USGS RESEARCH ON MINERAL RESOURCES—1994

PART A—PROGRAM AND ABSTRACTS

NINTH V.E. McKELVEY FORUM ON MINERAL AND ENERGY RESOURCES

Cosponsored by
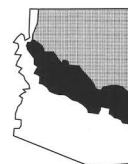
**ARIZONA
GEOLOGICAL
SOCIETY**

THE UNIVERSITY OF
ARIZONA
TUCSON ARIZONA
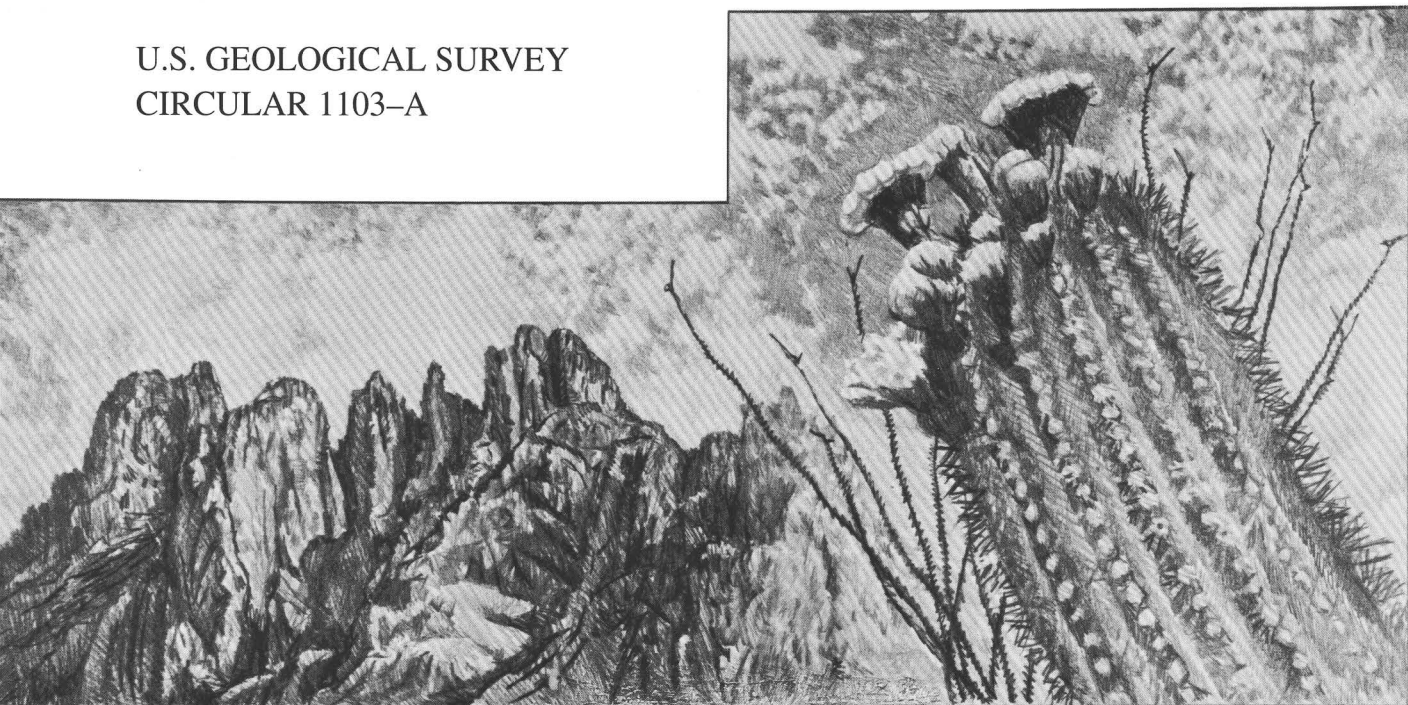
**Arizona
Geological
Survey**

U.S. GEOLOGICAL SURVEY
CIRCULAR 1103–A

USGS RESEARCH ON MINERAL RESOURCES—1994
PART A—PROGRAM AND ABSTRACTS

Edited by L.M.H. Carter, M.I. Toth, *and* W.C. Day

NINTH V.E. McKELVEY FORUM ON
MINERAL AND ENERGY RESOURCES

U.S. GEOLOGICAL SURVEY

Cosponsored by

Arizona Geological Society   University of Arizona   Arizona Geological Survey

9th V.E. McKelvey Forum
Mineral Resources
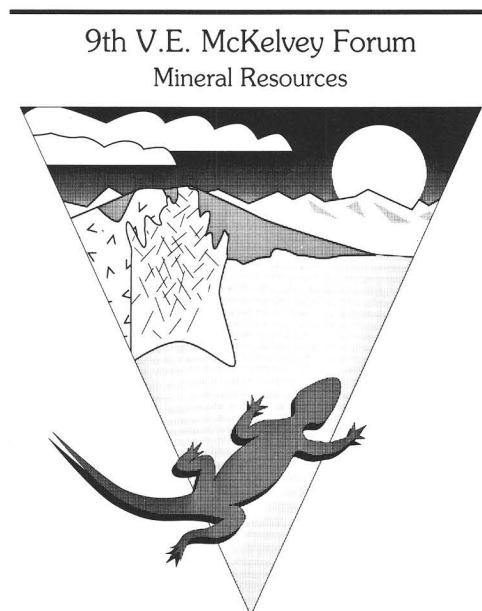
U.S. GEOLOGICAL SURVEY CIRCULAR 1103–A

U.S. DEPARTMENT OF THE INTERIOR
BRUCE BABBITT, Secretary

U.S. GEOLOGICAL SURVEY
Robert M. Hirsch, Acting Director

UNITED STATES GOVERNMENT PRINTING OFFICE, WASHINGTON : 1994

A society's wealth depends on the use it makes of raw materials, energy, and especially ingenuity.
                    —V.E. McKelvey

FOREWORD

The abstracts in this volume summarize talks and posters at the U.S. Geological Survey's Ninth V.E. McKelvey Forum on Mineral and Energy Resources. This year's Forum includes several innovations, chief among them being our cosponsors, the University of Arizona Department of Geosciences, the Arizona Geological Survey, and the Arizona Geological Society. Combining our efforts allows us to present a truly comprehensive program. Tucson was chosen as the site of the 1994 Forum in part to highlight activities of the U.S. Geological Survey (USGS) Tucson field office, our cosponsors, and the Center for Inter-American Mineral Resource Investigations (CIMRI). Tucson is also an excellent staging area for field trips, another innovation of this year's Forum. The field trips provide opportunities to explore the mining history and mineral deposits of one of the country's most important mining regions; further, they allow interaction with researchers who are reinterpreting the igneous geology of the Tucson Mountains and studying the relation of mineralization, rock type, and structural features of southeastern Arizona.

The McKelvey Forum was created to enhance communication between USGS scientists and members of the private sector, academia, and other government agencies; it is one of the main outreach activities of the USGS Geologic Division. Topics for the Forums have alternated between mineral and energy resources; this Forum concentrates on mineral resource issues.

Our program covers a broad spectrum of concerns—from the assessment and genesis of mineral resources to mineral-related environmental studies. A symposium on geology and mineral deposits of the southwestern United States and Mexico explores new ideas on the tectonic development and mineral endowment of this important region. Results are also presented from a USGS effort to reconstruct the tectonic history of the mineral-rich terrane of the Tucson-Mogollon corridor of eastern Arizona and western New Mexico. Another study examines the location, availability, and economics of industrial and metallic mineral deposits along the United States–Mexico border.

Mineral resource and environmental assessments are an integral part of wise and responsible land and resource management plans. Representatives from the U.S. Bureau of Mines, U.S. Forest Service, Bureau of Land Management, and Bureau of Indian Affairs will discuss their use of such information, along with presentations of the results of mineral resource assessment of the Coronado National Forest, Arizona and New Mexico; the Bureau of Land Management Roswell Resource Area, New Mexico; the Kaibab National Forest, Arizona; and the East Mojave National Scenic Area, California.

Summitville, Colorado, has been the focus of an intense effort to understand the geochemistry and environmental effects of cyanide and toxic metals released from the Summitville mine on downstream water supplies and crops. The distribution and movement of metals from mining districts of Coeur D'Alene, Idaho, and Rio Tinto, Spain are also ongoing environment-oriented projects for which results are presented here.

In light of the fact that in the private sector, emphasis for mineral exploration and development has shifted from a domestic to a global focus, this year's Forum also includes presentations of the results of mineral resource assessments of the Venezuelan Guayana shield; aeromagnetic data from the Brazilian part of the shield; new digital geologic information for Puerto Rico and Costa Rica; and studies of the regional framework and ore genesis from Bolivia, Brazil, Chile, Mexico, Peru, and the Venezuelan Andes.

Our cosponsors and I welcome you to the Ninth V.E. McKelvey Forum on Mineral and Energy Resources. I look forward to the lively exchange of ideas and information during the Forum, and I anticipate receiving valuable feedback that will help guide our program development within the USGS to continue to meet the needs of the Nation.

Robert M. Hirsch

Robert M. Hirsch, Acting Director
U.S. Geological Survey

NINTH V.E. McKELVEY FORUM ON MINERAL AND ENERGY RESOURCES

TUCSON, ARIZONA, FEBRUARY 22–25, 1993

PROGRAM OF LECTURES, DISCUSSIONS, AND FIELD TRIPS

All McKelvey talks and posters will be held in the
Tucson Convention Center Grand Ballroom

TUESDAY, FEBRUARY 22, 1994
Pre-meeting Field Trips

Trip 1 — Historic mining camps of southeastern Arizona
(*Brenda B. Houser*, USGS)

2 — Relationship of mineralization to key rock types and structural features of southeastern Arizona—Rincon and Santa Rita Mountains
(*Harald D. Drewes*, USGS, *and*
Stephen J. Reynolds, Arizona State University)

3 — Silver Bell porphyry copper deposit, Silver Bell Mountains, Arizona
(*Spencer R. Titley*, University of Arizona)

4:00–9:00 pm — Registration—Tucson Convention Center Lobby
6:00–8:00 — Open House—CIMRI, MIO, and ESIC
6:00–9:00 — Posters and Reception

WEDNESDAY, FEBRUARY 23, 1994

7:30 am — Registration
8:00 — Welcoming Comments and Overview
Officials of the U.S. Geological Survey
Elizabeth Ann Rieke (Assistant Secretary for Water and Science, U.S. Department of the Interior)

▽ *8:30–11:40* — *Minerals Related Environmental Studies*

Session Chairs: **Kathleen S. Smith** (USGS) and **Larry D. Fellows** (Director and State Geologist, Arizona Geological Survey)

8:30 — *Gilpin R. Robinson, Jr., and Larry P. Gough* (USGS), Overview of environmental mineral resources and related investigations in the Geologic Division, U.S. Geological Survey

8:50 — *William R. Miller, John B. McHugh, and Walter H. Ficklin** (USGS), The generation of natural acid drainage and the formation of iron bogs, Rocky Mountains, Colorado

9:10 — *Walter H. Ficklin*, Geoffrey S. Plumlee, and Kathleen S. Smith* (USGS), Geologic and geochemical controls on the composition of water draining from diverse mineral deposits

9:30 — *Trude V. V. King, Cathy Ager, Roger N. Clark, Gregg A. Swayze, and Andrea J. Gallagher* (USGS), Application of

*Walter H. Ficklin, deceased 10/11/93.

field and laboratory spectroscopic analysis to investigate the environmental impact of mining in the southeastern San Juan Mountains and adjacent San Luis Valley, Colorado

9:50 — *S.E. Church* (USGS), Use of lead isotopes to fingerprint sources of heavy-metal contamination in the environment

10:10–10:30 — Coffee Break and Poster Session

10:30 — *James R. Herring and Larry P. Gough* (USGS) Agricultural mineral mining, processing, and use—Environmental research opportunities

10:50 — *C.H. Nelson, A. Van Geen, P.J. Lamothe* (USGS), *and A. Palanques* (Ciencias del Mar, Barcelona, Spain), Heavy-metal contamination in river, estuary, and marine shelf sediment from the Rio Tinto mines, Spain

11:10 — *William P. Blacutt* (Univ. of Arizona), Recent environmental awareness in Latin America—The Bolivian case

11:30 — *Carroll Ann Hodges* (USGS), Mineral resources, environmental concerns, and land-use

12:00 — Luncheon (optional, preregistration requested)

12:30 — *Willis H. White* (USGS), Introductory remarks
Welcoming remarks from Cosponsoring Organizations and Organizing Committee
Larry D. Fellows (Director and State Geologist, Arizona Geological Survey)
Clement G. Chase (Chairman, Department of Geosciences, Univ. of Arizona)
Frances Wahl Pierce (President, Arizona Geological Society)
Warren C. Day (General Chair, Organizing Committee, USGS)

12:40 — Luncheon Speaker
Stephen D. Hoffman (Chief, Mining Section, Office of Solid Waste, U.S. Environmental Protection Agency), Developing a *rational* approach to regulating mining—Integrating the reauthorization of the Clean Water Act, CERCLA, and the reforming of the mining law of 1872

▽ *1:30–5:10* — *Symposium on Geology and Mineral Deposits of the Southwestern United States and Mexico*

Session Chairs: **Leslie J. Cox** (USGS) and **Clement G. Chase** (Univ. of Arizona)

1:30   *Stephen J. Reynolds* (Arizona State Univ.) *and Ed DeWitt* (USGS), Tectonic evolution of the southwestern United States

1:55   *Forrest G. Poole* (USGS), Geologic setting of mineral deposits in the Ouachita-Marathon-Sonora orogenic system along the southern margin of North America

2:20   *J. Ruiz, E. Centeno-Garcia, P.J. Coney, R. Torres-Vargas, P.J. Patchett, and P. Yanez* (Univ. of Arizona), Paleozoic and Mesozoic tectonic evolution of Mexico based on geochemistry of basement rocks

2:45   *Mark D. Barton* (Univ. of Arizona), *John-Mark G. Staude* (USGS), *and Lukas Zürcher* (Univ. of Arizona), Igneous-related mineralization in Mexico

3:10–3:30   Coffee Break and Poster Session

3:30   *Jaime Roldan Quintana* (Univ. of Mexico-Hermosillo), Brief description of the geology and mineral deposits of southern Sonora, Mexico

3:55   *John-Mark G. Staude* (USGS), Tectonic reconstruction of northwestern Mexico with implications for mineral resources—A new regional ore deposit synthesis and model

4:20   *Karen J. Wenrich and Miles L. Silberman* (USGS), Au-Ag polymetallic mineralization in the Music Mountain area, Arizona, along the southwestern edge of the Colorado Plateau

4:45   *Robert J. Kamilli* (USGS), The Mogollon mining district—Results from mapping, paragenesis, and fluid inclusion studies

5:10–7:00   Poster Session and Refreshments

THURSDAY, FEBRUARY 24, 1994

▽ *8:00–10:00 am Mineral Resource and Mineral Environmental Assessments for Land and Resource Management*

Session Chairs: **Martha S. Power** and
                  Joseph A. Briskey, Jr. (USGS)

8:00   *Panel Discussion on Land-Use Planning—*
Use of Minerals Information in Managing the Nation's Lands and Resources
Introduction: *Joseph A. Briskey, Jr.* (USGS)
Panel Members:
Ransom F. Read III (U.S. Bureau of Mines, Chief, Branch of Mineral Land Assessment)
G. Lynn Sprague (U.S. Forest Service, Director, Minerals and Geology Management)
Adam A. Sokoloski (Bureau of Land Management, Deputy Assistant Director, Energy and Mineral Resources)
Richard N. Wilson (Bureau of Indian Affairs, Chief, Division of Energy and Mineral Resources)
Summary: *Martha S. Power* (USGS)

9:00   *Geoffrey S. Plumlee, Steven M. Smith, Margo I. Toth, and Sherman P. Marsh* (USGS), Integrated mineral resource and environmental assessments of public lands—Applications in land-use management

9:20   *Dennis P. Cox, Joseph A. Briskey, Jr., Sandra H. D. Clark, Michael F. Diggles, Thomas D. Light, and Alan R. Wallace* (USGS), The national assessment of undiscovered deposits of copper, zinc, lead, silver, and gold—A progress report

9:40   *P. B. Barton, R. A. Ayuso, D. A. Brew, E. R. Force, B. M. Gamble, R. J. Goldfarb, D. A. John, K. M. Johnson, D. A. Lindsey, and S. D. Ludington* (USGS), Quantitative assessment of undiscovered, non-fuel mineral resources

10:00–10:20   Coffee Break and Poster Session

▽ *10:20–11:40 Results and Impact of Mineral Resource Assessments*

10:20   *J.M. Hammarstrom, M.L. Zientek, J.E. Elliott, R.R. Carlson, G.K. Lee, B.S. Van Gosen, and D.M. Kulik* (USGS), Mineral resource assessment of the Absaroka-Beartooth study area, Custer and Gallatin National Forests, Montana

10:40   *James P. Shelden and Sherman A. Sollid* (U.S. Forest Service), Mineral resource assessment of the Absaroka/Beartooth study area—A USFS perspective

11:00   *Jean Juilland and Jerry Dutchover* (Bureau of Land Management), Regional and Resource Area uses of mineral resource information

11:20   *Stephen A. Manydeeds* (Bureau of Indian Affairs), Utilization of U.S. Geological Survey mineral resource data by the Bureau of Indian Affairs

11:40   Director's Lecture: *John F. Slack* (USGS), Tourmalinites and strata-bound ore deposits—Geology, genesis, and exploration applications

12:20–1:30   No Host Deli Lunch and Poster Session (optional, preregistration requested)

▽ *1:30–5:00   Mineral Resource Activities in Latin America*

Session Chairs: **Barbara A. Eiswerth and Floyd Gray** (USGS)

1:30   *Douglas B. Silver* (Balfour Holdings), Trends in mineral exploration in Latin America

2:00   *Barbara A. Eiswerth* (USGS), Geological remote sensing—History and development in Latin America

2:20   *C.G. Cunningham, R.E. Zartman, E.H. McKee, R.O. Rye, C.W. Naeser, and G.E. Ericksen* (USGS), Timing and origin of ore deposition at the Cerro Rico de Potosi Ag-Sn and Porco Ag-Zn-Pb-Sn deposits, Bolivia

2:40   *Albert Hofstra[1], Luis Barrera[2], Richard Hardyman[1], Edwin H. McKee[1], and Orlando Sanjines[2]* ([1]USGS and [2]Servicio Geologico de Bolivia), La Espanola prospect—A multiple intrusive porphyry complex with low-grade gold potential, northwestern Altiplano, Bolivia

3:00–3:20   Coffee Break and Poster Session

3:20   *Richard I. Grauch* (USGS), Gold-bearing exhalative-hydrothermal systems in the Venezuelan Andes

3:40   *Richard M. Tosdal* (USGS), Lead sources in Oligocene and Miocene precious-metal deposits of the western Andean cordillera, southern Peru, western Bolivia, and northern Chile

4:00   *Edwin H. McKee* (USGS), *Peter Craig Gibson, Donald C. Noble, and Kirk E. Swanson* (Mackay School of Mines, Univ. of Nevada-Reno), Timing of igneous activity, alteration, and mineralization at the Orcopampa Ag-Au district, southern Peru

4:20   *Ed DeWitt[1], G. P. Landis[1], R. E. Zartman[1], Enzio Garaype[2], Sérgio Luiz Martins Pereira[3], Milton Guimarães Bueno do Prado[3], Frederico Wallace Reis Vieira[4], and C. H. Thorman[1]*, ([1]USGS, [2]São Bento Minerao S.A., Santa Barbara, Minas Gerais, [3]Unamgen Minerao e Metalurgia S.A., Santa Barbara, Minas Gerais, and [4]Minerao Morro Velho, Nova Lima, Minas Gerais), Isotopic and fluid inclusion data on the age and origin of the São Bento and Morro Velho gold deposits, Minas Gerais, Brazil

4:40   *Willis H. White* (USGS), Summary and concluding remarks

6:00   Cocktails—7:00 Dinner—Ramada Inn. Here's your chance to unwind and enjoy a casual review with your colleagues (optional, preregistration required)

FRIDAY, FEBRUARY 25, 1994
Post-meeting Field Trips

Trip 4   The Tucson Mountains caldera (*Peter W. Lipman*, USGS)

      5   New work in the San Manuel and Mammoth districts—An introduction via Tucson Wash (*Eric R. Force*, USGS, *and William R. Dickinson*, Univ. of Arizona)

      6   Silver Bell porphyry copper deposit, Silver Bell Mountains, Arizona—repeat of Trip 3 (*Spencer R. Titley*, Univ. of Arizona)

      7   Kitt Peak National Optical Astronomy Observatory (*Floyd Gray*, USGS)

V.E. MCKELVEY FORUM—POSTER SESSIONS

[Some of these abstracts share poster space]

Aleinikoff, J.N., Peterman, Z.E., Widmann, B.L., Walter, M., and Futa, Kiyoto—Isotopic tracers of gold mineralization in Late Proterozoic and Paleozoic limestones of southern Nevada

Armstrong, Augustus K.—Jurassic Todilto Limestone Member, facies, diagenesis, and mineralogy, Grants uranium district, New Mexico

Bartsch-Winkler, Susan—Mineral resource assessment of the Roswell Resource Area, New Mexico—A cooperative study by three Interior Department agencies

Bawiec, Walter J., and Ambroziak, Russell A.—Digital Geologic Information and its application in the mineral resource assessment of Puerto Rico

Bliss, James D.—Development of predictive models for sand and gravel deposits in the southwest United States

Bookstrom, Arthur, Box, Stephen, Smith, Cole, and Lindsay, James—Distribution and movement of metals derived from mining and mineral processing in the Coeur d'Alene River valley

Bouse, Robin M., Wooden, Joseph L., Titley, Spencer R., Ruiz, Joaquin, and Tosdal, Richard M.—Th/U ratios as a potential exploration tool for Ag- or Au-enriched crustal provinces

Bultman, Mark W.—A summary of the mineral resource assessment of Coronado National Forest, Arizona and New Mexico

Bultman, Mark W., and Gettings, Mark E.—New techniques of geophysical data analysis; an investigation of the geometry, structure, and bedrock lithology of the San Rafael basin, Arizona

Calderone, Gary J., Peterson, Donald W., Faulds, James E., and Butler, Robert F.—Paleomagnetism and magnetic fabric of the Apache Leap Tuff, central Arizona

Chaffee, M.A., Carlson, R.R., and Theodorakos, P.M.—Regional geochemical studies in the Kaibab National Forest, Arizona

Church, S.E., and Raines, G.L.—Geochemical maps of Arizona and the Great Basin

Clark, Roger N., and Swayze, Gregg A.—Mapping minerals with imaging spectroscopy—Examples illustrating the beginning of a new mapping era

Conway, Clay M.—Precambrian massive sulfide deposits in amphibolite and granulite-facies rocks, western Arizona and southeastern California

Cox, Leslie J.—Porphyry copper deposits in Arizona—An example of resource evaluation for the U.S. Geological Survey's national assessment of copper, lead, zinc, gold, and silver

Cunningham, Charles G., Fournier, Robert O., Vikre, Peter G., and Rytuba, James J.—Hot-spring textures in epithermal environments

Cygan, G.L., Hemley, J.J., and Doughten, M.W.—Fe, Pb, Zn, Cu, Au, and HCl partitioning between vapor and brine in hydrothermal fluids—Implications for porphyry copper deposits

Desborough, George A.—Capture of copper, lead, zinc by the zeolite-clinoptilolite in metal-polluted drainages of Colorado

Drewes, Harald—Geologic contributions to the mineral resource assessment of the Coronado National Forest, Arizona and New Mexico

du Bray, Edward A., and Pallister, John S.—Magmatic evolution of the Turkey Creek caldera, Chiricahua Mountains, Arizona

Erdman, J.A., and Smith, K.S.—Impact of the Summitville mine on irrigation water, agricultural soils, and alfalfa in the southwestern San Luis Valley, Colorado

Erickson, B.M., Briggs, P.H., and Peacock, T.R.—Metal concentrations in the wetland vegetation receiving acid mine drainage from St. Kevin Gulch, Leadville, Colorado

Folger, Helen, Hofstra, Albert, and Nowlan, Gary—A progress report on the southern California geochemical database and map

Force, Eric R.—Santa Catalina Mountains, southeastern Arizona—Laramide to Eocene paleodepths from field evidence, and implications for mineral potential

Gallagher, Andrea J., Watson, Ken, Knepper, Daniel H., Jr. and Ager, Cathy—Mapping alteration in hot spring environments using imaging spectrometry

Gettings, Mark E.—Constraints on mineral resource potential from analyses of geophysical data from the Coronado National Forest, southeastern Arizona

Gettings, Mark E.—Some structural features along the Tucson-Mogollon Corridor inferred from gravity and magnetic anomaly data

Gray, Floyd, Bliss, James D., Page, Norman J, Pierce, Herbert A., and Eiswerth, Barbara—Redefinition of lateritic bauxite deposit types, northern South America Shield

Gray, Floyd, Wynn, Jeffrey C., Orris, Greta J., Page, Norman J, Brooks, William E., Sidder, Gary B., Day, Warren C., Bliss, J.D., Cox, Dennis P., Detra, David, Unkefer, Jason, and Gutierrez, John—Mineral resource assessment of the Venezuelan Guayana Shield

Hoffman, J.D., and Marsh, S.P.—National Geochemical Data Base

Hon, Ken, and Lipman, Peter—Jurassic calderas in southeastern Arizona—The surface manifestation of a composite batholith

Houser, Brenda B.—Santa Ana–Reserve extension zone—A proposed zone of interactive northeast- and northwest-directed extension during the Cenozoic, New Mexico, Arizona, and Sonora

NOTE: Due to limitations of space and constraints on topics, several abstracts are included in this volume that are not presented in the Forum.

USGS RESEARCH ON MINERAL RESOURCES—1994 PROGRAM AND ABSTRACTS

Edited by L.M.H. Carter, M.I. Toth, and W.C. Day

ISOTOPIC TRACERS OF GOLD MINERALIZATION IN LATE PROTEROZOIC AND PALEOZOIC LIMESTONES OF SOUTHERN NEVADA

J.N. Aleinikoff, Z.E. Peterman, B.L. Widmann, M. Walter, and Kiyoto Futa

Disseminated gold deposits (Carlin-type) are important mineral exploration targets in the Great Basin. Many deposits occur in Late Proterozoic and Paleozoic limestones and dolomites that were mineralized in the Cretaceous and Tertiary by hydrothermal fluids which deposited micrometer- to submicrometer-sized gold particles. Commonly, ore deposition was structurally controlled, and in some areas shallow-dipping thrust or detachment faults were pathways for the mineralizing solutions.

Late Proterozoic and Paleozoic shelf carbonate rocks crop out extensively in the mountain ranges of southern Nevada. Bare Mountain, located about 100 miles (160 km) northwest of Las Vegas (immediately west of Yucca Mountain), is composed of heavily mineralized carbonate rock. Other ranges, such as the Striped Hills, Specter Range, and Spring Mountains, contain the same stratigraphic section, but the rocks apparently are mostly barren. We have measured Sr and Pb isotopic compositions and Sr, Rb, Pb, U, and Th concentrations in fresh (unaltered) and mineralized (altered) rocks, including samples collected along traverses that cross contacts between unaltered rocks and ore zones in an operating underground mine. The objectives of this study are to determine (1) if mineralized rock has Sr and Pb isotopic signatures indicative of fluid alteration and Carlin-type gold deposition, and (2) if these isotopic tracres can be used in exploration.

Marine limestones incorporate the $^{87}Sr/^{86}Sr$ value of sea water from which they are deposited. The oceans are isotopically uniform in strontium at any particular time, but $^{87}Sr/^{86}Sr$ values have varied systematically throughout Late Proterozoic and Phanerozoic time. However, if strontium of a different isotopic composition were added to or exchanged with strontium in the limestone, then the $^{87}Sr/^{86}Sr$ in these limestones might be significantly modified from its primary depositional value. Lead isotopic ratios ($^{206}Pb/^{204}Pb$, $^{207}Pb/^{204}Pb$, and $^{208}Pb/^{204}Pb$) in carbonate are a function of the age of the rock and the concentrations of Pb, U, and Th in the rock. Closed-system, modern-day Pb isotopic ratios in Paleozoic carbonate rocks are fairly high (such as $^{206}Pb/^{204}Pb$ >20).

Cretaceous and Tertiary alteration of Paleozoic carbonate rocks of southern Nevada produced an increase in Sr, Pb, U, and Th concentrations, an increase in $^{87}Sr/^{86}Sr$, and a decrease in $^{206}Pb/^{204}Pb$, $^{207}Pb/^{204}Pb$, and $^{208}Pb/^{204}Pb$. Although these modifications of the primary isotopic compositions and concentrations could have been caused by dolomitization or exchange among units during metamorphism, the changes were most likely caused by introduction of Sr, Pb, U, and Th by hydrothermal fluids that had acquired these elements from underlying Precambrian basement rocks. Thus, anomalously high $^{87}Sr/^{86}Sr$ and Pb (ppm), and low $^{206}Pb/^{204}Pb$, $^{207}Pb/^{204}Pb$, and $^{208}Pb/^{204}Pb$ could indicate hydrothermally altered and mineralized carbonate. For convenience and clarity, $^{87}Sr/^{86}Sr$ values are expressed as the per mil deviation ($\delta^{87}Sr$) from modern sea water $^{87}Sr/^{86}Sr$.

Both mineralized and barren Late Proterozoic and Paleozoic carbonates were collected from Bare Mountain. For comparison, suites of unmineralized samples were also collected from the Striped Hills, Spring Mountains, and various ranges in the vicinity of Indian Springs Valley. $\delta^{87}Sr$ values for Paleozoic carbonates from the Striped Hills, Spring

Mountains, and mountain ranges near Indian Springs Valley have a limited range of −1 to +2‰. Some of these values are slightly higher than would be expected for primary marine values, but we attribute this to relatively minor local exchange during dolomitization or metamorphism. In contrast, δ^{87}Sr values for Bare Mountain samples range widely and have values as high as +25‰. Low values (<+2‰) are from areas on Bare Mountain that do not appear to be mineralized or altered. δ^{87}Sr values of +3‰ or higher are from known mineralized areas such as the Sterling mine, the Gold Ace mine, Tungsten Canyon, Fluorspar Canyon, Secret Pass, and the Telluride mine. Similarly, unaltered rocks have very low Pb (0.81 ppm), U (0.35 ppm), and Th (0.78 ppm) and high Pb isotopic ratios (for example, $^{206}Pb/^{204}Pb=21.87$), whereas altered rock has high Pb (51.3 ppm) and Th (4.46 ppm) and low $^{206}Pb/^{204}Pb$ (19.08).

We conclude that hydrothermal alteration of gold-bearing Late Proterozoic and Paleozoic carbonate rocks is indicated by modifications of the Sr and Pb isotopic systematics. The isotopic ratios in the altered rocks presumably reflect the isotopic signature of underlying Precambrian basement through which the mineralizing fluids passed. Thus, we suggest that Sr and Pb isotopic tracers have considerable potential for identifying hydrothermal alteration in carbonate rocks of southern Nevada that may contain cryptic gold deposits.

JURASSIC TODILTO LIMESTONE MEMBER, FACIES, DIAGENESIS AND MINERALOGY, GRANTS URANIUM DISTRICT, NEW MEXICO

Augustus K. Armstrong

The Todilto Limestone Member, basal member of the Wanakah Formation (Middle Jurassic) of the Grants uranium district, is 1–30 ft (0.3–9.1 m) thick and records the change in depositional environments from a restricted marine embayment with an ephemeral connection to the Curtis-Summerville sea to a completely enclosed and shrinking body of gypsiferous water. The salina measured 300 miles (483 km) from east to west and 250 miles (402 km) from north to south, and was fringed by an extensive limestone-gypsum sabkha. The arenaceous-lime mudstone records a shoaling-upwards sequence deposited in subtidal to supratidal sabkha environments, in alternating brackish to hypersaline marine waters. Dolomite is absent in the study area. The calcite lime mudstones were derived primarily from an aragonite mud precursor and were subjected to extensive neomorphism. The aragonite-to-calcite diagenetic history is evident in the poorly preserved ooids.

The salina waters did not support a normal marine invertebrate fauna or flora. Bioclasts of the marine calcareous algae, dasyclads of the Tribe Salpingoporelleae, indicate short periods of near-normal marine water as a result of sea water influx into the Todilto embayment. Ostracodes lived in ephemeral-gypsiferous ponds and are abundant in the sabkha facies. The salinity of marine waters was influenced by seasonal influx from streams, by rainfall, by periods of drought, and by intermittent connections to the Curtis-Summerville sea. The overlying 0–110 ft (0–33.5 m)-thick gypsum unit found to the east of the study area was deposited in the center of the basin during the final salina phase. Lacustrine alkaline evaporites, such as trona and shortite, are not known from the Todilto Limestone Member.

Megapolygon mounds to intraformational folds of early diagenetic origin, in a vertical stack up to 10 ft (3 m) high and 45 ft (14 m) wide, occur in the supratidal facies and are associated with calcite pseudomorphs of anhydrite-gypsum and anhydrite ptygmatic-enterolithic layers. The fractures of the megapolygons may have acted as sites of preferential saline ground-water outflow. The intraformational folds are overlapped and buried by thick-bedded microbial mat, supratidal ostracode-lime mudstone. The Todilto Limestone Member was subjected to vadose solution that formed sinkholes, rundkarrens, and solution pipes that are filled with limestone breccias and ferruginous sands from the overlying Beclabito Member of the Wanakah. The smaller vadose solution cavities are partially filled with multiple cycles of spar calcite and iron-stained quartz sands. Commercial bodies of uranium ore are found in the Todilto intraformational folds and associated solution cavities. Isotopic ages (155–150 Ma) indicate that the uraninite is nearly syngenetic with the carbonates.

INTRUSION-RELATED MINERALIZATION IN MEXICO

Mark D. Barton, John-Mark G. Staude, and Lukas Zürcher

Igneous-related mineralization in Mexico can be broadly divided between (1) epithermal deposits that have broad temporal and spatial correlations with volcanism, and (2) mineralized deposits clearly associated with intrusive centers and exhibiting close relationships in composition, time, and space. We review herein patterns of intrusion-related mineralization and possible controls, based in part on continuing research and database compilation by the University of Arizona–mining industry–U.S. Geological Survey consortium on the mineral resources of Mexico.

In Mexico, intrusion-related mineral deposits are primarily Mesozoic to middle Tertiary in age. Although complex in detail, three broad periods are prominent in the mineralization record: the late Mesozoic, the Laramide, and
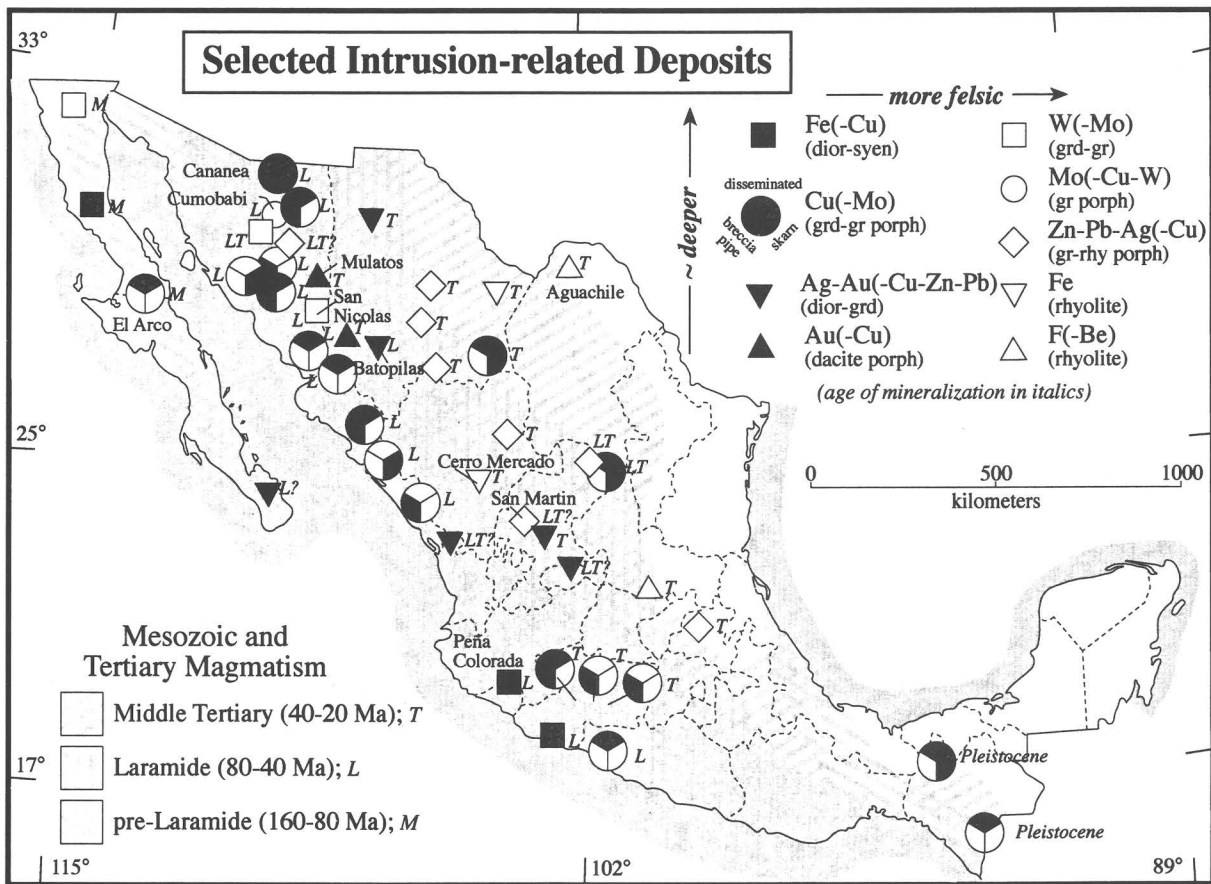
Figure 1 (M. Barton and others). Generalized distribution and timing of selected intrusion-related ore deposits in Mexico.

the middle Tertiary (fig. 1). Jurassic to Late Cretaceous calc-alkalic batholiths with sparse volcanic rocks occur along the Pacific margin mainly on eugeoclinal crust, although locally on continental crust (for example, in Sonora). Latest Cretaceous to early Tertiary ("Laramide") calc-alkalic batholithic, subvolcanic, and volcanic centers occur in an overlapping but somewhat more easterly band that extends with diminished intensity (and somewhat younger ages) into the Sierra Madre Oriental. Mid-Tertiary volcanism and local intrusive centers are widely developed, with a volume maximum of calc-alkalic felsic volcanics in the Sierra Madre Occidental, but extending as a more mafic middle to late Tertiary arc in the Sierra Madre del Sur in southern Mexico, and as a fringe of alkalic volcanic and subvolcanic centers in northeastern Mexico.

Mexico is characterized by multiple styles of intrusion-related mineralization. These can be divided by geologic associations, metal contents, and styles of alteration (table 1). Although more than 1,000 intrusion-associated mineral deposits are known, the scarcity of data requires a simplified approach focusing on major districts. The broad continuum

that exists in the types of mineralization products is a function of exposure level and igneous compositions, which in turn mainly reflect age and province.

Some inferences can be drawn from examination of these patterns:

• Igneous compositions vary in time and space in Mexico, but multiple compositions commonly were emplaced at different times in the same region. Temporal variations (as in Sonora) are as important as differences in province (as between Sonora and southern Mexico).

• Alteration and metal differences between alkaline and subalkaline, felsic and mafic magma suites (table 1) can be partly rationalized from equilibria among igneous minerals (see fig. 2, αAl_2O_3 vs αCaO [vs αSiO_2]) and magmatic metal contents (reflecting province and process).

• Exposure and preservation filter observed Mexican metallogeny. Erosion of the Mesozoic arc superstructure in the west leaves mainly tungsten skarns, burial of the Laramide arc in central Mexico interrupts porphyry copper patterns, and minimal exhumation of mid-Tertiary intrusive centers preserves distal vein/replacement systems.

3

Table 1 (M. Barton and others). Generalized characteristics of intrusion-related mineralization.

Deposit Type / (example)	Associated Igneous Rocks (IUGS)	Mineralization & Alteration	Time-space distribution (see also Figure 1)
Porphyry Cu(-Mo) (Cananea, SON)	bi-hbl-mt granodiorite to bi monzogranite porphyry	stockwork Cu w Kf-qz/ ser-py; Zn skarn	Laramide, minor pre-Laramide & Tertiary; inboard western
Porphyry Cu(-Mo-Au) (El Arco, BC)	px-hbl-qz diorite to bi-hbl granodiorite porphyry	stockwork Cu w bi-Kf-mt/chl-py-ser; ± Fe skarn	pre-Laramide & Tertiary (SW Mexico); outboard western
Fe(-Cu) (Peña Colorada, JAL)	px-hbl diorite to (bi) qz monzonite	Fe ± Cu skarn w Na- (±K-) silicate alteration	pre-Laramide and Laramide; outboard western
Ag-Au(-Cu-Zn-Pb) (Batopilas, CHI)	px-bi-qz diorite to bi granodiorite porphyry	Ag-Au(-Pb-Zn) qz-carb vein & replacement; ± stockwork Cu	pre-Laramide & Tertiary; inboard western & north-central
Au(-Cu) (Mulatos, SON)	bi-mt(-hbl) dacite to bi rhyolite	Au(-Cu-Ag) advanced argillic & sericitic zones	Tertiary; inboard western
W(-Mo) (San Nicolas, SON)	bi(-hbl) granodiorite to mu-bi granite	W(-Mo) skarns, pegmatite & greisen (mu-qz) W(-Mo)	pre-Laramide & Laramide; western
Mo(-Cu-W) (Cumobabi, SON)	bi granodiorite to bi granite porphyry	stockwork/pegmatitic Mo w Kf-qz-mu-py	Laramide; inboard western
Zn-Pb-Ag(-Cu) (San Martin, ZAC)	bi granodiorite to (bi) rhyolite porphyry	Zn-Pb-Ag(-Cu-W-Mo) skarn & replacement; ± stockwork qz	Tertiary, minor Laramide; north-central
Fe (Cerro de Mercado, ZAC)	px-mt qz latite to hbl-mt rhyolite	massive hm(after mt) (volcanic?) w Fe-pyroxene to Qz-clay-apat	Tertiary; north-central
F(-Be-Sn) (Aquachile, COA)	rieb syenite or bi qz latite to (bi-) alkali rhyolite	carbonate replacement fl-qz±Be, (± igneous Sn, Mo, topaz)	Tertiary; north-central & east
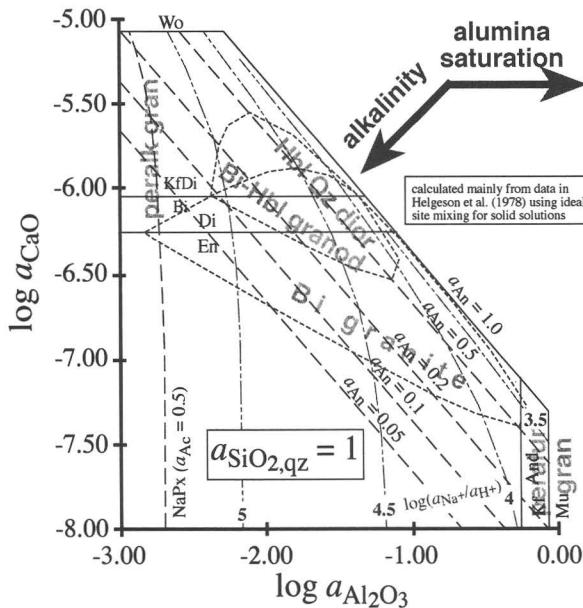
Figure 2 (M. Barton and others). Calculated αCaO vs. αAl$_2$O$_3$ diagram (at quartz saturation) showing simplified phase relations among igneous minerals and hydrothermal fluid. These relationships help rationalize differences between mineralization types associated with different kinds of quartz-bearing igneous rocks. Short dashed lines, limits of hornblende (logα$_{parg}$ = -2.7, appropriate for a plausible igneous composition) stability for potassium-bearing and potassium-lacking assemblages.

• The superimposed metallogenic patterns in Mexico have parallels with metallogenic patterns in the western United States in terms of the effects of preservation, process, and province.

Future work should focus on increasing the basic geologic data on mineral deposits and igneous rocks. Geochronology, petrology, and geochemistry studies would help better define the temporal, spatial, and compositional interrelations between tectonism, magmatism, and mineralization.

QUANTITATIVE ASSESSMENT OF UNDISCOVERED, NON-FUEL MINERAL RESOURCES

P.B. Barton, R.A. Ayuso, D.A. Brew, E.R. Force, B.M. Gamble, R.J. Goldfarb, D.A. John, K.M. Johnson, D.A. Lindsey, and S.D. Ludington

Since its establishment in 1879, it has been the responsibility of the U.S. Geological Survey to study and report on the mineral resources of the public domain. A wide variety of mineral deposits and identified resources have been described, and the circumstances and processes by which they formed have been extensively investigated. In recent years, there has been an expanded role in society for land-use

4

planning. Because mineral extraction is one of the activities competing for access to land, a need has grown for assessments of undiscovered mineral resources. As early as 1975, the USGS began using techniques to quantify its assessments, combining grade and tonnage models with estimates of the number of deposits to arrive at an estimate of the amounts of metals. In 1984, the first assessment was made in which these estimates were combined by means of a Monte Carlo simulation to provide probabilistic estimates of tonnages of metals.

These protocols have been and will continue to be subject to evolution and improvement. In response to internal dissent, the USGS commissioned an extramural panel, chaired by Dr. DeVerle Harris of the University of Arizona, to review the assessment methods. The report, released in March 1993 (USGS Open-file Report 93–258), examines and largely vindicates the methodology; it also contains an extensive list of suggested improvements. A series of in-house forums, held at six USGS facilities during fall 1993, were designed to evaluate the suggested improvements, seek out others, prioritize all suggestions, and analyze their implementation. The outcome of these forums will inform and determine future improvements in the assessment program.

MINERAL RESOURCE ASSESSMENT OF THE ROSWELL RESOURCE AREA, NEW MEXICO—A COOPERATIVE STUDY BY THREE INTERIOR DEPARTMENT AGENCIES

Susan Bartsch-Winkler

Comprehensive mineral resource reports on the Roswell Resource Area, N.Mex., were prepared by the U.S. Bureau of Mines (USBM) and the U.S. Geological Survey (USGS) for use by the U.S. Bureau of Land Management (BLM) (Bartsch-Winkler, 1992; Bartsch-Winkler and Donatich, in press; Korzeb and Kness, 1993). The work was conducted in order to assist the BLM in preparing the Resource Management Plan for the resource area, which encompasses 14 million acres of private, State, and Federal land in seven counties in the east-central part of the State (fig. 1). The reports result from two separate studies (a mineral inventory by the USBM and an assessment of mineral resources by the USGS) which are compilations of published and unpublished data, and integrate new findings on the geology, geochemistry, geophysics, mineral, industrial, and energy commodities, and resources. Both reports were guided in the data-gathering processes, field operations, and writing stages by the BLM staff in Roswell, who were developing the Management Plan for the Roswell Resource Area. In addition, the reports will be used in future nationwide

mineral and energy resource inventories and assessments, and as reference and training documents; they can also be used as public-information tools by the BLM, USBM, and USGS. The USGS also provided BLM with digital maps on the geology (LaRock and Moore, 1992), geochemistry (Tidball and Erdman, 1992), mine and prospect locations, and oil and gas well locations and fields and an interactive computer display on the geology and resources of the study area prepared for use in the Public Information Office of the BLM in Roswell (see Tidball and Bartsch-Winkler, this volume). A valuable link was established between the staffs of these agencies as a result of this study, and a working relationship continues.

The resource area is not now a major mineral producing area in the State; however, many metals, industrial mineral commodities, and energy resources are, or have been, produced or prospected in the past, and future exploration potential is discussed. Copper, gold, silver, thorium, uranium and (or) vanadium, rare-earth elements, iron, manganese, tungsten, lead, zinc, and molybdenum, as well as many industrial minerals (the most important being fluorspar and gypsum) and fuels and associated resources are evaluated in the assessment study. Important commodities that have yet to be identified in economic concentrations (have no past production) but are permissive in the area include potash, halite, polyhalite, anhydrite, sulfur, feldspar, brines, various gases associated with oil and gas exploration, and carbon dioxide.

REFERENCES

Bartsch-Winkler, Susan, ed., 1992, Mineral and energy resources of the BLM Roswell Resource Area, east-central New Mexico: U.S. Geological Survey Open-File Report 92–261, 153 p.

Bartsch-Winkler, Susan, and Donatich, A.J., eds., in press, Mineral and energy resources of the Roswell Resource Area, east-central New Mexico: U.S. Geological Survey Bulletin 2063. [Supersedes Open-File Report 92–261.]

Korzeb, S.L., and Kness, R.F., 1993, Mineral resource investigation of the Roswell Resource Area, Chaves, Curry, DeBaca, Guadalupe, Lincoln, Quay, and Roosevelt Counties, New Mexico: U.S. Bureau of Mines Open-File Report MLA 12–92, 229 p.

LaRock, E.J., and Moore, S.L., 1992, Digital geologic map of the Roswell Resource Area, New Mexico: U.S. Geological Survey Open-File Report 92–0328–A Discussion (paper copy), 92–0328–B Database (diskette), and 92–0328–C Command Files (diskette).

Tidball, E.R., and Erdman, J.A., 1992, NURE data for groundwater and stream sediments, BLM Roswell Resource Management Area, east-central New Mexico: U.S. Geological Survey Open-File Report 92–365–A Discussion (paper copy), 92–365–B Database (diskette).
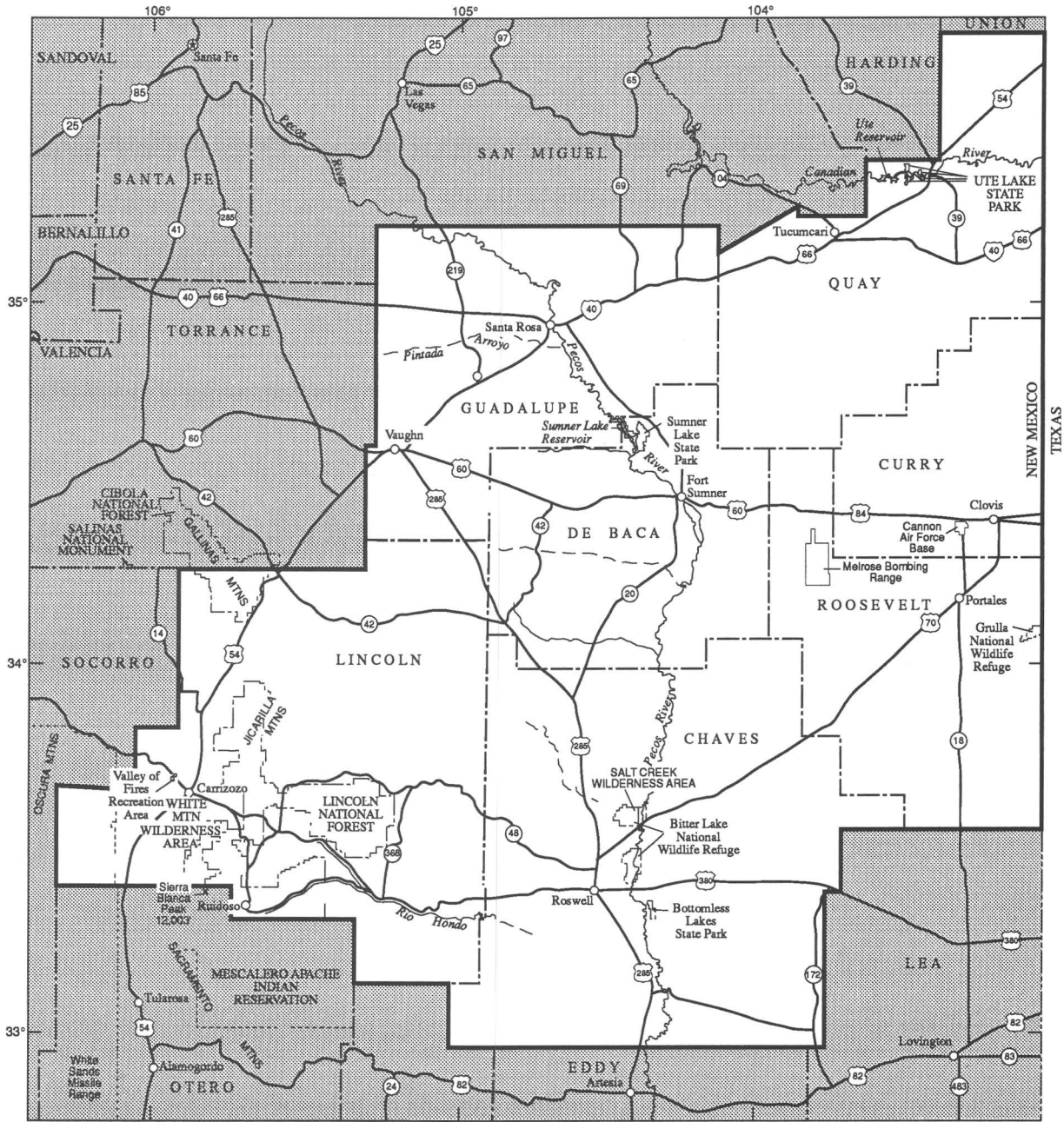
Figure 1 (Bartsch-Winkler). Index map of the Roswell Resource Area, east-central New Mexico.

6

DIGITAL GEOLOGIC INFORMATION AND ITS APPLICATION IN THE MINERAL RESOURCE ASSESSMENT OF PUERTO RICO

Walter J. Bawiec and Russell A. Ambroziak

The availability of new and diverse modes of digital information, particularly in the field of earth science, has led to a new cycle of innovative applications to earth-science-related issues. Included within these applications are mineral resource assessments, where digital databases of site-specific information and thematic layers of spatial data can be combined and manipulated to serve as an analytical tool. In the mineral resource assessment of Puerto Rico, we used digital data to produce both integrated and comprehensive derivative products. The digital thematic data will be available to the public on CD-ROM.

The USGS (U.S. Geological Survey), in cooperation with the Puerto Rico Department of Natural Resources and the University of Puerto Rico at Mayaguez, recently completed a mineral resource assessment of the Commonwealth of Puerto Rico as part of the USGS National Mineral Resource Assessment Program (NAMRAP). The objectives in conducting this assessment were to aid government officials in land-use planning, to inform the community of potential new areas of interest, and to compile Puerto Rican earth-science-related information, much of which previously had not been released.

This assessment is an example of the use and integration of digital data in the assessment process. The variety of digital data utilized includes geology, which permits selection of specific and (or) combinations of map units based on rock type or age; geophysics (including gravity and magnetic signatures), which infers subsurface structure and the extent of lithologies; geochemistry, which indicates surficial anomalous values for metallic and pathfinder elements; mineral occurrences, which provide information about the spatial distributions of known commodities; remote sensing (including SLAR (Side Looking Airborne Radar)), which represents surficial geomorphic features; and GLORIA (Geological Long Range Inclined Asdic) system, whose images of offshore landforms can be traced onshore.

Puerto Rico, the easternmost island of the Greater Antilles, is a volcanic island-arc whose geologic record spans approximately 150 million years. The island consists of volcaniclastic and epiclastic rocks of volcanic origin, sedimentary rocks of Late Jurassic to Paleocene-Eocene age, and intrusive mafic and felsic plutonic rocks of Late Cretaceous and early Tertiary age. These rocks are overlain unconformably by Oligocene and younger sedimentary rocks and sediments. The geology of Puerto Rico is represented by approximately 150 stratigraphic units. Twelve terranes based primarily on lithologic affinity and age (fig. 1) were the initial starting point for delineation of permissive mineral deposit-type terranes.

The rock types and depositional environments encountered in Puerto Rico are permissive for a wide variety of metallic and industrial mineral deposits associated with island-arc environments. (Table 1 lists our mineral deposit models and the probabilistic estimates of the number of undiscovered metallic deposits.) Porphyry copper deposits consist of a stockwork of veinlets of quartz, chalcopyrite, and molybdenite in or near a porphyritic intrusion. Copper skarn and iron skarn deposits are irregular or tabular-shaped ore bodies formed in carbonate or calcareous rocks near igneous contacts or in xenoliths in igneous stocks. Polymetallic veins consist of quartz-carbonate veins containing gold and (or) silver and associated with base-metal sulfides related to hypabyssal intrusions in sedimentary and metamorphic terranes. Volcanogenic manganese deposits include lenses and stratiform bodies of manganese oxide, carbonate, and silicate in volcanic-sedimentary sequences. Epithermal quartz-alunite gold deposits occur in island-arc and back-arc spreading centers and within vuggy veins and breccias in zones of high-alumina alteration. Copper- and zinc-bearing Kuroko massive-sulfide deposits occur in marine volcanic rocks of intermediate to felsic composition. Placer gold-PGE (platinum-group-element) deposits include detrital elemental gold and PGE alloys in grains in gravel, sand, silt, clay, and their consolidated equivalents.

Development of CD-ROM technology enhances the use, distribution, and availability of layers of digital data to all segments of the earth-science community. The USGS has been an innovator in the application of this rapidly expanding technology to earth-science-related activities. In studies of Puerto Rico, the interactive layering and manipulation of these digital layers have produced new insights and relationships, capable of being observed and interpreted readily on a computer screen.

HEAVY-METAL CONTENTS OF SEDIMENT FROM THE KUSKOKWIM RIVER, BETHEL, ALASKA— A BASELINE STUDY*

Harvey E. Belkin and Harold M. Sparck

The Kuskokwim River, at Bethel, Alaska, drains a major mercury-antimony metallogenic province in its upper reaches and tributaries. Gray and others (1991) and Nelson and others (1977) have reported anomalously high heavy-metal values (up to ≈1,800 ppm) for stream sediments in the river above Bethel that are invariably associated with

*Not presented at Forum.

7

Table 1 (Bawiec and Ambroziak). Estimates of undiscovered mineral deposits at specified probability levels, for Puerto Rico.

[MARK3 Input]

Model	Known mineral deposits	Known occurrences	Probability .90	.50	.10	.05	.01	Level of prospecting
Porphyry Cu	2	8	--	--	--	--	--	--
Copper skarn	2	10	1	4	8	--	--	Low.
Fe skarn	1	16	0	0	1	2	3	Mod/High.
Porphyry Cu-Au	5	2	2	3	5	8	10	High?
Polymetallic veins	2	59	1	4	15	--	--	Moderate.
Volcanogenic manganese	3	11	1	3	8	--	--	Moderate.
Epithermal qtz-alu Au (low grade)	2	3	1	2	4	--	--	Low.
Kuroko massive sulfide	0	0	0	0	1	--	--	Very low.
Placer Au-PGE	Ancient placer sites	3	0	0	--	--	1	Very high.

mercury-mineralized lode deposits. However, downstream from these lode deposits, approximately 10–25 km, they described a decrease of the heavy-metal content in the sediments to essentially background levels. This decrease is mainly due to dilution with relatively clean bed, bank, and hillslope material.

Bethel (population 4,000) is situated on the Kuskokwim River floodplain and draws its water supply from wells located in river-deposited sediment. These sediments may be secondary sources of containants to ground-water quality. These potential contaminants are not necessarily fixed as inorganic particulates but may be mobilized via biological and chemical processes within the sediment column and ground water, although biological processes may be minimal in this high-latitude environment. The Bethel area, typical of arctic tundra environments, is underlain by permafrost, and the ground is frozen for extended periods of time. Nevertheless, examining samples of the Kuskokwim River sediment is important in order to establish a baseline datum for heavy-metal concentration.

A boring on the riverbank down to and into permafrost (≈ 8 m) provided 11 samples that we analyzed for mercury, arsenic, antimony, and selenium. These elements are present in anomalously high concentrations in the upstream deposits (Nelson and others, 1977; Gray and others, 1991). All the sediment passed through a 150-μm sieve and was therefore mostly very fine sand and silt; we noted little visible organic matter. Splits of the dried sediment were analyzed as follows: total mercury by cold vapor atomic absorption spectrometry, arsenic and selenium by hydride generation atomic absorption spectrometry, and antimony by graphite furnace atomic absorption spectrometry. Aluminum was analyzed by inductively coupled plasma atomic emission spectrometry and was used as a normalizing factor.

The values of all the elements did not vary systematically with depth and ranged from (all ppm dry weight) [mean, 1 sigma]; Hg=0.08–0.29 [0.16, 0.06], As=2.7–4.2

[3.5, 0.4], Sb=0.53–1.5 [0.87, 0.27], and Se=0.2–0.3 [0.2, 0.0]. Aluminum (ppm×10^4) ranged from 5.91 to 6.27 [6.07, 0.12].

The values determined at Bethel represent the normal products of weathering and show no indication of contamination from mercury-antimony mineralized areas. This study helps to establish a useful baseline datum at Bethel for these elements and will be valuable if mining activities increase upstream.

REFERENCES

Gray, J.E., Goldfarb, R.J., Detra, D.E., and Slaughter, K.E., 1991, Geochemistry and exploration criteria for epithermal cinnabar and stibnite vein deposits in the Kuskokwim river region, southwestern Alaska: Journal of Geochemical Exploration, v. 41, p. 363–386.

Nelson, H., Larsen, B.R., Jenne, E.A., and Sorg, D.H., 1977, Mercury dispersal from lode sources in the Kuskokwim River drainage, Alaska: Science, v. 198(4319), p. 820–824.

RECENT ENVIRONMENTAL AWARENESS IN LATIN AMERICA— THE BOLIVIAN CASE

William P. Blacutt

The Bolivian national legislature recently passed a general environmental law to protect the environment and to promote sustainable development. This law delineates general principles of environmental policy; actual implementation procedures will be specified in future regulations. Much of the controversy surrounding this legislation may disappear when it is seen as a guide rather than an operational part of Bolivia's industrial policy.
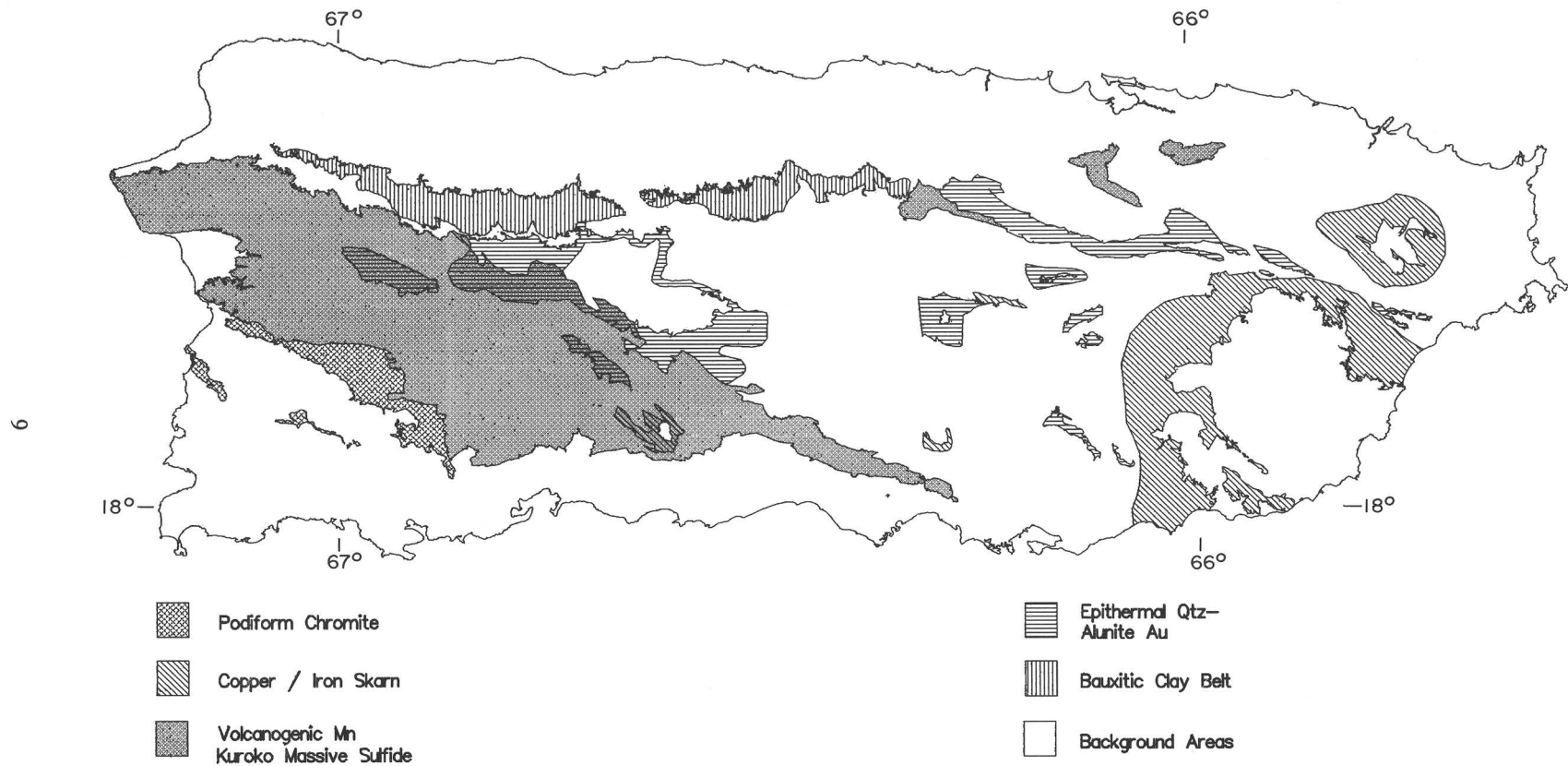
Figure 1 (Bawiec and Ambroziak). Permissive terranes for metallic mineral deposits of Puerto Rico.

Legend:
- Podiform Chromite
- Copper / Iron Skarn
- Volcanogenic Mn Kuroko Massive Sulfide
- Epithermal Qtz–Alunite Au
- Bauxitic Clay Belt
- Background Areas

Placer Au — PGE

Cu — Ag Manto

Porphyry Copper

Background Areas

Possible Gold Placer Areas
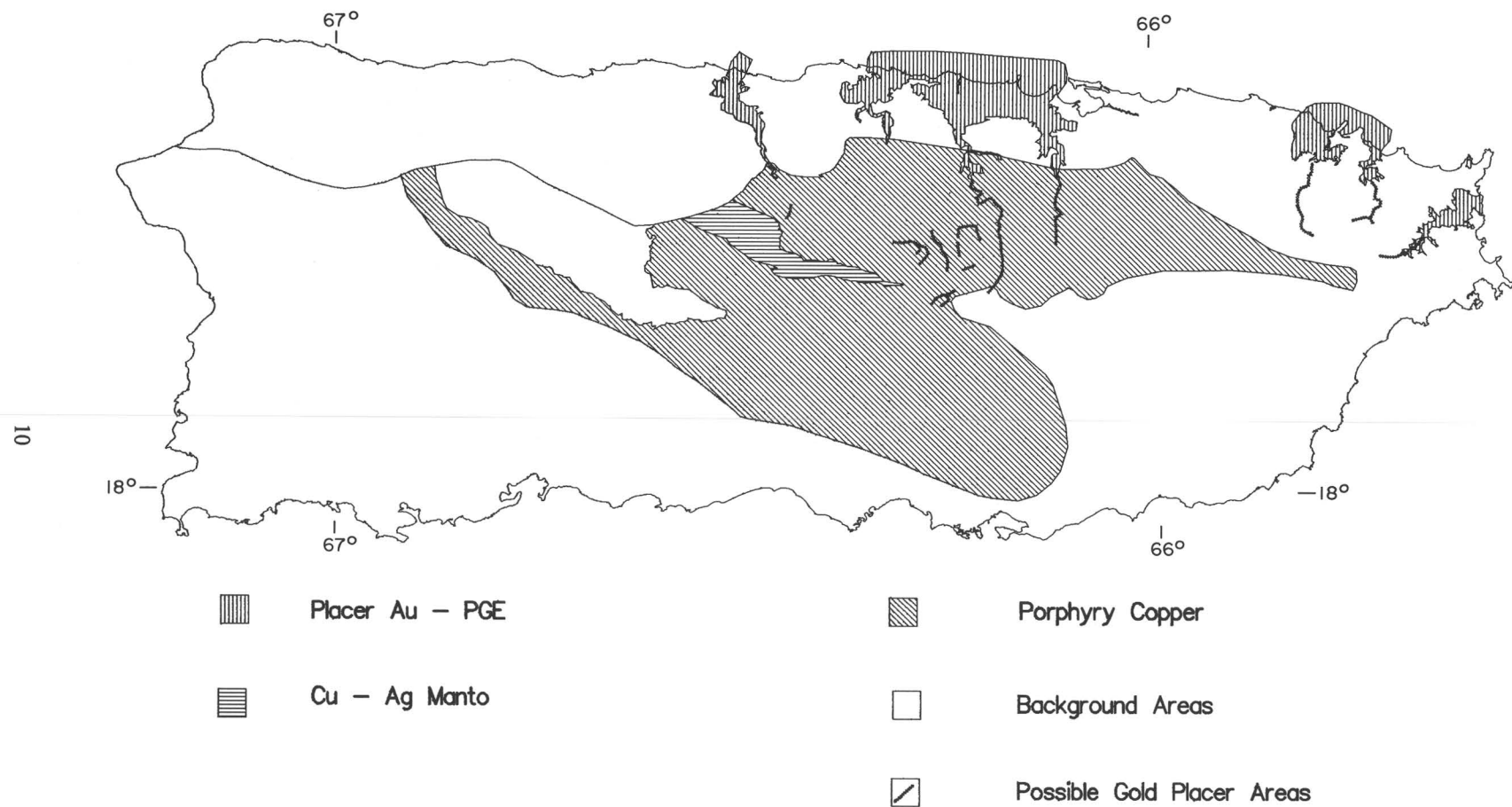
Figure 1 (Bawiec and Ambroziak) (Continued). Permissive terranes for metallic mineral deposits of Puerto Rico.

Bolivia's legislation illustrates the recent jump from practically nonexistent environmental awareness to an all-encompassing framework for rules and regulations. The law is in this respect an "encyclical" or "bill of rights" announcing that the society and the State are now ready to "guarantee everyone the right *** to enjoy a healthy and pleasant environment in the development and performance of all their activities." How this is done is left to subsequent regulations. The unfinished regulatory work can raise risk and apprehension for potential investors. For example, economic evaluation of the development of a hypothetical 500 t (metric ton)/day underground zinc mining and milling operation, located in the Bolivian Altiplano, indicates that excessive environmental regulation would render the project unprofitable at current commodity market prices.

Missing in much of the risk assessment is an appreciation for the compromises implied in Bolivia's multiple objective planning procedures. Trade-offs are to be expected given the nature of environmental and economic costs and benefits. Although major improvements in environmental quality are always possible at moderate implementation costs, efforts to eliminate hazardous waste altogether will founder on exponentially rising costs. Thus, limited economic resources available for environmental quality improvements will tend to limit mitigation costs to levels that will not threaten investment in industrial activities.

Under national and international pressure, all countries will ultimately find themselves compelled to implement adequate environmental standards that will permit and encourage rational resource development. That Bolivia has acted on this issue relatively early on may prove to be advantageous.

DEVELOPMENT OF PREDICTIVE MODELS OF SAND AND GRAVEL DEPOSITS IN THE SOUTHWEST UNITED STATES

James D. Bliss

Modeling of sand and gravel deposits needs to address (1) deposit size and geometry, (2) size distribution of rocks and mineral fragments within the deposit, (3) physical characteristics of the material, and (4) chemical composition and chemical reactivity of the material. Development of models to characterize size and geometry of some deposits was accomplished based on data from California and the United Kingdom (Bliss, 1993). With the exception of sand and gravel deposits in alluvial fans, nearly all significant sand and gravel deposits (for example, a minimum thickness of 1–2 m) can be described by a single volume model, and this model is valid for fluvial, glacial-fluvial, and other kinds of sand and gravel deposits found in California or the United Kingdom. The applicability of this model to the sand and gravel deposits in the Southwest United States has yet to be tested, but it is expected to be appropriate here as well.

Preliminary modeling of size distribution of clasts is currently underway for sand and gravel pits and prospects in New Mexico. The definition of deposits includes all sand and gravel bodies within 1.5 km of each other, but in the case of the 193 New Mexico sites, it is not always clear if "sites" are different deposits, which may bias the study in ways not recognized.

A model for size distribution of clasts in sand and gravel deposits must consider what percent of each deposit consists of sand and gravel. The definition of a *sand and gravel deposit* is that it must contain at least 25 percent gravel by weight (Langer, 1988). Sand and gravel deposits contain not only sand and gravel, but also cobbles and boulders, as well as silt. In practice, those searching for surficial sand and gravel deposits find and describe other types of deposits which fail to meet the 25-percent-gravel criterion. For these, several other subtypes of deposits are identified. Thus six subtypes can be distinguished using clast sizes: (1) sand deposits, (2) sand deposits with gravel, (3) sand deposits with gravel and boulders, (4) sand and gravel deposits, (5) sand and gravel deposits with boulders, and (6) boulder deposits with sand and gravel.

An outline of the standard classification rules (fig. 1) shows how the distributions of these subtypes of deposit (based on percent of clast sizes) for undiscovered sand and gravel deposits for a given population can be predicted. Three models are needed—the distributions of sand, silt, and gravel within deposits (fig. 1, models I, II, III). The values in brackets give the probabilities that a particular classification (fig. 1) occurred in the New Mexico data. In brief, all sand and gravel deposits contain sand and silt. Rarely was the sand subtype (without some gravel-sized clasts) described [p≈0.005], not a surprising result given that sand and gravel deposits were sought. The most common outcome [p≈0.76] was a sand and gravel deposit with boulders. Sand and gravel deposits without boulders [p≈0.11], sand deposits with gravel and boulders [p≈0.063], sand deposits with gravel but no boulders [p≈0.039], and boulder deposits with gravel and sand [p≈0.021] occurred less frequently. If the boulder deposits are suitable for crushing, 89 percent of the New Mexico sites are suitable for extraction of sand- and gravel-sized clasts and 11 percent for sand-sized clasts. These probabilities are not likely applicable to sand and gravel deposits strictly defined or to deposits found elsewhere. The standard classification scheme is sufficiently general in nature that it and the appropriate probability could be used in Monte Carlo simulation to predict the nature of undiscovered sand and gravel deposits anywhere in the world given models I, II, and III (fig. 1).

Figure 1 (Bliss). General outline for classifying subtypes of surficial deposit using clast sizes.

REFERENCES

Bliss, J.D., 1993, Modeling sand and gravel deposits—Initial strategy and preliminary examples: U.S. Geological Survey Open-File Report 93–200, 31 p.

Langer, W., 1988, Natural aggregates of the conterminous United States: U.S. Geological Survey Bulletin 1594, 33 p.

DISTRIBUTION AND MOVEMENT OF METALS DERIVED FROM MINING AND MINERAL PROCESSING IN THE COEUR D'ALENE RIVER VALLEY

Environmental Research Team (contact: Arthur Bookstrom, Stephen Box, Cole Smith, and James Lindsay, Spokane Field Office), USGS Office of Mineral Resources

The Coeur d'Alene River valley has been contaminated by metals from mine tailings flushed downriver during the past 100 years of mining in the Coeur d'Alene mining district. Large portions of the flood plain of the Coeur d'Alene River have been blanketed with tailings-contaminated sediments. Geochemical processes involving the interaction of sediment, surface and ground water, air, and plants modify the contaminants in the flood plain. The hazardous character of these contaminants was recognized as early as 1904, when the first lawsuits were filed by valley landowners against the mine operators.

The Environmental Protection Agency declared 21 square miles of the mining district as a Superfund site in 1986, and numerous Federal and local agencies are interested in evaluating the extent of contamination downstream of the Superfund site. The area is extensively used for farms, residences, recreational activities, and wildlife habitat, so the potential for human and wildlife health risks is significant.

A multidisciplinary USGS team, consisting of geologists, geochemists, and geophysicists in the Office of Mineral Resources, has begun a study of the distribution and movement of mining-derived metals in the valley of the Coeur d'Alene River between the mining district and Coeur d'Alene Lake. Surficial geologic mapping of flood deposits, together with reconnaissance characterization sampling, is being used to design a systematic geochemical sediment sampling program. Concentrations of Pb, Zn, Cd, Cu, Sb and As, as well as the mineral carriers of these elements, are being determined. Natural stream-cut banks and cores are being used to determine lateral thickness variations of the contaminated sediments, mostly limonite-cemented sand and silt. Heavy-metal content of gray clay, which underlies the tailings-contaminated sediments, also is being determined to indicate natural background concentrations of
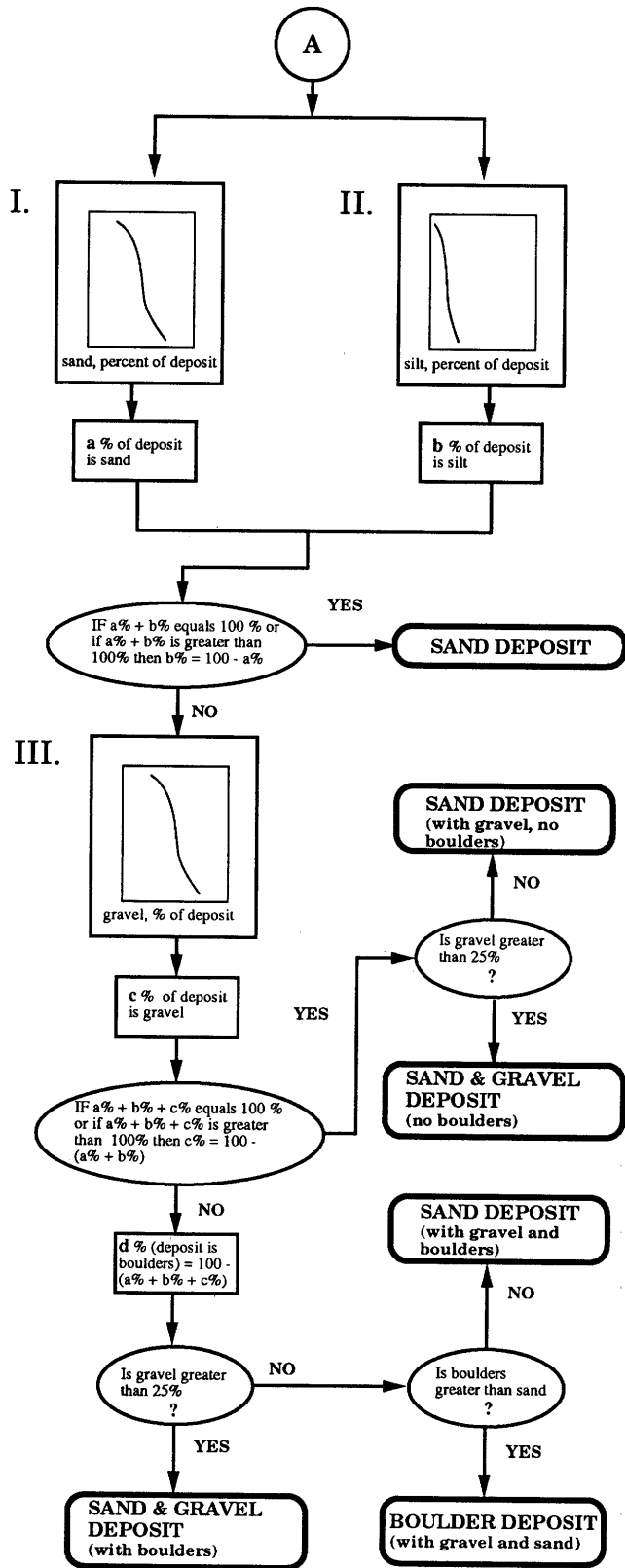
metals in sediments derived by weathering and erosion of the veins and altered rocks of the Coeur D'Alene district.

Multispectral satellite and hyperspectral aircraft images are being analyzed and will be used to map surficial variations in the character of the flood-plain sediments. Geophysical methods will be tested to aid in estimating thickness of the sandy-to-silty tailings-derived sediments, particularly in areas where thickness of contaminated sediment exceeds 1 meter. Geophysical studies combined with studies of pore-water chemistry will help us to understand the chemical mobility of heavy metals in the flood-plain environment. Proposed biogeochemical studies can indicate metal-uptake and fixation by plants. We are coordinating our studies with those of other agencies concerned with bioavailability and health risks of the contaminants to human and wildlife populations. Data will be made available in a geographic information system (GIS) database (Arc/Info). Results will be used to generate recommendations of remedial actions for present problem areas and preventive actions to lessen future problems.

Th/U RATIOS AS A POTENTIAL EXPLORATION TOOL FOR Ag- Or Au-ENRICHED CRUSTAL PROVINCES

Robin M. Bouse, Joseph L. Wooden, Spencer R. Titley, Joaquin Ruiz, and Richard M. Tosdal

Lead isotopic compositions and model Th/U ratios (based upon a 1.7 Ga formation age for Arizona crust) for ores from 50 mineral districts throughout Arizona fall into three groups on a $^{208}Pb/^{204}Pb$ versus $^{206}Pb/^{204}Pb$ diagram that mimic the regional lead-isotopic trends defined by Early Proterozoic whole rocks in the southwestern United States. The Early Proterozoic whole rocks (and the ores) define the crustal provinces: western Arizona and eastern Mojave Th/U>4; central Arizona Th/U≅2; and southeastern Arizona Th/U≅4.

Ore deposits in western Arizona and central Arizona have Ag/Au ratios that predominantly range between 0.5 and 10 and average about 4.5 ($n=120$), whereas ore deposits in southeastern Arizona have Ag/Au ratios that predominantly range between 30 and 300 and average about 90 ($n=116$). Low Ag/Au ratios correspond to crustal provinces with both the highest (western Arizona/eastern Mojave) and lowest (central Arizona) Th/U ratios. Thus, Au enrichment correlates with differential mobility in U and Th.

Silver enrichment and high Ag/Au ratios are found in the southeastern Arizona province, in which Th/U ratios and Th and U concentrations are similar to those of average crust. (Th/U=4 is approximately the crustal average.) This suggests that provinces with Th/U ratios either higher or lower than 4 have a higher potential for relatively gold rich deposits, whereas provinces with Th/U≅4 have a higher potential for relatively silver rich deposits. The hypothesis does not imply that gold- or silver-rich deposits are exclusive to a crustal province but that a predominance of silver-rich deposits will occur in crustal provinces with Th/U≅4 and that gold-rich deposits will predominate in crustal provinces depleted or enriched in Th or U.

For example, the Mojave province (Th/U>4) encompasses western Arizona, southeastern California, and a portion of the Great Basin, and is known to contain many gold-rich deposits. Island arcs also contain many gold-rich deposits and they commonly have Th/U ratios around 2. Southeastern Arizona and western New Mexico (Th/U≅4) have long been known for their silver production. Northern Chile (lat 23°–28° S.) also has Th/U around 4 and contains many silver-rich deposits. The Wyoming province has high Th/U ratios and is a possible gold-enriched province.

These observations strongly suggest that Th/U ratios and Th and U concentrations may be important indicators of Ag- and Au-enriched provinces and they should be considered as a general geochemical/isotopic exploration tool for evaluating crustal province-scale potential.

A SUMMARY OF THE MINERAL RESOURCE ASSESSMENT OF CORONADO NATIONAL FOREST, ARIZONA AND NEW MEXICO

Mark W. Bultman

The area in and around Coronado National Forest, Arizona and New Mexico, has been a major supplier of mineral resources for the Nation: its total metal production is valued at approximately 20 billion dollars. The U.S. Geological Survey was asked to provide a mineral resource assessment of Coronado National Forest, to assist the U.S. Forest Service in complying with regulations requiring them to provide information and interpretations so that the mineral resources can be considered with other types of resources in land-use planning. This presentation is a summary of the results of that assessment.

The procedure used to obtain the mineral resource assessment follows the concept of a mineral deposit model, which is systematically arranged information that describes the essential earth science attributes of a particular group or class of mineral deposits and their accompanying grade and tonnage models. First, all known and potential mineral deposits in the region are identified and classified into a mineral deposit model. Next, regions that are favorable for the occurrence of these mineral deposits are delineated on

mineral resource assessment tract maps. In order to provide land-use planners with the most useful information, the parts of the favorable tracts that have high potential are also delineated where possible. Finally, subjectively based team judgments of the number of deposits likely to occur are integrated with estimates of the likely grades and tonnages of ore deposits as they exist in and around the forest. This last step produces a probabilistic estimate of the number of metric tons of ore and metal that may occur in the forest.

The metallogeny of Coronado National Forest consists of a porphyry copper zone and a gold- and silver-bearing vein zone. Each zone contains mineral deposits unique to that zone in addition to deposits common to both zones. The porphyry copper zone is coincident with a northwest-striking belt of world-class porphyry copper deposits and passes through the portion of the forest southwest of Tucson. The porphyry copper zone is characterized by large, multiphase, and dispersed deposits in which the value of produced copper far outweighs the value of other metals. Besides typical porphyry deposits, the zone contains stockwork deposits, breccia pipes, and large, irregular, composite ore deposits. The gold- and silver-bearing vein zone covers the eastern portion of the forest, extending to the east into New Mexico and to the south into Chihuahua. These small to (rarely) medium sized deposits are mostly vein deposits but do include some small pipes and contact metasomatic deposits.

Lead, zinc, gold, and silver, mostly in polymetallic vein deposits, may be present throughout the forest; the more complex and dispersed types of these deposits are more typical of its southwestern part. Fluorite and manganese are present in small but minable concentrations in the eastern portion of the forest. Minable tungsten deposits are most likely to be present in its southwestern part. Although these generalizations represent an oversimplification of the metallic mineral deposits in the forest, they offer a useful framework for consideration of metallic mineral resource distribution therein.

Initially, delineation of favorable mineral resource tracts was based solely on geologic evidence. The boundaries established were then modified through consideration of extensive geochemical, geophysical, remote sensing, and mineral resource data. The earth science database and the interpreted mineral resource tracts are the major product of the assessment; they will benefit future land-use planning, mineral resource assessment, and mineral resource exploration in and around the forest.

Finally, consensus subjective estimates of the number of undiscovered deposits for each mineral deposit model in each tract were reached by team members. These estimates were combined with estimates of the grades and tonnages of mineral deposits from their respective mineral deposit models. The result is a series of estimates for the contained producible metal in each tract, which are summed to create a combined contained metal estimate for the entire Coronado National Forest. Users of contained metal estimates should realize that these estimates contain large variances and a low level of precision, and incorporate a variety of possible errors.

NEW TECHNIQUES OF GEOPHYSICAL DATA ANALYSIS; AN INVESTIGATION OF THE GEOMETRY, STRUCTURE, AND BEDROCK LITHOLOGY OF THE SAN RAFAEL BASIN, ARIZONA

Mark W. Bultman and Mark E. Gettings

Large undiscovered conventional mineral deposits may be concealed by alluvium in basins in productive terranes. Research on assessment and exploration for such deposits has focused on the acquisition and interpretation of high-spatial-resolution total intensity magnetic field data collected at ground level through a truck-mounted proton precession magnetometer. Previous investigations recognized a strong similarity between these magnetic field profiles and certain profiles of fractal behavior (especially those known as self-affine fractals). These high-quality magnetic field profile data are integrated with more conventional geophysical data and interpreted so that basin structure and geometry can be precisely modelled. Also, the fractal character of these magnetic field profiles is used to assign a textural "fingerprint" to the magnetic field acquired from specific lithologies. These "fingerprints" can be used to help identify the lithology of some concealed magnetic field source rocks.

In order to identify concealed lithologies, we compare magnetic field profile data from exposed candidate lithologies with data from covered areas. It is necessary to account for the attenuation in high spatial frequencies in the component of the data from the concealed lithology due to depth of burial. We have done this by upward continuing data acquired from exposed candidate rocks by an amount equal to the depth of burial of the bedrock whose lithology is unknown. The depth estimates and the upward continuation are iterated until a self-consistent model is achieved. An estimate of the magnetic field due to the cover itself is then added to the continued data. This estimate is generally determined from simulations or by high pass filtering of data acquired over thick basin fill. The field resulting from the sum of the upward-continued field (upward continuation of the exposed candidate lithology) and the estimated field due to cover is then compared with the observed field acquired over the covered area. Comparisons are based on various statistical measures of the data, including the fractal dimension of the profiles. If appropriate, cluster analysis is applied to the data.

An analytic approach to geoscience data integration and visualization is an aid in developing models of basin geometry and structure. Multivariate statistical methods are applied to reduce the dimensionality of the many layers of

geoscience data sets. Image processing tools are used to analyze patterns and textures in an attempt to correlate these data to exposed and subbasinal features. Scientific visualization tools are used to display the resulting three-dimensional model. The product of the investigation is a three-dimensional model incorporating basin geometry, structural geology, and interpretations of concealed lithologies where possible.

We selected the San Rafael basin, Arizona, for the application of these techniques due to its high resource potential, a shallow accumulation of sediment, and proximity to the Coronado National Forest, the subject of a recent mineral resource assessment. The east margin of the basin lies along the Sawmill Canyon fault complex, a northwest-trending system that may control the placement of Laramide intrusive bodies elsewhere along its length. A complex assemblage of volcanic rocks, with some mineral production history, forms the north margin of the basin. The Patagonia Mountains and the Harshaw Creek fault, which form the west margin, define an area with a rich history of ore production. Our investigation shows that many of the structural features and lithologies necessary but not sufficient for ore deposit formation can be found concealed under the San Rafael basin. One large anomaly, 15 km east-southeast of the Red Mountain porphyry copper deposit, can be modelled as a small stock or cupola. This anomaly may be an attractive target.

PALEOMAGNETISM AND MAGNETIC FABRIC OF THE APACHE LEAP TUFF, CENTRAL ARIZONA

Gary J. Calderone, Donald W. Peterson, James E. Faulds, and Robert F. Butler

The 20-Ma Apache Leap Tuff is a zoned ash-flow tuff deposited on a surface of considerable topographic relief over an area of at least 1,000 km^2 near the mining districts of Superior, Miami, and Globe in central Arizona. Analyses of paleomagnetic remanence directions from 353 samples from 39 sites at 16 localities in the Apache Leap Tuff agree with conclusions made earlier, based on geologic evidence, that the tuff is a single cooling unit. The tuff records an essentially instantaneous direction of the Miocene geomagnetic field at D=5.3°, I=40.9° (α_{95}=6.7°, k=31.0, R=15.5164, n=16), which corresponds to a virtual geomagnetic pole (VGP) at lat 79.6° N., long 42.3° E. (A$_{95}$=6.7°, K=31.7, R=15.5273, N=16). Site mean anisotropy of magnetic susceptibility (AMS) typically deviates only a few percent from an isotropic state and varies considerably in the shape of the fabric ellipsoid. AMS ellipsoids range from prolate uniaxial forms to oblate uniaxial forms, and most ellipsoids exhibit either prolate or oblate triaxial forms. The AMS shape parameters do not correlate with stratigraphic zones in the Apache Leap Tuff. Bulk susceptibility, however, decreases

up-section by an order of magnitude from the lower densely welded brown zone to the upper nonwelded white zone, most probably the result of increased deuteric oxidation in the white zone.

At each locality, the mean minimum AMS axis is subvertical whereas the intermediate and maximum AMS axes define a subhorizontal plane of magnetic foliation. The maximum axis defines a magnetic lineation in the plane of the magnetic foliation. Both the magnetic lineation and the magnetic "imbrication" (as defined by the azimuths of the minimum AMS axes) exhibit a crudely radial geographic pattern, although the pattern of magnetic lineations is much better defined. The convergence of these radial patterns, in association with other geologic and geophysical constraints, is consistent with a source in the vicinity of the Haunted Canyon cauldron (about 12 km north of Superior) near the west-central margin of the known exposures of the tuff.

REGIONAL GEOCHEMICAL STUDIES IN THE KAIBAB NATIONAL FOREST, ARIZONA

M.A. Chaffee, R.R. Carlson, and P.M. Theodorakos

The Kaibab National Forest, northern Arizona, consists of three separate areas—the North Kaibab area, located north of the Grand Canyon; the Tusayan area, located just south of the Grand Canyon; and the Chalendar area, located farther south near the Mogollon Rim. The regional geology of the three areas is relatively simple and consists of a sequence of generally flat lying Paleozoic sedimentary rocks that are locally folded and (or) faulted and locally covered by volcanic rocks. In the North Kaibab area, most outcrops are of the carbonate-dominant Lower Permian Kaibab Formation. Outcrops in the Tusayan area mostly include the Kaibab Formation and Tertiary and Quaternary volcanic flows, tuffs, and cinder deposits. Rocks in the Chalendar area consist predominantly of Tertiary and Quaternary volcanic flows. The region is semiarid, and the forest contains no perennial streams.

The major known mineral resources of the Kaibab National Forest are in breccia pipes, formed in collapse structures in Paleozoic sedimentary rocks in and near the Tusayan area and just west of the North Kaibab area. Hundreds of pipes have been identified; many of these pipes are mineralized and some contain economic deposits of copper and (or) uranium. Associated elements commonly include Ag, As, Bi, Cd, Co, Fe, Mo, Ni, Pb, S, Sb, V, and Zn.

For our investigations, 478 samples of bulk sediment were collected rom dry first- and second-order stream channels in the forest. The samples included organic-rich to clean mixtures of sand, silt, and (or) clay-sized material. In order to create a uniform sample medium, all samples were wet

sieved and two fractions (0.5 to 2 mm and <0.25 mm) were saved. Samples from both fractions were analyzed for 39 elements (Ag, Al, As, Au, Ba, Be, Bi, Ca, Cd, Ce, Co, Cr, Cu, Eu, Fe, Ga, K, La, Li, Mg, Mn, Mo, Na, Nb, Nd, Ni, P, Pb, Sb, Sc, Sn, Sr, Th, Ti, U, V, Y, Yb, and Zn). The analyses of the coarser fraction were found to be the most useful because more analytical results of the mineral deposit-related elements were in the range of determination.

On a regional scale, the areal extents of the different major lithologies can be delineated on the basis of their chemistry. Of the 39 elements determined, Ba, Ce, Cr, La, and Na are particularly good lithologic discriminators. The regional chemical changes within a single formation can also be seen. In the North Kaibab and Tusayan areas, Ca and Mg show a distinct regional zoning within the areas containing the Kaibab Formation, with low concentrations in the topographically higher core areas and higher concentrations in the lower perimeters. This zoning may be related to differences in annual precipitation at different elevations. This variation can affect the rate at which these two elements are leached from the relatively soluble material forming the stream alluvium.

Of the ore-related elements listed, three (As, Mo, and Sb) were derived solely from mineralized breccia pipe deposits and showed the best spatial correlation with known mineralization. In the Chalendar area, with limited exposure of Paleozoic sedimentary rocks, no significant geochemical anomalies were found that could be related to Cu/U-rich breccia pipe mineralization. The North Kaibab area contains hundreds of sinkholes; however, none has yet been found to form a breccia pipe at depth or to be mineralized. Mineralized pipes are known only to the west of this part of the forest. In the Tusayan area, widespread, significant anomalies for many ore-related elements extend well beyond the areas of known deposits, suggesting that additional mineralized breccia pipes may be present in that part of the forest.

USE OF LEAD ISOTOPES TO FINGERPRINT SOURCES OF HEAVY-METAL CONTAMINATION IN THE ENVIRONMENT

S.E. Church

The isotopic composition of lead in rocks varies as a direct result of the decay of uranium and thorium. During the formation of ore deposits, lead is isolated from its parent isotopes, uranium and thorium, and has a specific lead-isotopic composition of limited range that is preserved at the time of ore formation. In many ore deposits, lead is a major constituent, and is present in either galena or some other lead-bearing phase. Thus, many ore deposits, especially those associated with magmatic hydrothermal systems, have a

characteristic lead-isotopic composition. As a consequence, ore deposits can be "fingerprinted" by their lead-isotopic signatures.

Weathering of hydrothermal deposits containing sulfide minerals results in the oxidation of sulfide minerals. In the oxygenated surface waters of streams, secondary iron and manganese oxides form as a result of this weathering process. Metals released are sorbed by the iron and manganese oxides that coat sand grains in the stream. By analyzing the lead-isotopic variation in the $HCl-H_2O_2$ extractable fraction in stream sediments, we can maximize the signal caused by the weathering of sulfide minerals in the ore deposits exposed in a drainage basin. This lead-isotope signature and the concomitant trace-metal signature of individual deposits can then be traced into larger drainage basins and the effect of the heavy metals from a specific source can be traced downstream. This procedure has application in the study of environmental consequences of mining and industrial activity on the geochemical landscape.

This lead-isotopic tracer technique has been used to distinguish between the base-metal veins that surround the Mount Emmons, Colo., porphyry molybdenum deposit and the deposit itself. The base-metal veins have variable lead-isotopic compositions ($^{206}Pb/^{204}Pb$ generally >17.9 and $^{208}Pb/^{204}Pb$ generally >38.1) that differ from that of the porphyry molybdenum deposit ($^{206}Pb/^{204}Pb$=17.3–17.5 and $^{208}Pb/^{204}Pb$=37.9–38.1). Furthermore, the Pb-isotopic signatures of both deposit types differ greatly from that of the surrounding country rock ($^{206}Pb/^{204}Pb$ generally >19.0 and $^{208}Pb/^{204}Pb$ generally >38.8). Isotopic studies of the composition of lead sorbed by the iron and manganese oxide coatings on pebbles from the streams showed that the lead-isotopic composition in the leaches from the pebbles varies over short lateral distances. This indicates rapid sorption of lead from the stream by iron and manganese oxide coatings and validates the leaching procedure as a valuable tool in environmental geochemistry.

Application of the method in the upper Arkansas River drainage basin, Colorado, has demonstrated that lead from tributaries to the river above Leadville, Colo., has a variable, but radiogenic lead-isotopic signature ($^{206}Pb/^{204}Pb$ generally >18.4 and $^{208}Pb/^{204}Pb$ generally >38.6), indicating a crustal rock source. In contrast, the high concentrations of lead from the ores from Leadville totally overwhelm the lead occurring in the sediments. Stream-sediment samples from all the drainages within the Leadville mining district, as well as the samples from the Arkansas River collected immediately below the town of Leadville, contain substantial amounts of lead and other base metals, and have the lead-isotopic "fingerprint" of the ores from the Leadville mining district ($^{206}Pb/^{204}Pb$ from 17.95 to 18.25 and $^{208}Pb/^{204}Pb$ from 38.4 to 38.6). Cores taken in the Arkansas River below Leadville show that the baseline concentrations for heavy metals prior to mining were similar to those in the upper Arkansas River basin above Leadville. These data

demonstrate that mining, rather than natural processes, has resulted in the present distribution of heavy metals in the Arkansas River at Leadville, Colo.

GEOCHEMICAL MAPS OF ARIZONA AND THE GREAT BASIN

S.E. Church and G.L. Raines

Stream-sediment geochemical data for the elements Cu, Mo, Pb, Zn, As, Sb, Ag, and Au have been used to produce a series of maps for Arizona and the Great Basin. The data were collected during the NURE and various USGS regional sampling programs over the last 30 years. Evaluation of the quality of the data from the four different NURE laboratories and the USGS laboratories has been made in terms of the detection limit (DL) and the analytical resolution (AR) of the analytical methods used. When element concentrations are expressed in terms of the crustal abundance (CA) of the element, that is in clarke units, useful regional geochemical maps can be made. Copper is the only element that has been satisfactorily determined by all methods used in these laboratories over this time period; nevertheless, useful data showing the character of the geochemical landscape can be derived from the data of lower quality.

Approximately 50,000 stream-sediment samples from these two regions were collected at variable sampling densities appropriate for sampling programs at map scales ranging from 1:500,000 to 1:50,000. In the present study, several approaches have been used to effectively evaluate geochemical variations resulting from variable sampling densities, analytical noise, interlaboratory variability, and analytical resolution. To reduce the effect of individual samples and variable sample densities on the geochemical data base for Arizona, the data were gridded into 25 km^2 cells and the highest value in the cell was assigned to the cell. This procedure resulted in about 7,500 cells for the map of Arizona. Analytical resolution of the gridded data is sufficient to assign five concentration intervals for several elements, based on the clarke values, to make individual geochemical maps: DL to $\frac{2}{3}$×CA, $\frac{2}{3}$ to 1$\frac{1}{2}$×CA, 1$\frac{1}{2}$ to 2$\frac{1}{2}$×CA, 2$\frac{1}{2}$ to 4×CA, and >4×CA. Experiments with more than five intervals resulted in maps that displayed various types of noise and were difficult to interpret.

Comparison of composite geochemical maps with distribution of ore deposits and districts shows a good correspondence with known base-metal districts. The correlation of the precious metals, As, and Sb with epithermal metal districts is severely limited by the analytical quality, detection limits, and analytical gaps in the geochemical data base. The geochemical distribution of Au, determined during the NURE program, appears to be random. We conclude that, in general, these data are useful to define regional geochemical baselines and to outline areas of elevated metal concentrations for a number of metals where analyses are complete. These geochemical maps are a valuable resource for land-use planning, mineral resource assessment, and environmental geochemical evaluations. Significant and cost-effective improvements in data quality could be achieved by reanalysis of samples collected during these previous studies.

MAPPING MINERALS WITH IMAGING SPECTROSCOPY—EXAMPLES ILLUSTRATING THE BEGINNING OF A NEW MAPPING ERA

Roger N. Clark and Gregg A. Swayze

Imaging spectroscopy is a new mapping tool and the next generation in remote sensing technology. The narrow spectral channels of an imaging spectrometer form a continuous reflectance spectrum of the Earth's surface, contrasting with the 4–7 channels of the previous generation of imaging instruments such as the MSS (Landsat Multispectral Scanner) and TM (Thematic Mapper) instruments. Systems like Landsat can distinguish general brightness and slope differences in the reflectance spectra of the surface; imaging spectroscopy not only does that, but also resolves absorption bands in the spectrum that can be used to identify specific materials. Spectroscopic analysis of imaging spectroscopy data allows any material (mineral, vegetation, man-made, water, snow) to be mapped if it has unique absorption features in the measured spectral region.

Imaging spectrometers have improved remarkably over the last 3 years. The NASA AVIRIS (Advanced Visual and Infra-Red Imaging Spectrometer) instrument is now producing excellent data with a signal:noise ratio in the hundreds. AVIRIS acquires data in the spectral range from 0.4 to 2.45 μm in 224 spectral channels. The instrument is flown in an ER-2 aircraft (a modified U-2 reconnaissance plane) at 19,800 m (65,000 ft). The ground resolution is 20 m, the swath width about 11 km (614 pixels), and the flightline length as much as 1,000 km.

Spectral analysis algorithms have matured to the point that identification and discrimination of even similar minerals are possible, producing astonishingly detailed maps. For example, not only can clays be mapped, but also specific identification of alteration minerals (such as kaolinite, montmorillonite, or muscovite) can be achieved. The relative crystallinity of clays can be determined spectroscopically (for example, kaolinite, dickite, and halloysite can be distinguished from each other). Iron-bearing minerals are another class of minerals that can be spectrally distinguished. For instance, hematite, goethite, jarosite, chlorite, and nontronite have been identified at Cuprite, Nev., with AVIRIS data. In addition, AVIRIS data may allow us to differentiate

pyroxenes, amphiboles, and olivines at Barstow, Calif. In the case of sulfates, like alunite, the solid solution series (from sodium to potassium) has been spectrally identified showing chemical zonation in a hydrothermal alteration zone. Swayze and others (work in progress) have also found that the spectra of alunites appear different depending on their hydrothermal formation temperature. Thus paleotemperature mapping is possible and is being applied to decipher tectonic movements in the Basin and Range province.

Many rocks are composed of mineral assemblages which are spectrally detectable (for example, clays, carbonates, micas, evaporites, and fe-hydroxides) over the spectral range of the AVIRIS instrument. We have found that simple combinations of these minerals in proper proportions serve to uniquely identify rock types. Experimental mapping in Arches and Canyonlands National Parks in Utah, using AVIRIS data, shows that we can produce spectrolithologic maps that correspond remarkably well with geologic maps. In fact, these spectrolithologic maps show mineralogical changes so subtle (normally undetectable by human eye or in airphotos) that we have subdivided previously undivided formations. We believe that this capability has direct applications for sedimentary provenance studies.

Imaging spectroscopy can also address global change and environmental problems. For example, the continuous spectral coverage and fine spatial resolution of the AVIRIS instrument make it unique among remote sensing instruments, in determining accurate albedos of earth materials. Albedo information is of critical importance to Global Circulation Models. Snow and ice grain sizes have been remotely mapped in the Sierra Nevada of California using AVIRIS data. Vegetation communities have also been mapped, even in low vegetation cover terrains such as those in the Colorado Plateau. We also believe that imaging spectroscopy analysis has great potential for mapping surface contamination in areas experiencing environmental problems.

PRECAMBRIAN MASSIVE SULFIDE DEPOSITS IN AMPHIBOLITE- AND GRANULITE-FACIES ROCKS, WESTERN ARIZONA AND SOUTHEASTERN CALIFORNIA

Clay M. Conway

Volcanogenic massive sulfide deposits have long been known in amphibolite-grade metamorphic rocks in the Early Proterozoic volcanic belts at Bagdad and at Boriana Canyon (Hualapai Mountains) in western Arizona. However, the metamorphic character of these deposits and especially of associated footwall alteration zones has not been appreciated. In particular, recent recognition of metamorphosed altered rocks at Bagdad has shown the altered zones to be far more extensive than previously thought and thus to indicate new exploration potential in the Bagdad volcanic belt. Additionally, reconnaissance mapping in western Arizona has revealed similar metamorphosed alteration zones in new localities (for example, northern Hualapai Mountains, Grand Wash cliffs, lower Grand Canyon), suggesting further exploration potential.

Detailed work by the USGS at Bagdad indicates at least four alteration types in the silicic to mafic volcanic rocks that host the massive sulfide deposits: albitized, epidotized, silicified, and chloritized rocks. Of these, the chloritized rocks are easiest to recognize and are most proximate to the massive sulfide deposits. They form "chlorite pipes" immediately subjacent to the massive sulfide deposits. Chloritized rocks provide an excellent regional exploration tool. The chloritized areas at Bagdad have a distinctive yellow tinge on infrared aerial photographs.

Chloritized rocks at Bagdad and elsewhere in amphibolite-facies rocks in western Arizona exist primarily as a chlorite-garnet-magnetite assemblage or a higher grade assemblage containing orthoamphibole (anthophyllite)+ cordierite±garnet. Cordierite-anthophyllite rocks have long been recognized in Canada and elsewhere as metamorphosed chlorite pipes in association with massive sulfide deposits; however, this association has sometimes been overlooked in the southwestern United States. Some cordierite-anthophyllite exposures at Bagdad were previously mapped as gabbro.

Preliminary work in the Turtle Mountains, eastern Mojave Desert, southeastern California, suggests that Cu-Zn deposits in the Horn Spring area are volcanogenic massive sulfide deposits metamorphosed to granulite facies. A regional granulite-facies metamorphism occurred during the Ivanpah orogeny at about 1.7 Ga and may be responsible for the metamorphism of these deposits. Metamorphosed hydrothermally altered rocks associated with gossans contain combinations of chlorite, quartz, orthoamphibole, garnet, phlogopite, spinel (pleonaste?), and cordierite(?). These magnesian metamorphic rocks occur as layers and pods immediately adjacent to the gossan layers, suggesting the familiar deposit-footwall relationship of massive sulfide deposits. This is apparently the first documentation of massive sulfide deposits in the high-grade metamorphic terrane of southeastern California. However, reports do exist of pods (or thin layers) of orthoamphibole-cordierite in the Old Woman Mountains, gedrite schist in the Halloran Hills, and chlorite-talc or orthoamphibole-cordierite in the eastern Transverse Ranges. These magnesian assemblages hint at volcanogenic metasomatism and thus invite exploration for massive sulfide deposits in the Mojave Desert country.

THE NATIONAL ASSESSMENT OF UNDISCOVERED DEPOSITS OF COPPER, ZINC, LEAD, SILVER, AND GOLD— A PROGRESS REPORT

Dennis P. Cox, Joseph A. Briskey, Jr., Sandra H.D. Clark, Michael F. Diggles, Thomas D. Light, Barry C. Moring, and Alan R. Wallace

The mineral resource assessment of the United States, proposed by McCammon and Briskey (1992), focuses on resources in deposits as yet undiscovered (as opposed to those in extensions of known deposits) and is limited to deposits of the five most commonly explored for metals. The goal of the assessment is to decrease the time required to respond to requests for mineral resource information on the public lands, requests that have come with increasingly shorter deadlines and which involve increasingly larger areas, some with uncertain boundaries. The assessment will create a large digital database to be published at a small map-scale (1:2.5–3.5 million), but available also at intermediate scales (1:750,000 to 1:1 million), that will provide mineral information for the whole country.

The assessment follows procedures outlined by Singer (1993): (1) teams of experts on mineral deposits, regional geology, geochemistry, and geophysics delineate tracts permissive for undiscovered deposits of one or more deposit types using known relationships between deposit types and geologic environments; (2) the teams use grade-tonnage models based on worldwide reserve and production data to represent the probable tonnage and metal grades of undiscovered deposits of each type; and (3) the teams estimate the number of undiscovered deposits of each type within the permissive tracts that are consistent with the grade-tonnage models, using a depth range of 1,000 m. These estimates, presented as three or more probability distributions (number of deposits, tonnage, and grade of one or more metals), have been combined by Monte Carlo simulation (Root and others, 1992) to produce probabilistic estimates of tons of undiscovered metal.

The teams, based in Reston, Va., Denver, Colo., Menlo Park, Calif., Anchorage, Alaska, Spokane, Wash., Reno, Nev., and Tucson, Ariz., also have compiled estimates of past production and remaining resources of the five metals in the important known deposits of each type in the regions being assessed. These estimates can be compared conveniently with the tonnages of metals estimated for undiscovered deposits.

At this writing (November 1993) digital tract maps and resource estimates from each region are being reviewed internally, and an external review process is planned.

REFERENCES

McCammon, R.B., and Briskey, J.A., Jr., 1992, A proposed national mineral-resource assessment: Nonrenewable Resources, v.1, no. 4, p. 259–266.

Root, D.H., Menzie, W.D., and Scott, W.A., 1992, Computer Monte Carlo simulation in quantitative resource estimation: Nonrenewable Resources, v. 1, no. 2, p. 125–138.

Singer, D.A.,1993, Basic concepts in three-part quantitative assessments of undiscovered mineral resources: Nonrenewable Resources, v. 2, no. 2, p. 69–81.

PORPHYRY COPPER DEPOSITS IN ARIZONA—AN EXAMPLE OF RESOURCE EVALUATION FOR THE U.S. GEOLOGICAL SURVEY'S NATIONAL MINERAL ASSESSMENT OF COPPER, LEAD, ZINC, GOLD, AND SILVER

Leslie J. Cox

Porphyry copper deposits in Arizona contain 53 percent of the copper in all known deposits in the United States as well as significant amounts of lead, zinc, gold, and silver. The U.S. Geological Survey's numerical assessment of the potential for new porphyry copper deposits took the following steps: selection of a grade and tonnage model that describes the probable characteristics of undiscovered deposits, delineation of a tract permissive for porphyry copper deposits, and estimation of the number of undiscovered deposits in the permissive tract.

A general porphyry copper deposit model was used to guide the delineation of tracts permissive for the occurrence of this deposit type and related porphyry Cu-Au, porphyry Cu-Mo, and porphyry Cu skarn-related deposits. This model was based on deposits worldwide and incorporates the known characteristics of the geologic and tectonic setting, rock type and ages, ore (including grades and tonnages), alteration, association with other deposit types, and geochemical and geophysical expression. Permissive tracts were defined as the areas remaining after exclusion of terrains where expecting a deposit of the type in question to be present is unreasonable, based on our present understanding of the characteristics of this deposit type and the geology of Arizona. Tracts permissive for the occurrence of porphyry copper deposits were drawn for Arizona at the scale of 1:1,000,000 (fig. 1).

Estimates of the number of undiscovered porphyry copper deposits in Arizona were obtained by the following process: the geologist who led a team of scientists in the tract delineation made a short presentation about the permissive tract and the favorable features contained within it. Additional information was offered by the regional geologic

114°   111°

36°

ARIZONA

IV

○ Flagstaff

III

II

V

Phoenix ○

33°

I

0   50 KILOMETERS

EXPLANATION

● Porphyry copper deposits that contain at least 50,000
   metric tons of copper metal, pre-production

— Boundary separating geologic basement-defined
   terranes (I-V) of Titley and Anthony (1989, p. 489)

- - - - - Boundary separating Terrane I into east and west sections

▨ Tract permissive for the occurrence of porphyry copper deposits

Figure 1 (L. Cox).   Tracts permissive for the occurrence of porphyry copper deposits in Arizona.

experts, the team geochemist, and the team geophysicist. This presentation was followed by group discussion of the data, analog areas, perceived history of exploration, the appropriateness to Arizona of the deposit model and the associated grade and tonnage distributions, and the ratio of the area covered by 0–1-km-thick strata of Eocene and younger age to the area covered by exposed pre-Eocene rocks.

We then decided to make separate probability estimates for each of five geologic terranes (fig. 1) rather than for the State as a whole. Terrane I was divided into east and west sections (fig. 1), based on the differences in the amounts of Eocene and younger cover (not shown in fig. 1). The estimation method stipulates that the distribution of the deposits estimated in each area considered must have the same distribution of tonnages and grades as the worldwide porphyry copper model. The initial, individually made assessments were followed by discussion of geologic and informational issues identified by each assessor as most sensitive to his or her estimate. A second assessment was made and the scores compiled. A consensus score, close to the mode, was attached to each probability distribution.

REFERENCE

Titley, S.R., and Anthony, E.Y., 1989, Laramide mineral deposits in Arizona, in Jenney, J.P., and Reynolds, S.J., eds., Geologic evolution of Arizona: Tucson, Ariz., Arizona Geological Society Digest, v. 17, p. 485–514.

SPECTRAL PROPERTIES OF SELECTED INDUSTRIAL MINERALS AND ORES— POTENTIAL FOR REMOTE SENSING DETECTION AND EXPLORATION*

James K. Crowley

Visible and near-infrared (0.4–2.5 μm; VNIR) reflectance spectra and thermal infrared (8.0–13.5 μm; TIR) emission spectra were measured for 19 industrial minerals and ores to evaluate prospects for mineral detection with spectroscopic remote sensing data. The minerals and ores selected for study (table 1) occur in surficial exposures and have moderately high intrinsic value, making them potentially viable targets for remote sensing exploration programs. High-purity quartz sand and calcitic carbonate rock samples were also examined, because remote sensing exploration for these less valuable commodities might be practical in some situations. The study is not comprehensive, as a number of industrial minerals and ores are not included, and minerals

represented here by only one or two samples may exhibit considerable spectral variation.

The laboratory spectra show that many industrial minerals and ores exhibit VNIR and (or) TIR spectral features that might be useful for detecting the minerals remotely. The two different wavelength ranges are complementary, in that minerals lacking absorption bands in one part of the spectrum commonly exhibit spectral features in the other. VNIR spectral data may be especially useful for discerning borates, pyrophyllite, talc, and vermiculite (fig. 1), as well as carbonates, diatomite, and gypsum. Spectral discrimination in the VNIR is generally based on the occurrence of narrow, diagnostic, absorption bands attributable to hydroxyl groups and hydrate water molecules, and (or) the borate and carbonate anion groups. Such features can be observed remotely with suitable instruments, such as the NASA Airborne Visible/Infrared Imaging Spectrometer (AVIRIS). Thermal-infrared spectral data may be particularly useful for locating barite, quartz, perlite, phosphorite, and thenardite (fig. 2). TIR remote sensing prospects for the industrial minerals and ores were evaluated by convolving the sample spectra to the six spectral bandpasses of the NASA Thermal Infrared Multispectral Scanner (TIMS). A spectral library of 43 well-characterized igneous and sedimentary rocks was also convolved to the TIMS bandpasses, permitting the rock spectral responses and the industrial mineral spectral responses to be compared. Diagnostic TIR spectral features are produced by vibration modes of the borate, phosphate, silicate, and sulfate molecular groups. Some important industrial minerals, such as zeolites, may not be amenable to remote sensing detection because of near-infrared absorption interference by atmospheric water vapor and the minerals' occurrence in fine-grained samples that have low TIR spectral contrast. In practice, the remote sensing detection of industrial minerals is also likely to be affected by soil, rock, and vegetation mixtures, as well as by weathering processes that may degrade the spectral signatures.

Table 1 (Crowley). Industrial minerals and ores examined in this study.

Barite (2)	Phillipsite
Calcite	Phosphorite
Colemanite	Pyrophyllite
Diatomite	Quartz sand
Erionite	Talc
Graphite schist	Thenardite
Gypsum	Ulexite
Kimberlite	Vermiculite
Perlite (2)	

*Not presented at Forum.
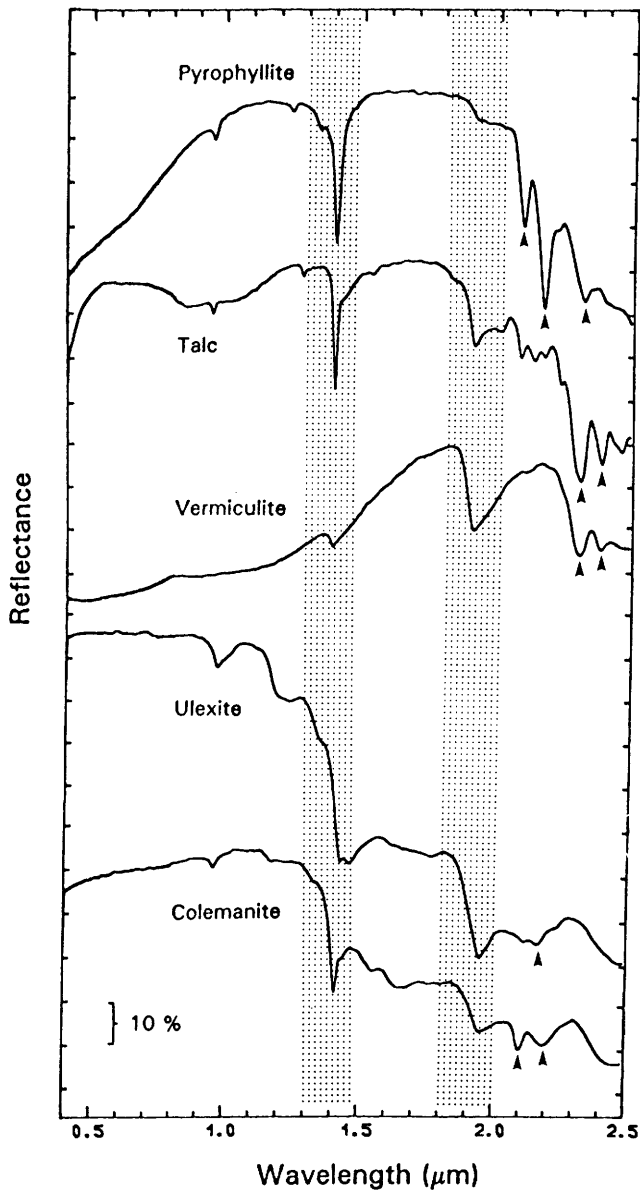
Figure 1 (Crowley). Visible and near-infrared reflectance spectra of selected industrial minerals. Spectra are offset vertically for viewing purposes. Arrowheads, positions of diagnostic VNIR absorption features. Dot pattern, wavelength region obscured by atmospheric water-vapor absorption. Tickmarks on vertical axis show reflectance intervals of 10 percent.
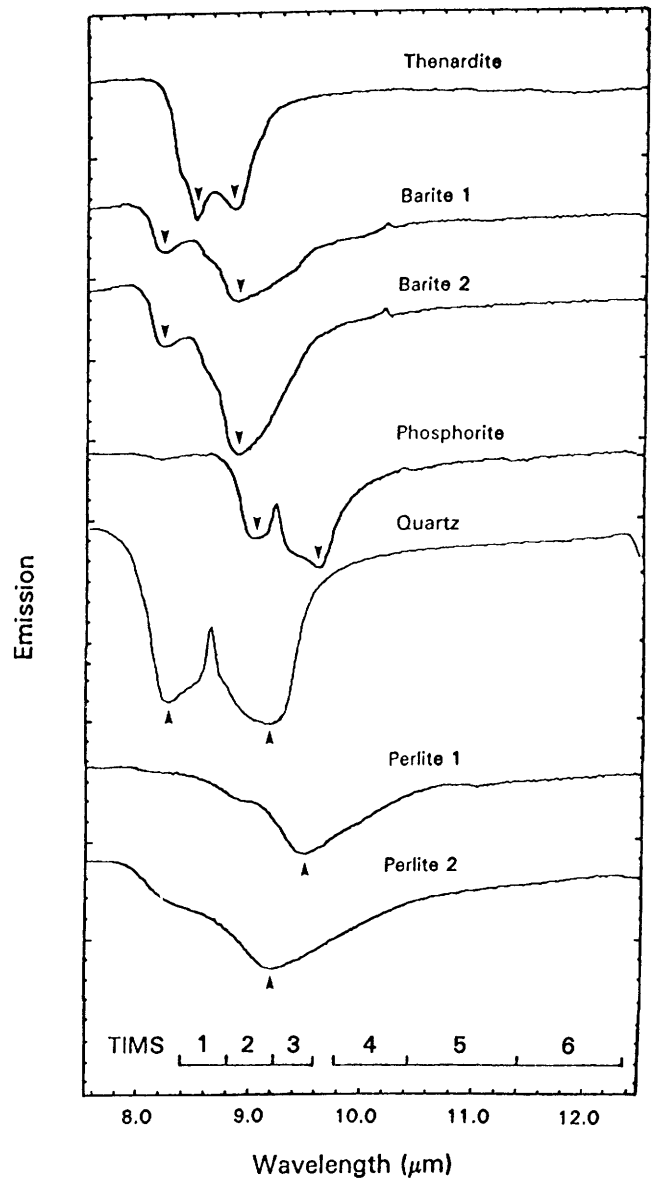
Figure 2 (Crowley). Thermal emission spectra of selected industrial minerals and ores. Spectra are offset vertically for viewing purposes, and TIMS scanner bandpasses are shown on the lower part of the figure. Arrowheads, positions of diagnostic emission features. Tickmarks on vertical axis indicate emission intervals of 5 percent.

HOT-SPRING TEXTURES IN EPITHERMAL ENVIRONMENTS

Charles G. Cunningham, Robert O. Fournier, Peter G. Vikre, and James J. Rytuba

Hot-spring systems are the modern analogs of many Tertiary precious-metal-bearing epithermal systems.

Several distinctive textural features in modern hot springs are commonly also preserved in fossil systems, and they can help to differentiate sinter from similar-appearing silicified sediments and airfall tuff. These textural features include mud cracks, bubble tubes, geyserite, terraces, filamentous and conophyton bacteria, and reeds. Where textures are absent to definitively identify sinter from silicified sediments or tuff, a very low Al_2O_3 content and lack of TiO_2 and ZrO_2 can be diagnostic of sinter.
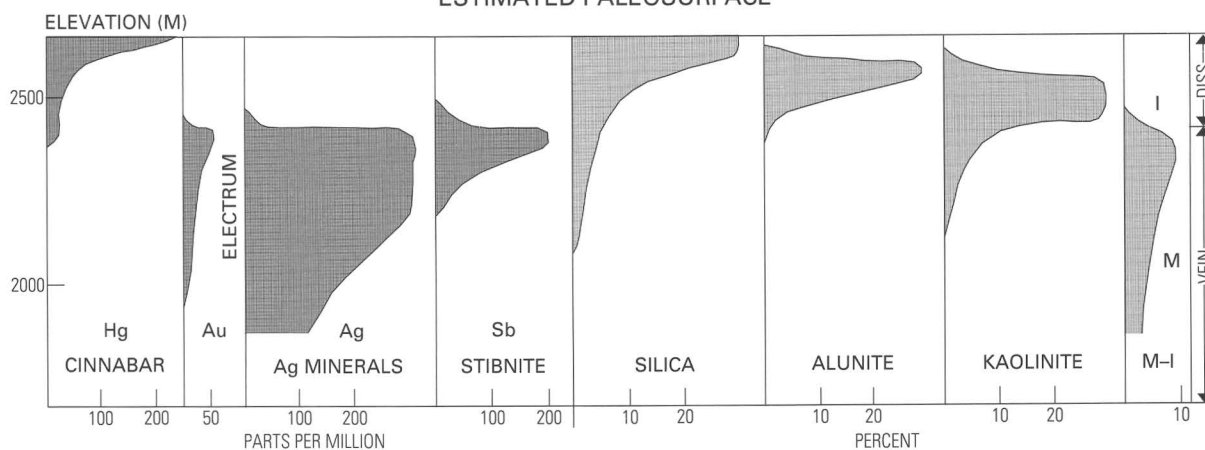
Figure 1 (Cunningham and others).   Abundance of vertically zoned hydrothermal phases and components in the Buckskin Mountain precious-metal deposit. M, muscovite; I, illite. Modified from Vikre (1985).

Hydrothermal explosion features are also near-surface manifestations of epithermal systems. These features include breccia aprons, craters, and hot-spring pools as indicated by fossil conophyton bacteria, and fossil filamentous bacteria marking the outflow of the pools. Hydrothermal breccias often mark the location of the upflowing part of a hydrothermal system, where pressure and temperature changes are greatest, and where precious-metal deposits tend to form.

Hot-spring systems have distinctive physical, chemical, and mineralogical vertical variations that reflect the results of active processes and the consequent thermochemical environments. The Miocene Esperanza silver-gold deposit in the Maricunga district of Chile is one of the best documented examples of hot springs superimposed on acid-sulfate deposits in the Andes. The deposit formed in a dacitic volcanic dome environment, and much of the known precious-metal mineralization was contained within vuggy silica formed by volcanic degassing and acid-sulfate alteration. The deposit, however, contains many hot-spring features preserved at the paleoground surface in the extremely arid environment of this part of the Andes. The tops of some hydrothermal systems, at the paleoground surface, are marked by explosion craters with rims of ejecta. Breccia fragments in these rims include fragments of vuggy silica that are indicators of the acid-sulfate alteration processes that occurred at depth; this vuggy silica marks the zones of higher permeability that localized later mineralizing fluids. Some of the outflow channels of the former pools in explosion craters contain fossil filamentous bacteria.

Well-documented examples of fossil hot-spring systems in which most of the upper part is preserved and the subsurface is exposed by mining and drilling exist throughout the world. Vertical variations in minerals and selected elements at the Buckskin, Nev., precious-metal deposit are illustrated in figure 1. The distribution of silica, as sinter with

interbedded hydrothermal explosion breccias, at the paleoground surface, results from the large temperature gradient near the ground surface. Mercury is commonly concentrated in the sinter because it can travel through the lower part of the system as a vapor and is condensed at the ground surface. The zonation of alunite immediately beneath the silica, and kaolinite mostly beneath the alunite, reflects the interaction of the hydrothermal system with atmospheric oxygen, the oxidation of hydrogen sulfide at a fluctuating water table, and the resulting distribution of temperature, pH, and sulfate activity. The distribution of precious metals reflects the changes in gold and silver solubility as the upwelling near-neutral-pH alkali-chloride fluids encounter the low-pH, oxygenated environment near the ground surface.

REFERENCE

Vikre, P.G., 1985, Precious metal vein systems in the National District, Humboldt County, Nevada: Economic Geology, v. 80, p. 360–393.

TIMING AND ORIGIN OF
ORE DEPOSITION AT THE
CERRO RICO DE POTOSI Ag-Sn AND
PORCO Ag-Zn-Pb-Sn DEPOSITS, BOLIVIA

C.G. Cunningham, R.E. Zartman, E.H. McKee,
R.O. Rye, C.W. Naeser, and G.E. Ericksen

Cerro Rico de Potosi is the world's largest silver deposit, having produced an estimated 30,000 to 60,000 t (metric tons) of fine silver from high-grade Ag and Ag-Sn

Mining zinc and silver, Porco, Bolivia.

veins that cut a dacitic volcanic dome. Recent dating by a variety of isotopic techniques indicates that the deposit is large because it was mineralized several times. Interpretation of U-Th-Pb isotope systematics on zircon from the Potosi dacite dome is complicated by the presence of inherited components, but extrapolation to the time of dome extrusion constrains the timing of extrusion of the dome to about 14 Ma. The main episode of alteration and mineralization took place shortly after dome extrusion at 12.4±0.4 Ma. A second alteration-mineralization episode is temporally bracketed by K-Ar age determinations on widespread sericite of 11.1±0.4 Ma and 10.5±0.4 Ma and a fission-track age on zircon of 12.5±1.1 Ma. The mineralization resulted in a core enriched in Sn-W-Bi with a peripheral zone of Pb-Zn-Ag. As the hydrothermal system collapsed, Pb-Zn-Ag minerals were overprinted on the core zone. A third significant episode of mineralization occurred ≈6–8 Ma and is documented by K-Ar ages on sericite (7.3±0.6 Ma) and vein alunite (5.7±0.2 Ma, 6.3±0.1 Ma, 6.4±0.2 Ma, and 8.3±0.5 Ma). The vein alunite was deposited contemporaneously with sulfides; ^{18}O partitioning between SO_4 and OH in the alunite indicates deposition temperatures of 240–290 °C for this event. The δD values (–69 to –74 per mil) of alunite require a magmatic fluid origin for the alunite, and by inference, for the related sulfides. The $\delta^{34}S$ values of coexisting

alunite and pyrite are out of equilibrium and probably indicate rapid ascent of alternating liquid and vapor-phase fluids. This third mineralizing event occurred at about the same time as most of the Los Frailes ash-flow tuffs were erupted from multiple caldera sources northwest of Potosi. This event is part of a regionally extensive 6–9 Ma magmatic, tectonic, hydrothermal episode in southern Bolivia.

The Porco Ag-Zn-Pb-Sn deposit, ≈35 km southwest of Potosi, was a major silver producer in the 16th century and is currently the largest zinc producing mine in Bolivia. It is located within a 3×5 km resurgent caldera that formed in response to the eruption of the dacitic Porco tuff that extends northward beneath the ≈6–9 Ma Los Frailes tuffs. K-Ar ages on biotite from the Porco tuff indicate the age of eruption at 12.0±0.4 Ma and 12.1±0.4 Ma. Mineralization appears to be genetically related to the central Huayna Porco stock, which is at the center of a system of radial dikes and zoned metal and alteration mineral patterns. A K-Ar age on sanidine from

Tomas Vila (left), Chief Geologist of Minero Anglo American Chile, and Skip Cunningham at the volcanic-hosted, zoned, Aldebaran porphyry gold-copper and epithermal precious-metal deposit, Maricunga district, northern Chile. Andesitic volcanic host rocks in background show transition from the porphyry to the epithermal hot-spring environment.
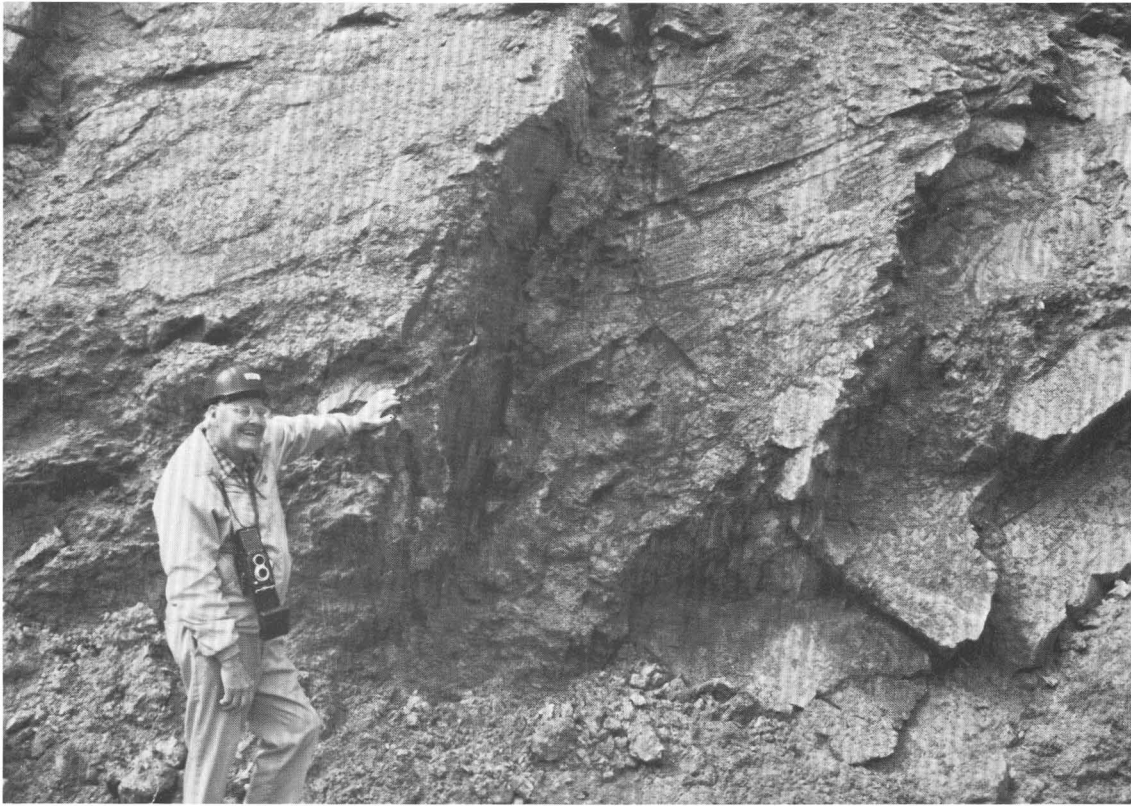
La Joya district, Bolivia; the only volcanic-hosted disseminated gold producer in Bolivia. George Ericksen at left.

the Huayna Porco stock indicates an age of intrusion of 8.6±0.3 Ma. The known ore deposits occur in steeply dipping irregular and curvilinear veins that cut the intracaldera Porco tuff about 1 km east of the Huayna Porco stock. The distribution of metals is zoned, with Sn concentrated nearer the stock and Pb-Zn-Ag farther away; additionally, Ag increases upwards in the base-metal veins. Geologic mapping has indicated that the known Pb-Zn-Ag veins are localized along the east side of the ring fracture of the caldera; the west side of the ring fracture has not been explored.

Fe, Pb, Zn, Cu, Au, AND HCl PARTITIONING BETWEEN VAPOR AND BRINE IN HYDROTHERMAL FLUIDS—IMPLICATIONS FOR PORPHYRY COPPER DEPOSITS

G.L. Cygan, J.J. Hemley, and M.W. Doughten

Hydrothermal fluids experiencing decompression will eventually split into two phases, one high density and one low density, each with very different chemistry. Base metals are partitioned between these two conjugate fluids. We have measured the KCl, $FeCl_2$, $PbCl_2$, $ZnCl_2$, CuCl, HCl, and AuCl partitioning coefficients and phase separation systematics of the $KCl-H_2O$ system. Two devices are used: (1) a flexible-volume Au bag of approximately 20 mL capacity at 500 °C in a large-volume extraction vessel, and (2) a fixed-volume extraction vessel. Pressures were monitored with calibrated transducers (accuracy of ±0.2 percent). Measurements were made at isothermal conditions and decreasing pressure to determine the characteristics of a single-phase KCl fluid as it splits into two fluids of differing density. Results are similar to but more detailed than those given earlier on liquid-vapor partitioning in a quartz monzonite-buffered, sulfide-bearing system at 500 °C, 500 bars (Hemley and others, 1992; Hemley and Hunt, 1992).

Our results for $KCl-H_2O$ relations agree with Tkachenko and Shmulovich (1992) at 500 °C although the liquid phase is shifted slightly to higher concentrations. Addition of base metals has an insignificant effect upon the pure $KCl-H_2O$ system. Partition coefficients $K'_d = ppm_i^{vapor}/ppm_i^{liquid}$, for Fe, Pb, Zn, and Cu decrease with decreasing P. Values at 500 °C, 550 bars are 0.17, 0.09, 0.07, and 0.19 for Fe, Pb, Zn, and Cu, respectively; at 400 °C, 250 bars, they are 0.024, 0.008, 0.006, and 0.014. The effect of pressure upon the distribution coefficient, $D_{Me^+}^{V/L} = (C_{Me^+}^{V} / C_{KCl}^{V}) / (C_{Me^+}^{L} / C_{KCl}^{L})$ is small to insignificant, where C_{Me^+} refers to individual metal concentrations. Adding 0.1 molal HCl to the system, similarly, did not significantly alter the pure $KCl-H_2O$ system relations. The vapor tended to be significantly more acid than the liquid—by a factor of two. Total molal quench acidity
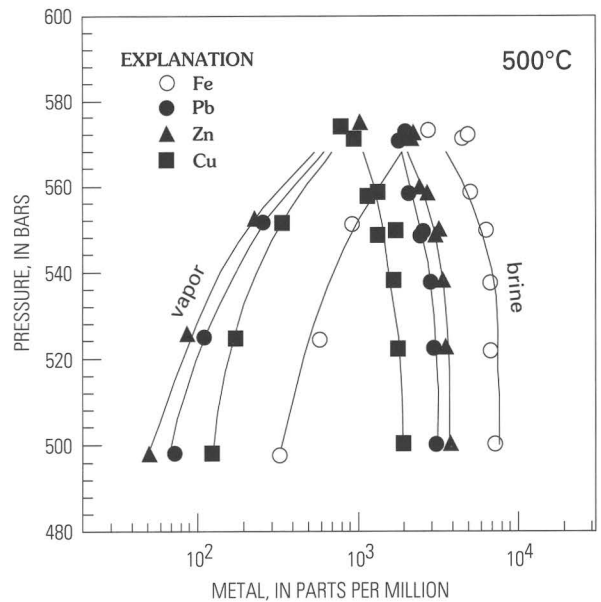
Figure 1 (Cygan and others). The vapor-liquid relations at 500° C plotted versus pressure. Initial base-metal concentrations used in this experiment for Fe, Pb, Zn, and Cu are, in ppm, 5,600, 2,000, 2,000, and 1,000, respectively. These values represent the approximate fluid composition in equilibrium with a quartz-monzonite-buffered single-phase hydrothermal solution at 500 °C, 1,000 bars (Hemley and others, 1992). The Fe curve is displaced to higher concentrations as expected, but the other metals show their own individuality. Copper shows the smallest difference between liquid and vapor concentrations; zinc shows the greatest. In this sense, copper is favored in vapor phase partitioning relative to zinc and lead, but the difference between vapor and liquid concentrations is still a factor of 16 at 500 bars.

values at 500 °C, 550 bars are 0.074 and 0.037 for vapor and liquid phases (K_d=2.0). Figure 1 shows the relative concentrations of base metals measured in both brine and vapor phases. Note that whereas all metals are more concentrated in the liquid phase, copper concentrations are increased relative to lead and zinc in the vapor. Gold measurements, which ranged as high as 10 ppm, indicate behavior similar to base metals—that is, partitioning favors the liquid phase.

These data demonstrate the potential for a rising, decompressing hydrothermal fluid to undergo phase separation and partition and transport metals through a fractional vaporization process. The concentrations of metals, especially iron, and the relatively high mobility of the low-density vapor suggest that the mineralizing potential of the vapor may be significant in hydrostatic pressure regimes where vapor may dominate. Furthermore, HCl is strongly partitioned into the low-density vapor phase compared with the liquid phase at these P, T conditions, and this process results in a highly reactive mobile fluid that may migrate

through the host rock. This fluid would produce intense hydrolytic alteration characterized by an advanced argillic assemblage, with accompanying pyrite and minor copper mineralization, as is seen in acid-sulfate precious-metal systems and in the upper levels of the porphyry copper deposits.

REFERENCES

Hemley, J.J., Cygan, G.L., Fein, J.B., Robinson, G.R., and d'Angelo, W.M., 1992, Hydrothermal ore-forming processes in the light of studies in rock-buffered systems—I, Iron-copper-zinc-lead sulfide solubility relations: Economic Geology, v. 87, p. 1–22.

Hemley, J.J., and Hunt, J.P., 1992, Hydrothermal ore-forming processes in the light of studies in rock-buffered systems—II, Some general geologic applications: Economic Geology, v. 87, p. 23–43.

Tkachenko, S.I., and Shmulovich, K.I., 1992, Liquid-vapor equilibria in the systems water salt (NaCl, KCl, CaCl₂, MgCl₂) at 400–600°C: Doklady Akademii Nauk, v. 326, p. 1055–1059.

CAPTURE OF COPPER, LEAD, AND ZINC BY THE ZEOLITE-CLINOPTILOLITE IN METAL-POLLUTED DRAINAGES OF COLORADO

George A. Desborough

Clinoptilolite-rich rocks (CRR) from 10 deposits in the western United States and one from British Columbia were tested for ion-exchange capture of copper, lead, and zinc in several Colorado mine and stream drainages with pH ranging from 4 to 9. Spring and summer 1993 tests evaluated element capture by CRR samples from Buckhorn, N.Mex. (BNM); Castle Creek, Idaho (CCI); Creede, Colo. (CCO); Fish Creek, Nev. (FCN); Ft. LaClede, Wyo. (FLW); Harney Lake, Ore. (HLO); Princeton, B.C. (PBC); South Dakota (SD1, SDA, SDC); St. Cloud mine, N. Mex. (SNM); Sheaville, Ore. (SVO); and Tilden, Texas (TT). Sized 20-g packets of CRR (1.7–4.7 mm) in 2×3-mm-mesh nylon bags were immersed in the drainages, with a maximum of eight side-by-side tested simultaneously. Test periods were from 19 hours to 28 days. After testing, the samples were dried, sieved to remove sand-sized particles and Fe-hydroxide precipitates, pulverized, and analyzed for K, Ca, Fe, Cu, Zn, Rb, Sr, Cd, Ba, and Pb using three radioisotope X-ray sources and a Li-drifted detector. The drainage waters, all containing significant heavy metals, were anlyzed for nine elements at a commercial laboratory.

Mine-tunnel or adit drainages that were tested vary only slightly in pH, temperature, flow rate, and composition, temporally, and thus "appear" to be point sources (for example, Argo drain, Idaho Springs; Rawley adit, Bonanza; Wellington mine drain, French Creek, Breckenridge). Other larger, metal-polluted drainages, such as the Alamosa River, California Gulch, Leadville, Mineral Creek, Silverton, and St. Kevin Gulch (northwest of Leadville), vary significantly in pH, temperature, flow rate and composition. Thus, remediation treatment of water in each drainage must be tested prior to selection of remediation methods. Some possible complexities of water treatment for heavy-metal remediation are shown by the variations in CRR metal capture at the lower California Gulch test site; pH varied from 4.3 on 5/29/93 during highest flow rates, to a pH of 9 on 8/3/93 during the low summer flow (table 1).

Data in table 1 show that large amounts of Zn were captured by FLW (Fort LaClede) at low pH, but much smaller amounts were captured at high pH. At the highest pH, SDA (South Dakota) and SVO (Sheaville, Ore.) captured significantly more Zn than the other CRR samples. For the water, between 6/4/93 and 8/3/93, the amount of Cu decreased by one-fourth, the amount of Zn decreased by one-half, Cd decreased by one-fifth, and Pb decreased by one-third. The greatest concentrations of heavy metals of interest here were present during peak spring runoff.

Based on 1993 testing of 138 samples in seven drainages in Colorado, Cu was readily captured by the best performing CRR at aqueous concentrations as low as 0.06 mg/L. Significant amounts of Pb were captured by the best performing CRR at dissolved concentrations of 0.1 mg/L. At Zn concentrations of 1 mg/L, or more, the most efficient CRR captured significant amounts of this metal. Only minor amounts of Cd were captured at concentrations of 0.2 mg/L.

ISOTOPIC AND FLUID-INCLUSION DATA ON THE AGE AND ORIGIN OF THE SÃO BENTO AND MORRO VELHO GOLD DEPOSITS, MINAS GERAIS, BRAZIL

Ed DeWitt, G.P. Landis, R.E. Zartman, Enzio Garaype, Sérgio Luiz Martins Pereira, Milton Guimarães Bueno do Prado, Frederico Wallace Reis Vieira, and C.H. Thorman

The São Bento and Morro Velho mines in the state of Minas Gerais, Brazil, exploit stratabound gold-arsenic deposits within stratified rocks of the Late Archean Nova Lima Group. Models ranging from syngenetic sea-floor hot springs to epigenetic quartz veins in shear zones have been proposed for these and other similar deposits in Minas Gerais. In order to more precisely determine the origin of each deposit, we applied techniques of thin- and polished-section petrography, U-Th-Pb geochronology, Pb-Pb

Table 1 (Desborough). Concentrations of elements in the water and elements gained or lost (–) by CRR during four test periods at the lower California Gulch test site, west of Stringtown, Colo.

[n.d., not determined. FLW, Ft. LaClede, Wyo; SD1, SDA, SDC, South Dakota; TT, Tilden, Texas; CCO, Creede, Colo.; FCN, Fish Creek, Nev.; HLO, Harney Lake, Ore.; PBC, Princeton, B.C.; SVO, Sheaville, Ore.]

	K	Ca	Cu	ZN	Rb	Sr	Cd	Ba	Pb
	$ppm \times 10^3$		parts per million						
5/29/93–6/4/93 (6 days)			pH=4.3–4.9, T=12–14 °C						
FLW	0.2	1.1	10	1,625	0	55	1	–230	640
SD1	–0.2	–1.1	30	680	85	60	1	–285	790
SDA	–0.3	–0.1	55	1,180	0	45	<1	–55	525
SDC	–0.1	0.4	50	995	–10	35	1	25	660
TT	–0.3	1.2	50	810	0	20	1	–335	790
6/4/93–6/13/93 (9 days)			pH=4.9–6.1, T=14.5–17 °C						
water (mg/L)	2.6	145	0.4	21	n.d.	n.d	0.11	0.4	0.3
FLW	0.3	1.5	0	1,335	0	70	<1	–105	570
SD1	–0.2	–0.5	40	790	75	50	<1	–200	530
SDA	–0.3	0.6	30	1,095	–10	45	<1	–50	810
SDC	–0.2	0.3	40	910	–10	60	<1	–20	785
TT	–0.6	–0.1	0	565	–10	–15	<1	–155	535
6/13/93–7/2/93 (19 days)			pH=6.1–7.4, T=15–17 °C						
FLW	0.3	1.9	0	1,300	–10	115	<1	–160	210
SD1	–0.3	0.1	55	1,360	–10	85	<1	–400	165
SDA	–0.2	–0.3	0	1,020	0	65	<1	–315	155
SDC	–0.4	0.7	0	1,190	–15	80	1	–155	175
TT	–1.3	0.4	0	485	–10	70	<1	–160	200
7/20/93–8/3/93 (14 days)			pH=8.2–9.2, T=15–17 °C						
water (mg/L)	2.5	218	<0.1	10.3	n.d.	n.d.	0.02	0.04	0.11
CCO	–0.2	0.4	0	1,400	–45	10	<1	160	40
FLW	0.4	2.1	0	1,185	–10	80	<1	–255	0
FCN	0	0.6	0	1,320	–45	55	<1	45	45
HLO	0	0.5	0	915	15	45	<1	75	35
PBC	0.2	0.5	0	645	–20	–65	<1	–80	50
SDA	–0.7	0.9	0	2,130	0	45	<1	55	50
SVO	–0.8	0.6	0	1,945	–20	60	<1	65	110

analyses, and in-place mass spectrometry of gases in fluid inclusions to selected samples.

The São Bento deposit is hosted by siderite-rich iron-formation interbedded with carbonaceous phyllite and minor volcaniclastic material. Primary arsenopyrite-pyrite-pyrrhotite ore has a distinctly bedded appearance, with the greatest concentration of sulfide grains in siderite- and albite-rich beds. Pretectonic quartz veins are common and most numerous in the siderite-rich ore, but are also present in carbonaceous phyllite and surrounding rock units. Remobilization textures and recrystallization of primary pyrrhotite and pyrite adjacent to quartz veins are well documented. Chert beds within iron-formation have variably recrystallized to form quartz veins parallel to bedding. The nonsulfide mineralogy of veins that cut beds is controlled by host rock type: veins that cut siderite beds are only quartz; veins that cut siderite-rich iron-formation are quartz-siderite; veins that cut magnetite iron-formation are quartz-magnetite.

Gas chemistry of fluid inclusions from a variety of quartz veins, Pb-Pb analysis of arsenopyrite and pyrite from

primary ore, and thin-section petrography indicate that most veins at São Bento formed in place from siderite-rich iron-formation during regional metamorphism. Inclusions from veins in phyllite are water rich; all other veins are water poor. Veins in siderite-rich iron-formation are methane rich and have variable to high carbon dioxide concentration. Veins in magnetite iron-formation are the only ones to contain significant nitrogen. Veins that cross from phyllite to siderite-rich iron-formation have the gas composition of those in siderite-rich iron-formation. Pb-Pb analyses of refractory arsenopyrite and pyrite from bedded and remobilized ore plot on a single-stage growth curve at 2.65 Ga. Pyrrhotite, which is more easily recrystallized than the other sulfide minerals, plots slightly off the growth curve but within the field of Late Archean remobilized lead.

The Morro Velho deposit is hosted by the Lapa Seca, an iron-rich dolomite containing volcanic(?) grains of albite to oligoclase. The Lapa Seca is interbedded with slate and greenschist-facies shale-rich volcaniclastic strata. Ore ranges from disseminated arsenopyrite-pyrrhotite-pyrite within bedded, laminated Lapa Seca to massive ore of the same minerals within a minor siderite-dolomite gangue. Quartz veins are very minor, and remobilization features that disrupt the primary ore are minimal. Pb-Pb data from arsenopyrite, pyrite, and pyrrhotite from the 26-level of the M- and X-orebodies contain such low concentrations of lead (6–14 ppm) that meaningful interpretations are difficult—other than to say that Late Archean or Early Proterozoic lead originally present in the sulfide grains has been modified significantly during Early Proterozoic metamorphism and deformation.

GEOLOGIC CONTRIBUTIONS TO THE MINERAL RESOURCE ASSESSMENT OF THE CORONADO NATIONAL FOREST, ARIZONA AND NEW MEXICO

Harald Drewes

A mineral resource assessment of the Coronado National Forest of southeastern Arizona and southwestern New Mexico was recently completed by six U.S. Geological Survey scientists. The forest comprises 12 separate units which total about 7,500 km^2 (fig. 1).

Metallic mineral production from the forest areas was mainly copper, lead, zinc, molybdenum, silver, and gold, obtained from vein, stockwork, replacement, porphyry, and placer deposits. Production of nonmetallic commodities was minor. Current value of metals produced from the immediate forest region (forest units plus tracts between them) is $0.5–1 billion; about $20 billion has been produced from an extended region (50 mi; 80 km) around the forest. Mineral resource assessment is a key element to land-use planning for this forest.

A complex geologic history of deposition, intrusion, and tectonism is apparent in many of these areas within the forest and belies the apparent surface simplicity of others. This study focuses on five partly interdependent geologic factors that contributed to the final geologic assessment map; geochemistry and geophysics are covered separately.

A porphyry copper metallogenic belt extends through the western part of the forest region and contains most of the large mineral deposits of the extended region. Location of a forest area within this metallogenic belt is one of the favorable geologic factors. This belt is associated with a particular magmatic-tectonic zone (western intermediate zone) of the Cordilleran orogen and is favorable for the occurrence of differentiated granodioritic plutons and their hydrothermal systems bearing base and precious metals. Under present market conditions, deposits east of the porphyry copper belt would not as likely be economically viable without having a substantial amount of precious metals.

A second favorable geologic factor is the presence of a hydrothermal system. A tract having all other favorable factors but no sign of hydrothermal alteration or scattered weak signs of mineral accumulation does not have a particularly high mineral potential. In many of the forest units, observations have been made on the distribution of mobile metals, silicified rock, and clay-mineral alteration; these indicators augment the geochemical and geophysical studies, which are more concerned with quantitative factors.

A third geologic factor is proximity to plutonic rocks of favorable composition and age. Plutons of granite to diorite composition were emplaced in rocks of the forest during (1) Early and Middle Proterozoic (1,650–1,450 Ma), (2) Middle Proterozoic (1,100 Ma), (3) Jurassic (190–140 Ma), (4) Late Cretaceous and Paleocene (70–55 Ma), (5) Paleocene-Oligocene (55–30 Ma), and (6) Oligocene (30–25 Ma). Of prime importance are plutons of group (4), particularly those having multiple compositional phases from diorite to alkali granite, and in several mining districts, to a quartz latite porphyry, known as the "ore porphyry." Such compositionally diverse plutons occur mainly in the western part of the forest region; plutons of group (4) are fewer and smaller to the east. Of secondary importance are plutons of groups (3) and (6): Two of five Jurassic stocks are associated with mineral deposits, one a major mining district; many Oligocene stocks are associated with small mines and prospects but in places have concentrated large amounts of precious metals. Plutons of group (5) may have had a negative influence on ore accumulation. These peraluminous muscovite-biotite-garnet granites, which are associated with gneiss-cored domes (core complexes), may have come from partially melted lower crust that was impoverished in metals and whose late thermal history and high topographic and structural position favored the presence of outward-flowing hydrothermal systems prone to flush out, rather than accumulate, metals.
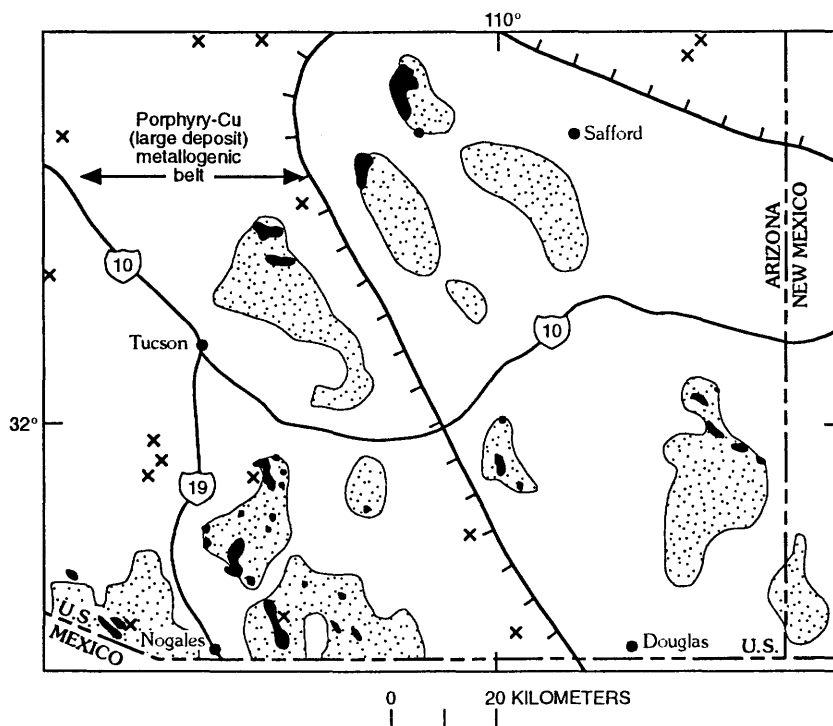
Figure 1 (Drewes). Tracts of high mineral resource potential, based on geologic factors alone (solid black), in Coronado National Forest area (stipple pattern). ×, major mine or mining district.

A fourth favorable factor is proximity to northwest-trending steep faults. Faults of many orientations, ages, and origins cut rocks of the forest, and most have the potential for channeling ore fluids. Northwest-trending structures, which may have begun in the Proterozoic as left-slip faults, are somewhat sinuous in plan but always steep, and they are widely spaced through the region, as if they controlled major crustal block movements. These faults appear to have been the dominant control of fluid movement at deep levels; faults of other trends and inclinations dispersed fluids at shallower levels. Neogene low-angle normal faults (glide faults) seem to be of little consequence to ore fluids because they postdate most known ore deposits of the region.

A fifth favorable geologic factor is the presence of a receptive host rock. The forest region is underlain by more than 10 km of sedimentary, volcanic, and metamorphic rocks that are potential hosts for mineral deposits. Although some mineral deposits are found in most rocks, only a few are particularly good hosts, because of either their chemical or physical properties, their age, or their spatial distribution relative to other geologic factors. The most favorable host rocks are the Middle and Upper Cambrian Abrigo Formation and overlying Upper Devonian Martin Formation, both mixed clastic and carbonate rocks widespread in the western part of the forest region. Andesite volcanic rocks of Late Cretaceous or Paleocene age are also good host rocks in many places, for they are brittle, are intruded by late orogenic plutons, and are abundant to the west. In some places, the Mississippian Escabrosa Limestone, Pennsylvanian and Lower Permian Horquilla Limestone, and Mural Limestone-equivalent beds of the Lower Cretaceous Bisbee Group, and other Mesozoic volcanic rocks are also favorable hosts. In covered or only slightly mineralized areas, in which other factors are favorable, these host rocks have potential for subsurface mineral deposits.

Although the five geologically favorable factors have been considered separately, all typically act together to define the geologic characteristics used in evaluating mineral resource potential. The resulting tracts of high potential (fig. 1) and of lower levels of potential (given in full report) were then collated with evaluations derived from the other studies to provide a final assessment of resource potential.

MAGMATIC EVOLUTION OF THE TURKEY CREEK CALDERA, CHIRICAHUA MOUNTAINS, ARIZONA

Edward A. du Bray and John S. Pallister

The Turkey Creek caldera is a 20-km-diameter volcanic collapse structure in the Chiricahua Mountains, Ariz. Caldera magmatism began with development of a shallow,

30

compositionally stratified magma reservoir in which rhyolitic magma overlay dacitic magma across a sharp interface. Stratigraphic relations and overlapping ages indicate that both magmas were present simultaneously in the source reservoir. Caldera formation was initiated by eruption of 500–1,000 km³ of the Rhyolite Canyon Tuff. Lava flows and tuff erupted after caldera formation record the compositional evolution of the underlying magma reservoir. The caldera floor is not exposed, and zones of megabreccia are rare in the Turkey Creek caldera. The caldera's deeper levels have been exhumed by faulting and erosion, exposing the roof of the crystallized magma reservoir.

The caldera evolved through three principal stages:

1. The rapid, voluminous eruption of Rhyolite Canyon Tuff caused magma withdrawal and concomitant caldera collapse into the partially evacuated reservoir. The outflow facies of the tuff, composed of lower, middle, and upper members, is as much as 400 m thick and consists of multiple ash flows that represent a series of eruption pulses; ash flows spread laterally from the caldera and accumulated in topographic lows during the paroxysmal eruptions. The intracaldera facies of the tuff, which ponded to a thickness of more than 1.2 km inside the caldera, is compositionally and petrographically akin to only the upper member of the outflow facies. Equivalents of lower and middle members of the tuff either were not deposited within the caldera or are concealed therein.

2. Following eruption of the Rhyolite Canyon Tuff, dacitic magma from beneath the compositional interface formed an intrusion, and associated lava flows were erupted on the floor of the caldera. Emplacement of the dacite intrusion, a >1-km-thick laccolith, within the collapsed floor of the caldera bowed up the caldera's central region and caused formation of a dome-encircling moat within the collapse crater. Interpretation of the intrusion as an intracaldera laccolith, rather than a core pluton, explains the lack of exposed floor rocks, scarcity of megabreccia within the caldera, and the absence of intracaldera equivalents of most of the outflow tuff: each is presumed to be concealed beneath the laccolith. Dacite lava flows were erupted from caldera-collapse ring faults, vents that previously fed ash-flow eruptions. A sequence of locally glassy, vesicular, and flow-ramped dacite lava flows are >0.5 km thick in the moat. Unerupted dacite was trapped in and beneath the vents and solidified to form a ring dike at depth.

3. A period of volcanic quiescence and erosion is represented by a sequence of sedimentary rocks deposited in the caldera moat; these rocks are in turn overlain by ≈135 km³ of mainly crystal poor rhyolite lava that represents the final phase of caldera-related volcanism. The sedimentary rocks are rich in Rhyolite Canyon Tuff debris and are mainly poorly sorted breccias and ash-rich sandstone that were deposited within the caldera moat on or near the eroded caldera wall. Rhyolite erupted following moat sedimentation records generation of a voluminous new batch of mainly

high silica rhyolite with a distinct geochemical signature. Initial, volumetrically minor low-silica rhyolite is overlain by three sequences of high-silica rhyolite lava and minor associated tuff. Despite complex internal flow folding, lava-flow map units are remarkably planiform sheets. Rhyolite dikes and feeder zones for the moat rhyolite are rare; the moat rhyolite units may overlie their own vents.

$^{40}Ar/^{39}Ar$ data are consistent with all of the Turkey Creek caldera rocks being broadly cogenetic; ages on sanidine for the Rhyolite Canyon Tuff and the dacite are 26.9±0.1 Ma, whereas ages for two samples of moat rhyolite are 26.9±0.1 and 26.6±0.1 Ma. These ages constrain the erosional interval between emplacement of the dacitic rocks and eruption of the moat rhyolite to < 300,000 years.

GEOLOGICAL REMOTE SENSING— HISTORY AND DEVELOPMENT IN LATIN AMERICA

Barbara A. Eiswerth

The use of remote sensing technology in geologic mapping and mineral exploration programs in Latin America and the Caribbean region has increased dramatically in the last 5 years. Factors such as the need for reliable assessments of a country's mineral endowment, the current favorable investment terms for multinational companies, accelerated technology transfer, improved data availability, and expanded variety of data types and uses have all contributed to this increase.

Latin America and the Caribbean region are ideal for the application of remote sensing technology because many areas are remote and isolated, accurate base maps are not always available, and infrastructure is often limited. Analysis of multispectral and radar images contributes to mineral resource studies by providing a rapid and efficient means of delineating major tectonic and volcanic features, lithologies, and hydrothermally altered rocks. Interpretation of remotely sensed data, coupled with conventional mapping, is used to enhance and augment exploration efforts.

The shift in mining exploration from the United States and Canada toward Latin America results in part from favorable changes in investment laws throughout Latin America. In 1992, 203 Canadian and 42 United States companies had mining interests in Latin America and the Caribbean region (Don E. Howell, Mining Record, oral commun., 1993). Accompanying this shift is the export of modern tools and technology including innovative image processing, and the use of remote sensing and GIS (geographic information systems).

Specialized centers exist to train Latin American geoscientists in the application of remote sensing techniques.

More universities offer courses in remote sensing and GIS for geoscience applications than in the past. Foreign governments facilitate transfer of technology through cooperative research programs involving equipment acquisition, intensive training, and practical application of methods learned. Many national geological surveys and other government agencies in Latin America and the Caribbean have developed remote sensing laboratories that specialize in earth science investigations and provide information for mineral development in their respective countries.

The variety of digital data types available has increased rapidly over the last 10 years. Landsat MSS (Multispectral Scanner) data have been collected since 1972 and TM (Thematic Mapper) data since 1982. TM data have been useful in exploring for gold placer deposits in heavily vegetated areas in Central and South America. Data collected by the French SPOT (Satellite Probatoire pour l'Observation de la Terre) have been available since 1986. Analyses of SPOT data have been used to identify potential bauxite deposits in Venezuela. Imaging radar data from Seasat and the SIR (Shuttle Imaging Radar) systems have been used extensively since the 1970's for geologic mapping, especially in areas obscured by cloud cover or dense vegetation. Radar images are the sole source of areal coverage for parts of the Brazilian Amazon Basin and are often used for regional structural interpretation as well as lithologic mapping.

The 1992 launch of Japan's JERS-1 and the European Space Agency's ERS-1 satellites will produce unprecedented continent-wide radar coverage. The JERS-1 satellite also is equipped with visible and near-infrared spectral bands. Landsat 6 was unfortunately lost during launch in 1993, but Landsat 5 is expected to continue functioning until Landsat 7 is launched in 1997. The sensor aboard Landsat 7 will provide higher spatial and spectral resolution. RADAR-SAT, a Canadian satellite scheduled for launch in 1994, will provide improvements on past systems such as variable and high spatial resolution and changeable incidence angles.

Several hyperspectral airborne imaging spectrometers, both commercial and government sponsored, are actively collecting data in areas in Latin America. These systems include AVIRIS (Airborne Visible and Infrared Imaging Spectrometer), TIMS (Thermal Infrared Imaging Spectrometer), Geophysical Environmental Resources' GER-63 channel sensor, and GEOSCAN's 24 channel sensor. Since 1980, Intera Information Technologies' airborne radar system, STAR-1, has been providing very high spatial resolution data with stereoscopic capabilities. Commercial data from both the GER-63 sensor and the GEOSCAN sensor are being used by mining companies in Chile to map distinct zones of hydrothermal alteration associated with porphyry copper and volcanic-hosted epithermal precious-metal deposits. The variety and utility of remote sensing data will have great impact on the systematic exploration and geologic mapping of Latin America and the Caribbean region.

IMPACT OF THE SUMMITVILLE MINE ON IRRIGATION WATER, AGRICULTURAL SOILS, AND ALFALFA IN THE SOUTHWESTERN SAN LUIS VALLEY, COLORADO

J.A. Erdman and K.S. Smith

Contamination from the Summitville gold mine in the San Juan Mountains has raised concerns over the effects of low pH and metal-laden surface waters carried down the Alamosa River. These waters enter the Terrace Reservoir, which provides irrigation water to the southwestern part of the San Luis Valley. The purpose of this study was to assess whether significant differences exist between the effects of two source waters on the compositions of alfalfa and the associated soils, respectively. The two source waters are Terrace Reservoir water and Rio Grande River water and (or) confined ground water.

Sampling was conducted June 3–6, 1993, just prior to the first cutting of alfalfa. Irrigation water, soils, and alfalfa were collected from four sprinkler-irrigated Terrace Reservoir fields and from similarly irrigated "control" fields using a balanced one-way analysis-of-variance design. Four sites were selected randomly within each of the eight fields.

The water samples were taken from the irrigation system of each field. The pH values of the Terrace Reservoir waters ranged from 5.6 to 6.8 and the samples contained no measurable alkalinity. Preliminary chemical data indicate that these waters contained anomalous concentrations of copper (60–350 µg/L), zinc (150–190 µg/L), and manganese (360–520 µg/L) in unfiltered samples. In contrast, the pH of irrigation waters originating from sources other than Terrace Reservoir ranged from 7.6 to 9.2, and the concentration of dissolved metals was less than 2 µg/L, 25 µg/L, and 20 µg/L for copper, zinc, and manganese, respectively. It appears that fields irrigated with waters originating from the Terrace Reservoir receive more acidic water and higher concentrations of dissolved metals than do fields using irrigation waters from another source.

Results of total analyses of soils from sites irrigated with Terrace Reservoir water are similar to those of the soils irrigated with other sources of water. Differences in element concentrations were not significant at the 0.01 probability level, but were significant at the 0.05 level for copper and phosphorus. When compared with geometric means for soils from the western United States (Shacklette and Boerngen, 1984), soils we collected from the southwestern part of the San Luis Valley contain higher concentrations of aluminum, barium, beryllium, cobalt, copper, iron, manganese, potassium, sodium, strontium, titanium, vanadium, and zinc. These higher concentrations probably reflect the composition of the alluvial parent material from which the soils were derived. This fan material is detritus shed from weathering of

Figure 1 (Erdman and Smith).   View of one of eight alfalfa fields sampled, all of which were irrigated by a center-pivot sprinkler system similar to the one shown here. Photograph taken June 4, 1993.

volcanic rocks and mineralized areas in the Alamosa River drainage basin. All of our soil data from the southwestern part of the San Luis Valley are within geochemical baselines for soils from the western United States (Shacklette and Boerngen, 1984).

Stem-and-leaf samples of alfalfa were collected from 10 points within a 1-m radius of each soil pit. An analysis-of-variance for 15 elements showed no significant differences in alfalfa irrigated by the two source waters when tested at the 0.01 probability level. However, concentrations of copper and manganese between the two sources were significantly different at the 0.05 level. More importantly, concentrations of these metals in alfalfa affected by both water sources (1) meet published nutritive requirements for ruminants, (2) are far below concentrations reported to be toxic to cattle, and (3) are comparable to concentrations in alfalfa found in other parts of the country.

In conclusion, preliminary results indicate that the metal concentrations of the irrigation water affected by the Summitville mine may be anomalous. Yet these waters have no measurable effects on the total soil chemistry and seem to have had a minimal impact on the nutritional value of the associated alfalfa.

REFERENCE

Shacklette, H.T., and Boerngen, J.G., 1984, Element concentrations in soils and other surficial materials of the conterminous United States: U.S. Geological Survey Professional Paper 1270, 105 p.

METAL CONCENTRATIONS IN THE WETLAND VEGETATION RECEIVING ACID MINE DRAINAGE FROM ST. KEVIN GULCH, LEADVILLE, COLORADO

B.M. Erickson, P.H. Briggs, and T.R. Peacock

Acid mine drainage (AMD) from St. Kevin Gulch, Leadville, Colo., drains into a 26-ha (hectare) subalpine wetland. The wetland is a sedge meadow with two ecosystem components: (1) sedges growing on top of hummocks—the drier component (*Carex canescens* L.); and (2) sedges growing between or off hummocks—the aquatic component (*Carex utriculata* Boott.). The purpose of this study was to evaluate the affects of the AMD on the wetland sedges. Two main tasks were identified. The first task was to establish the expected baseline trace-element concentrations in the sedges to delineate areas of possible effects. The second task was to examine seasonal variation and establish biomass production estimates to determine the amount of metals being removed from the AMD by the wetland.

As of the 1989 growing season, no signs of metal stress were visible on the wetland vegetation. However, the AMD has affected the metal concentrations of the sedges growing on the wetland. Sedge concentrations of Cd, Cu, Fe, Pb, Mn, and Zn, known to be high in the AMD waters, are higher in the area of direct inflow than the sedge baseline geometric

means (GM) reported for the wetland. Concentrations higher than the GM in other areas of the wetland are evidence for contamination from other sources. Maximum cattle dietary levels reported in the literature for Cd (0.5 ppm) and Zn (500 ppm) are exceeded in some areas of the wetland and could present a nutritional problem for the cattle grazing this wetland each year. Vegetation toxicity levels for Cu (20–100 ppm) and Pb (30–300 ppm) are not exceeded, but Pb concentrations are higher in the inflow area and may indicate that accumulation is occurring. Iron deficiency, common in vegetation and foodstuffs, was not detected in the sedges of this wetland. Manganese concentrations above the 500 parts per million level, reported in the literature as resulting in signs of visible stress in vegetation, are present in most areas of the wetland. The Fe/Mn ratio necessary for healthy vegetation (1.5 to 2.5), occurs only in the areas with the higher Fe concentrations. Presently the only element being removed from the AMD waters by the wetland is Fe. If the sedges accumulate higher levels of Fe, the ratio of Fe/Mn will not necessarily be improved. Iron and manganese are physiological antagonists, and at toxic Mn levels, iron absorption could reverse, resulting in more stress and eventual loss of biomass.

GEOLOGIC AND GEOCHEMICAL CONTROLS ON THE COMPOSITION OF WATER DRAINING FROM DIVERSE MINERAL DEPOSITS

Walter H. Ficklin, Geoffrey S. Plumlee, and Kathleen S. Smith

Pyrite may be the most abundant of all the sulfide minerals. It occurs in some form in almost all mineral deposits. The oxidation of pyrite initiated by atmospheric oxygen is responsible for one of the most widespread environmental problems that will be encountered in the utilization of mineral deposits: acid rock drainage. The reaction is catalyzed by bacteria, and the main products are acid, sulfate, and dissolved and solid forms of iron. Many other minerals are dissolved in the process. Once the reaction is established, it does not stop until one or more of the reactants is exhausted. The overall reaction is slow enough that pyrite deposits may not be completely exhausted for several thousand years. Yet it is fast enough that a mineral deposit undergoing oxidation may seriously affect the quality of water draining that deposit.

The composition of water samples draining from mines located throughout the Colorado Mineral Belt is quite variable. Out of approximately 40 sample locations tested, the pH varies from 1.7 to 7.8. Iron concentrations range from not detectable to 8,000 mg/L; zinc concentrations range from 20 to 700,000 µg/L; and copper concentrations range from not detectable to 500,000 µg/L. Uranium, thorium, the rare earth elements, and several other metals are present in concentrations that are far greater than would be found in suitable drinking water.

The Colorado Mineral Belt hosts a broad spectrum of mineral deposits, each having characteristic structural features, host rocks, wallrock alteration, gangue minerals, and trace metals. The composition of waters draining diverse deposit types is a function of several factors: (1) the acid-buffering capacity of mineral-deposit host rocks and gangue material; (2) the types and abundance of metal-bearing sulfide minerals in the deposits; (3) the exposure of the sulfides to weathering; and (4) the availability of dissolved oxygen for the sulfide oxidation process. The mining method used in exploitation of mineral deposits has a bearing on the composition of water. As a generalization, open-pit mines produce water having low pH and high concentrations of metals, whereas underground mines produce water of intermediate to low pH and relatively lower concentrations of metals. Tunnels draining several mines often produce low-pH and high-metal waters.

In light of the observed range of pH and metals, we have developed an empirical metal-pH classification scheme for mine drainage. This scheme uses pH as a master variable that conveniently summarizes large amounts of data and provides a means for comparing mine water composition from different geologic settings. A plot of the sum of copper, zinc, lead, cadmium, cobalt, and nickel concentrations from mine drainage samples collected throughout Colorado as a function of pH is presented in figure 1. These base metals are of environmental concern and are present in nearly all drainage water. Samples of similar mineral deposit type and geology are outlined. Sulfide-rich deposits of low buffering capacity plot as a group in the upper left corner. On the other hand, deposits situated where the acid is neutralized by carbonates or other water-rock reactions plot in the lower right corner. Even though (as indicated in fig. 1) the most environmentally damaging water is derived from sulfide-rich–low-buffering deposits with pH values of less than 3, many of the mines with pH values greater than 5.5 still contain significant quantities of metals. Our interpretation of mine drainage chemistry in a geologic context is enabling us to develop a model that can be used to predict drainage chemistry from analogous undeveloped mineral deposits.

REFERENCES

Ficklin, W.H., Plumlee, G.S., Smith, K.S., and McHugh, J.B, 1992, Geochemical classification of mine drainages and natural drainages in mineralized areas, in Kharaka, Y.K., and Maest, A.S., eds., Proceedings of the 7th International Symposium on Water-Rock Interaction-WRI-7, Park City, Utah, July 13–18, 1992: Rotterdam, A.A. Balkema, p. 381–384.
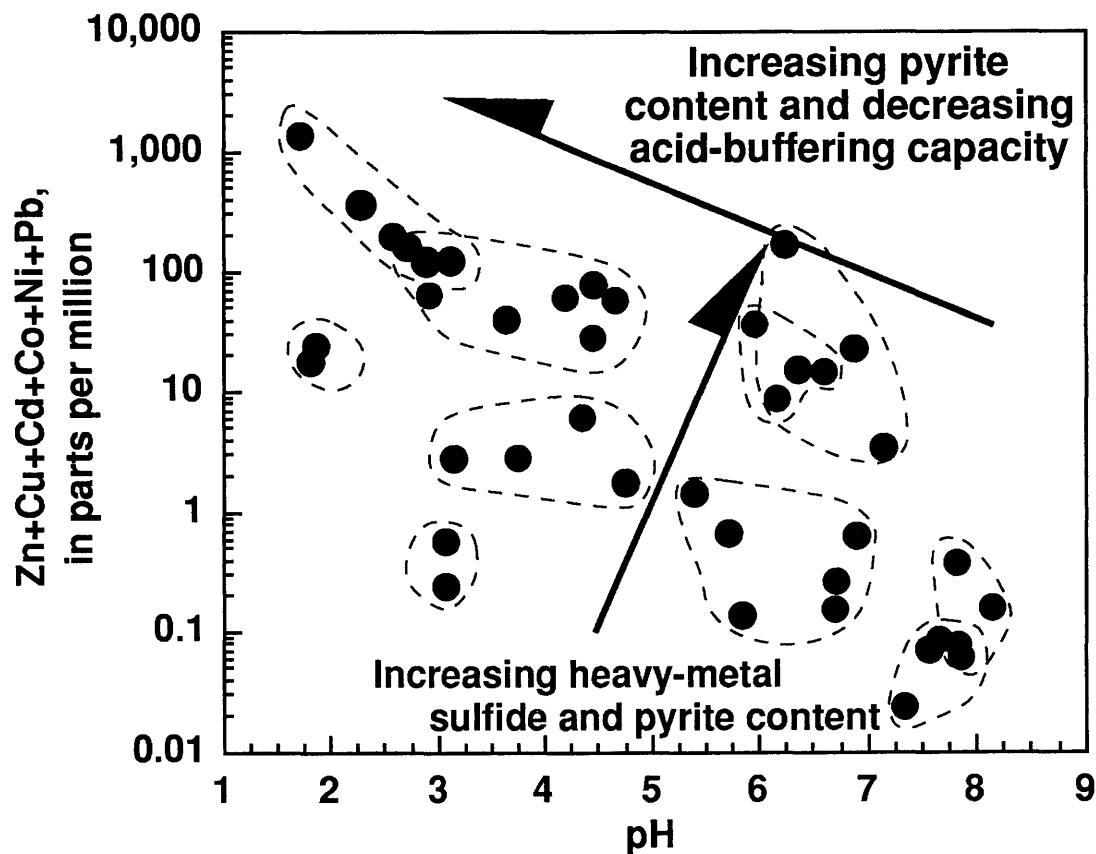
Figure 1 (Ficklin and others). Geologic controls on the pH and dissolved metal content (black dots) of diverse mine drainage waters from Colorado. Data from Ficklin and others (1992) and Plumlee and others (1993). Mineral deposit types are defined by differences in their geologic characteristics, which largely control the composition of mine draining waters. The dashed lines enclose waters that drain mineral deposits with similar geologic characteristics. These characteristics can be used to predict, plan for, and remediate potential environmental effects caused by natural weathering or mining of these deposit types.

Plumlee, G.S., Smith, K.S., Ficklin, W.H., Briggs, P.H., and McHugh, J.B., 1993, Empirical studies of diverse mine drainages in Colorado—Implications for the prediction of mine-drainage chemistry, *in* Planning, Rehabilitation and Treatment of Disturbed Lands, Sixth Billings Symposium, Billings, Mont., March 21–27, 1992: Reclamation Research Unit, Montana State University, p 176–186.

A PROGRESS REPORT ON THE SOUTHERN CALIFORNIA GEOCHEMICAL DATABASE AND MAP

Helen Folger, Albert Hofstra, and Gary Nowlan

A 5-year mineral resource assessment of southern California was initiated in 1991, as part of NAMRAP (National Mineral Resource Assessment Program). Using existing data, we have compiled a preliminary regional geochemical database and constructed a distribution map of selected elements for southern California. Review of the data showed good correlation between the geochemical anomalies exhibited in the map and known mining districts and metallogenic provinces. We present here an element-distribution map based on the existing database and outline future plans for the project.

The study focused on the region between lat 37° N. and the Mexican border. The southern California study area includes parts of the following physiographic provinces: Basin and Range, Mojave Desert, Sonoran Desert, Salton Trough, and Transverse and Peninsular Ranges. The study area includes the Monterey, Fresno, Death Valley, San Luis Obispo, Bakersfield, Trona, Kingman, Santa Maria, Los Angeles, San Bernardino, Needles, Long Beach, Santa Anna, Salton Sea, El Centro, and San Diego 1°×2° quadrangles.

Our data were compiled from three principal databases: the U.S. Geological Survey RASS and PLUTO databases, and the Department of Energy NURE database. Because these databases contain samples from many different studies collected over a long period of time, sample media, sample density, analyzed elements, and analytical methods vary both within and among the three databases. Nevertheless,

we have successfully constructed a coherent regional geochemical database for the study area.

The compiled regional geochemical database is based on the analyses of minus-80 mesh and minus-100 mesh stream-sediment and soil samples. We evaluated a total of 9,650 NURE samples and 9,797 RASS and PLUTO samples. The geochemical map we constructed uses vector symbols to represent relative concentrations for lead, zinc, copper, gold, silver, arsenic, antimony, and molybdenum, "pathfinder" elements selected for their common association with precious- and base-metal deposits. All data plotted on the geochemical map were gridded at a scale of 4 km^2. By gridding the samples, we generated a composite sample—by selecting the highest concentration value for each element from samples located within the grid. Only values considered anomalous are depicted by vectors.

Where adequate sample coverage exists, the geochemistry reflects areas of known mineralization. However, not all quadrangles have sufficient coverage to adequately evaluate the resource potential. A preliminary interpretation of this database indicates that it was inadequate for mineral resource assessment; additional samples and analyses were needed. Only the Fresno, San Luis Obispo, Bakersfield, Kingman, and Salton Sea quadrangles have samples that have been analyzed for some of the eight pathfinder elements shown on the geochemical map. In all quadrangles within the study area, low-level gold, arsenic, and antimony analyses are almost completely lacking.

In order to adequately evaluate the resource potential of this region, we needed an improved, updated geochemical database. Thus several thousand NURE samples are being reanalyzed for 40 elements by inductively coupled plasma-atomic absorption spectroscopy (ICP-AES) methods as well as by graphite-furnace atomic absorption (AA) for low-level gold (0.002 ppm detection limit). Additional stream-sediment samples collected in areas of sparse existing coverage are being analyzed by the same methods. These new data will provide greater sample coverage for a suite of elements with lower detection limits. We plan to complete and update the database and map of the regional geochemistry for Southern California by the end of 1996.

SANTA CATALINA MOUNTAINS, SOUTHEASTERN ARIZONA—LARAMIDE TO EOCENE PALEODEPTHS FROM FIELD EVIDENCE, AND IMPLICATIONS FOR MINERAL POTENTIAL

Eric R. Force

Reconstruction of paleosurfaces in the Santa Catalina Mountains suggests that Laramide (Late Cretaceous–Paleocene) paleodepths vary from zero in the Stratton-Peppersauce area in the northern part of the range, through about 2 km at the Geesaman fault on the north slope, to about 4 km

at the range crest. These figures are based on the following chain of reasoning:

1. Sedimentary rocks of the Upper Cretaceous American Flag Formation and a subaerial-vent facies of the older subunit of Rice Peak porphyry record a Laramide paleosurface in the Stratton-Peppersauce area;

2. Supracrustal rocks dipping gently east and northeast as a result of post-Laramide deformation can be used to extrapolate this paleosurface southward to the Geesaman fault;

3. The Geesaman, an earlier Laramide fault, was intruded by Laramide Leatherwood quartz diorite. Thus Laramide paleodepths north and south of the fault are the same; and

4. The Leatherwood quartz diorite forms a nearly concordant sheet that cuts almost all structures including thrust faults between the Geesaman fault and the range crest. The Marble peak syncline which deforms all these features is the exception, but its effect can be calculated. The angle between the Leatherwood sheet and sedimentary host rocks is constant; extrapolation of the paleosurface using this angle and dip of supracrustal rocks gives a 4.1±0.5-km paleodepth for the range crest.

In the Eocene, seven leucogranite sills of the Wilderness suite were intruded below this pile. The sills total 3.9 km thickness in only 0.7 km of host-rock screens. Sill intrusion caused Eocene paleodepths to increase to 8.8 km at the structural base of the forerange at the south end of the range (fig. 1). However, Eocene paleodepths of exposed rocks northward from the range crest remained about the same because these rocks overlie the sills.

These field-controlled paleodepths imply that Laramide phyllitic fabrics and tight sheath folds in the range-crest area formed as shallow as about 4 km, consistent with low grades of Laramide metamorphism except for contact metamorphism. Previously published Laramide paleodepths based on "magmatic" epidote in the Leatherwood quartz diorite are incorrect; those depths are geologically impossible and the epidote is not magmatic. Later mid-Tertiary mylonitization apparently occurred at depth ranges of about 8.7 to 4.5 km in the forerange (assuming little late Eocene–early Oligocene erosion); these are the most deep-seated events recorded in the Catalinas.

The Catalinas have been considered a mid-crustal metamorphic core complex, and this view has implied minimal resource potential for metallic minerals in deep-seated mylonitic rocks. Actually, only the forerange should be considered such a complex, and the newly calculated Laramide paleodepths are permissive of a variety of upper-crustal mineral-deposit types in the rest of the range. Paleodepths represented by the few already-known Laramide deposits are about 2 km or less.

In addition, many more of the northern parts of the range than previously supposed consist of favorable host rocks. For example, the Abrigo Formation forms extensive

36
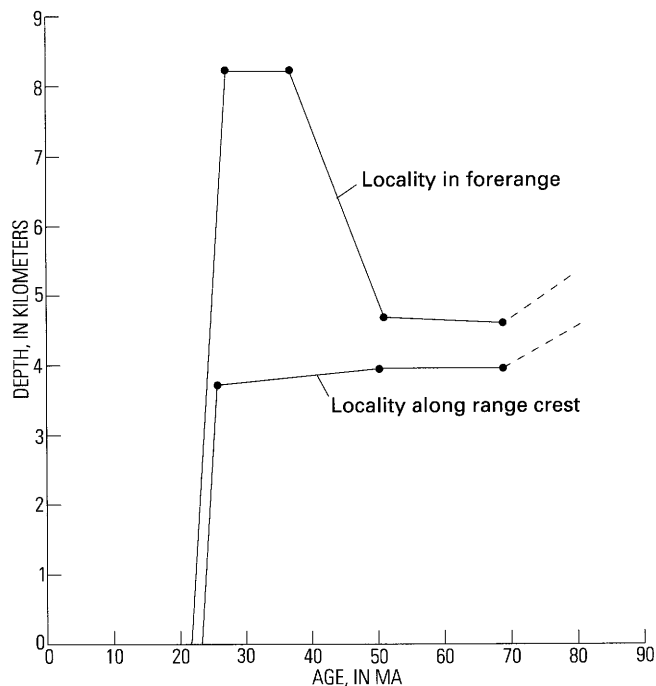
Figure 1 (Force). Paleodepths versus age from field evidence in the Santa Catalina Mountains, southeastern Arizona.

dip-slopes south of Edgar-type thrust faults, with Laramide paleodepths of about 3 km, and contains previously unreported Laramide skarns. The Geesaman fault, a deformed left-oblique fault with about 7 km displacement, is the locus of a previously unrecognized zoned population of mid-Tertiary deposits.

MAPPING ALTERATION IN HOT SPRING ENVIRONMENTS USING IMAGING SPECTROMETRY

Andrea J. Gallagher, Ken Watson, Daniel H. Knepper, Jr., and Cathy Ager

In August 1992, TMS (Thematic Mapper Simulator) and AVIRIS (Airborne Visible and Infrared Imaging Spectrometer) data were acquired over a portion of the Rio Grande Rift in south-central Colorado containing four hot springs areas. The primary objective of this study is to determine the distribution of epithermal minerals at each hot springs site and to relate them to differences in the geologic settings. A secondary task is to evaluate each site's vegetation characteristics as a function of the epithermal mineral distribution.

TMS has spatial resolution of 20 m per pixel and has 10 channels in the 0.4 to 2.5 μm region. AVIRIS acquired data with a spatial resolution of 20 m per pixel, and measures 224 channels from 0.4 to 2.5 μm. These narrow, contiguous bands form reflectance spectra for each pixel measured. Characteristic spectral features of minerals, and thence the minerals, can be mapped by comparing the AVIRIS data with reference mineral spectra measured in the laboratory. Using TMS data we can detect the presence of clay or carbonate minerals, but with AVIRIS data we are able to identify the specific mineral.

Many epithermal minerals associated with hot springs deposits and hydrothermal alteration are ideal for mapping with imaging spectrometry data because they have characteristic absorption features in the 0.4 to 2.5 μm region. Such minerals include iron oxides, clays, carbonates, micas, jarosites, and ammonium minerals such as buddingtonite. Subtle differences in the crystallinity or chemistry of these minerals may be detected in reflectance spectra.

The four hot springs areas in the study area occupy different geologic settings. Valley View Hot Springs is on the east edge of the San Luis Valley along the Neogene fault that bounds the west edge of the Sangre de Cristo Mountains. Mineral Hot Springs lies in the Tertiary and Quaternary valley-fill sediments of the San Luis Valley, at the projected intersection of two fault zones. Poncha Hot Springs is in Precambrian rocks along the northern boundary fault of the west-trending horst block separating the Arkansas River Valley and the San Luis Valley. Waunita Hot Springs is located on a fault in Cretaceous sedimentary rocks intruded by Tertiary rocks.

Preliminary mineral mapping results using the AVIRIS data show a calcite signature associated with the travertine mound at Mineral Hot Springs. A halo of amorphous iron oxide or combination of iron oxides extends up to a mile (≈1.6 km) from the hot springs. This suggests that the areal extent of alteration from the hot springs is much greater than that determined from field observations. Iron oxide and illite map together in an area east of Mineral Hot Springs, which may indicate alteration along another fault set that extends into the San Luis Valley. In progress are clay mineral maps that should help further characterize the epithermal alteration. At the other hot springs locations, we expect to detect similar alteration patterns, although the mineralogy may vary with the geologic setting.

CONSTRAINTS ON MINERAL RESOURCE POTENTIAL FROM ANALYSES OF GEOPHYSICAL DATA FROM THE CORONADO NATIONAL FOREST, SOUTHEASTERN ARIZONA

Mark E. Gettings

Regional gravity and aeromagnetic anomaly data, NURE (National Uranium Resource Evaluation) low-level aeromagnetic and aeroradiometric flightline data, and

detailed ground magnetic data have been analyzed to assist in evaluation of the mineral resource potential of the Coronado National Forest, southeastern Arizona. Regional-scale structures derived from interpretation of complete Bouguer gravity anomaly and regional aeromagnetic data define a rectangular pattern of elongate-to-the-northwest structural blocks that define the style of post-Laramide extension. The northwest and southeast ends of the individual blocks are terminated by northeast- or north-northeast-trending structures across which differential extension has occurred. If we assume that the northeast- and northwest-trending block boundaries correspond to deep fractures of crustal scale, then we can reasonably assume that the movement of both heat and mass during and following extension may be concentrated near the block boundaries. In southeastern Arizona, many of the post-Laramide plutons are proximal to these geophysically defined boundaries. Geologic and geophysical studies have shown that within the regional blocks, extension has also occurred, and at least some instances of post-Laramide mineralization can be shown to be localized to extensional faults. Thus proximity to extensional domain boundaries is one criterion for favorability of post-Laramide mineralization. Many of the block boundaries may be determined by preexisting structure; if so, proximity to these boundaries becomes a favorability criterion for older mineralization as well, and it may explain why many known deposits are located on the edges of mountain ranges, which often are block boundaries.

In some areas of the forest, several plutons or plutonic complexes are of large enough volume (as determined by geophysical modeling) and near enough in age to the times of crustal extension to be heat sources for detachment-related precious-metal deposits. This definition fits several areas of favorability in the Santa Catalina, Galiuro, and Santa Teresa Mountains. Analysis of the aeromagnetic data in the Whetstone Mountains, supported by gravity anomaly and physical property data, suggests that the mountain range may be entirely underlain by intrusive rocks, probably of Tertiary age. The intrusives have "rafted" the range up and by their own thickness constitute a significant proportion of the uplift of the range. Geologic work by E.R. Force (described elsewhere in this volume) has demonstrated the same effect in the Santa Catalina Mountains. The intrusives constitute significant heat and possibly metal sources and render areas of the northern Whetstone Mountains favorable for replacement-type deposits where favorable host rocks are present. This type of model applies to several areas in the Coronado National Forest, notably the Chiricahua, Dragoon, and Santa Rita Mountains, in addition to those already listed.

Analysis of the gravity anomaly map of the Santa Rita Mountains and surrounding vicinity suggests that extension in at least the southern part of the range contains a strong rotational component in a clockwise sense. This component is presumably due to differential rotation across a boundary to the east with the Patagonia Mountains and the Canelo

Hills. The rotation is the apparent source of the tensional regime resulting in the east-west-trending zone of dikes that underwent silver mineralization. On the basis of this analysis, the favorable area for mineralization can be extended into areas of cover.

Although flightlines of the NURE study are too widely spaced (5 km) to be contoured onto maps for resource evaluation purposes, the flightline data can be projected and plotted onto maps that overlay geologic maps. In the Chiricahua Mountains, the gamma ray spectrometer data were used to show that the rhyolitic rocks in the southeastern part of the range were distinct from the Turkey Creek rhyolites in the rest of the range, even though no definitive mapping had been done in much of the southeastern region. Throughout the forest study area, the best data available for depth-to-source estimates came from NURE aeromagnetic profiles, because the flightline profiles preserve the observed gradients of the magnetic field rather than a smoothed version produced by a map. In the northern Santa Catalina Mountains, a consistent set of sources with depth-to-top of about 2 km below the surface was observed. These sources are probably magnetic contrasts in the host rocks below the Wilderness granite, and they provide additional evidence for a sill-like overall structure of the Wilderness suite. In the Patagonia Mountains, gamma ray spectrometer data from the NURE survey defined several areas of potassic metasomatism, one of which is mineralized. As all the areas of potassium metasomatism are somewhat favorable for mineralization by other criteria, the radiometric data provide another constraint on favorability for mineralization.

SOME STRUCTURAL FEATURES ALONG THE TUCSON-MOGOLLON CORRIDOR INFERRED FROM GRAVITY AND MAGNETIC ANOMALY DATA

Mark E. Gettings

Interpretation of a complete Bouguer gravity anomaly map and a regional aeromagnetic anomaly map has delineated several structural patterns, suggesting that in southeastern Arizona, regional-scale extension has occurred transverse to elongate, northwest-trending, generally tilted, structural blocks about 30 km in width (northeast-southwest) and with length:width ratios of about 4:1 for the major blocks. Structural blocks are cut off by northeast- or north-northeast-trending wrench zones that offset blocks by as much as a block width. The gravity anomaly map generally exhibits this regional-scale pattern of rectangular blocks more clearly, whereas on the aeromagnetic map, the pattern is overprinted by many lithologic variation anomalies; locally the aeromagnetic patterns define the northeasterly trending block-terminating structures. Preliminary estimates

of southwest-northeast extension suggest that it is of the order of 50–100 percent across the map area.

The Santa Catalina Mountains and Pinaleno Mountains metamorphic core complexes are included in the area of study, and both have similar gravity and magnetic anomaly patterns. These patterns are general gravity anomaly highs relative to the surrounding basins, but they include large superimposed anomalies caused by plutons and other sources in and adjacent to the complexes. Magnetic anomaly patterns over the core complexes are intricate; large lows correspond to the Eocene "Wilderness granite" (Shakel, 1978) sills of the Santa Catalina and Rincon Mountains and some of the gneisses and granites of the Pinaleno Mountains. A consistent relationship is gravity anomaly highs wherever there are mapped detachment faults and fragments of the upper plate exposed; the maximum of the high is slightly displaced from the detachment fault and over the upper plate. In the case of the Santa Catalina core complex, the anomaly maximum falls over the northern Tucson basin, a fact which has led to difficulties in regional-residual field separation in other gravity anomaly studies in the area. In the Pinaleno core complex, the gravity anomaly shows that the upper plate–lower plate boundary trends nearly south from the Santa Teresa Mountains across the range at Eagle Pass. The entire Mount Graham portion of the Pinaleno Mountains from Eagle Pass to the eastern terminus of the range appears to be a wrench or accommodation zone, with the upper plate absent. The gravity anomaly map suggests (but does not require) an upper plate–lower plate boundary at the east end of the range. Neither the gravity nor the magnetic data indicate the presence of a detachment fault along the northwest-trending edge of the range where it bounds the San Simon Valley. The upper–lower plate boundary also has a consistent magnetic high anomaly, which is displaced to magnetic south from the gravity anomaly maximum, as would be expected for a magnetic dipolar response. Thus, interpretation of the magnetic anomalies corroborates that of the gravity anomalies with regard to the location and trend of the detachment structures. Models of the correlative gravity and magnetic highs suggest that the Santa Catalina core complex actually has its axis of uplift approximately along the south edge of the Santa Catalina Mountains, as suggested on geologic evidence by E.R. Force (this volume). The presence of both gravity and magnetic highs requires a mafic composition for the material in the core of the core complex. Model calculations, together with measurements of magnetic susceptibility and bulk density, strongly suggest that the Pinaleno Mountains also are underlain by a similar mafic intrusive mass.

Constraints on extension in a structural block have been obtained in the Galiuro Mountains area. Gravity survey data in the Galiuro Mountains and surrounding San Pedro and Sulphur Springs Valleys have delineated a large circular gravity minimum about 40 km in diameter, interpreted to represent the gravity effect of the volcanotectonic depression

of the Galiuro Volcanics (Oligocene and Miocene). The circular gravity anomaly contains numerous northwest-trending gradients that correlate with faults exposed in the Galiuro Mountains and indicate the location of faults beneath the valley fill. The inference of buried faults in the San Pedro Valley has been corroborated by interpretation of detailed magnetic profiles collected with a truck-mounted magnetometer. These faults are the result of syn- and post-volcanic extension of the area along a northeast-southwest trend. A minimum extension in the mountain range of 15 percent can be demonstrated from exposed offsets of volcanic units on faults. Assuming similar dips for the faults beneath cover, a minimum extension of 15 percent since approximately 26 Ma (the oldest faulting dated by field relations in the Galiuro Volcanics) can be established for the area from the easternmost Santa Catalina Mountains bedrock in the Peppersauce Wash area to the westernmost outcrops of bedrock of the Pinaleno Mountains at the foot of Eagle Pass. Spacing between faults in this domain is of the order of 5 km with length:width ratios of about 4:1.

REFERENCE

Shakel, D.W., 1978, Supplemental road log number 2—Santa Catalina Mountains via Catalina Highway: New Mexico Geological Society 29th Field Conference Guidebook, p. 105–111.

GOLD-BEARING EXHALATIVE-HYDROTHERMAL SYSTEMS IN THE VENEZUELAN ANDES

Richard I. Grauch

Three regions (Mucuchies, Burbusay, Canaguá) of previously unrecognized, submarine exhalative-hydrothermal activity have been recognized in the Venezuelan Andes. Coticule (spessartine-quartz rock) and tourmalinite interlayered with pelitic schist, amphibolite, and felsic gneiss are indicators of premetamorphic, submarine exhalative-hydrothermal activity. Protoliths of the coticule were probably manganiferous chert and silt, whereas that of the tourmalinite was most likely boron-metasomatized sediment. At least one region, Mucuchies, contains gold in upper amphibolite-facies metamorphites, specifically in coticule, tourmalinite, and sulfide-rich gneiss.

In the Mucuchies region, coticule occurs as thin (as much as 1 cm thick) interlayers in quartz-biotite–two-feldspar schist that is part of a Paleozoic(?) sequence of sillimanite-grade schist, amphibolite, and felsic gneiss. Peridotite is a minor component of the sequence and is associated with an abnormal amount of amphibolite. Garnet in the coticule is fine grained (1–3 mm in diameter), optically unzoned, and

compositionally homogeneous (approximately 30 percent spessartine, 60 percent almandine, 7 percent pyrope, and 3 percent grossular). The predominant opaque phase is Mn-Zn-bearing ilmenite. Trace amounts of a Fe-Cu-Zn-S phase, a REE-P (rare-earth-element–phosphorus) phase, and a Au-Te phase with minor Ag are also present. The Au-Te phase occurs as small (<1 μm long) grains on the rims of garnet and as inclusions in biotite and both feldspars. The tourmalinite (>80 volume percent tourmaline) has been found only as float but must be part of the same lithologic sequence as the coticule. Translucent phases are dravite (MgO/FeO=0.6 to 1.0), quartz, biotite, two feldspars, and trace amounts of a REE-P phase. The opaque assemblage consists of graphite, Mn-bearing ilmenite, chalcopyrite, and trace amounts of phases composed of Fe-S, Pb-S, and Au-Te with minor Ag. The Au-Te phase occurs as small inclusions in tourmaline and quartz. The sulfide-rich gneiss occurs about 10 km along strike from the coticule. It is composed of quartz, two feldspars, biotite, muscovite, almandine garnet, and a REE-P phase. Minor amounts of Mn-bearing ilmenite and Fe-S, Fe-Cu-S, Fe-Cu-Zn-S, and Au-Te phases make up the opaque assemblage. The Au-Te phase has minor Ag and occurs as small inclusions in biotite. Cordierite-bearing gneiss in the vicinity of the sulfide-rich gneiss may be a further indication of premetamorphic hydrothermal activity (magnesium metasomatism) in the region.

Tourmalinite in the Burbusay region occurs in a middle to late Paleozoic sequence of staurolite-bearing pelitic schist, quartzite, and amphibolite. Fine-grained garnetiferous quartzite (possibly coticule) is a minor but widely distributed portion of the sequence. The tourmalinite is a two-mica-tourmaline (approximately 30 volume percent)-quartz schist. Apatite, a REE-P phase, and a Y-P (yttrium-phosphorus) phase are minor components of the rock. Tourmaline compositions are more magnesian than those in the Mucuchies region; MgO/FeO values exceed 1. Opaque phases include ilmenite and chalcopyrite; the latter phase occurs as inclusions in tourmaline and quartz.

Tourmalinite in the Canaguá region occurs within the same stratigraphic unit as that in the Burbusay region. Although the exact nature of the surrounding lithologies is not known, they are, in general, greenschist-facies phyllite (in part, graphitic) and amphibolite. Forty kilometers across strike from Canaguá, the same unit hosts the small, high-grade Bailadores massive Zn-Pb-Cu sulfide deposit.

The lithologic packages, especially in the Mucuchies region, that host the coticule and tourmalinite are indicative of ocean floor deposition. Graphite in the tourmalinite indicates that at least some of the original sediments were deposited in a restricted basin. Base metals within the coticule and tourmalinite are strong indications of metalliferous, exhalative-hydrothermal activity in a marine environment, and their presence suggests the possibility of sediment-hosted base-metal deposits in regions far removed from the Bailadores deposit. The gold and tellurium in the Mucuchies region

represent unusual, but not unprecedented, metal accumulations in exhalative, marine environments. Their economic and petrogenetic significance remains to be examined.

REDEFINITION OF LATERITIC BAUXITE DEPOSIT TYPES, NORTHERN SOUTH AMERICA SHIELD

Floyd Gray, James D. Bliss, Norman J Page, Herbert A. Pierce, and Barbara Eiswerth

Bauxite deposits are widely variable in their origin and geological settings, and various classification schemes can be found in the literature (Harder, 1952; Patterson, 1967, 1986; Hill and Ostojic, 1984). Many of the classifications for the important deposits of northern South America combine genesis, elevation, age, parent rock, and tectonic setting, although they generally recognize two important groupings: bauxite developed in upland areas and those deposits formed on lowland peneplains in sedimentary settings (Van Kersen, 1956; Moses and Michell, 1963; Bleackley, 1964; Grubb, 1973a, b; Aleva, 1981; Aleva and Hilversum, 1984; Menendez and Sarmentero, 1984). We propose to redefine the known and potential bauxite resources of the northern margin of the Guayana Shield as being of two broadly defined types: *remnant* and *continentally derived detrital* (fig. 1). These two types are distinguished by their stratigraphic profile and geomorphologic settings. Other characteristics such as age, thickness, elevation, chemistry, textural variation, and cover sequences cannot be used to discriminate between these deposits.

Remnant deposits result from weathering of underlying bedrock. The deposits grade downward from the bauxite horizon into kaolinized bedrock, weathered bedrock, and unweathered bedrock material (fig. 1, profile A–B). Bedrock can include various aluminum-bearing igneous, sedimentary, and metamorphic rocks, although unmetamorphosed sedimentary rocks are rare. Bauxitization is a complex, multistage process that may have begun as early as Late Cretaceous in South America, although the majority of the deposits studied are Eocene to recent in age. These deposits

Figure 1 (Gray, Bliss, and others) (facing page). Generalized profiles of lateritic bauxite types, northern South America. Three types of exposures for remnant-type deposits are presented in cross section A-B. Two types of exposures for continentally derived detrital deposits are represented by cross section C-D. The three types of outcrops for remnant deposits shown are (1) topographically prominent deposits subject to dissection, (2) topographically indistinct deposits subject to continued bauxitization (may be partly buried with younger sediments), and (3) blind deposits totally covered with sediments. The two types of continentally derived detrital deposits are (4) topographically prominent deposits, and (5) blind deposits covered by recent sediments. Modified from Van Kersen (1956).

Transgressive cover rocks
Bauxite
Kaolinite-bauxite

Weathered bedrock

Unweathered bedrock

A

1

2

3

B

Arkosic sand

unconformity

Bauxite with carbonaceous clay lens

Sedimentary kaolinite with carbonaceous clay lens (bauxitized)

unconformity

Weathered bedrock

Unweathered bedrock

C

4

White coastal sands

5

D

NOT TO SCALE

EXPLANATION

Sediments   Weathered bedrock

Bauxite   Crystalline bedrock

Kaolinite   Arkosic sand

can be at high elevations or at sea level but are predominantly residual in origin. Pakaraima Mountains, Guyana, Nassau Mountains, Suriname, and Los Pijiguaos, Venezuela are examples of this deposit type.

Continentally derived detrital deposits are found in sediments shed off the margin of the Precambrian crystalline basement complex (fig. 1, profile C–D) as typified in the coastal plain of Suriname. Arkosic sandstone is the dominant lithology with variable minor occurrences of intercalated carbonaceous sandy clay lenses, kaolin, and shale. The sedimentary sequence hosting this deposit type is part of deltaic and (or) large alluvial basin systems and unconformably overlies crystalline basement rocks that may include remnant-type bauxite horizons. Bauxitization of the transported sedimentary beds has resulted in bauxite and kaolin-rich beds resting unconformably above weathered bedrock.

The sedimentary deposits historically have formed the bulk of the production of low-iron refractory-grade bauxite in northern South America since the turn of the century, principally from Guyana (Ituni, Mackenzie) and eastern Suriname (Onverdacht, Moengo). A high-grade (refractory) exception is the large Venezuelan Los Pijiguaos deposit, which overlies alkaline leucogranite. Remnant deposits found on the shield have been exploited but generally produce a nonrefractory-grade, high-iron bauxite with variable and lower ore grades (Aleva and Hilversum, 1984).

Redefinition of the classification of bauxite deposits may affect (1) delineation of areas with potential for undiscovered deposits; (2) development of grade, tonnage, and exploration models; and (3) environmental characterization. Exploration for remnant deposits is best facilitated by analysis of regional erosion surfaces using elevation, geobotanical mapping by Thematic Mapper and radar, and field sampling (shallow core). Exploration for continentally derived detrital deposits requires profiles of edges of basin structures using gravity or seismic data, age and subsidence rate analysis, core drilling, and sampling. Regional tectonic analysis is important in the assessment for both deposit types. For example, the rate of uplift of the Imataca terrane (Venezuela) and the Bakhius Mountains horst (Suriname) affected the isostatic equilibrium of the shield and the subsidence rates of adjoining basins in northern South America, thereby affecting the shape of potential domains for bauxite resources. Using these newly defined deposit types to assess lateritic bauxite potential may change the calculated bauxite reserves for the area, and these newly defined models may be applied to other regions of South America as well as to other continental regions where lateritic processes occur.

REFERENCES

Aleva, G.J.J., 1981, Essential differences between the bauxite deposits along the Southern and Northern edges of the Guiana Shield, South America: Economic Geology, v. 76, p. 1142–1152.

Aleva, G.J.J., and Hilversum, A.H., 1984, Bauxite in West Suriname—Known deposits and potential, *in* Leonard, Jacob, Jr., ed., Bauxite; Proceedings of the 1984 Bauxite Symposium, Los Angeles, Calif., Feb. 27–March 1: New York, Society of Mining Engineers AIME, p. 319–348.

Bleackley, D.,1964, Bauxites and laterites of British Guiana: British Guiana Geological Survey Bulletin 34, 154 p.

Grubb, P.L.C., 1973a, Genesis of bauxite deposits in the Lower Amazon Basin and Guianas Coastal Plain: Economic Geology, v. 74, p. 735–750.

———1973b, High-level and low-level bauxitization—A criterion for classification: Mineral Science and Engineering, v. 5, p. 213–231.

Harder, E.C., 1952, Examples of bauxite deposits illustrating variations in origin: Proceedings from Problems of Clay and Laterite Genesis Symposium, Society of Mining Engineers AIME, p. 35–64.

Hill, V.G., and Ostojic, Slavko, 1984, The characteristics and classification of bauxites, *in* Leonard, Jacob, Jr., ed., Bauxite; Proceedings of the 1984 Bauxite Symposium, Los Angeles, Calif., Feb. 27–March 1: Society of Mining Engineers AIME, p. 31–48.

Menendez, Alfredo, and Sarmentero, Alberto, 1984, Geology of the Los Pijiguaos bauxite deposit, Venezuela, *in* Leonard, Jacob, Jr., ed., Bauxite; Proceedings of the 1984 Bauxite Symposium, Los Angeles, Calif., Feb. 27–March 1: Society of Mining Engineers AIME, p. 387–407.

Moses, J.H., and Michell, W.D., 1963, Bauxite deposits of British Guiana and Suriname in relation to underlying unconsolidated sediments suggesting two-step origin: Economic Geology, v. 58, p. 250–262.

Patterson, S.H., 1967, Bauxite reserves and potential aluminum resources of the world: U.S. Geological Survey Bulletin 1228, 176 p.

———1986, Descriptive model of laterite type bauxite deposits, *in* Cox, D.P., and Singer, D.A., eds., Mineral deposit models: U.S. Geological Survey Bulletin 1693, p. 255.

Van Kersen, J.F., 1956, Bauxite deposits in Surinam and Demerara (British Guiana): Liedse Geologische Mededelingen, v. 21, p. 249–373.

MINERAL RESOURCE ASSESSMENT OF THE VENEZUELAN GUAYANA SHIELD

Floyd Gray, Jeffrey C. Wynn, Greta J. Orris, Norman J Page, William E. Brooks, Gary B. Sidder, Warren C. Day, J.D. Bliss, Dennis P. Cox, David Detra, Jason Unkefer, and John Gutierrez

A quantitative mineral resource assessment of the Venezuelan Guayana Shield is the result of a 5-year cooperative scientific program sponsored by U.S. Geological Survey and the Corporacion Venezolana de Guayana, Tecnica Minera C.A. Products of the assessment include a series of

Table 1 (Gray, Wynn, and others). Probability estimates of undiscovered deposits in the Venezuelan Guayana Shield.

Deposit type	Chance of occurrence				
	90 percent	50 percent	10 percent	5 percent	1 percent
Algoma iron	9 or more	26 or more	90 or more		
Low sulfide gold-quartz veins	20 or more	40 or more	50 or more		
Carbonate	2 or more	5 or more	12 or more		
Kuroko massive sulfide				1 or more	
Synorogenic-syn-volcanic nickel-copper					1 or more
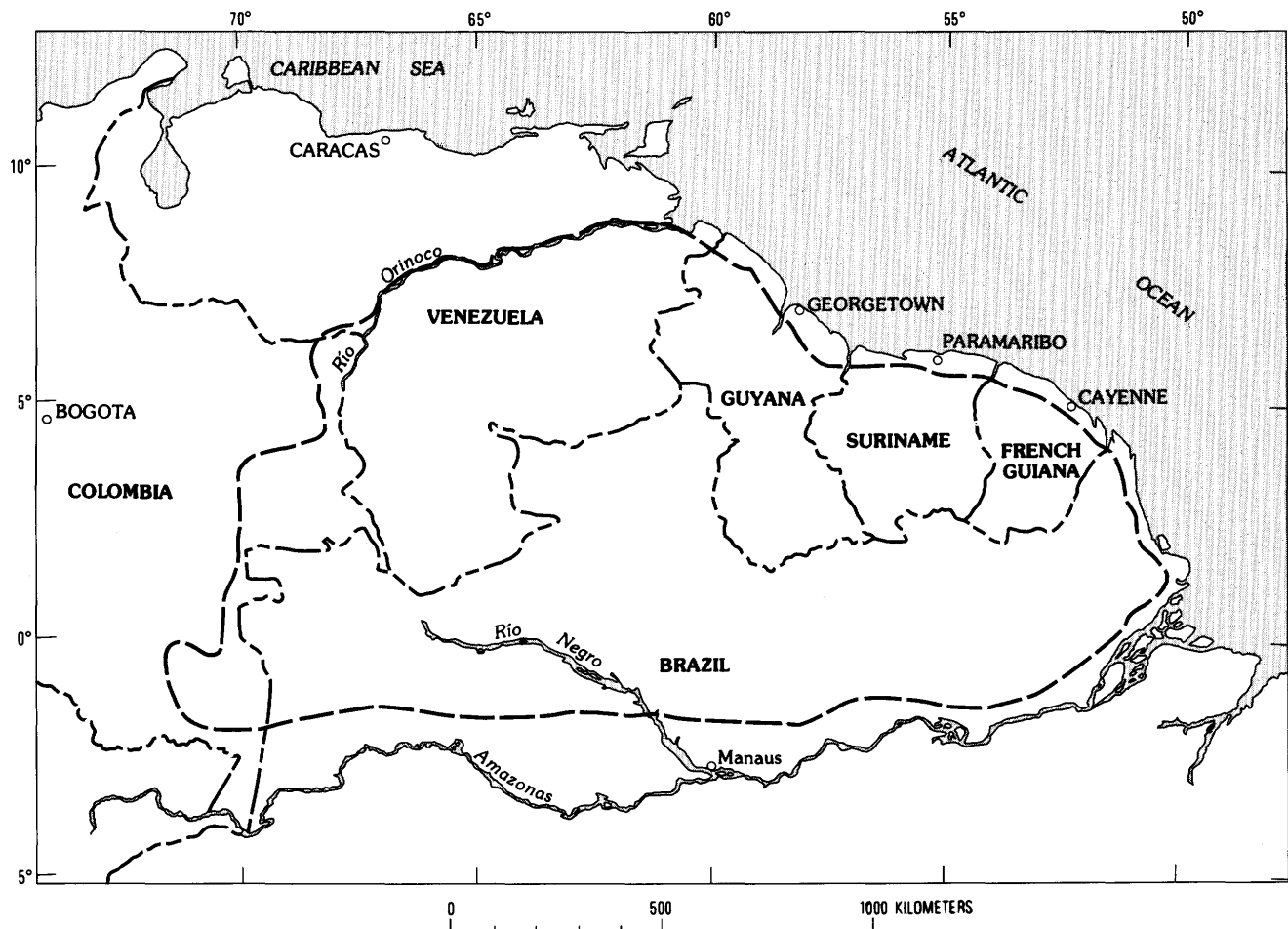
Figure 1 (Gray, Wynn, and others). Index map showing location of Venezuelan Guayana Shield (dashed outline) in northern South America.

1:1,000,000-scale maps and accompanying text, which characterize the mineral potential of the Venezuelan Guayana Shield, an area of Precambrian terrane in the south and east half of Venezuela, encompassing more than 415,000 km². These are supported by a geographic map, geologic and tectonic map, simple Bouguer gravity anomaly map, side-looking airborne radar (SLAR) image, two mineral occurrence maps, and two permissive domain maps.

U.S. Geological Survey mineral resource assessment methodology comprises three parts: (1) selection of

appropriate descriptive deposit models and delineation of areas permissive for each deposit type; (2) construction of a grade-tonnage model for each deposit model; and (3) probabilistic estimation of the number of undiscovered deposits for model types with sufficient data. These estimates are made using the deposit density and the target counting methods. Thirteen known deposit types are identified in the Venezuelan Guayana Shield, and nine other deposit types are possible. Quantitative estimates of undiscovered deposits were made for five deposit types: Algoma iron, low-sulfide gold-quartz veins, carbonatite, kuroko massive sulfide, and synorogenic-synvolcanic nickel-copper (table 1); data are insufficient to estimate the number of undiscovered deposits for the remainder.

Deposits in deeply eroded regions, such as the Imataca and Pastora-Supamo terranes, contain mineral deposits that (1) were formed in the Archean and Early Proterozoic, infolded with their host rocks, and metamorphosed; or (2) were formed during, or soon after, regional metamorphism associated with the Trans-Amazonian orogeny. These deposits include stratiform iron and manganese at Cerro Bolivar and El Pao, and deposits of gold in quartz veins from the El Callao, Kilometer 88, and Lo Increible districts, and elsewhere.

Sedimentary rocks of the Roraima Group, volcanic rocks of the Cuchivero Group, and epizonal plutonic rocks that intrude Cuchivero Group rocks form a supracrustal terrane that is a potential host for deposits formed near, or within a few kilometers of, the surface during the Early to Middle Proterozoic. These deposits include carbonatite and diamond pipes, as well as yet to be discovered deposit types such as tin greisen, porphyry copper, volcanic-hosted iron deposits, and polymetallic or epithermal veins.

Surficial processes such as erosion and chemical weathering, followed by uplift of the Venezuelan Guayana Shield, have created many permissive environments for mineral deposition. Deposits formed by leaching and residual enrichment of metals and nonmetals include bauxite, iron, kaolinite, and possibly nickel laterite. Transport and deposition of metals and minerals produced placer deposits of gold, diamonds, tin, and titanium. In the northern part of the shield, most placer deposits were formed during Miocene to Quaternary time, coinciding with the time of maximum uplift. Some deposit types, for example, sedimentary kaolin, are produced by a combination of these processes.

This study provides information for mineral-related land-management decisions affecting future mining activity and a framework for identifying areas affected by past and present mining activity needing environmental mitigation and concurrent reclamation. A careful review of the data obtained during the course of this cooperative agreement will form the basis for future studies. Results of these investigations will serve, in part, to guide the growth and development of the Venezuelan mineral sector in the future.

MINERAL RESOURCE ASSESSMENT OF THE ABSAROKA-BEARTOOTH STUDY AREA, CUSTER AND GALLATIN NATIONAL FORESTS, MONTANA

J.M. Hammarstrom, M.L. Zientek, J.E. Elliott, R.R. Carlson, G.K. Lee, B.S. Van Gosen, and D.M. Kulik

The Absaroka-Beartooth study area encompasses approximately 1.4 million acres in the Custer and Gallatin National Forests of southwestern Montana. The area contains most of the identified lode resources of platinum-group elements and the largest identified chromium resource in the United States. Mines have operated in the area since the 1860's and have produced gold, silver, copper, lead, zinc, arsenic, tungsten, chromium, platinum-group elements, and travertine. Exploration by industry since 1970 led to the discovery and development of platinum-group element deposits of the Stillwater mine and gold deposits of the Mineral Hill mine and the discovery of gold-copper-silver deposits in the New World district. Recent exploration efforts have focused on gold, chromium, platinum-group elements, and oil and gas.

A 2-year study of the geology, geochemistry, geophysics, exploration history, and nature and distribution of mineral occurrences enabled a USGS team to delineate nine tracts of land as geologic environments deemed permissive for the occurrence of 20 different types of mineral deposits. Favorable areas for undiscovered deposits are delineated within some permissive tracts. Important geologic controls on the occurrence of mineral deposits in the study area include the following: (1) an Archean metasedimentary package of rocks that includes banded iron-formation and hosts a lode gold (+arsenic+tungsten) deposit at the Mineral Hill mine; (2) the Stillwater Complex, an Archean layered mafic intrusion that hosts disseminated to massive copper-nickel sulfide deposits near its base, chromite layers, and a thin, laterally persistent horizon enriched in platinum-group elements (the J-M Reef), which is partially exploited by the Stillwater mine; and (3) at least five deeply eroded Cretaceous to Eocene stratovolcano centers that have associated porphyry copper-gold-molybdenum and related copper-gold skarns and polymetallic vein deposits.

Estimates of undiscovered resources for selected commodities are made by combining probabilistic estimates of numbers of undiscovered mineral deposits with grade and tonnage models (Cox and Singer, 1986; Theodore and others, 1991) in a computer simulation (Root and others, 1992) to describe expected distributions of commodities contained in-place in undiscovered mineral deposits. Results of the simulation for four types of mineral deposits (Archean lode gold, banded iron-formation, porphyry copper, and

gold-bearing skarn) indicate a 50 percent chance that undiscovered deposits contain at least 90 t (metric tons) of gold, 700 t of silver, 3.1 million t of copper, 35,000 t of molybdenum, 62 million t of iron, and 3,000 t of phosphorus (as a byproduct of potential iron ore). These results provide a quantitative basis for including mineral information in land-use planning; however, an economic analysis must be conducted to estimate any potential net worth of minable resources.

Evaluation of exploration data for three additional types of mineral deposits in the Stillwater Complex indicates that approximately 225,000 t each of copper and nickel and 6.5 million t of chromium may be present in undiscovered deposits. Extensions of identified resources within the Stillwater Complex may contain additional resources of these commodities as well as gold and platinum-group elements.

REFERENCES

Cox, D.P., and Singer, D.A., eds., 1986, Mineral deposit models: U.S. Geological Survey Bulletin 1693, 379 p.

Root, D.H., Menzie, W.D., and Scott, W.A., 1992, Computer Monte Carlo simulation in quantitative resource estimation: Nonrenewable Resources, v. 1, p. 125–138.

Theodore, T.G., Orris, G.J., Hammarstrom, J.M., and Bliss, J.D., 1991, Gold-bearing skarns: U.S. Geological Survey Bulletin 1930, 61 p.

AGRICULTURAL MINERAL MINING, PROCESSING, AND USE— ENVIRONMENTAL RESEARCH OPPORTUNITIES

James R. Herring and Larry P. Gough

The agricultural minerals (nitrogen, phosphate, potash, sulfur, zeolites) are responsible for providing or moderating release of the principal agricultural nutrients (N, P, and K) and are vital to the United States agricultural industry and economy. Their value to the national economy is the sum of (1) their intrinsic value as mined commodities (equal to 10 percent of nonconstruction mineral value to the U.S. economy); (2) their additional contribution because of manufacturing-added value (about 5 billion dollars); (3) export value and contribution to the balance of payments and foreign trade; and (4) their use as required nutrients to grow food in the Nation, 40 percent of which is exported and further contributes to trade (about 15 billion dollars export value). Continued production and best use of these minerals depend greatly on understanding their environmental interactions; consequently, our goals are twofold: (1) to use these minerals in ways most beneficial and least harmful to the ecosystem and (2) to understand the optimal rates and methods of mining use that will allow their sustained availability to a growing society.

Zeolites offer possibilities for environmental remediation principally by their ion exchange properties. This technology may be useful to many industries, for example, metal mining, where waste-water streams must be cleaned of metallic and other impurities to meet certain discharge criteria.

In the United States, most sulfur is used to produce sulfuric acid; in turn, most of the sulfuric acid is used to produce phosphoric acid for fertilizers. About half the sulfur used in the United States is obtained through the frasch process, which produces a clean, reagent-grade product. However, much of the remainder of the sulfur—obtained from secondary recovery from mineral and fossil fuel processing—involves association between sulfur and trace elements of environmental concern, such as zinc, cadmium, and arsenic, that are released during cleaning, processing, or use of the fuel. Residual sulfur compounds left in coal, both sulfides and organosulfur compounds, also contain noxious trace elements that are released during combustion. USGS efforts address these considerations in the coal-quality program.

Nitrogen fertilizer is not a rock-sourced nutrient but subsequently enters the geosphere because of application, plant uptake, and soil interaction. The environmental concerns associated with agricultural nitrogen involve its release to surface, vadose, or ground waters after application as a crop nutrient. Current interest in the USGS is in nitrogen interaction with these waters and is focused in the toxic-substances and water-quality programs.

In the United States, the bioessential nutrient phosphorus is obtained from world-class deposits of phosphorite. Because of inequities in world resource distribution and interplay of politics and economics in use of global reserves, phosphate is regarded as the most critical agronutrient and the key to world food supply. U.S. production supplies its internal needs as well as providing about 30 percent of world phosphate trade (about 3 billion dollars in trade revenue). Major environmental concerns result from the complete phosphate use cycle, from mining and manufacturing to use and disposal. Current USGS research involves characterization of clay type (important to settling characteristics of the fine-grained waste), other waste products (acidic gypsum heaps), radioactivity, and trace element assemblages in presently mined and potential future reserves of phosphorite. Also being studied are depletion models of known reserves and scenarios for best future use that will lead to optimal resource demand for a sustainable global food supply.

The United States produces only 30 percent of the potash that it uses, all from evaporite deposits. The principal environmental consideration associated with the production of potash is disposal of waste salt and clay. Waste salt is produced at approximately 2 tons per ton of mined potash.

Significant environmental considerations are involved with the mining, pressing, manufacturing, and use of these agricultural minerals. Some of these considerations are being addressed by present USGS research. However, many additional environmental concerns offer future research opportunity.

MINERAL RESOURCES, ENVIRONMENTAL CONCERNS, AND LAND-USE

Carroll Ann Hodges

Among the most vigorously debated issues in U.S. economic geology circles is the extent to which nonfuel minerals industries, and thereby the Nation, are adversely affected by land restrictions and environmental regulations, and public advocacy thereof (Ward, 1992; Hale, 1992). A presumed grave consequence is the departure of mining companies for more hospitable shores. (See, for example, Cameron, 1986.) The relative importance of factors such as labor costs, ore tonnage and grade, political stability, investment incentives, and exploration potential—as well as U.S. foreign policy interests—is seldom addressed in public commentary. The global political and economic cataclysms that introduced the 1990s presage far more extensive international interdependence in world minerals trade as centrally planned economies strive to become market-driven. The producer oligopoly that prevailed in the decades of strong economic growth following World War II is dramatically diminished in today's global metal markets (Bomsel, 1990).

Contrary to predictions from the 1950s through the early 1980s, persistent, widespread shortages of nonfuel minerals have never occurred, partly because exploration has been remarkably successful. Despite increased rates of consumption, present estimates suggest that world mineral supplies are adequate for the foreseeable future (McLaren and Skinner, 1987; Pearse, 1991; Vogely, 1993). Stable or declining prices, the potential availability of new and presumed large ore resources abroad (due in part to the demise of the Soviet economy as well as to new discoveries elsewhere), increased recycling, technological innovation and substitution—all affect supplies of raw materials and thus are relevant to policy decisions regarding mineral development, use of U.S. public lands, and attendant environmental concerns.

The 1991 "Earth Summit" in Rio de Janeiro demonstrated that environmental consciousness is not unique to the industrialized world; prevention and mitigation of environmental problems are increasingly required elsewhere, partly as a result of United Nations encouragement and recent dictates from the World Bank. The Berlin Guidelines, established at a United Nations conference in June 1991, mandate attention to environmental impacts, while at the same time ensuring the long-term economic and social benefits that mineral development can provide, specifically to resource-rich countries of the Third World. Social (external) costs of mining historically have not been incorporated in commodity prices, but that may change on world markets; developing nations have made it clear that environmental protection is of major concern internally and not merely "a luxury item peddled by first world participants" (United Nations, 1993). The newly created (March 1991) International Council on Metals and the Environment (ICME) was established specifically to promote sound environmental policy for the industry worldwide. Rigorous adherence to high standards for environmental protection may be as applicable abroad as in the United States sooner rather than later; the "writing is on the wall" (Mining Journal, 1991).

Since World War II, U.S. policy objectives have included acquisition of necessary raw materials at lowest possible prices, consistent with the interests of our trading partners and with other foreign policy goals (President's Materials Policy Commission, 1952). Self-sufficiency is no longer even remotely possible, and thus a major goal must be to ensure adequate and dependable foreign sources of supply. Interests of the Nation may now include (in *addition* to domestic jobs) economic development in those countries dependent on mineral rents, without which improvement in education and living standards and a consequent reduction in birth rates are unlikely. Continued population growth at rates between 2 and 4 percent in much of the less developed Southern Hemisphere (World Resources Institute, 1992) poses dire implications not only for those nations striving to improve economic status, but also for the industrialized North and for the planet's entire ecosystem. It may behoove the United States to take the less parochial view that investment in mineral deposits overseas is advantageous politically and economically, abetting improved education and living standards in developing countries, while maintaining favorable consumer prices at home. Transfer of efficient "green" technology abroad can ensure that the pollution we now attempt to clean up will be avoided altogether in new projects overseas. The issues are complex, but the United States may, like Japan, become increasingly dependent on foreign raw materials, irrespective of domestic environmental regulations—or mining law reform.

As world tensions diminish and trade expands, concerns about U.S. self-sufficiency and military security no longer seem overriding. Of greater importance may be the contribution of mineral resources to the economic rescue of some emerging nations—and a consequent reduction of fertility rates, without which environmental concerns are ultimately irrelevant.

46

REFERENCES

Bomsel, Olivier, 1990, Mining and metallurgy investment in the third world—The end of large projects?: Development Centre Studies, OECD, 221 p.

Cameron, E.N., 1986, At the crossroads—The mineral problems of the United States: New York, John Wiley, 320 p.

Hale, Alma, 1992, Public lands legislation—Drowning in a sea of bills: AMC Journal, August 1992, p. 5–6.

McLaren, D.J., and Skinner, B.J., eds., 1987, Resources and world development: Chichester, U.K., John Wiley, 940 p.

Mining Journal, 1991, Writing is on the wall: Environment Supplement, v. 317, no. 8140, p. 1.

Pearse, P.H., 1991, Scarcity of natural resources and the implications for sustainable development: Natural Resources Forum, February 1991, p. 74–79.

President's Materials Policy Commission, 1952, Resources for freedom, Summary of Volume I: 82 p.

United Nations, 1993, Interregional seminar on guidelines for the development of small/medium scale mining; Seminar Report, U.N. Department of Economic and Social Development (UNDESD) and Government of Zimbabwe, 15–19 February 1993, Harare, Zimbabwe: 38 p., 7 annexes.

Vogely, W.A., 1993, An economist looks at resource assessment: Non-Renewable Resources, v. 2, no. 2, p. 67–68.

Ward, Milton H., 1992, Mining law repeal effort is 'wrong-headed' AMC Journal, February 1992, p. 26–27.

World Resources Institute, 1992, World resources, 1992-'93, A guide to the global environment: New York, Oxford, p. 246–247.

NATIONAL GEOCHEMICAL DATA BASE

J.D. Hoffman and S.P. Marsh

The National Geochemical Data Base (NGDB) contains data from geochemical surveys conducted by the U.S. Geological Survey and other Federal Government agencies, including data from the NURE (National Uranium Resource Evaluation) HSSR (Hydrogeochemical and Stream Sediment Reconnaissance) program (1976–1980) from the National Wilderness Program (1965–present) and from numerous mineral resource assessment and geologic projects. The NGDB is maintained and controlled by the geochemistry staff of the U.S. Geological Survey. Administrators, land-use planners, and scientists can use this multipurpose data base to influence their decisions concerning health, the environment, and mineral resources. Because large portions of the data were collected in the 1960's and 1970's, they can be used in "baseline" studies to establish background values for many metals in areas that have since been developed.

The portion of the NGDB that most represents regional coverage for the United States is the data collected during the NURE HSSR. These data represent the only regional geochemical data base for the conterminous United States and Alaska. Most of these data were compiled from analyses of stream sediments, soils, and ground water and surficial water. Each sample was analyzed utilizing various chemical methods including INA (induced neutron activation), AA (atomic absorption), and ES (emission spectrography) for uranium and as many as 58 other elements, plus sulfate. The USGS has undertaken the reanalysis of the NURE HSSR samples using multi-element inductive coupled plasma (ICP) and low-level (parts per billion) gold techniques.

The history of the NURE HSSR program is complex. Starting in 1974, NURE program personnel acquired and compiled geologic and other information required to evaluate the extent and distribution of uranium resources and to determine areas favorable for the occurrence of uranium in the United States. The HSSR survey sampling component of the program began in 1976 and ended in 1980. Initially, the samples were analyzed only for uranium. In 1977, analyses for other elements were added.

Four DOE (Department of Energy) national laboratories were involved in the survey: Lawrence Livermore Laboratory, Los Alamos Scientific Laboratory, Oak Ridge Gaseous Diffusion Plant, and Savannah River Laboratory. Each developed its own procedures for sample collection, analyses, and data management; these procedures were sometimes altered during the life of the program. In 1977, the laboratories were instructed to conform all sampling and data management to the 1°×2° NTMS grid system. This decision resulted in incomplete coverage in some States, mainly along their borders; also, some quadrangles were sampled by more than one laboratory. An inevitable consequence of using the analytical capabilities of all four laboratories and the multiple procedural changes was the generation of 47 different data formats. In addition, some of the national laboratories subcontracted analytical work to one or more of the other national laboratories and to private laboratories.

Under contract to the DOE, the Information Systems Programs of the Energy Resources Institute, University of Oklahoma, Norman, reorganized substantial portions of the data into one format (1983–1985). In 1985, a memorandum of understanding between the DOE and the Department of the Interior transferred responsibilities for maintenance of HSSR samples and HSSR data collected under the NURE program to the U.S. Geological Survey.

The NURE HSSR data for the western United States, using the reformatted data, have been published as USGS Publication DDS-0001 using Compact Disc-Read Only Memory (CD-ROM) technology. A CD-ROM for the Alaska NURE HSSR data and a CD-ROM containing all the NURE HSSR data for the conterminous United States are also being developed. A fourth CD-ROM publication is to contain the NURE HSSR data in the original formats, plus indexes and a user's guide. In all, the NURE HSSR data encompass 428 1°×2° quadrangles in the conterminous United States and Alaska, totaling about 850,000 records.

Data may be retrieved from Publication DDS-0001 according to sample type, quadrangle, latitude and longitude, element, element concentration range, or any combination of these criteria. Once the requested data are found, they may

be written in dBASE format or several different ASCII formats to the user's hard disk. Context-sensitive help files are available. The prototype Alaska and conterminous United States CD-ROM's have similar structures and capabilities.

LA ESPAÑOLA PROSPECT—A MULTIPLE INTRUSIVE PORPHYRY COMPLEX WITH LOW-GRADE GOLD POTENTIAL, NORTHWESTERN ALTIPLANO, BOLIVIA

Albert Hofstra, Luis Barrera, Richard Hardyman, Edwin Mckee, and Orlando Sanjines

La Española prospect lies in the Bolivian portion of the Neogene to Quaternary magmatic arc of the central Andes (lat 17°14′ S., long 69°31′ W.). La Española was selected for study because it is the most intense color anomaly on remote sensing imagery of this part of the arc and because gold was found during recent prospecting. Field mapping, geochronology, exploration geochemistry, and fluid-inclusion studies were conducted by geologists from GEOBOL (Servicio Geologico de Bolivia) and the USGS in an effort to determine the origin of the gold-anomalous rocks at La Española. The results suggest that La Española can be characterized as a multiple intrusive porphyry complex with epithermal alteration/mineralization assemblages superimposed on deeper porphyry-style assemblages.

The hydrothermal system is centered on a 1.5×3 km composite andesite to dacite porphyry stock that intrudes Oligocene to middle Miocene andesite to dacite flows, lahars, and volcaniclastic sedimentary rocks. The stock consists of at least four early intrusive phases, including one distinguished by an abundance of miarolitic cavities. In most places these intrusions are pervasively altered to an assemblage of quartz, sericite, and pyrite, although potassic and propylitic alteration is also present. These altered porphyries are intruded by several small unaltered dacite porphyry dikes and plugs. K-Ar determinations on hornblende in premineralization dacite flows (11.2±0.7 Ma) and on biotite from a premineralization intrusive phase in the stock (11.8±0.8 Ma) indicate the stock was emplaced between about 12.6 and 10.5 Ma. Alunite, associated with vuggy silica alteration that crosscuts the early altered porphyries, is dated at 10.3±0.3 Ma, indicating that alteration and mineralization soon followed emplacement. The volcanic edifice inferred to have overlain La Española has been completely stripped away. Nearby volcanoes, 1–2 km higher in elevation than La Española, are dated at 4–8 Ma.

Four types of alteration/mineralization are recognized at La Española: (1) black, porphyry-style stockwork veinlets, in potassically altered portions of the stock, consist of quartz, ±pyrite, ±bornite, ±chalcopyrite, ±magnetite, ±gold; (2) stockwork veinlets, in phyllically altered portions of the stock, consist of pyrite, sericite, quartz, ±gold; (3) quartz–base-metal veins with sericitic alteration, in fractures marginal to the stock, contain pyrite, chalcopyrite, sphalerite, ±galena; (4) acid-sulfate alteration, along structures within and marginal to the stock, is characterized by an early stage of vuggy silica and quartz-alunite alteration and a second stage of silicification with pyrite, barite, ±enargite, ±silver sulfosalts, ±galena, ±sphalerite, ±gold.

Altered rocks contain low but anomalous concentrations of Au, Ag, As, Cu, Hg, Mo, Pb, Sb, and Zn. Rock samples from the stockwork zones show that gold is correlated with elevated copper values whereas the acid-sulfate zones are characterized by elevated Ag, As, Sb, ±Au and base metals. Gold potential is primarily in stockwork zones in the altered porphyries. Bulk samples from stockwork zones at the surface have gold values of 0.05 to 1.7 ppm. Samples of stream sediment collected from drainages surrounding the stock contained low parts per billion-level gold values below each of the known mineralized areas. Heavy-mineral concentrates and moss were less effective sample media.

Secondary fluid inclusions in quartz lining miarolitic cavities are either hypersaline, containing halite daughter minerals, or undersaturated with halite. Preliminary homogenization temperature data vary widely from 400 to 200 °C. Fluid inclusions in quartz–base-metal veins and acid-sulfate mineralization are undersaturated with halite and have homogenization temperatures from 300 to 200 °C.

La Española records multiple intrusive episodes and hydrothermal activity over a period of about 1 million years. The early stockwork potassic and phyllic alteration/mineralization assemblages have the earmarks of the porphyry copper environment, with the exception that the copper grade is subeconomic and the quartz and associated alteration minerals are fine grained (≤1mm). The acid-sulfate alteration/mineralization is typical of the high sulfidation epithermal environment that is thought to occur at shallow levels above porphyry intrusions. The fact that acid-sulfate-altered rock crosscuts potassic- and phyllic-altered porphyries suggests that rapid erosional unroofing of the porphyry intrusive complex occurred during the life span of the system. The acid-sulfate alteration at the surface suggests the presence of a deeper, unexposed porphyry intrusion. Undiscovered stockwork mineralization may therefore exist at depth within the system.

JURASSIC CALDERAS IN SOUTHEASTERN ARIZONA—THE SURFACE MANIFESTATION OF A COMPOSITE BATHOLITH

Ken Hon and Peter Lipman

Volcanic deposits from three overlapping calderas of Jurassic age, recently identified in the Canelo Hills and Huachuca Mountains of southern Arizona, chronicle the

emplacement of a large composite batholith. Smaller plutonic complexes were also emplaced near Bisbee and Gleeson at approximately the same time.

The Montezuma caldera, the oldest of the three, erupted within a cluster of andesitic to dacitic volcanoes. Although no sections of these early rocks are preserved intact, large blocks and shattered masses of andesite and dacite form extensive megabreccia lenses within the Montezuma caldera, indicating the presence of a thick sequence of lavas on the rim during caldera collapse. Intracaldera accumulations of crystal-rich dacite tuff (68 percent SiO_2) also interfinger with massive landslide lenses consisting of blocks of Paleozoic limestone, dolomite, and sandstone, and Jurassic(?) sandstone and siltstone. The intracaldera crystal-rich dacite is overlain by thin rhyolitic outflow sheets from the Turkey Canyon and Parker Canyon calderas. A similar outflow sequence is found in the Mustang Mountains some 20–30 km to the north.

Following caldera collapse, a large composite granitic intrusion was emplaced into the intracaldera dacite tuff. The intrusion consists of a medium- to coarse-grained, porphyritic granite (70 percent SiO_2) containing 2–3 cm phenocrysts of orthoclase and a medium- to coarse-grained equigranular granite that ranges from hornblende granite (70 percent SiO_2) to biotite granite (76 percent SiO_2). Aplite dikes cut both the porphyritic and equigranular granites but are more common in the former. Cuspate blebs (10–20 cm) of dark andesite-dacite are found in both granites but are more plentiful in the porphyritic granite. Similarly, discontinuous basalt dikes (50 percent SiO_2) are more common within the porphyritic granite.

After a short hiatus, crystal-poor rhyolite tuff erupted from the Turkey Canyon caldera. This welded tuff is strongly rheomorphic within the caldera and in the Mustang Mountains. High volatile contents are indicated by the presence of abundant lithophysae and secondary potassium feldspar related to pervasive vapor-phase alteration of this unit. Similar strongly rheomorphic, crystal-poor rhyolite tuffs are known to have erupted at relatively high temperatures (800–900 °C) in mid-Tertiary western United States.

The youngest of the three calderas, the Parker Canyon caldera, erupted a crystal-rich rhyolite tuff consisting of ≈40 percent crystals of quartz, potassium feldspar, and biotite. The high crystal content of this unit suggests that it records the eruption of a cooling pluton. The intracaldera tuff is intruded by a rhyolite porphyry of similar composition but does not appear to be structurally domed.

Sediments interbedded between the three ash-flow tuffs indicate a time break between caldera-forming events. The amount of sedimentation within the Montezuma caldera is similar to that found within Tertiary calderas, which take tens of thousands to hundreds of thousands of years to accumulate.

The nested nature of the three Jurassic calderas suggests that they formed during emplacement of successive cupolas
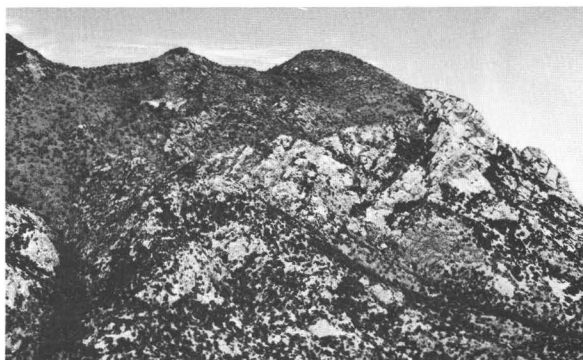
Resurgent granite (lower, light-colored cliffs) intruding hornfelsed intracaldera dacite tuff (upper, slope-forming exposures) within the Montezuma caldera, southern Huachuca Mountains. By Ken Hon.

of a composite batholith. The general progression from early andesitic volcanism to more silicic ash-flow tuff eruptions mimics well-documented patterns seen in many of the mid-Tertiary volcanic fields of the western United States.

Important porphyry copper mineralization of Jurassic age is associated with emplacement of the Juniper Flat Granite and the associated Sacremento Hill stock at Bisbee. Weak copper skarn mineralization is widespread near contacts of limestone megablocks and limestone pendants with the resurgent pluton in the Montezuma caldera. The two systems are approximately coeval, but it appears that development of a porphyry copper system in the Huachuca Mountains was thwarted by eruption of the Montezuma caldera. Hydrothermal activity associated with emplacement of the resurgent intrusion and a later dike swarm appears to have scavenged enough copper and other metals from the intracaldera dacite tuff to make the small skarn deposits.

SANTA ANA–RESERVE EXTENSION ZONE—A PROPOSED ZONE OF INTERACTIVE NORTHEAST- AND NORTHWEST-DIRECTED EXTENSION DURING THE CENOZOIC, NEW MEXICO, ARIZONA, AND SONORA

Brenda B. Houser

Studies of the tectonic setting of the Sierrita-Mogollon transect project indicate that the transect coincides with a proposed system of Cenozoic northeast-trending faults and grabens (fig. 1). This system can be traced from northern Sonora, Mexico, to north of Reserve, N.Mex., where it was recognized earlier as the Morenci-Reserve fault zone (Ratté, 1989). The entire system is named the Santa Ana–Reserve extension zone (SAREZ) for towns near the southwest and northeast ends of the zone, respectively. As currently
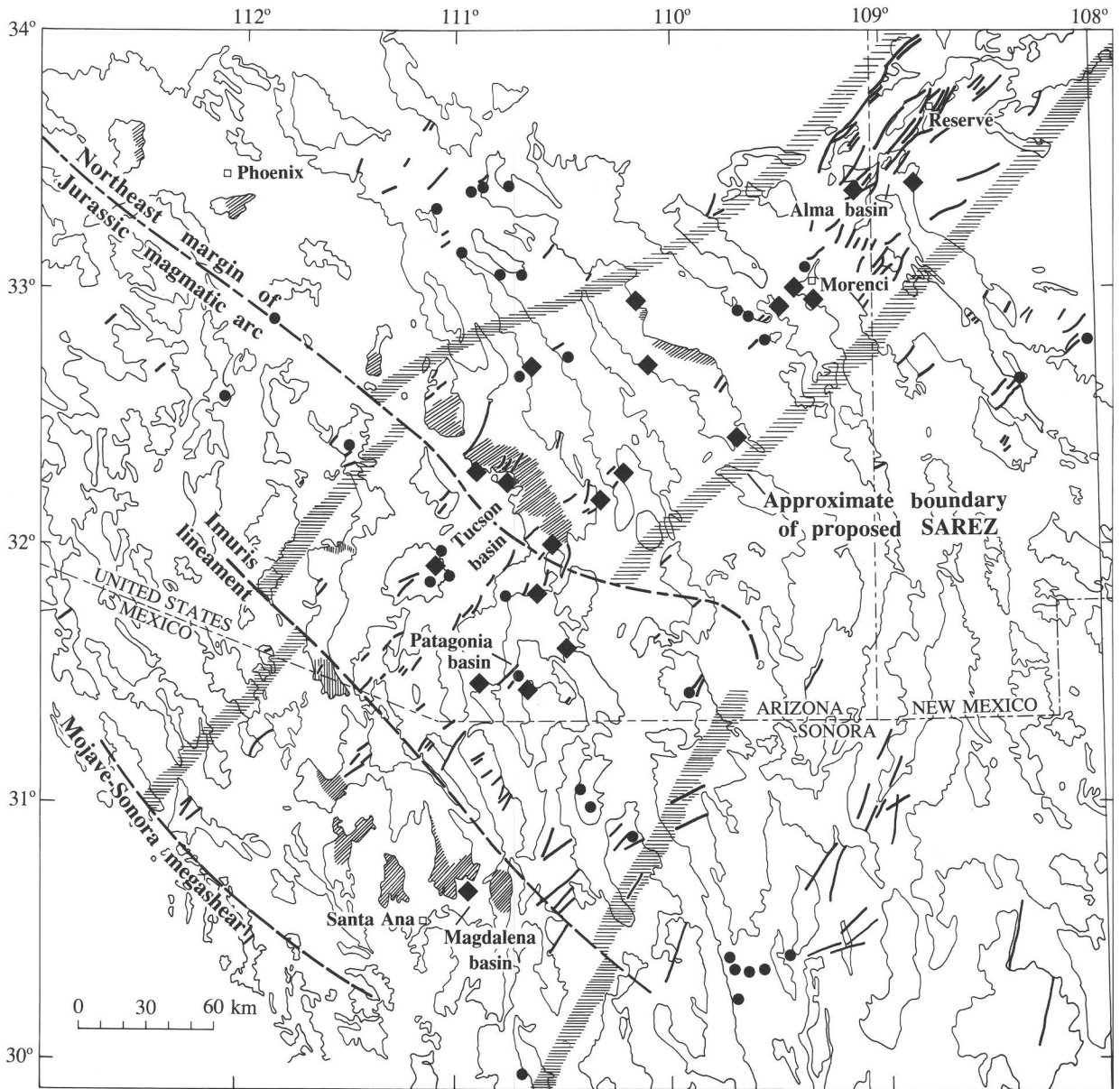
Figure 1 (Houser). Approximate location of proposed Santa Ana–Reserve fault zone in relation to exposures of mid-Tertiary sedimentary units (older than 18 Ma), porphyry copper deposits, and to pattern of faults, basins, ranges, and other tectonic elements of the southern Basin and Range province.
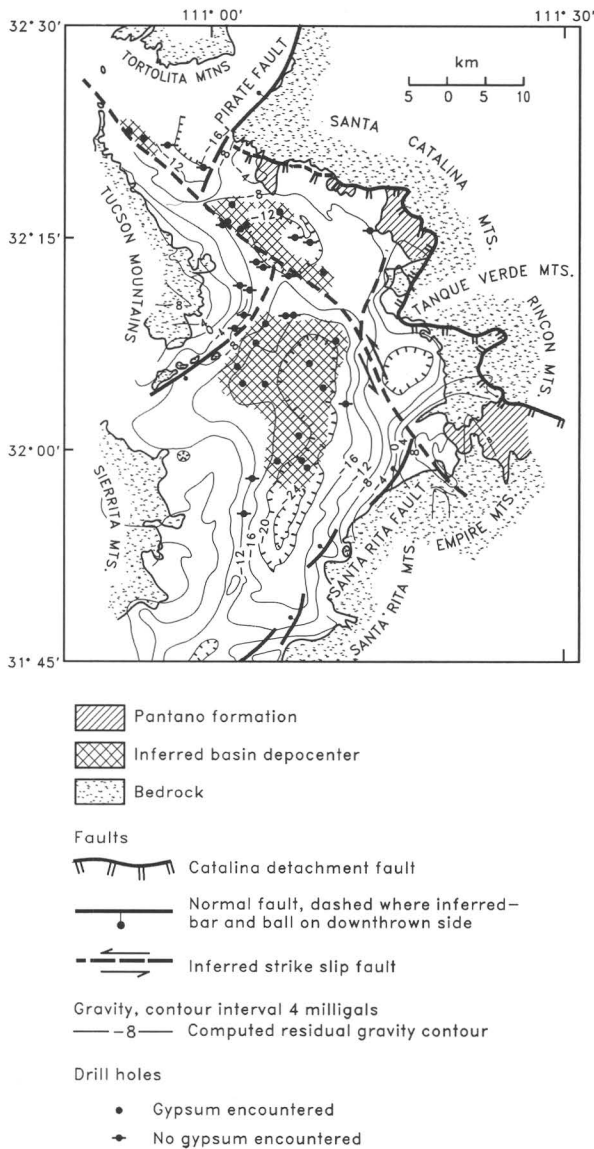
Figure 2 (Houser). Tectonic map of Tucson basin showing off-set of basin depocenters that may be related to inherited displacement along an inferred northwest-trending fault.

defined, it is about 500 km long and widens from 60 km at the northeast end to 200 km at the southwest end.

The SAREZ is characterized by horsts and grabens bounded by chiefly high angle normal faults trending N. 30°–60° E., by local occurrences of thick mid-Tertiary sedimentary deposits, by metamorphic core complexes, and by porphyry copper deposits. Mid-Tertiary sedimentary deposits (about 30 to 18 Ma) such as the conglomerate of Bonita Creek and Pantano, Mineta, and lower Cloudburst Formations in Arizona, probably the Magdalena Formation in

Sonora, Mexico, and various unnamed pre-18 Ma sedimentary units throughout the zone are inferred to have been deposited in northeast-trending grabens of the SAREZ that have since been disrupted by oppositely directed basin-and-range extension (post-18 Ma) and by core complex uplift. Many of these deposits have not been studied in detail, but those plotted in figure 1 have well-constrained ages between 30 and 18 Ma, are as thick as 3,000 m, are complexly faulted and tilted, and have two other significant features in common: (1) their facies bear no relationship to the present topography, and (2) most contain clasts that have no known source nearby. Similar deposits are uncommon in the region outside the SAREZ.

Tectonic activity in the SAREZ continued through the Miocene and Pliocene as evidenced by ages of basin-fill sediments in northeast-trending grabens such as the Patagonia, Tucson, and Alma basins. Pleistocene activity in the zone is demonstrated by northeast-trending fault scarps that cut Pleistocene pediment gravel along the Santa Rita fault on the southeast side of the Tucson basin (fig. 2) and along unnamed faults on the northwest side of the Alma basin, New Mexico.

In addition to northeast-trending faults and grabens, the SAREZ is the locus of a large number of metamorphic core complexes (fig. 1). Uplift of these core complexes may have been localized along the SAREZ by virtue of greater tectonic extension within the zone—that is, the interactive effects of the northwest-directed extension of the SAREZ (1) with the northeast-directed midcrustal extension at about 24 Ma that produced the mylonite fabric of the core complexes, and (2) with the regional northeast-directed basin-and-range extension after about 18 Ma. The two directions of extension may have had the effect of producing a northeast-trending zone of greater attenuation in the upper crust, which in turn resulted in locally greater crustal buoyancy and concentration of core complex uplift along the zone.

The chief barriers to recognizing and tracing the SAREZ have been that southwest of Morenci, the zone was disrupted by uplift of the core complexes, and southwest of Tucson, it was obscured further by the fragmented terrane of the Jurassic magmatic arc and by more core complexes. The map pattern shown in figure 1 suggests that south of the Tucson basin, northeast-trending grabens and fault segments have been progressively offset to the southeast, possibly by an inherited (but not necessarily reactivated) pattern of left-lateral offset on northwest-trending strike-slip faults in the Jurassic terrane. This southeast offset is also indicated in figure 2, a gravity and tectonic map of the northeast-trending Tucson basin, that shows apparent offset of Pliocene(?) depocenters along an inferred northwest-trending strike-slip fault. The depocenters are defined by the presence of evaporite minerals (chiefly gypsum) at depths of about 150 m. Because there is no surface evidence for Neogene reactivation of this fault, the segmented shape of the Tucson basin may have been predetermined by earlier offset by the fault.

51

Figure 1 shows that Laramide porphyry copper deposits tend to be clustered along the SAREZ but are less common outside the zone; this northeast-trending distribution has been noted previously by many investigators. Spatial coincidence of the copper deposits and the proposed SAREZ suggests the possibility of a genetic relationship, but the coincidence may simply be a function of exposure. Late Cenozoic uplift associated with the many core complexes in the zone could have resulted in exposure of more porphyry copper deposits relative to areas outside the zone.

REFERENCE

Ratté, J.C., 1989, Geologic map of the Bull Basin quadrangle, Catron County, New Mexico: U.S. Geological Survey Geologic Quadrangle Map GQ–1651, scale 1:24,000.

THE MOGOLLON MINING DISTRICT—RESULTS FROM MAPPING, PARAGENESIS, AND FLUID-INCLUSION STUDIES

Robert J. Kamilli

The Mogollon district in southwestern New Mexico comprises numerous silver-copper-gold epithermal veins of Miocene age. The district is situated along the Queen fault, a reactivated north-northeast-trending segment of the structural wall of the Oligocene Bursum caldera (fig. 1).

The hypogene paragenesis is complex, owing to repeated episodes of hydrothermal brecciation, mineralization, and faulting. Any individual episode generally commenced with hydrothermal brecciation, followed by deposition of quartz-rich (commonly chalcedonic) veins containing chlorite, adularia, pyrite, electrum, copper sulfides, and copper-silver sulfides. This ore-forming event commonly was followed by a period of calcite±fluorite deposition, accompanied by dissolution of calcite and concomitant replacement by quartz.

Fluid-inclusion petrography and filling temperatures confirm that boiling of the hydrothermal fluids was a common phenomenon throughout the district. The restriction of the most productive ore horizons to an elevation interval of about 200 m, regardless of depth below the current land surface, supports the hypothesis that fluid boiling was an integral part of the ore-deposition process, as do anomalously high filling temperatures in quartz, up to 461 °C. However, the abundance of chalcedony and other forms of recrystallized silica in many specimens precludes the rigorous demonstration that boiling was the primary ore-deposition process because fluid inclusions in such material are notoriously untrustworthy. Most filling temperatures for quartz are 210–290 °C, for calcite 180–260 °C, for sphalerite 230–260
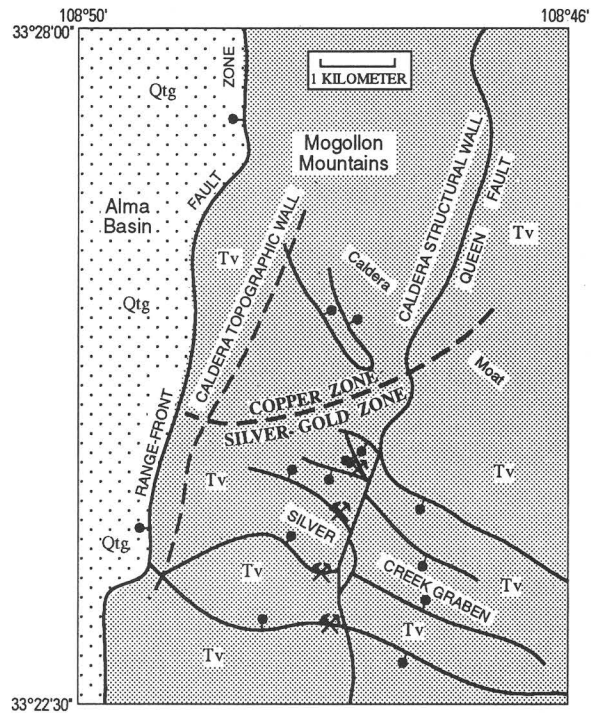
Figure 1 (Kamilli). Generalized map of the Mogollon district. QTg, Quaternary and Tertiary gravels; Tv, Tertiary volcanics. Bar and ball symbol denotes dip of fault. Crossed pick and hammer, principal mine.

°C, and for fluorite 120–200 °C. Most salinities are less than 2 weight percent NaCl equivalent. A few values are as high as 5 weight percent NaCl equivalent; this is probably due to the concentrating effects of boiling rather than to the presence of a second fluid.

Several lines of evidence are consistent with the presence of a buried porphyry-type intrusion in the district. Although all dated igneous rocks in the district are at least 23.2 Ma, an $^{40}Ar/^{39}Ar$ date of 16.7 Ma on vein adularia suggests that the thermal event represented by the mineralization at Mogollon could not have occurred during the formation of the Bursum caldera (28 Ma), but must be related to a buried intrusion or to increased heat flow caused by basin-and-range extensional faulting (Ratté, 1989). The presence of an intrusion is suggested by the existence of the box or ladder mosaic patterns of the Silver Creek graben in the central part of the district. This pattern may have been caused by doming above the hypothesized intrusion. Other suggestive evidence includes the presence of a major porphyry molybdenum prospect 11 km south of the district along the trace of the Queen fault and the presence of 21–16 Ma rhyolite intrusions southwest of the district (Ratté and Brooks, 1991).

Underground mapping has demonstrated that ore-grade mineralization extends to the range-front fault zone, which separates the Mogollon Mountains from the Alma basin on

the west. It seems likely therefore that mineralization may extend beneath the late Cenozoic basin fill at a depth between 1,000 and 350 m. However, these depth estimates assume that movement along the range-front fault is entirely post-mineralization. If some displacement along the basin-and-range faults predates mineralization, as is likely, the depth to the buried mineralized horizon could be much less and basin fill itself could be mineralized.

Audio-magnetotelluric resistivity profiles through the district indicate that as much alteration occurs east of the Queen fault as occurs to the west, where all historical production occurred (Senterfit and others, this volume). The veins east of the Queen fault are predominantly calcite±chalcedonic quartz. The character of the veins, the geophysical data, and probable offset along the Queen fault of several hundred meters are seen as permissive evidence that the part of the district east of the Queen fault, where there has been no production, may contain significant mineral deposits.

REFERENCES

Ratté, J.C., 1989, Days 3 and 4—Selected volcanic features of the western Mogollon-Datil volcanic field, in Ratté, J.C., Cather, S.M., Chapin, C.E., Duffield, W.A., Elston, W.E., and McIntosh, W.C., Excursion 6A—Eocene-Miocene Mogollon-Datil volcanic field, New Mexico, in Chapin, C.E., and Zidek, J., eds., Field excursions to volcanic terranes in the western United States, volume 1, Southern Rocky Mountain region: New Mexico Bureau of Mines and Mineral Resources Memoir 46, p. 68–91.

Ratté, J.C., and Brooks, W.E., 1991, Rhyolite rift zone in southwestern New Mexico—A possible target for precious metals exploration: Geological Society of America Abstracts with Programs, v. 23, no. 4, p. 58.

APPLICATION OF FIELD AND LABORATORY SPECTROSCOPIC ANALYSIS TO INVESTIGATE THE ENVIRONMENTAL IMPACT OF MINING IN THE SOUTHEASTERN SAN JUAN MOUNTAINS AND ADJACENT SAN LUIS VALLEY, COLORADO

Trude V.V. King, Cathy Ager, Roger N. Clark, Gregg A. Swayze, and Andrea J. Gallagher

A series of laboratory, field, and theoretical studies have recently been completed to support the interpretation of airborne imaging spectroscopy data to be collected by NASA's AVIRIS (Airborne Visible and Infrared Imaging Spectrometer) in August/September 1993. This investigation is part of an integrated environmental study of the southeastern San Juan Mountains and adjacent San Luis Valley in Colorado. The Alamosa River and its tributaries drain several highly mineralized areas that are sources for both natural and mining-related contamination. This contamination is of concern due to the extensive downstream use of the Alamosa River for irrigation in the San Luis Valley, for domestic use, and as a source for water in the Monte Vista Wildlife Refuge.

The AVIRIS data are obtained over the wavelength interval of 0.4 to 2.5 µm at a spatial resolution of 20 m and a spectral resolution previously attained only by laboratory instruments (9–15 nm). AVIRIS data will be obtained for the Summitville mine (a possible source of contamination from mining-related activities) and downstream areas in the San Luis Valley, thus providing a synoptic view not available through other techniques.

The primary emphasis for the preflight portion of the investigation has been to determine if absorption features related to materials introduced by mine drainage can be detected in vegetation and mineral spectra. To examine the influence of water chemistry on alfalfa, a field investigation was undertaken to determine if, and to what extent, variations in irrigation sources (some possibly high in metals and other contaminants) would affect the spectral signature. In addition, a series of measurements was made to determine the spectral effects of liming (an agricultural method to control the pH of soil) in fields irrigated with Alamosa River water. These data will provide the calibrations necessary to map species distribution, and potentially their vigor, from the AVIRIS data.

Laboratory spectroscopic studies and previous studies using AVIRIS data (Clark and others, 1993) show that it is possible to detect and map the distribution of minerals based on slight changes in chemistry and crystal structure. Laboratory studies indicate that it is possible to identify mixtures of matrix (soil constituents) and cyanide compounds based on diagnostic absorption features that should allow their identification in AVIRIS data. The laboratory calibration data suggest that it will be possible to use AVIRIS data to produce mineral, soil, and contamination maps for a large area.

Preliminary spectroscopic examination of soil samples taken from a drainage ditch in the San Luis Valley indicate that material is being deposited on the banks that is not a common mineral phase associated with agricultural activity. The spectral signature of this material is diagnostic and could readily be mapped with AVIRIS. However, the full extent to which the AVIRIS data will be effective for mapping potential environmental contaminants in the region must be determined.

REFERENCE

Clark, R.N., Swayze, G.A., and Gallagher, Andrea, 1993, Mapping minerals with imaging spectroscopy, *in* Scott, R.W., Jr., and others, eds., 1993, Advances related to United States and international mineral resources—Developing frameworks and exploration techniques: U.S. Geological Survey Bulletin 2039, p. 141–150.

GEOELECTRIC CONTRIBUTIONS TO THE MINERAL RESOURCE ASSESSMENT, CORONADO NATIONAL FOREST, SOUTHEASTERN ARIZONA—BURIED STRUCTURE AND ALTERATION IN MAGMATIC CENTERS

Douglas P. Klein

Audiomagnetotelluric (AMT) traverses within and adjacent to the Coronado National Forest, southeast Arizona, provide electrical resistivity information at depths from about 10 to 3,000 m. The data provide information on the location and extent of buried low-resistivity features, including geothermal fluid, hydrothermal alteration, and fault breccia, as well as contrasts in resistivity from lithologic changes across faults, and high-resistivity intrusions. These geologic features delineate potential targets for ore deposition, provided other geologic and geophysical conditions are favorable. Four specific areas studied within the Coronado National Forest (fig. 1) are west-central Winchester Mountains, northern Dragoon Mountains, northern Chiricahua Mountains, and central Chiricahua Mountains. These areas are all underlain by volcanic or plutonic rocks either in outcrop or at shallow depth.

In the Winchester Mountains area (Martin, 1986; Martin and others, 1982), AMT data sense the location of a narrow low-resistivity zone along the western margin of the mountains; this zone is interpreted to represent conductive gouge of a range-front fault. Farther west into the basin, a low-resistivity layer at an average depth of about 400 m is inferred to represent basin brine or thermal fluid; hot springs above and possibly emanating from this layer are found about 5 km west of the mountain range.

Across the northern Dragoon Mountains (Baer and Klein, 1984), high resistivity is associated with intrusive rock of the mountain core, and moderate resistivity is associated with localized sedimentary overburden. The data allow estimates of the maximum thickness of sedimentary rock overlying the resistive intrusive. Beneath alluvium about 5 km west of outcrop and coincident with an aeromagnetic anomaly, a low-resistivity anomaly at about 350 m depth below basin fill may indicate altered intrusive rock.
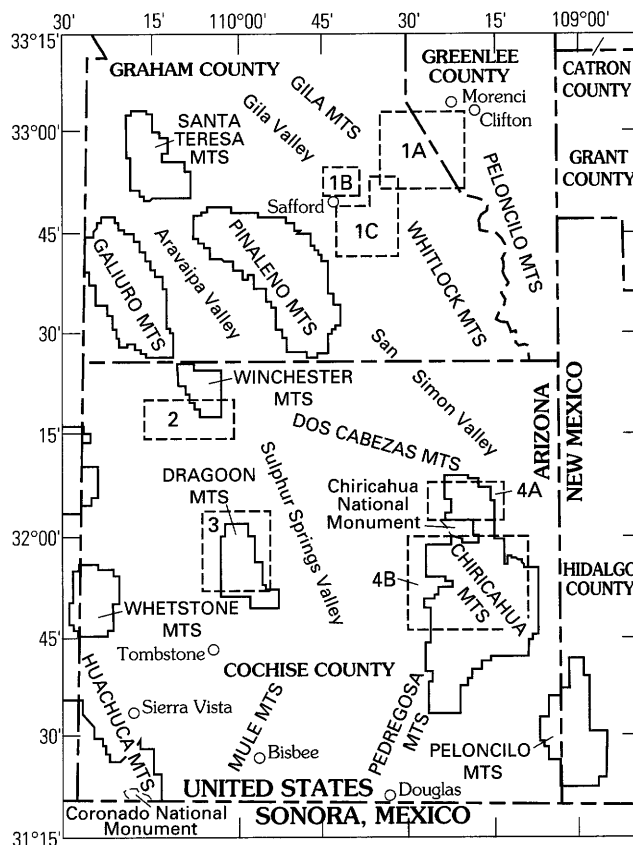

Figure 1 (Klein). Location of AMT electrical surveys in southeastern Arizona (dashed lines). Segments of the Coronado National Forest are enclosed by solid lines. Areas discussed in this report are 2, 3, 4A, and 4B.

In the Emigrant Pass area of the northern Chiricahua Mountains (Nervick and Boler, 1981), inferences from AMT resistivity data indicate a possible intrusion buried under lower-resistivity volcanic rock. AMT stations here provide data consistent with the interpretation that the inferred intrusion is either altered at a depth of 300–500 m, or that the intrusion bottoms near this depth.

Traverses on the northeast boundary of Turkey Creek caldera (Senterfit and Klein, 1991) reveal moderate to low resistivity peripheral to the inferred core of a highly resistive ring intrusion (fig. 2, between A and C′). This low-resistivity rock is inferred to represent hydrothermal alteration associated with intrusion. Mine prospects and also small abandoned mines are found in this area, but major ore deposits are

Figure 2 (Klein) (facing page). Location map (top), resistivity cross section (middle), and interpretation (bottom) of part of an AMT electrical survey, Turkey Creek caldera, Coronado National Forest, southeastern Arizona.

54

ARIZONA

109'10"
┬ 32'00"

N

Tfc

Kb

Kb

B
23
22
19
21 20
18
17 16 15 13
A
Qls
B'
C
5
6
7 3
8
9
C'
4 14
D
10
11
12
D'

Trc

Tmp

Tmp

Tmp

Trc

E
32
29
30
Trc
31
E'

F
1
28
27
26
25
24
F'

Tmp

Trc

Trc

0   5   10 KILOMETERS
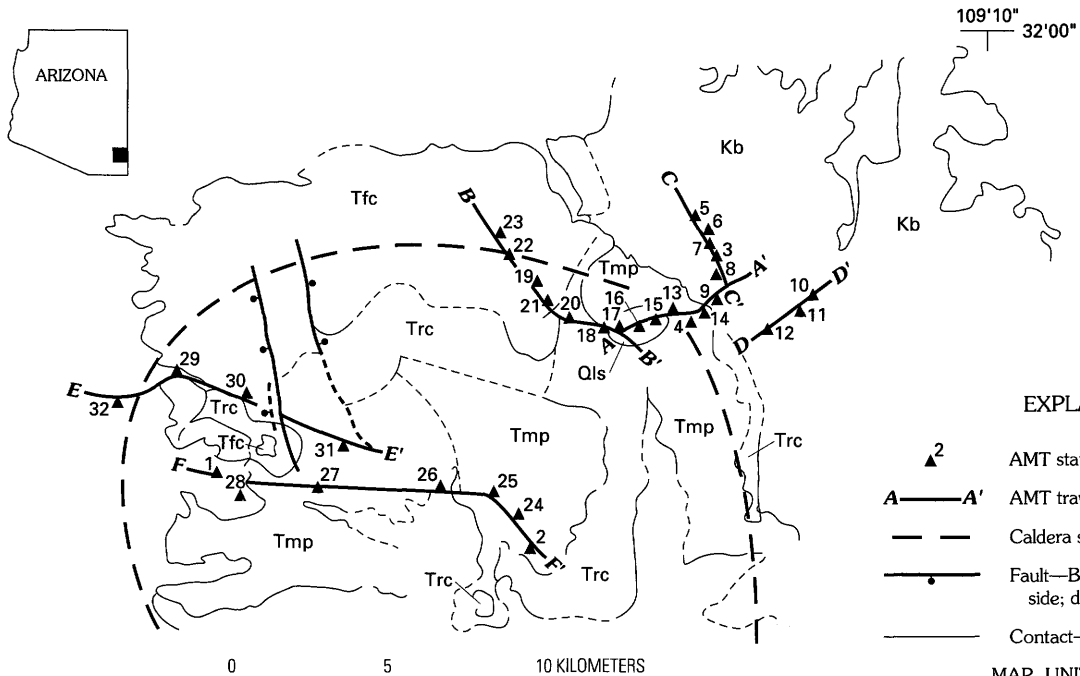
GEOLOGIC MAP SHOWING LOCATION OF AMT STATIONS AND PROFILES

EXPLANATION

▲2   AMT station location

A————A'   AMT traverse

— — —   Caldera structural margin

—•—   Fault—Bar and ball on downthrown
          side; dashed where uncertain

————   Contact—Dashed where uncertain

MAP UNITS (top) AND INFERRED
UNITS AT DEPTH IN THE
RESISTIVITY SECTION (bottom)

Qls   Landslide breccia (Quaternary)

Trc   Welded tuffs (Rhyolite Canyon
          Tuff—Oligocene)

Tfc   Moat lavas and tuff of Fife Canyon
          (Tertiary)

Tl   Welded tuffs and lava flows (inferred
          to be low in the section—Tertiary)

Tmp   Monzonite porphyry (core and
          ring—Tertiary)

Ti   Intrusive rock (Tertiary, but may
          include older granitic rocks and
          Proterozoic basement that is
          indistinguishable from intrusive
          rock by resistivity values)

Kb   Sedimentary rocks (mostly
          Cretaceous Bisbee Formation)

KPzs   Sedimentary rocks (mostly carbonate
          rocks of Cretaceous and (or)
          Paleozoic age)

OTHER SYMBOLS

F   Fault(s)

BFA   Brecciation, faulting and alteration

22   AMT station

B
BEND
0   2
B' A
BEND
4
C'
6
D
OFFSET
8   10   12
D'

KILOMETERS
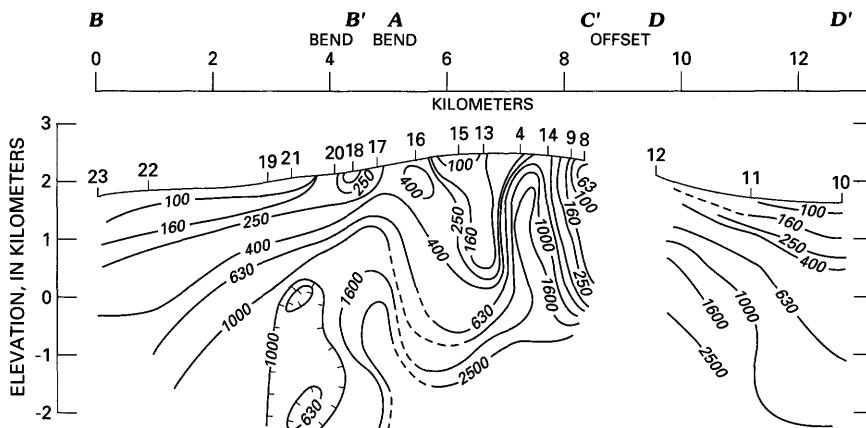
DEPTH-RESISTIVITY SECTION
(resistivity contours in ohm-m, dashed where uncertain)

0   2   4   6   8   10   12

KILOMETERS

OUTCROP ◄————Tfc————|Trc|——Qls——|—Tmp—|————Kb————►
F
(ring intrusion)
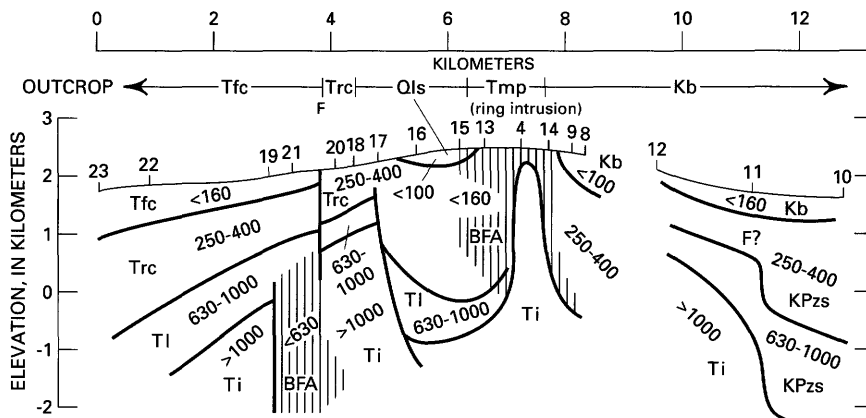
INTERPRETIVE SKETCH OF INFERRED SUBSURFACE LITHOLOGIES AND STRUCTURES
(resistivity values in ohm-m)

55

unknown. To the northwest where the AMT traverse crosses an area of outcropping tuff, the resistivity generally increases with depth, however; one area of buried lowered resistivity is anomalous (near station 20, fig. 2). Faults mapped in this area seem to indicate that the low resistivity represents breccia or gouge along the faults, or alteration associated with hydrothermal fluids guided by the faults.

Along part of a traverse in the west-central part of Turkey Creek caldera, AMT soundings indicate anomalously low resistivity at a depth of about 300 m (fig. 2, top, near station 26). This area is inside the inferred caldera boundary. The anomaly is believed to be related to faulting. Subsequent to the analysis of this profile, faults were identified in nearby outcrops.

REFERENCES

Baer, M.J. and Klein, D.P., 1984, Audio-magnetotelluric data in the Dragoon Mountains Roadless Area, Cochise County, Arizona: U.S. Geological Survey Open-File Report 84–417, 59 p.

Martin, R.A., 1986, Geophysical maps of the Winchester Roadless Area, Cochise County, Arizona: U.S. Geological Survey, Miscellaneous Field Studies Map MF-1851, scale 1:24,000.

Martin, R.A., Sherrard, M.S., and Tippens, C.L., 1982, Station location map and audio-magnetotelluric data log for an area between Hooker's Hot Springs and the Winchester Mountains, Arizona: U.S. Geological Survey Open-File report 82–779, 8 p.

Nervick, K.H., and Boler, F.M., 1981, Audio-magnetotelluric investigations of the North End Study Area, Cochise County, Arizona: U.S. Geological Survey Open-File Report 81–774, 6 p.

Senterfit, R.M., and Klein, D.P., 1991, Audiomagnetotelluric investigation at Turkey Creek Caldera, Chiricahua Mountains, southeastern Arizona: U.S. Geological Survey Bulletin 2012, p. K1–K9.

THE U.S. GEOLOGICAL SURVEY SIDE-LOOKING AIRBORNE RADAR (SLAR) MOSAICS—A REGIONAL VIEW FOR MINERAL EXPLORATION

Allan N. Kover and James W. Schoonmaker, Jr.

The U.S. Geological Survey has acquired SLAR (side-looking airborne radar) image data for more than 40 percent of the conterminous United States and Alaska, plus Puerto Rico and the U.S. Virgin Islands (fig. 1). These data are an under-used resource for mineral exploration. Many of the mineralized areas of the Southwest are particularly well covered, as are other areas of potential discovery. For convenience, the image data are assembled into 1°×2° mosaic quadrangles (1°×3° north of lat 59° in Alaska), and afford an unparalleled synoptic and cloud-free view of terrain. The radar system's imaging geometry provides enhancement of subtle structural geologic features, especially when acquired with optimum look direction and depression angle. The design of mission flight plans takes advantage of these special attributes of radar images.

The SLAR image data used to prepare the mosaics have a swath width of 20–46 km, depending upon the acquisition system, and are generally available in unbroken strips of at least quadrangle length. Images are collected with 60 percent sidelap to provide stereoscopic models and to facilitate mosaicing. All post-1984 image strip data are available on computer-compatible tape (CCT), and many earlier data sets are now available in digital form. Since 1991, data have been routinely provided on CD-ROM.

The SLAR image strips are assembled into 1:250,000-scale mosaic quadrangles that conform to the national topographic map series. (For names of individual conterminous U.S. quadrangles see USGS *Index of Small Scale Maps of the United States*, April 1, 1992, and for Alaskan quadrangle names consult the State Index. Both are available, without charge, from the local USGS Earth Science Information Office (ESIC), or call 1–800–USA MAPS.) The mosaics can be ordered as photographic prints, positive or negative transparencies, or diazo copies from the USGS EROS Data Center (EDC), User Services Section, Sioux Falls, SD 57198. Other USGS SLAR data, available from EDC, include indexes (microfiche, and 1:250,000- and 1:1,000,000-scale prints), image strips, nine-track tape (CCT), and CD-ROM. Custom laboratory products can be provided.

A composite SLAR mosaic of the State of West Virginia and parts of five adjoining States was compiled for the USGS at 1:500,000 and 1:1,000,000 scale. These mosaics can be ordered from EDC. Twenty other regional composite mosaics were prepared as value-added products by a private contractor and are not available from the USGS.

The USGS SLAR data have been an aid in improving geologic mapping and in selecting areas for resurvey. Several CUSMAP (Continental U.S. Mineral Assessment Program) quadrangles include analysis of SLAR mosaics. Lineament studies have been useful in identifying potential mineralized areas in a number of States, including New York–New Jersey (lead-zinc), California, Connecticut, Idaho, Utah, North Carolina, Montana, and Michigan. Uranium-rich breccia pipes in northern Arizona are more easily identified on SLAR images in both forested and desert locations. An adequate water supply is necessary for many mining operations, and lineaments located on SLAR mosaics have been particularly useful in finding new sources of ground water.
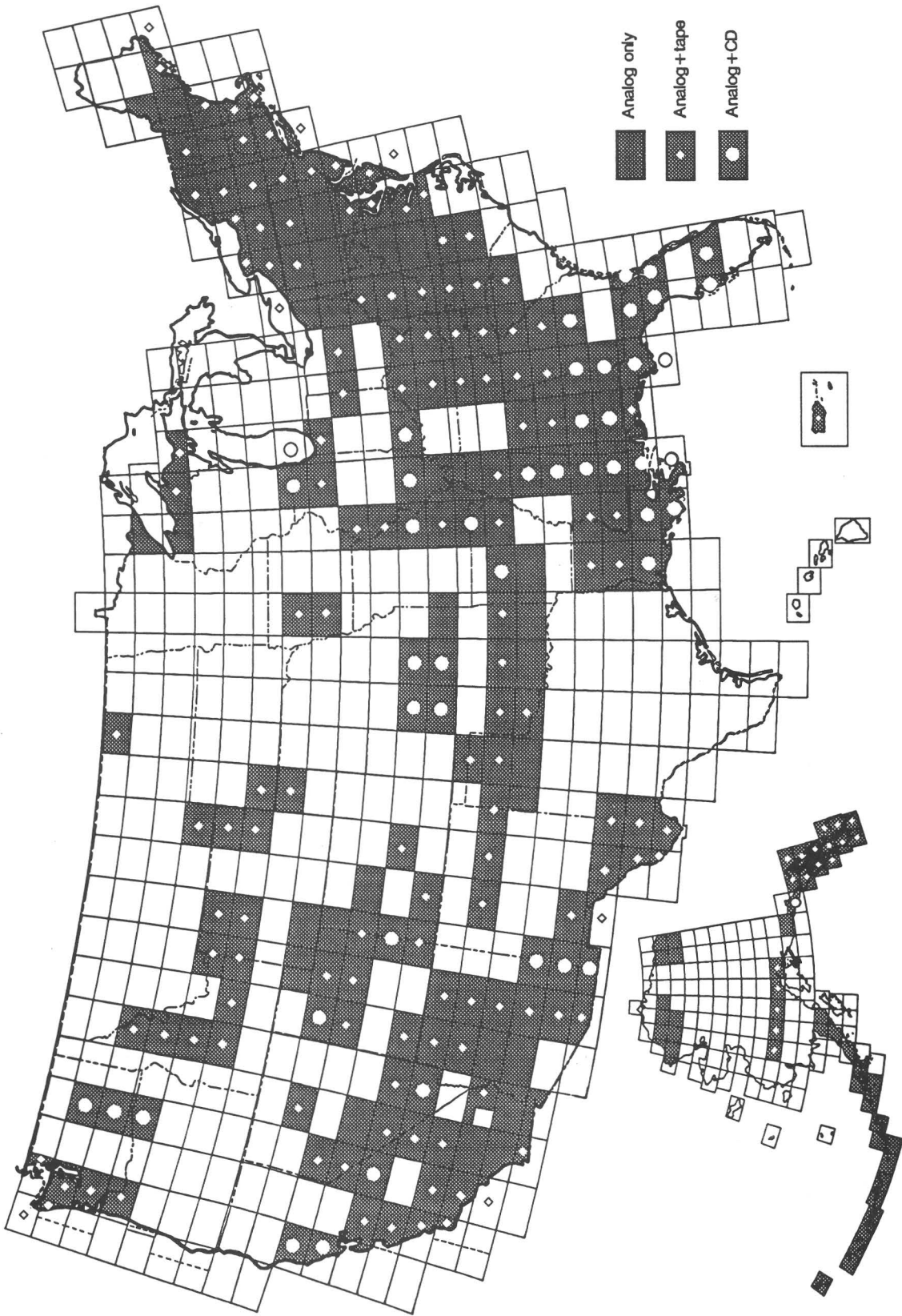
Figure 1 (Kover and Schoonmaker). USGS SLAR program 1980–1993.

Analog only

Analog+tape

Analog+CD

TESTING TEMPORAL DATA SETS FOR REGIONAL ENVIRONMENTAL ANALYSIS OF WEST VIRGINIA*

M. Dennis Krohn, Robert C. Clark, and
Charles W. Tremper

Two distinctive vegetation units (fig. 1) were mapped in western West Virginia from an analysis of temporal vegetation and hydrologic data sets from 1990. The analysis was conducted as part of a statewide mineral resource assessment to test whether analysis of temporal data would have any utility for regional environmental studies. Two new data sets published on CD-ROM now make such an analysis feasible in the conterminous United States and Alaska. Vegetation response is depicted on a mosaic of weather satellite images from the AVHRR (Advanced Visible High Resolution Radiometer) sensor. A ratio index of vegetation reflectance is measured at a resolution of 1 km for 19 biweekly intervals. Hydrologic response is measured from comparison of modern stream gauge readings to historic records from the HCDN (Hydro-Climatic Data Network). Fifteen gauging stations in West Virginia meet the HCDN criteria that minimize cultural influences on stream-flow readings.

The most distinctive vegetation unit is located in the southwest part of the State (diagonal lines, fig. 1) and corresponds mainly to an area of Pennsylvanian-age coal-bearing rocks of the Conemaugh Group. The unit appears in the AVHRR mosaics as a slightly less vigorous response during the greening of vegetation in late April. Land-use practices over the coal-mining areas coupled with the primarily siliceous bedrock of the area are the likely causes of the delay in vegetation greening. A second, less distinctive unit (stipple pattern, fig. 1) is mapped in the north-central part of the State and corresponds in part to a north-south outcrop pattern of Permian sedimentary rocks. The eastern border of the southern area (solid lines, fig. 1) and the western border of the northern area (dashed line, fig. 1) seem to be marked by north-south-trending linear features. The linear features align with part of the New River, but only partially correspond to previously mapped linear features from analysis of structures, such as lateral ramps, and features from other statewide geologic compilations.

The hydrologic records at this time are quite useful at eliminating spurious patterns observed in the satellite mosaics related to local meteorological effects. No relation is yet observed between vegetation units mapped from the satellite and patterns from the hydrologic records. The gauging records do show, however, that stream flow within the same drainage basin exhibits sufficiently distinctive patterns in the same time interval to be a poten-
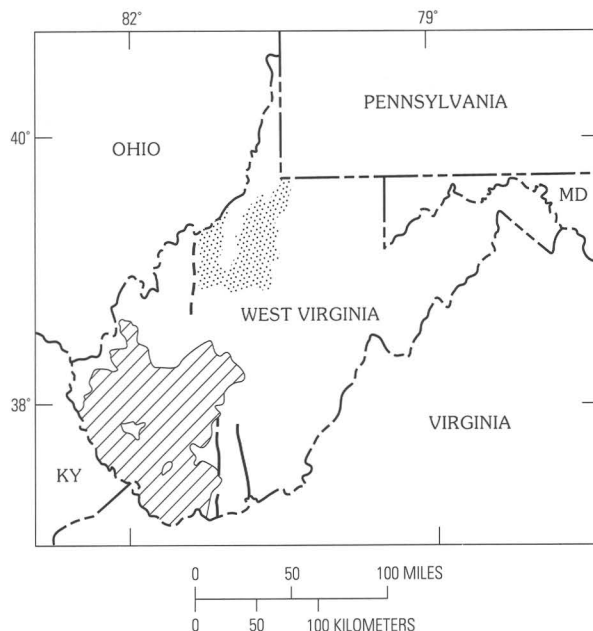
Figure 1 (Krohn and others). Vegetation units and linear features derived from analysis of 1990 temporal data sets for West Virginia.

tial source of variation for the vegetation response. The minimum biweekly flow values appear to be the best indicator of subsurface stream-flow conditions that would affect a regional area.

Initial analysis of the AVHRR and HCDN data sets shows that candidate vegetation areas and unmapped linear features can be recognized and would likely be components in a regional environmental analysis as well as in other resource assessments.

*Not presented at Forum.

GRAVITY AND MAGNETIC INTERPRETATIONS APPLIED TO MINERAL RESOURCE ASSESSMENT OF THE BUREAU OF LAND MANAGEMENT ROSWELL RESOURCE AREA, EAST-CENTRAL NEW MEXICO

Dolores M. Kulik

Gravity and aeromagnetic data were evaluated in conjunction with geologic, geochemical, and aerial gamma-ray data in determining the mineral resource potential of the Bureau of Land Management Roswell Resource Area, east-central New Mexico.

Three broad magnetic highs occur along the eastern boundary of the study area, and generally coincide with high gravity anomalies. They are interpreted to result from mafic intrusions within the basement complex of the Central Basin Platform.

Broad, low-amplitude magnetic anomalies present in the east half of the study area are caused by differences in lithology of the rocks of the Delaware Basin shelf and differences in depth to basement beneath these sedimentary rocks. Quaternary basalts, which frequently have associated magnetic anomalies, have no characteristic associated anomalies in the study area, suggesting that the basalts are thin.

The Lincoln County porphyry belt in the westernmost part of the study area, where Tertiary intrusive rocks crop out, is characterized by short-wavelength magnetic anomalies with magnitudes up to 1,000 nT. Similar anomalies extend to the northeast from the porphyry belt where only Permian sedimentary rocks are exposed. The presence of these magnetic anomalies suggests that intrusive rocks similar to those of the porphyry belt occur at shallow depth in this broad area. A magnetic high is associated with the syenite and syenogabbro of Baxter Mountain, which are hosts for the White Oaks ore deposits; this anomaly indicates that a large body of similar composition extends to the southeast and includes the west flank of Carrizo Mountain. Magnetic lows in the Gallinas Peak and Rough Mountain areas are caused by hydrothermal alteration of the intrusive rocks. The occurrence of magnetic lows in the Tecolote Hills area suggests that the rocks here are also altered. Magnetic anomalies of 1,600-2,000 nT extending southeast of the porphyry belt are attributed to uplifted Precambrian crystalline rocks of the Pajarito Mountain area.

A T-shaped gravity anomaly indicates that relatively high density rocks underlie (1) the Lincoln County porphyry belt, (2) most of the northeast extension of the belt interpreted from magnetic data, (3) the area just northwest of the exposed intrusive rocks where similar rocks are probably also present in the subsurface, and (4) the area of Precambrian rocks southeast of the porphyry belt at Pajarito Mountain. The T-shaped gravity anomaly appears to be caused by a composite source including both Tertiary intrusive and Precambrian rocks. The shape of the anomaly suggests that the Tertiary rocks were emplaced in a northeast-trending zone, orthogonal to the north-northwest trend of the Precambrian Pedernal Uplift. The magnetic data show no consistent correlation of the intrusive rocks with either magnetic highs or lows, and some of the larger bodies are spatially associated with both high and low anomalies. The lack of any consistent correlation indicates widely variable magnetite content in the intrusive rocks.

In the south-central part of the study area, strong northeast-trending gravity gradients parallel wrench faults, termed buckles, with normal, reverse, and strike-slip components. The continuity of the gradients suggests that the buckles, which are prospective for oil and gas, extend to the

northeast in the subsurface for many miles beyond mapped exposures. Similar strong northeast-northwest-trending gradients extend in a zigzag pattern across northeastern New Mexico and southeastern Colorado, and may represent a crustal transition and (or) change in basement character associated with crust-penetrating tectonic zones.

SPATIAL AND TEMPORAL VARIABILITY IN THE CHEMISTRY OF TREE RINGS DOWNSTREAM FROM THE SUMMITVILLE MINE

Frederick E. Lichte, James A. Erdman, Larry P. Gough, Thomas M. Yanosky, and Laurie S. Balistrieri

The Summitville mine, located near the old mining town of Summitville in Rio Grande County, Colo., began operating in July 1986 as a large-tonnage open-pit heap-leach gold mine and ceased operating in December 1992. During the mine's 6 years of existence, the trace-metal levels in drainage water from the site were elevated over historical (pre-1986) levels (Moran and Wentz, 1974) due to input from three sources—heap-leach water, seeps that occur throughout the mine workings, and an increase in the metal load of water coming from the old Reynolds Adit. Drainage waters flow into Wightman Fork, a small tributary of the Alamosa River, which in turn flows east into the San Luis Valley. The increase in the trace-metal burden of the Alamosa River watershed is of concern to farmers, fishermen, and Federal and State wildlife agencies. (Also see companion abstracts concerning Summitville in this volume.)

Our purpose was to chart potential spatial and temporal trace-metal trends in individual tree rings from about 1978 to the present. Metals, absorbed through the roots and transported to the aerial portions of a tree (such as the cellulose tissue of which rings are composed), may reflect changes in the bioavailability of metals being transported by both surface and ground water (Yanosky and Vroblesky, 1992). Tree rings have been used successfully to document changes in ground-water chemistry down-slope from point-sources of metal contamination. The analysis of tree-ring chemistry can be difficult to interpret, however, due to (1) potential inhomogeneity within a ring, (2) translocation of metals laterally between rings, (3) difficulties in tree-ring crossdating, and (4) differentiating among various metal sources (such as local vs. transported metals in ground water).

Samples of narrow-leaf cottonwood (*Populus angustifolia*) tree-ring cores were collected from riparian, mixed forest communities along the Alamosa River from just below its confluence with Wightman Fork to a point down river about 25 miles where the river water is extensively diverted

into irrigation laterals on the San Luis Valley floor. Nine sites, spaced approximately 3 miles apart, were established. At each site cores were extracted from each of two mature trees and samples of river water and sediment were collected. Variability in the elemental concentrations of the tree rings was partitioned among various sources, including (1) analytical, (2) between cores within a tree, (3) between trees at a site, and (4) among sites. We obtained ring chemistry results for both spatial (across the watershed) and temporal (among dated rings) trends.

This study utilizes a laser-ablation inductively coupled plasma mass spectrometer (ICP-MS) (Lichte, 1993), which has the capability of determining ≈16 elements in plant material (including the metals Cu, Fe, Hg, Mn, Ni, Pb, and Zn) at the µg/g concentration level over an area of the tree ring with a diameter as small as ≈0.5mm. The analysis of tree rings by laser-ablation ICP-MS utilizes both the technique's high sensitivity and its spatial resolution. Rings were analyzed in place, as part of an increment core, by suspending them in an enclosed sample cell and ablating the zone of interest with a neodymium/yttrium-aluminum-garnet (Nd/YAG) laser.

REFERENCES

Lichte, F.E., 1993, The analysis of small mineral grains by laser ablation inductively coupled plasma mass spectrometry; Abstract 201 *in* Proceedings of 35th Rocky Mountain Conference on Analytical Chemistry, July 25–29, Denver, Colo.: Society for Applied Spectroscopy.

Moran, R.E., and Wentz, D.A., 1974, Effects of metal-mine drainage on water quality in selected areas of Colorado, 1972–73: Denver, Colo., Colorado Water Conservation Board, Colorado Water Resources Circular 25.

Yanosky, T.M., and Vroblesky, D.A., 1992, Relation of nickel concentrations in tree rings to groundwater contamination: Water Resources Research, v. 28, p. 2077–2083.

ECONOMIC FUNDAMENTALS OF MINING LAW*

Keith R. Long

Mineral-bearing lands are typically owned by persons other than those able and willing to explore and to develop such lands. Mining law establishes the terms under which mineral lands are traded for purposes of exploration and development. From an economic perspective, an efficient mining law creates the conditions for maximizing social gains from such trades.

Gains from trading mineral lands depend on the prices of mineral commodities, costs of production, cost of capital, mineral endowment, exploration efficiency, and other factors. Under competitive conditions, involving many landowners and many mining firms, market forces will efficiently sort out which trades will yield the largest private gains. In the absence of externalities, including adverse environmental impacts, social gains from these trades will also maximize.

Private trading of mineral lands should be adequately regulated by commercial law that guarantees enforceability of contracts and compensation for damages. Where governments own mineral lands, a competitive market for mineral lands can be created using the principle of self-initiation, limiting the size of claims, and granting at least *de facto* private property rights to claim holders. Under self-initiation, competing firms decide when, where, and how much exploration and development to undertake. Parceling out claims to many firms prevents monopolization of mineral lands. Property rights allow claim holders to trade claims among themselves, secure financing, enforce contracts, and obtain compensation if mineral lands are expropriated for public use.

A conflict of interest arises between government as a landowner and government as a guardian of public welfare. As a landowner, government seeks to maximize the economic return from its lands. As a monopoly supplier of mineral lands, governments are able to garner excess returns by limiting supply. Noncompetitive limitations on land availability, excess taxes or holding fees, and selective granting of concessions in return for special considerations are forms of profiteering that inhibit economic growth and set a poor example for the private sector.

Governments that encourage competition, however, enhance public welfare by minimizing costs to the mineral consumer. Governments would then expect to receive no more, and no less, than fair market value for mineral rights. Yet fair market value cannot be determined in the absence of a competitive market for mineral rights. A government monopoly on mineral rights, regulated by government, may not be a convincing substitute.

Mineral lands are traded in return for some compensation. Ideally, mineral lands are a commodity having an undisputed market value. In reality, that value depends on expectations as to the type, quantity, and quality of minerals that might be found and profitably developed on a particular mineral property. The considerable uncertainty about that value leads to the almost universal acceptance of some form of risk-sharing between landowner and mining firm. Revenue or profit sharing distributes the risk of variations in earnings between landowner and the mining firm.

Tax payments as a percentage of profits are more equitable and efficient than payments based on gross receipts from mineral sales (gross revenues). In an internationally competitive mineral market, a country that adopts a tax on gross revenue forces its mineral industry to absorb the full cost of the tax. That tax can only be paid out of profits. A

tax on gross revenues is then an implicit tax on net income. Two firms with identical gross revenues will pay a greater or lesser share out of their net income depending on their relative profitability. A tax on gross revenue is regressive because firms earning less profits will pay a greater percentage of net income than firms earning greater profits. Equity can only be restored by explicitly stating a percentage of net income that will be collected.

Gross revenue taxes alter the production decisions of mining firms by raising cut-off grades and rendering marginally profitable operations uneconomic. Under a gross revenue tax, individual mines will produce less and close earlier than under a net income tax, shrinking the tax base and reducing employment of labor and capital. Lost production will be compensated by opening new mines elsewhere.

Although the essence of mining law is the trade in mineral lands, other important considerations include resolution of land-use conflicts, provisions for due diligence, capture of exploration information, and internalization of external (principally environmental) costs. Competition generally insures that lands will be acquired for their highest-value use. Diligence is insured by setting holding costs for mining claims just high enough to exclude acquisition by persons with no real interest in exploring and developing mineral rights. Prudent landowners, public or private, will retain information generated from exploration of their lands, even if the minerals found are not of current economic interest.

To maximize the social return from mineral development, mining firms must account for and internalize environmental costs in their production decisions. When faced with these costs, firms are better able to select the most efficient mitigation approach. Cost-effective instruments for internalizing these costs include legal actions to obtain compensation for damages, taxes on pollutants, and tradable permits for allowable emissions.

*Not presented at Forum.

DISTRIBUTION, COMPOSITION, AND AGE MAPS OF EARLY AND MIDDLE CENOZOIC VOLCANIC CENTERS, ARIZONA, NEW MEXICO, AND WEST TEXAS

Robert G. Luedke

Two new maps (Distribution and composition; Mode of origin and age) of Arizona, New Mexico, and West Texas are the first of a series to show the distribution, composition, and age of early and middle Cenozoic volcanic rocks and eruptive centers in the western conterminous United States. This map series is primarily a data base of igneous centers, a major geologic environment related to and host to mineral deposits throughout western North America.

The volcanic and associated plutonic rocks that were emplaced within the early and middle Cenozoic, about 58 to 16 Ma, are divided into three principal time increments. An earlier published map series (USGS I–1091) designed as a guide for the evaluation of igneous-related geothermal resources had 16 Ma as its maximum cutoff age. The igneous rocks also are classified compositionally into five major groups using a nongenetic system based upon the known or inferred silica content. This rock classification emphasizes the dominant rock type within a designated area, although several rock types may be intermixed.

Some Laramide magmatic and tectonic events that began in the Late Cretaceous or Paleocene continued into the middle Eocene, or at least served as precursors of similar events later in the Cenozoic. However, most of the early and middle Cenozoic igneous rocks shown on the maps are related principally to volcanotectonic activity that started in early or middle Eocene time. Following a quiescence of volcanic activity in the late Eocene, widespread volcanism commenced in the very latest Eocene and continued on a major scale through the Oligocene into the Miocene, to the onset of late Cenozoic bimodal volcanism and associated extensional tectonism characteristic of the Basin and Range province.

Most volcanic rock units shown on the maps fit within the selected time intervals, but, in some localities, a few rock units were included with the dominant younger or older unit in order to maintain geologic, petrologic, and tectonic continuity. For example, the widespread andesitic units occupying much of west-central New Mexico and east-central Arizona include domal eruptive centers, extensive lava flows, and assemblages of stratovolcano deposits consisting of vent and alluvial outflow facies that range in age from Oligocene to early Miocene.

The data base of igneous systems shown on these maps provides the basic information necessary for derivative regional and topical studies such as the development of geologic concepts to identify and assess igneous-related mineral deposits or mineralized systems. Not only do the widespread early and middle Cenozoic volcanic rocks, particularly throughout the south half of Arizona, southwest quarter of New Mexico, and the Big Bend region of West Texas, possibly cover undiscovered base- and precious-metal vein and replacement deposits, but also they may serve as hosts for ore deposits. Caldera source areas and related volcanic rocks, mostly siliceous ash-flow tuffs, are potential sites for mineral deposits.

These new maps show the temporal and spatial relations of the igneous rocks and their geochemical associations, at a single common scale (1:1,000,000), within the many different igneous centers. The maps can also be used as a base for studies of volcanology, volcanotectonics, and the general geology of volcanic and related rocks.

UTILIZATION OF U.S. GEOLOGICAL SURVEY MINERAL RESOURCE DATA BY THE BUREAU OF INDIAN AFFAIRS

Stephen A. Manydeeds

The economic return to Indian mineral owners from development of mineral resources historically has been between 75 and 85 percent of the total income generated on Indian Trust lands. On some Indian lands, the mineral income has exceeded 95 percent of the total income generated. In general, three categories of activities are carried out by the Division of Energy and Mineral Resources (DEMR) and Indian mineral owners: (1) energy and mineral assessments, (2) outreach programs, and (3) educational programs. The U.S. Geological Survey (USGS) plays a role in each of these activities, supplying their expertise in resource assessments and the mineral resource data bases they maintain. All agencies of the Department of the Interior (DOI) share a mandated trust responsibility for Indian Lands that includes mineral resources.

1. The DEMR accomplishes in-house mineral ASSESSMENT activities through its own staff. This activity makes use of public domain mineral resource data generated from a variety of USGS internally funded programs. The DEMR also funds the USGS to provide expertise in cost-effective sharing of networked computer resources and mineral resource data bases. DEMR funding is provided directly to Tribal governments to carry out mineral assessment projects under the direction of their own staff with technical monitoring by the DEMR. Some of these funds go to USGS to perform reservation-scale mineral assessment activities.

2. An OUTREACH program developed by the DEMR addresses several issues: (1) aiding Tribal governments for funding proposals to develop mineral resource assessment programs appropriate to their needs in land-use planning, (2) providing forums for public presentation of the results of mineral assessment and land-use programs on Indian lands, and (3) fostering communication between mineral resource development companies and Indian land-use planners. The DEMR has sponsored four national meetings in Denver, Colo., three poster sessions at the Northwest Mining Association meetings, and regional conferences on oil and gas resources of the Southern Ute, Uinta and Ouray, and Wind River reservations, and mineral resources of the Annette Islands Reserve. The USGS has been a major contributor of posters and papers to these meetings and associated publications.

3. In the category of EDUCATION, the DEMR addresses the issue of limited expertise within Tribal governments to effectively utilize energy and mineral resource data for land-use planning. A program has been developed with the Colorado School of Mines to train Tribal natural resource managers in effective utilization of energy and mineral resource technical information.

The Annette Islands Reserve (Alaska) and the Wind River Reservation (Wyoming) provide two case histories of how the BIA and USGS share mineral resource information and expertise. In the Wind River project, a Tribal government staff dedicated to energy resource development has examined unconventional oil and gas resources. In the Annette Islands Reserve project, a limited staff of resource specialists working closely with the Tribal government has produced a metallic mineral assessment. Both projects have resulted in public presentations of resource assessments, outreach, and educational activities that have benefited the Tribes.

ARSENIC AND ANTIMONY ANOMALIES IN NURE SEDIMENTS SHOW MINERALIZED AREAS IN NORTHWESTERN NEVADA*

Dawn J. McGuire and George V. Albino

Sediment geochemical data from the NURE (National Uranium Resource Evaluation) program collected in northwestern Nevada in 1976–1979 show enrichments in arsenic and (or) antimony which correlate with known mineralized areas and suggest possible mineral deposits in less-explored areas (fig. 1). We examined these data as part of a mineral-resource pre-evaluation of existing regional geochemical data in northwestern Nevada.

Trace elements were analyzed by NURE contractors using instrumental neutron activation analysis on sediments of different size fractions in four 1:250,000-scale quadrangles: Winnemucca and Lovelock (20–40 mesh), and Reno and McDermitt (<100 mesh). The difference in size fractions probably contributed to differences in arithmetic means for As: 33 ppm and 27 ppm for the coarser size fractions analyzed in the Winnemucca and Lovelock quadrangles, and 7 ppm and 5 ppm for the finer size fractions analyzed in the Reno and McDermitt quadrangles, respectively. Although arsenic was analyzed by contractors in all four quadrangles, antimony was analyzed only in the Winnemucca and Lovelock quadrangles. Samples were collected at about one site per 18 km², but not all samples were analyzed for arsenic and antimony. The number of analyzed samples for each element and the replaced minimum (min), maximum (max), and arithmetic mean values for each quadrangle are as follows: Winnemucca, As, 601 samples, min 2.2 ppm, max 587.3 ppm, mean 32.6 ppm; Winnemucca, Sb, 1,018 samples, min 0.5 ppm, max 1,800.0 ppm, mean 10.0 ppm; Lovelock, As, 575 samples, min 1.7 ppm, max 827 ppm, mean 27.1 ppm; Lovelock, Sb, 617 samples, min 0.3 ppm, max
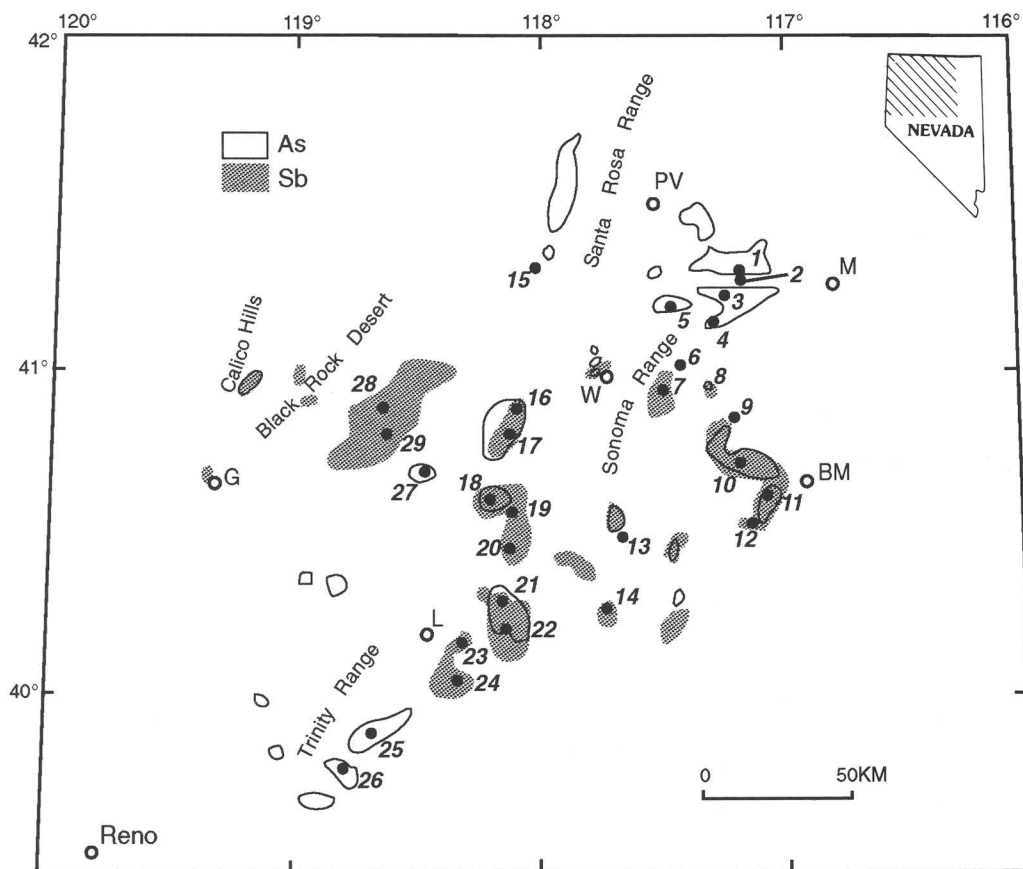
Figure 1 (McGuire and Albino). Areas of As and Sb enrichment in sediments collected and analyzed in the NURE program. BM, Battle Mountain; G, Gerlach; L, Lovelock; M, Midas; PV, Paradise Valley; W, Winnemucca. 1, Chimney Creek; 2, Rabbit Creek; 3, Getchell; 4, Pinson; 5, Dutch Flat; 6, Preble; 7, Kramer Hill; 8, Iron Point; 9, Lone Tree; 10, Marigold; 11, Copper Basin; 12, Copper Canyon; 13, Goldbanks; 14, Kennedy; 15, Sleeper; 16, Central; 17, Mill City; 18, Florida Canyon; 19, Starr; 20, Unionville; 21, Rochester; 22, Relief Canyon; 23, Muttleberry; 24, Wild Horse; 25, Lake; 26, Desert; 27, Majuba Hill; 28, Sulphur; 29, Rosebud.

473.7 ppm, mean 7.3 ppm; Reno, As, 956 samples, min 1 ppm, max 50 ppm, mean 6.9 ppm; McDermitt, As, 1,320 samples, min 1 ppm, max 44 ppm, mean 4.7 ppm. Geochemical interpretations are based on single-element plots of the 75th, 90th, 95th, and 97.5th percentiles of arsenic and antimony in each quadrangle.

Arsenic is present in a variety of minerals in the different mineral deposits in the area, including arsenopyrite and arsenian pyrite, and the arsenic sulfides orpiment and realgar. Antimony-bearing minerals in deposits include stibnite, tetrahedrite, and lead-antimony and arsenic-antimony sulfosalts.

Many areas of known mineralization can be identified in single-element geochemical plots of both arsenic- and antimony-enriched sediments: Florida Canyon hot springs gold mine, Rochester mine (Ag-Au), Relief Canyon mine (Au), Mill City tungsten district, Central district (polymetallic veins), the Battle Mountain district including the

Marigold mine (Au) and Copper Basin (Cu-Mo-Au), among others. The larger, more productive gold mines such as Florida Canyon and Marigold had not yet been discovered in the late 1970's when the NURE samples were collected and analyzed. Antimony enrichments, without arsenic enrichments, surround hot-springs gold deposits of the Sulphur district, Rosebud district (Au-Ag), Unionville district (Ag), Kramer Hill mine (Au), and other deposits. Arsenic enrichments, without antimony enrichments, characterize areas near the arsenic-enriched Chimney Creek (Twin Creeks), Getchell, and Pinson sediment-hosted gold deposits and the Kelley Creek valley to the east, as well as other areas.

Several areas lack known significant mineralized rock but are enriched in both arsenic and antimony: the southern Calico Hills, the east-central part of the East Range northwest of the hot springs gold-mineralized area of Goldbanks Hills, and the east side of the Tobin Range (east of the Big

Mike base-metal mine). Areas showing arsenic-enriched sediments without antimony enrichment include basins north of Chimney Creek (northern Eden and Kelley Creek valleys and adjacent areas south of the Humboldt River), Spring Creek (north of Hot Springs Peak and the Humboldt River), the Quinn River valley area, and a small area at the northern tip of Slumbering Hills (northeast of the Sleeper mine). Areas containing antimony-enriched stream sediments without arsenic enrichment include the East Range near and southeast of Kyle Hot Springs, the southern East Range northeast of McKinney Pass and southeast of Granite Mountain, and other, smaller areas with single-sample anomalies such as Granite Point near Gerlach, an area west of Pahsupp Mountain, and two areas in the southern part of the Black Rock Desert.

The significance of these results is that the distribution of arsenic- and antimony-enriched NURE sediment clearly shows some known districts and mines, including mines that only recently were discovered and became significant gold producers in the late 1980's. The correspondence of arsenic- and antimony-enriched sediments with known mineralized rocks suggests that similar anomalies in the less-explored areas listed herein may indicate locations of undiscovered mineral deposits of various types.

*Not presented at Forum.

DIVERGENT FOLD ORIENTATIONS IN LOWER PALEOZOIC ROCK UNITS INDICATE MULTIPLE TECTONIC EVENTS IN NORTH-CENTRAL NEVADA—OSGOOD MOUNTAINS, EDNA MOUNTAIN, AND THE HOT SPRINGS RANGE*

Dawn J. McGuire and A. Elizabeth Jones

Our studies have documented divergent orientations of folding in lower Paleozoic rocks in the Osgood Mountains, Edna Mountain, and the Hot Springs Range of north-central Nevada. These various orientations require either a single mid-Paleozoic tectonic event with multiple vergence directions in the different rock units (a complicated pattern of deformation during the Antler orogeny), or more likely, multiple tectonic events with differing stress orientations affecting these units during both Paleozoic and Mesozoic time.

We have recognized three lower Paleozoic lithotectonic units based on stratigraphic and structural characteristics: (1) the Proterozoic(?) and Lower Cambrian Osgood Mountain Quartzite, the Lower Cambrian to Lower Ordovician Preble Formation, and rocks mapped as Ordovician Comus Formation on the east side of the Osgood Mountains; (2) Lower Ordovician to Lower Silurian rocks mapped as Valmy and Vinini Formations and the Middle Ordovician Comus For-

mation at Iron Point (on the northeastern flank of Edna Mountain); and (3) the Upper Cambrian Paradise Valley Chert and overlying Upper Cambrian and Lower Ordovician(?) Harmony Formation in the Hot Springs Range.

The first lithotectonic unit includes the Osgood Mountain Quartzite and the gradationally overlying Preble Formation (Hotz and Wilden, 1964; Madden-McGuire and Marsh, 1991). Folds in the Preble Formation are predominantly west-vergent and south-plunging as observed along the strike of the unit for 60 km from Anderson Canyon in the northern Osgood Mountains to Hot Springs Ranch on the east side of the Sonoma Range. Poles to foliation and bedding cluster together on stereonet plots, based on more than 200 measurements. Rocks previously mapped as the Comus Formation, on the east side of the Osgood Mountains, have more scattered fold orientations. Plots of more than 200 poles to foliation and bedding show a cluster resulting from west-vergent folds similar to those of the Preble Formation, along with additional, scattered points, suggesting refolding. Stratigraphic evidence suggests that metamorphism and west-vergent folding occurred in middle Paleozoic time, between Late Ordovician (the age of the youngest involved strata) and Middle Pennsylvanian, when the Battle Formation is thought to have been deposited on an unconformity above metamorphosed lower Paleozoic rocks. Later movement along the unconformable contact created a low-angle fault above the Preble Formation and associated units (the "Iron Point thrust" of Erickson and Marsh, 1974). Exposed metasedimentary rocks of the first lithotectonic unit are inferred to have contributed to late Paleozoic sedimentation, because coarser parts of the upper Paleozoic units exposed on Edna Mountain contain clasts of quartzite, phyllite, and limestone (Erickson and Marsh, 1974).

Later deformation is evident in the northwestern Osgood Mountains, where a post-Pennsylvanian-Permian tectonic event locally folded and faulted the Middle Pennsylvanian to Lower Permian(?) Etchart Limestone and refolded the Preble Formation in a west-vergent orientation. The extent of this Mesozoic(?) deformation is unknown, but certain areas clearly have been affected by post-Paleozoic west-vergent deformation.

The second lithotectonic unit includes the Valmy Formation in the northern Osgood Mountains and the Vinini and Comus Formations to the south, at Iron Point. These units show east-vergent folding that is clearly different from folding in the Preble and Harmony Formations, based on more than 250 poles to bedding and foliation. East-vergent folding took place between Early Silurian (the age of the youngest involved rocks) and Middle Pennsylvanian deposition of the Etchart Limestone over the lower Paleozoic rocks, as seen on "Etchart hill" near the Getchell mine (Madden-McGuire and Marsh, 1991). Original stratigraphic continuity between the first and second lithotectonic units would require a complex and divergent structural history, and cannot be proven because of their differing fold orientations.
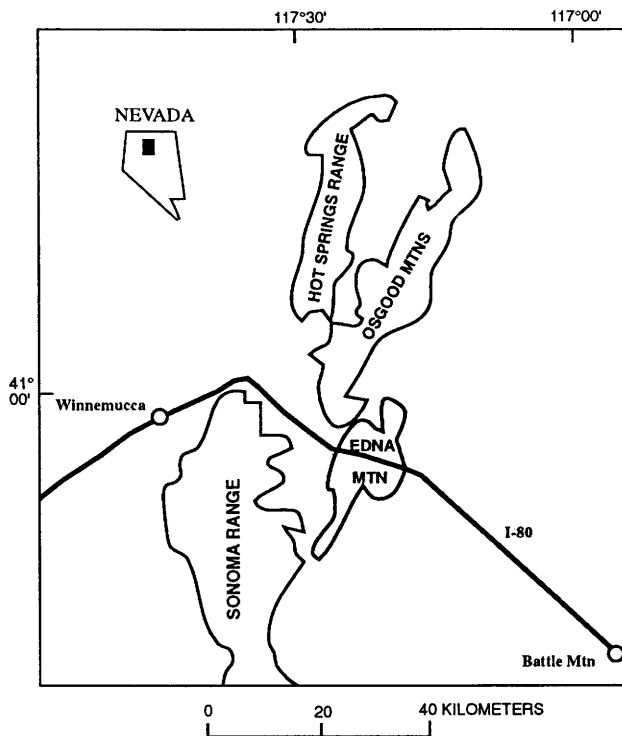
Figure 1 (McGuire and Jones). Location map showing Osgood Mountains, Edna Mountain, and surrounding area, Humboldt County, Nev.

The third unit contains the Paradise Valley Chert and overlying Upper Cambrian (Hotz and Willden, 1964) and Lower Ordovician(?) (Madden-McGuire and others, 1991) Harmony Formation. These units show west-vergent folding in the southern part of the Hot Springs Range (based on more than 1,600 poles to bedding and foliation in the Harmony Formation and 76 poles to bedding in the Paradise Valley Chert; Jones, 1993). Approximately 300 facing-known poles to bedding in the Harmony Formation show that the steeply east dipping beds are generally the overturned ones, indicative of west-vergent folding (Jones, 1993). Folding of the Harmony Formation in the Hot Springs Range predates the intrusion of a small Cretaceous(?) granitic plug at Dutch Flat. The pervasive west-vergent folding of the Harmony Formation and Paradise Valley Chert and the lack of evidence for multiple folding events suggest that these units were not affected by east-directed "Antler" deformation during the middle Paleozoic. The unusual arkosic lithology of the Harmony Formation suggests that it is allochthonous with respect to the partly coeval Preble Formation. It is not clear whether the west-vergent folding in the Harmony Formation is related to the west-vergent folding of the Preble Formation, or to later Mesozoic(?) deformation that affected both the Etchart Limestone and the Preble Formation in the northwest Osgood Mountains. This later deformation is inferred to correlate with the post-Triassic "Willow Creek"

belt, which is exposed to the south in the East Range and Sonoma Range.

The lower Paleozoic units show evidence for a combination of west- and east-directed Paleozoic and west-directed Mesozoic deformational events. Their structural history cannot be explained by a single east-directed tectonic event, commonly known as the Antler orogeny.

REFERENCES

Erickson, R.L., and Marsh, S.P., 1974, Geologic map of the Golconda quadrangle, Humboldt County, Nevada: U.S. Geological Survey Geologic Quadrangle Map GQ-1174, scale 1:24,000.

Hotz, P.E., and Willden, R., 1964, Geology and mineral deposits of the Osgood Mountains quadrangle, Humboldt County, Nevada: U.S. Geological Survey Professional Paper 431, 128 p., scale 1:62,500.

Jones, A.E., 1993, Northwest vergent folding in the Harmony Formation, north-central Nevada—Lower Paleozoic tectonics revisited: Geological Society of America Abstracts with Programs, Cordilleran Section Meeting, v. 25, no. 5, p. 59.

Madden-McGuire, D.J., Hutter, T.J., and Suczek, C.A., 1991, Late Cambrian/Early Ordovician microfossils from the allochthonous Harmony Formation at its type locality, northern Sonoma Range, Humboldt County, Nevada: Geological Society of America Abstracts with Programs, Cordilleran Section Meeting, v. 23, no. 2, p. 75.

Madden-McGuire, D.J., and Marsh, S.P., 1991, Lower Paleozoic host rocks in the Getchell gold belt—Several distinct allochthons or a sequence of continuous sedimentation?: Geology, v. 19, p. 489–492.

*Not presented at Forum.

TIMING OF IGNEOUS ACTIVITY, ALTERATION, AND MINERALIZATION AT THE ORCOPAMPA Ag-Au DISTRICT, SOUTHERN PERU

Edwin H. McKee, Peter Craig Gibson, Donald C. Noble, and Kirk E. Swanson

The Orcopampa Ag-Au district is located in southern Peru about 160 km northwest of Arequipa. It is one of a group of epithermal precious-metal deposits, including Arcata, Cailloma, Shila, and Suyckutambo, of Miocene age in the central Andes. Orcopampa is in a belt of calcalkaline volcanic rocks of intermediate to silicic composition; common volcanic features include stratovolcanos, calderas, and dome complexes. The mineral deposits in the Orcopampa district are in a series of generally northeast striking veins within steeply dipping normal faults. Several distinct periods of hydrothermal alteration are recognized. Precious-metal mineralization is associated with the youngest period, which

was characterized by potassium metasomatism and quartz-adularia-sericite alteration.

Potassium-argon and $^{40}Ar/^{39}Ar$ dating of 10 samples of unaltered volcanic rock in the region and 9 samples of altered wallrock and vein material are the basis for the geochronology at Orcopampa. Volcanic activity began with the formation of a stratovolcano complex at about 21 Ma. Rocks in this complex are mostly pyroxene andesite breccias, lavas, and associated silicic tuffs that are intruded by dikes, sills, and irregular bodies of andesite. These rocks are propylitized. Overlying this complex with slight unconformity is a regionally widespread rhyolite ash-flow sheet named the Manto Tuff (Gibson and others, 1990). Outflow sheet tuffs and intracaldera tuffs of the Manto Tuff exposed near or within its source, the Chinchón caldera about 15 km southeast of the Orcopampa district, are about 20 million years old. The Manto Tuff is not propylitically altered near the mines. Dacite lava flows, domes, and dikes of the Sarpane volcanics (Gibson and others, 1990) in the Orcopampa district were emplaced about 1.5 million years after eruption of the Manto Tuff. Three K-Ar dates on biotite and hornblende phenocrysts from dacite domes in the Sarpane volcanics are 18.3±0.6, 18.6±0.6, and 19.4±0.6 Ma. Hydrothermal breccia along veins in the Sarpane volcanics in the eastern part of the district contains quartz, alunite, and kaolinite and is associated with zones of silicification and argillic alteration. K-Ar age determinations on three samples of alunite from the Santiago Norte vein yielded ages of 18.4±0.5, 18.4±0.6, and 19.5±0.6 Ma, which is the same, within analytical uncertainty, as the Sarpane volcanics. The veins that contain precious-metal ore are associated with quartz-adularia-sericite alteration. K-Ar and $^{40}Ar/^{39}Ar$ dates on wallrock and vein adularia from the Manto, Calera, Santiago Norte, and Tudela veins are 17.0±0.5, 17.0±0.5, 17.6±0.6, 17.4±0.4, 17.7±0.6, 17.9±0.5, 17.9±0.5 Ma; the preferred age of mineralization is 17.7 Ma, about 1 m.y. younger than the alunite. A number of paragenetic substages within this low-sulfidation assemblage are recognized, but they are too close to the same age to be distinguished by our radiometric dates.

The total span of igneous and hydrothermal activity in the Orcopampa district is no more than about 3.5 to 4 million years (21 to 17.5 Ma). Within this short interval, the evolution of the volcanic hydrothermal system produced first volcanic rocks, followed by quartz-alunite alteration, in turn followed by quartz-adularia-sericite alteration. None of the earlier magmatic and hydrothermal events can be unequivocally related genetically to the 17.7 Ma episode of Ag-Au mineralization.

REFERENCE

Gibson, P.C., Noble, D.C., and Larson, L. T., 1990, Multistage evolution of the Calera Epithermal Ag-Au vein system, Orcopampa district, southern Peru—First result: Economic Geology, v. 85, p. 1505–1520.

GEOLOGY AND MINERAL RESOURCES OF THE LORETO–SAN JAVIER AREA OF NORTHERN BAJA CALIFORNIA SUR, MEXICO—RESULTS OF RECONNAISSANCE FIELD MAPPING

Hugh McLean

The Loreto and part of the San Javier 1:50,000 quadrangles in the northeastern part of Baja California Sur, Mexico, were mapped in reconnaissance by U.S. Geological Survey personnel in the mid-1980's. Field studies focused on the distribution and structural relations between Mesozoic granitic and metamorphic rocks and overlying Tertiary and Quaternary sedimentary and volcanic rocks.

The oldest rocks in the Loreto area are volcaniclastic sandstone and breccia that are metamorphosed to greenschist facies by the intrusion of Upper Cretaceous granitic rocks. The granitic rocks are locally exposed and are interpreted to be part of the peninsular batholith which crops out discontinuously from southern California to the southern tip of the Baja peninsula. Sedimentary lithofacies that unconformably overlie the Mesozoic basement rocks include red and white crossbedded sandstone, impure phosphatic sandstone, and volcaniclastic sandstone interbedded with welded tuffs that yield Oligocene radiometric ages. The locally exposed crossbedded sandstones may be as old as Eocene.

A section of lower Miocene volcaniclastic/volcanogenic sandstone, conglomerate, and breccia that is as thick as 1,500 m constitutes the bulk of the mountainous areas in the Loreto area. Along the coast of the Sea of Cortez, massive flows and breccia represent a near-vent volcanic facies. Coeval strata exposed in mountains to the west were deposited mainly by fluvial processes and are thinner and finer grained than the near-vent facies. Approximately 6 km west of the town of Loreto, swarms of dark-colored basaltic andesite dikes intrude the lower Miocene near-vent breccia. Light-colored felsic dikes also intrude the breccia in the same area. The felsic dikes are several tens of meters thick and are visible on aerial photographs for as much as 6 km. Alteration of the host breccia by the intrusion of the mafic and felsic dikes has produced a suite of clay and zeolite minerals. Geochemical surveys are needed to determine the extent of metallic mineralization. Hornblende from an andesitic stock associated with the silicic dikes yielded a K-Ar age of 19.4±0.9 Ma.

Epidote- and pyrite-bearing prebatholithic greenschist-facies rocks have been explored by small prospects with no reported recovery of valuable metals. Detrital modes indicate that impure phosphatic sandstone that unconformably overlies granitic rock contains as much as 60 percent pelloidal phosphate.

Extensional faulting that appears to be associated with the opening of the Gulf of California juxtaposes fossiliferous Pliocene marine strata with granitic basement rocks and pre-Pliocene strata. Rhyodacitic tuffs interbedded with the marine beds yield radiometric ages that range from 1 to 3 Ma. Quaternary rocks include basaltic lavas, cinder cones, and pyroclastic ejecta of local extent. Elevated Quaternary alluvial terrace deposits are in various stages of dissection.

INDUCTIVELY COUPLED PLASMA MASS SPECTROMETRY—A POWERFUL ANALYTICAL TOOL FOR MINERAL RESOURCE AND ENVIRONMENTAL STUDIES

Allen L. Meier, David J. Grimes, and
Walter H. Ficklin

The analytical technique of inductively coupled plasma mass spectrometry (ICP-MS) is being used for both mineral resource and environmental studies. Ground water associated with disseminated-gold deposits in Nevada is analyzed by ICP-MS to study elemental dispersion patterns around these deposits. The technique is also used to analyze surface water draining from mineralized and previously mined areas in Colorado to determine elemental mobility from these sources, for use in environmental studies. ICP-MS is extremely useful in these applications because of its ability to rapidly determine as many as 60 elements directly in the sample without the need for preconcentration or dilution and with detection limits in the sub-part-per-billion range and a linear range of six orders of magnitude or more.

Calibration for this extensive elemental coverage is accomplished by using a standard containing known concentrations of easily ionized elements across the elemental mass range as well as a few elements that are less likely to be totally ionized by the ICP. A response curve of the observed intensity for easily ionized elements versus mass is constructed using a second-order equation for a best fit over the entire mass range. The ion temperature and electron number density of the plasma are estimated using the data from the harder-to-ionize elements. These are used to estimate the degree of ionization for all elements in the plasma. By using the response curve derived, the degree of ionization, and the natural isotopic abundance, semiquantitative estimates of concentration for all elements can be made in samples without the need of a calibration standard for every element.

The main limitations of the technique come from drift due to clogging of sampling orifices; changes in ion transfer efficiencies due to sample matrix effects, plasma conditions, nebulizer, or electronics; and isobaric interference from polyatomic or doubly charged ions. Internal standards are used to correct for drift; interferences are minimized by

Figure 1 (Meier and others). A ground-water sample being collected from a drill hole using a double-check valve bailer. Photograph by David J. Grimes.
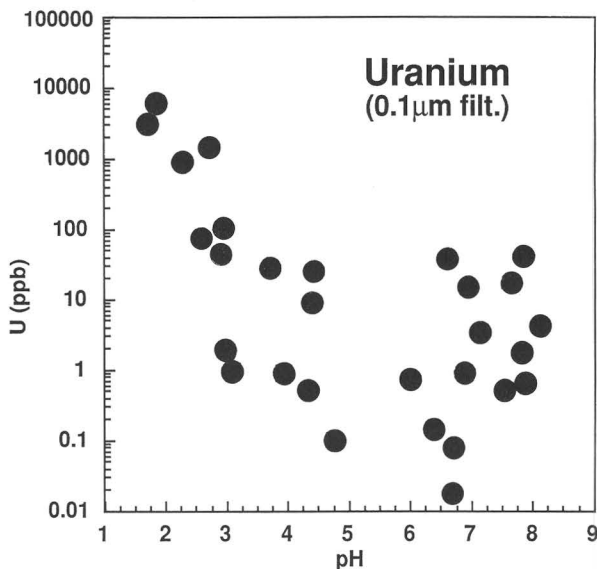
Figure 2 (Meier and others). Uranium concentrations determined by ICP-MS in water samples collected throughout Colorado plotted as a function of pH.

selection of the isotope used for determination or by mathematical correction.

The ICP-MS technique has been applied to the analysis of ground-water samples collected from drill holes near known covered disseminated gold deposits in northern Nevada, to study the hydromorphic mobility of ore-associated elements such as arsenic, antimony, and tungsten.

Ground-water samples were collected during active drilling and from old exploration drill holes. The water from the old drill holes was sampled at and below the water table using a custom-built double-check valve bailer (fig. 1). At each sample site, a 40 mL portion of water was filtered through a 0.45 μm membrane filter, acidified to a pH of approximately 2 with four drops of concentrated nitric acid, and stored in polyethylene bottles for ICP-MS analysis.

Results of the ICP-MS analysis of drill-hole water samples indicate the presence of hydromorphic dispersion anomalies for arsenic, antimony, and tungsten near the buried disseminated gold deposits. In these ground-water samples, the arsenic concentrations ranged from 14 to 130 μg/L; antimony, from 2.6 to 82.0 μg/L; and tungsten, from 15 to 99 μg/L. The low determination limits provided by the ICP-MS technique also enabled local background levels for the ore-associated elements in ground water to be established.

ICP-MS has been used in an environmental study of mine drainage in Colorado. Because of its capability to quantify a range of elements, it is useful in assessing the role of elements that are not ordinarily determined in mine water samples. The major cations in mine water are ordinarily calcium, magnesium, sodium, and potassium. In many low-pH mine waters, the concentration of iron, manganese, copper, and zinc can equal or exceed the concentration of the major cations. All these elements are easily determined by either atomic absorption or ICP-AES. However, the rare-earth elements, uranium, and many other metals that occur in small concentrations are not detectable by the more conventional methods used. Figure 2 shows uranium concentrations plotted as a function of pH for mine water samples collected throughout Colorado. This example demonstrates the low limits and range of the ICP-MS technique for uranium.

GENERATION OF NATURAL ACID DRAINAGE AND FORMATION OF IRON BOGS, ROCKY MOUNTAINS, COLORADO

William R. Miller, John B. McHugh, and Walter H. Ficklin

Pyrite oxidation in altered and mineralized areas in the Colorado Mineral Belt has led to the generation of natural acid drainage (NAD) that has impacted surface waters in areas where mining is absent or limited. The naturally acidic waters are similar in composition to some of the more familiar acid mine drainage (AMD) waters. The concentrations of Fe, Mn, and Al in stream waters are usually less than 10 mg/L but can reach several hundred mg/L; Cu, Ni, and Zn are usually less than 1 mg/L but can reach several mg/L, and other metals such as Pb are generally less than 0.01 mg/L. The metal contents of low-flow seeps may exceed these concentrations, but their impact on stream-water chemistry is usually insignificant.

Geneva Creek in the Front Range of Colorado is an example of a drainage impacted by NAD. The Geneva Creek drainage basin is underlain by Proterozoic metamorphic and igneous rocks, which have been intruded by Tertiary felsic stocks with associated pyritic alteration. Oxygen-charged waters from snow and rain strongly oxidize and dissolve pyrite, releasing H^+, Fe^{2+}, SO_4^{2-}, and trace metals to the waters of the study area. The dominant source of trace metals in the waters is trace-metal-bearing disseminated pyrite. The Fe^{2+} reacts with water, forming hydrous iron-oxide precipitates that accumulate along changes in slope and at the base of permeable zones. In these places iron bogs and iron-oxide zones can occur either as masses or as material cementing clastic and organic matter. Large accumulations of hydrous iron-oxide precipitates also occur locally along Geneva Creek. Substantial amounts of these precipitates are scoured out and removed from the upper basin each season during spring runoff, but are preserved in the lower gradient areas. Wetlands and terraces trap the

precipitates and prevent the spring runoff from removing this material, thus establishing iron bogs along the drainages.

For these NAD waters, metals are present in the stream waters as simple cations. Chemical modelling calculations suggest that the concentrations of Fe and Al in stream waters are controlled by the mineral phases ferihydrite and jurbanite. At most sites the Cu, Ni, and Zn concentrations are controlled by sorption onto precipitating hydrous metal oxides.

The range of metal contents in waters and the processes controlling the concentrations of metals in water in the study area can probably be considered typical for other similarly altered and mineralized areas underlain by geochemically comparable rocks in the Colorado Mineral Belt. The results of this study can aid in establishing natural geochemical backgrounds for waters draining areas affected by AMD and in the understanding of processes controlling the concentrations of metals in surface waters. The study suggests that it may be difficult to impossible to remediate AMD sites to unnatural conditions that are more pristine than those present prior to mining.

ASSESSMENT OF MINERAL RESOURCES AND TECTONIC SETTING DERIVED FROM DIGITAL AEROMAGNETIC DATA IN THE GUAYANA SHIELD, NORTHWESTERN BRAZIL

Fernando P. Miranda and Anne E. McCafferty

Reconnaissance geologic mapping is usually the first step of mineral exploration projects in tropical, remote regions of Latin America. The objective of such an enterprise is to quickly determine as much as possible about the geology of an unknown area. Reconnaissance maps at scales of 1:250,000 or less are typically based on photogeologic and SLAR (Side Looking Airborne Radar) interpretations and on incorporation of geology from published reports; only a minimum amount of time can be spent on the ground to identify rock types. A reconnaissance geologic map can also be obtained using information derived from the digital manipulation of data acquired in regional aerogeophysical surveys. This is especially true in dense jungle of the Guayana Shield.

Our study area is situated in the Pico da Neblina and Ica quadrangles, northwest Brazil, and covers an area of approximately 54,500 km². A geologic reconnaissance of the region was included in the RADAMBRASIL Project, a government enterprise that mapped the whole Brazilian territory from 1971 to 1976 (Correa, 1980). Final geologic maps were presented by the RADAMBRASIL Project at 1:1,000,000 scale (Pineiro and others, 1976; Fernandes and others, 1977). The region is mostly underlain by Middle Proterozoic crystalline rocks of the Guianense Complex,

which includes a complex association of gneissic and granitoid rocks not mapped as separate units on the RADAMBRASIL geologic map. However, Dall'Agnol and Abreu (1976) recognized three main lithologic types in order of abundance: sphene- and amphibole-bearing biotite granitoids and gneisses; two-mica granites and gneisses; and amphibolites and metabasic rocks.

Serious logistical difficulties exist for geologic studies in the area: (1) the regional scale (1:1,000,000) of the only available geologic maps; (2) dense vegetation and thick soil cover (the area is nearly devoid of rock exposures); (3) poor accessibility; (4) flat topography (lithologic boundaries and geologic structures have no evident geomorphic expression). Therefore, the main objective of our research is to produce useful maps by digitally processing and analyzing the available aeromagnetic data in order to facilitate the assessment of mineral resources and the study of the tectonic setting of the region.

The digital aeromagnetic data used in our research were obtained in 1987 and are part of a larger reconnaissance aeromagnetic survey that covered the border region with Venezuela, Colombia, and Brazil. A reduced-to-pole magnetic anomaly map was calculated in order to correct for the severe anomaly distortion caused by the low geomagnetic latitude of the area and to facilitate the interpretation of anomalies located over their causative sources. A terrace-magnetization map was calculated that delineates induced magnetization boundaries and outlines geologic structures that have contrasting magnetic properties. Maxima of the horizontal gradient of pseudogravity were calculated to map abrupt lateral changes in magnetization interpreted to reflect steep structural or lithologic contacts.

Digital manipulation of the aeromagnetic data allowed the recognition of induced magnetization domains possibly associated with unreported intrusive bodies in the crystalline rocks of the Guianense Complex. Magnetization boundary lines extending for tens of kilometers may represent shear zones not portrayed in the geologic maps of the RADAMBRASIL Project. These features are potential target areas for future mineral exploration (gold in particular). However, follow-up ground geologic work is necessary to determine if a connection between the inferred targets and mineral resources exists. Results of the research are an extension of a similar methodology carried out in the Guayana Shield by Miranda and others (in press).

REFERENCES

Correa, A.C., 1980, Geological mapping in the Amazon Jungle—A challenge to side looking radar: Jet Propulsion Laboratory Publication 80–61, p. 385–416.

Fernandes, P.E.C.A., and others, 1977, Geologia, Chapter 1 of Projecto RADAMBRASIL, folha SA.19, Ica: Rio de Janeiro, Brazil, Departamento Nacional da Producão Mineral, p. 17–124, 5 plates, scale 1:1,000,000.

Miranda, F.P., McCafferty, A.E., and Taranik, J.V., in press, Reconnaissance geologic mapping of a portion of the rain forest covered Guiana Shield, northwestern Brazil, using SIR-B and digital aeromagnetic data: Geophysics.

Pineiro, S.S., Fernandes, P.E.C.A., Pereira, E.R., Vasconcelos, E.G., Pinto, A.C., Montalvao, R.M.G., Issler, R.S., Dall'Agnol, R., Teixeira, W., and Fernandes, C.A.C., 1976, Geologia, *in* MME Projecto RADAMBRASIL, Levantamento de Recursos Naturais, Folha NA.19—Pico da Neblina: Rio de Janeiro, Brazil, Departamento Nacional da Producão Mineral, v. 11, p. 17–137.

SLEEPER GOLD-SILVER DEPOSIT, HUMBOLDT COUNTY, NEVADA—IMPORTANCE OF MIOCENE EXTENSIONAL TECTONICS*

J. Thomas Nash and Wayne Trudel

The world-class deposit of gold and silver at the Sleeper mine, Nevada, formed at about 15–16 Ma in a local volcanic field during the early stages of basin-and-range extension. Bonanza veins of opal-adularia-electrum contain more than 1.5 million oz Au, and widespread, bulk-mineable Ag-Au-bearing quartz-FeS_2 stockworks and breccias contain more than 1 million oz Au. Both ore types exhibit strong structural controls in brittle, formerly glassy rhyolite flows or a flow-dome complex. Ore-associated alteration is dominated by opaline and microcrystalline silica. Silicification decreases downward, over about 100 m, and grades laterally into argillic- and perlitic-altered rhyolite. Adjacent andesitic rocks, broadly altered to quartz-sericite-pyrite, are bulk-mined for their 0.02–0.1 oz Au/t. The Sleeper deposit has many of the features of the adularia- sericite class of epithermal deposits, except that it has a high Au:Ag ratio and lacks chlorite and base metals at depth.

Basin-and-range extensional tectonics played a major role in creating and protecting the ore. The basal Tertiary unit of clastic sedimentary rocks, about 200 m thick, formed in an extension-related lacustrine basin of probable Miocene age. Bimodal volcanic eruptions occurred from >17 to 13 Ma along normal faults. Andesitic and basaltic lavas about 150 m thick are sulfidized and altered over a broad area below ore. Lapilli tuff and tuff cones were deposited locally on the lavas. The glassy rhyolite of the Sleeper mine, here called Sleeper rhyolite (about 17 Ma), is the main ore host; this rhyolite unit is shattered by pre- and post-ore fractures and faults. Ash-flow tuffs (16.1 and 15.6 Ma, about 100 m thick), erupted from the McDermitt caldera complex (80 km north), probably covered the Sleeper rhyolite at the time of ore formation. After a period of substantial erosion, rhyolite lavas erupted at 13.6 Ma and probably covered ore. Multiple stages of normal faulting crushed but did not dismember ore zones; ore was down-dropped about 1,000 m, oxidized at several stages, and in part eroded into nearby placers.

Reconstruction of district geology suggests a larger role for structure and pre-Tertiary rocks than volcanism in ore formation. Geologic, geochemical, and geochronologic data do not indicate a pluton-driven geothermal system. Rather, the system probably was driven by high regional heat flow and deep meteoric circulation in active normal fault and fracture zones. Gold-adularia veins (17 Ma) in Mesozoic phyllite at the Jumbo mine, 6 km to the southeast, and in phyllite below the Sleeper orebody are manifestations of the moderately hot (<300 °C) waters in basement rocks. Reactions in metapelitic rocks would have produced fluid compositions similar to those advocated for Carlin-type gold deposits (high CO_2, CH_4, HS^-). Based on volumes of altered rocks and likely flow paths, we favor a source of gold in metapelitic rocks.

Sleeper ores formed at very shallow depth, probably <200 m below the contemporary land surface, and at temperatures of <200 °C. Conditions fluctuated repeatedly from local hydrothermal explosion breccias to open-standing large veins filled by delicately banded ore and gangue. Deposition probably was initiated by boiling, fluid mixing, and cooling. The bonanza zones are small targets that are difficult to anticipate in exploration, but the postulated extension-related geothermal system, with variable low- to high-grade ore, could have developed in diverse rock packages in many parts of the Basin and Range province.

*Not presented at Forum.

HEAVY-METAL CONTAMINATION IN RIVER, ESTUARY, AND MARINE-SHELF SEDIMENT FROM THE RIO TINTO MINES, SPAIN

C.H. Nelson, A. Van Geen, P.J. Lamothe, and A. Palanques

The Rio Tinto mine in the eastern Iberian Pyrite Belt (fig. 1) is the world's largest sulfide deposit (>170 million t (metric tons)) and longest continually operating mine (>5,000 years)(Schermerhorn, 1982; Wilson, 1981). Extensive mining activities began during Roman times and supported the conquests and currency of the Roman Empire. An initial 500–750 million tons of ore may have been removed by erosion prior to man's mining activities. The natural erosion and especially the later mining activities of this ore, which contains 0.7 percent copper, 2.9 percent zinc, 1.1 percent lead, and 0.6 percent arsenic, have supplied heavy metals to sediment, river water, and seawater in the Strait of Gibraltar region.

70
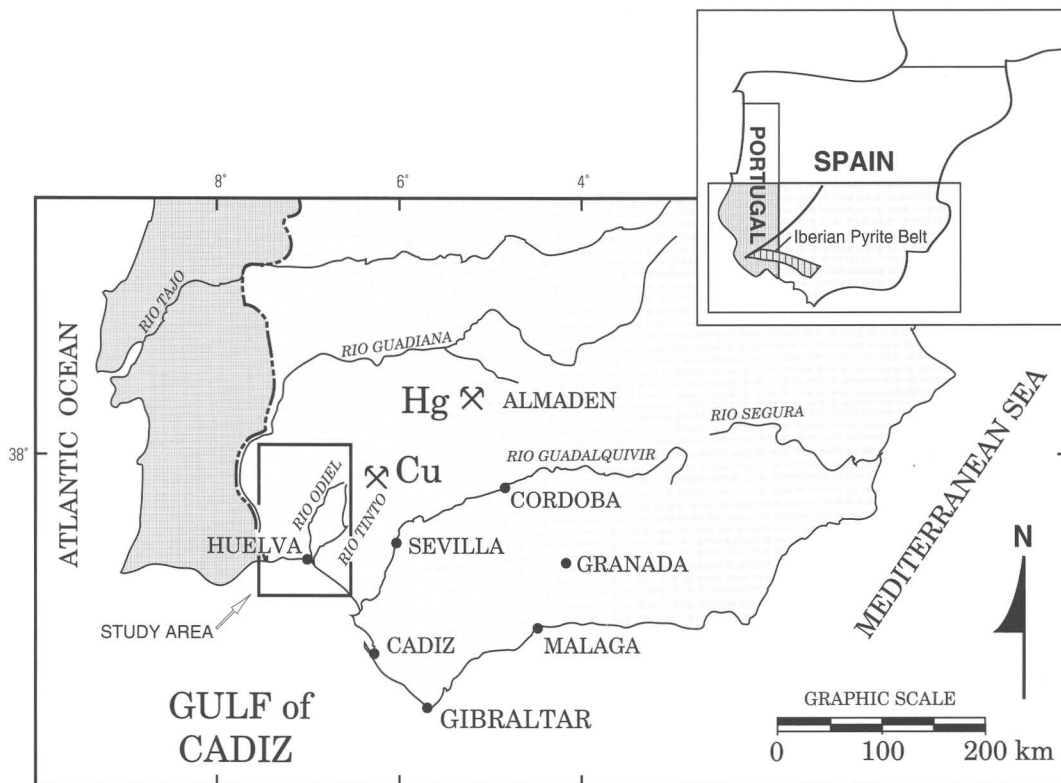
Figure 1 (Nelson and others). Location map of the Rio Tinto and Rio Odiel study area showing the region of the Iberian Pyrite Belt and the main Tinto copper sulfide deposit in relation to the river drainage systems.

The Tinto and Odiel Rivers drain 100 km from the east and west sides of the Rio Tinto sulfide mining district, and join at a 20-km-long estuary entering the Atlantic Ocean. A reconnaissance study of heavy-metal anomalies in river and estuary bottom sediment by semiquantitative emission dc-arc spectrographic analysis shows the following upstream to downstream ranges, in ppm: As (3,000– <200), Cd (30–<0.1), Cu (1,500–10), Pb (2,000–<10), Sb (300–<150) and Zn (3,000–<200) (fig. 2). Organic-rich (1.3–2.6 percent TOC-total organic carbon) sandy-silty overbank clay has been analyzed to represent suspended load materials. The high content of heavy metals in the overbank clay throughout the river and estuary systems indicates the importance of suspended sediment transport for dispersing heavy metals from natural erosion and anthropogenic mining activities of the sulfide deposit. The organic-poor (0.21–0.37 percent TOC) river-bed sand has been analyzed to represent bedload transport of naturally occurring sulfide minerals. The sand exhibits high metal contents upstream, but these decrease an order of magnitude in the lower estuary. Although concentration in estuary-mouth beach sand has been diluted to background levels, estuary mud exhibits increased contamination of heavy metals that is apparently related to finer grain size, higher organic carbon content, and precipitation

of river-dissolved solids. The contaminated estuary mud disperses to the inner-shelf mud-belt (IGME, 1974) and offshore suspended sediment, which exhibit metal anomalies from river sulfide sources (for example, Cu, Zn; fig. 2). The heavy metal contamination of Tinto-Odiel river sediment reaches or exceeds the highest levels encountered in other river sediment of Spain and throughout Western Europe.

The mud blanket of the middle to outer continental shelf in the Gulf of Cadiz contains a historical record of metal input to the ocean from the Rio Tinto mining region. Preliminary results show 3- to 15-fold Cu and Zn enrichments in surface sediment over the whole mud blanket relative to deeper intervals in 2-m gravity cores. Dating of these sediment cores currently underway will help to define the onset of metal enrichment in the mud blanket and provide a time frame for comparison with known activities in the Rio Tinto mining region. Extremely high dissolved Cu and Zn concentrations observed in the water column of the Gulf of Cadiz (Atlantic Ocean), the Strait of Gibraltar, and the Alboran Sea (Mediterranean Sea) are directly traceable to input from the Tinto estuary. The distribution of sediment and water-column enrichments demonstrates the impact of the Rio Tinto mining activities in late Holocene time.

71
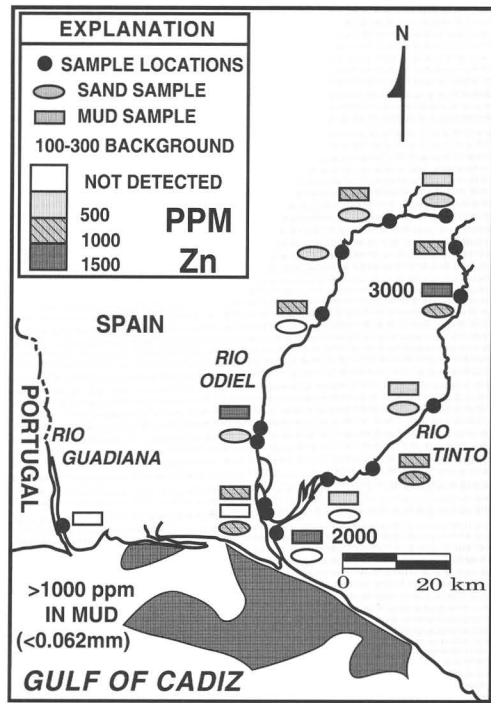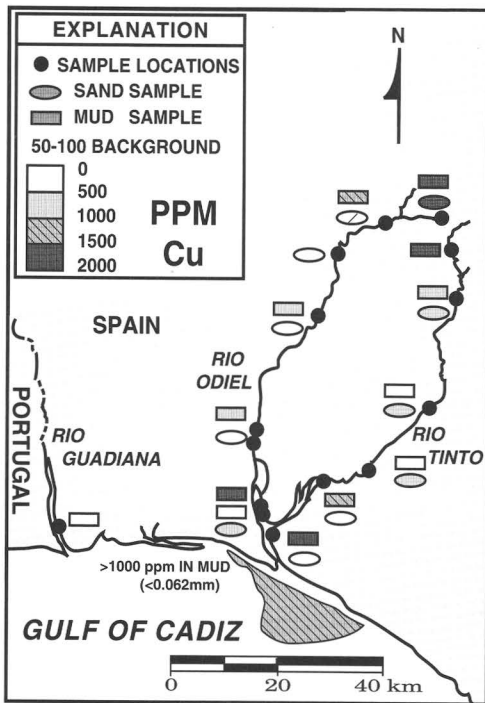
Figure 2 (Nelson and others). Content of copper and zinc in Tinto and Odiel river-bed sand and river-bank mud. Off-shore data are modified from IGME (1974) and typical background values are from Levinson (1974, table 2–1, p. 44–45).

REFERENCES

Instituto Geologico y Minero de Espana (IGME), 1974, Investiga-cion Minera Submarina en el Subsector "Huelva 1" Golfo de Cadiz: Madrid, Servicio de Publicaciones Ministerio de Indus-tria, 89 p.

Levinson, A.A., 1974, Introduction to exploration geochemistry: Wilmette, Ill., Applied Publishing Limited, 924 p.

Schermerhorn, L.J.G., 1982, Framework and evolution of Hercyn-ian mineralization in the Iberian Meseta: Comunicacione Geo-logica Iceo, Portugal, t. 68, fasc. 1, p. 91–140.

Wilson, A.J., 1981, Archaeologists find "Missing Link" in Rio Tin-to Mining History: Queensland Government Mining Journal, p. 32–33.

GEOCHEMISTRY CONTRIBUTIONS TO THE MINERAL RESOURCE ASSESSMENT OF THE CORONADO NATIONAL FOREST, ARIZONA AND NEW MEXICO

Gary A. Nowlan

The metal geochemistry of the Coronado National For-est and adjacent areas, Arizona and New Mexico, was eval-uated as part of a U.S. Geological Survey study of the mineral resource potential of the forest. The geochemical data base consisted of (1) data from existing U.S. Geological Survey data bases, (2) data from analyses of additional samples from areas of sparse coverage, and (3) new data from analyses of the existing samples. The geochemical evaluation is based mainly on stream-sediment data, because the stream-sediment sample coverage is much more exten-sive than that of other sample media.

A total of 3,874 stream-sediment samples in this study were analyzed by 31-element, semiquantitative, direct-cur-rent arc emission spectrography. In addition, 2,537 stream-sediment samples were analyzed for Au by graphite-furnace atomic-absorption spectrophotometry and for Ag, As, Au, Bi, Cd, Cu, Mo, Pb, Sb, and Zn by inductively coupled plasma-atomic emission spectroscopy. The geochemical evaluation is based principally on abundances of Ag, As, Au, Ba, Bi, Cd, Cu, Mn, Mo, Pb, Sb, Sn, W, and Zn because they are commonly associated with hydrothermal ore deposits known or suspected to occur in Coronado National Forest; these include porphyry copper and molybdenum deposits, epithermal precious-metal deposits, veins and replacements, various types of skarns, various types of tin, tungsten, and beryllium deposits, and pegmatites.

Based on geology, the forest was subdivided into 35 areas that were ranked on a geochemical intensity scale. Rankings are based on the number of elements present in anomalous concentrations, the percentage of samples with anomalous concentrations, and the magnitude of concentra-tions in individual samples. The most anomalous area was assigned a value of 10. Parts of the Patagonia Mountains are highest on the geochemical intensity scale and parts of the
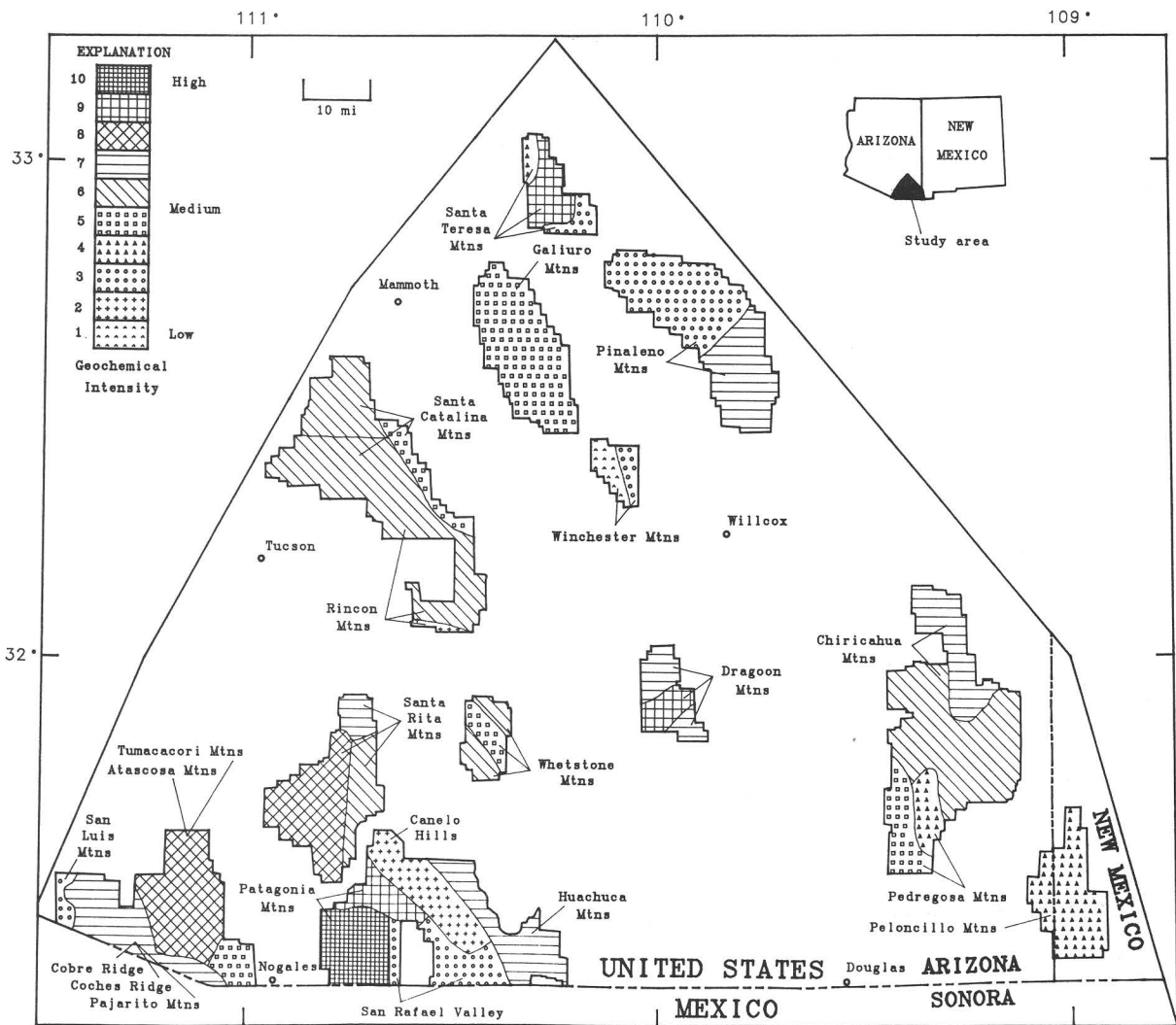
Figure 1 (Nowlan). Geochemical intensity rankings of subdivisions of the Coronado National Forest (patterned areas), southeastern Arizona and southwestern New Mexico, based on analyses of stream-sediment samples.

Winchester Mountains are the lowest. The areas and their geochemical intensity rankings are shown in figure 1.

MINERAL RESOURCES AND ECONOMICS OF THE UNITED STATES–MEXICO BORDER REGION

Greta J. Orris, Floyd Gray, Keith R. Long, Norman J Page, John-Mark G. Staude, and Karen S. Bolm

In anticipation of increasing mineral trade with Mexico, the Center for Inter-American Mineral Resource Investigations (CIMRI) initiated a project in 1992 to study the mineral economics of nonfuel mineral resources in the United States–Mexico border region. The study area was defined to include much of the southern parts of the States of California, Arizona, New Mexico, and Texas in the United States and the northern portions of the States of Baja California Norte, Sonora, Chihuahua, Coahuila, Nuevo Leon, and Tamaulipas in Mexico (fig. 1). As a first step in the border project, CIMRI began to construct a database of the known mines and mineral occurrences in and adjacent to the study area. This information is stored in the Mineral Resources Data System (MRDS), the U.S. Geological Survey's publicly accessible computerized system for storage of mine and mineral occurrence data. The most current versions of the border region data are available from the Minerals Information Office (MIO) at 340 North 6th Avenue, Tucson, AZ 85705.
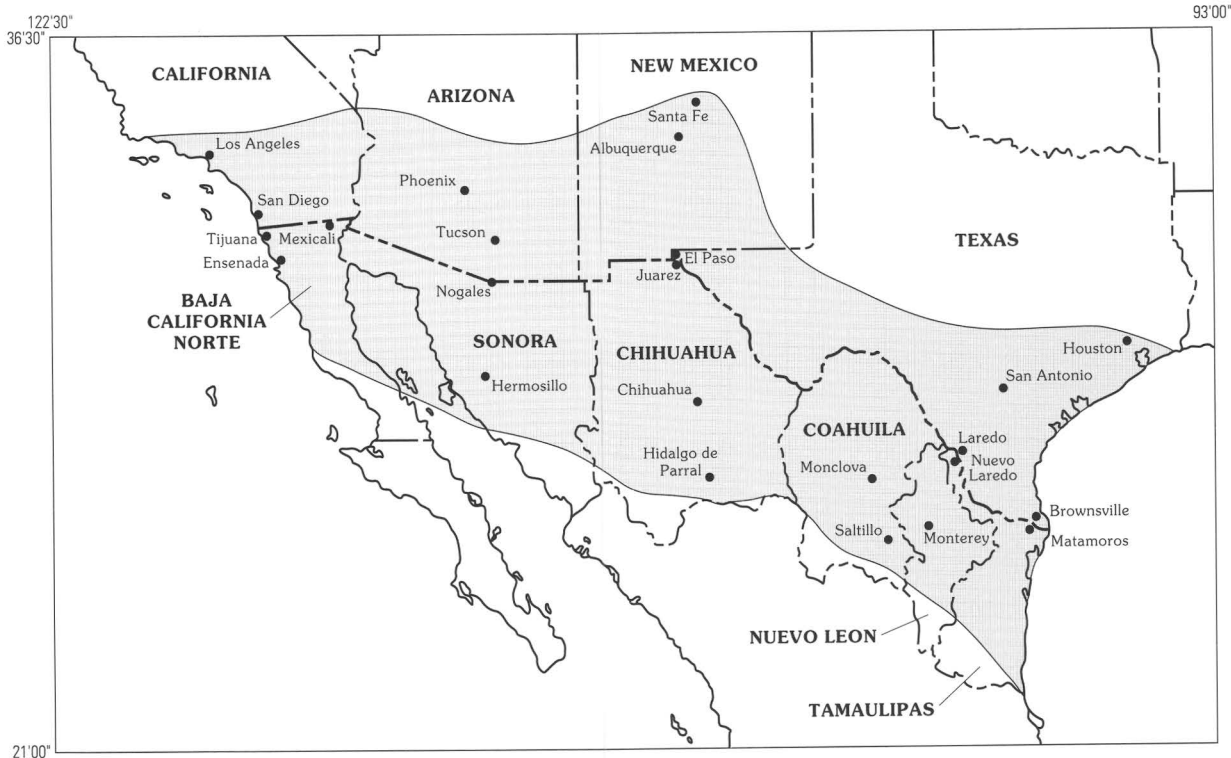
Figure 1 (Orris and others). The CIMRI United States–Mexico border region study area (shaded).

Prior to CIMRI's project, data in MRDS for the border region consisted of data sets for Arizona, New Mexico, California, Baja California Norte, and Sonora that were compiled by the USGS and contractors in the late 1970's and early 1980's. These data sets were incomplete with regard to both mineral discoveries of the last 10 years and industrial minerals. Essentially no data were stored in MRDS for the States of Texas, Tamaulipas, Nuevo Leon, Cohuila, or Chihuahua. As of summer 1993, CIMRI has made a first pass at completing and updating mine and mineral occurrence information for most of the study area and entered that information in MRDS. Data sets known to be incomplete after the first pass include the data set for southern California, industrial minerals for north-central Mexico, and sand and gravel for Arizona.

In addition to mineral resource data, as part of the border region project, CIMRI is also compiling data related to geology, infrastructure, transport, mineral processing, tariffs, electric power sources, and other data related to the mineral economics of the area. These data will allow CIMRI to address such issues as the relationship of mineral deposits to geology and the adequacy of mineral resources in the border region for infrastructure construction and rebuilding, environmental mitigation, and agricultural support.

PRELIMINARY INTERPRETATION OF AEROMAGNETIC DATA IN NORTHEASTERN NICARAGUA— POSSIBLE RELATION BETWEEN STRUCTURE AND ECONOMIC MINERAL DEPOSITS

Herbert A. Pierce

In northeastern Nicaragua, Mesozoic rocks host economic mineral deposits, some of which are associated with structures identified through aeromagnetic surveys. The dominant aeromagnetic anomalies extend northeast-southwest for more than 110 km, and in places they are several kilometers wide.

Aeromagnetic data are available for 11,764 km^2 located between lat 13°30′N. and 14°15′ N. and long 85°00′ W. and 83°45′ W. The original data were gathered under a program financed by the United Nations in 1964 and 1965. Data were collected along east-west flightlines spaced 500 m apart and plotted on eight 1:50,000-scale maps. The data were digitized and subsequently merged and gridded to create two

1:200,000-scale maps for the interpretation of structure and geology of the upper crustal rocks. For one map, the International Geophysical Reference Field (IGRF) and a secondary residual field were removed and the residual data plotted. For the second, the IGRF was removed, data were reduced to the pole, and maximum horizontal gradient locations were calculated before plotting.

The data show a northeast-southwest-trending series of curvilinear magnetic anomalies extending across and probably beyond the survey area. A second, less obvious linear set of magnetic features cuts orthogonally across the northeast-southwest-trending features. Interpretation of two high-frequency, high-amplitude magnetic areas suggests two separate groups of volcanic-intrusive rock. An area of low magnetic response representative of basin-filling sediments suggests a small basin adjacent to and north of the predominant northeast-southwest-trending anomalies. A circular feature 60 km in diameter and near the center of the survey area is proximal to and southeast of the main anomalies and appears to contain a smaller, nested (though less distinct) circular anomaly of unknown origin.

To the north, near the common border between Honduras and Guatemala, curvilinear structures of similar scale and trend have been identified by geologic mapping, topographic features, Landsat, and interpretation of SIR-A radar data (Short and Blair, 1986). One major structure, the Rio Motagua–Polochic fault system, separates the Chortis block on the south from the Mayan block to the north (Molnar and Sykes, 1969). This fracture system has multiple placer and vein gold deposits along its strike. In central Honduras, another feature of similar scale and trend, the Guayape fault, cuts across the central region of the country and has placer, stockwork, and vein gold deposits dotted along its strike (D.G.M.H., 1989).

In the west half of the Nicaraguan study area, existing geologic maps show Tertiary arc-related volcanic rocks and Cretaceous plutons exposed by erosion; in the east half of the area, Quaternary platform sediments are dominant (Dengo and others 1969; Case and Holcomb, 1980; Muehlberger, 1992). However, recent geologic work (M. Venerable, written commun., 1993) suggests a more complex picture. Preliminary mapping in the southern portion of the northeast-southwest-trending anomaly identified serpentinites and other ultramafic rocks containing podiform chromite deposits. These rocks may represent back-arc terrane, marking the contact between the continental Chortis block (nuclear Central America) to the north and the oceanic crust of southern Central America to the south. Gold districts are associated with the magnetic anomalies. Two districts, Bonanza and Siuna, are proximal to the main northeast-southwest-trending series of anomalies; a third district, Rosita, is located along the northern boundary of the large circular feature described previously. Cumulative production (≈1901–1991) from these districts comprises 35,000 tons Pb; 102,260 tons Cu; 217,170 tons Zn; 2,504,590 oz Ag; and 850,100 oz Au (USGS, 1993).

Rock type is not consistent along the trend of the magnetic anomalies. The only consistent relation is that the deposits tend to cluster along the magnetic linears. If the trend of anomalies delineates a boundary, fault, or set of faults, these breaks in the crust may have served as conduits and control of mineral-bearing fluids. Exploration geologists should consider these trends in their exploration programs.

REFERENCES

Case, J.E., and Holcomb, T.L., 1980, Geologic-tectonic map of the Caribbean region: U.S. Geological Survey Miscellaneous Investigations Series Map I–1100, scale 1:2,500,000.

Dengo, G., Levy, E., Bohnenberger, O., and Caballeros, R., 1969, Metallogenic map of Central America: Instituto Centroamericano de Investigation y Technologia Industrial, scale 1:2,000,000.

Direccion General de Minas e Hidrocarburos (D.G.M.H.), 1989, Mapa Metalogenetico de la Republica de Honduras: Scale 1:500,000.

Molnar, P., and Sykes, L.R., 1969, Tectonics of the Caribbean and Middle America regions from local mechanisms and seismicity: Geological Society of America Bulletin, v. 87, p. 1639.

Muehlberger, W.R., 1992, Tectonic map of North America: American Association of Petroleum Geologists, scale 1:5,000,000.

Short, N.M., and Blair, R.W., Jr., eds., 1986, Geomorphology from space, a global overview of regional landforms, chapters 3 and 6: National Aeronautics Space Administration, p. 216–217; 388–389.

U.S. Geological Survey, 1993, Mineral Resources Data System.

THORIUM, URANIUM, AND POTASSIUM AERORADIOACTIVITY MAPS OF ARIZONA—GEOLOGIC INTERPRETATION AND METALLOGENIC SIGNIFICANCE

James A. Pitkin, Clay M. Conway, and Gordon B. Haxel

We have prepared and interpreted maps (1:1,000,000 scale) of thorium (Th), uranium (U), and potassium (K) concentrations for Arizona from aerial gamma-ray spectrometer (aeroradioactivity) data acquired during the National Uranium Resource Evaluation program of the U.S. Department of Energy. The maps were made from 3–km square grids of Th, U, and K for the conterminous United States (Phillips and others, 1993). The grid values are in ppm (parts per million) for Th and U and in percent for K; these values represent the near-surface (to 50 cm depth) concentrations of the natural radioelements. With a few important exceptions, the spatial patterns of Th, U, and K are similar. We emphasize

the distribution of Th, for which the patterns are most pronounced and systematic, probably reflecting the generally greater mobility of U and K and the dual oxidation states of U in the upper crust.

The Colorado Plateau as a region exhibits relatively low to moderate and homogeneous radioelement concentrations in the widespread Paleozoic and Mesozoic sandstones and limestones. Areas of elevated relative concentrations are underlain by Cretaceous strata that include shale and coal around Black Mesa, lacustrine beds of the Neogene Bidahochi Formation, ash-bearing mudstones of the Upper Triassic Chinle Formation, silicic and alkaline Tertiary volcanic rocks, and, locally, redbeds of the Lower and Middle Triassic Moenkopi Formation. Detailed features in the radioelement maps suggest areas of higher potential for U within these more radioactive formations.

Aeroradioactivity data in the Basin and Range–Colorado Plateau Transition Zone and the Basin and Range province show greater range, spatial variability, and generally higher radioactivity than are evident for the Colorado Plateau. The more radioactive rocks include 1.4-Ga granite, some 1.7–Ga granites, Jurassic granitoids, Tertiary volcanic rocks, and basin detritus from these bedrock sources.

An anomalous belt of low radioactivity, most pronounced in the Th data, extends from the Prescott-Jerome region in the Transition Zone southwestward to the region between Gila Bend and Yuma in the Basin and Range province. In the Transition Zone, this belt corresponds closely to the distribution of 1.75–1.72-Ga calc-alkaline volcanic and plutonic suites unique to this part of Arizona. This belt includes very little 1.4–Ga granite, in contrast to the rest of the Transition Zone. The metallogeny of this low-radioactivity region is characterized by unusually abundant Proterozoic massive sulfide deposits, and abundant Laramide and Proterozoic base- and precious-metal veins. The aeroradioactivity maps suggest that this metallogenic province may extend southward into the Basin and Range province.

Within the generally high radioactivity of the Basin and Range, a broad, irregular corridor of low radioactivity about 50–80 km wide trends northwestward from Douglas in southeastern Arizona to Parker in west-central Arizona. This corridor parallels and includes the Arizona metamorphic core complex belt. Individual metamorphic core complexes, both within this belt and south of it in the Baboquivari Mountains area, generally are characterized by pronounced radioactivity lows. The core complex belt is also a region of low heat flow, which may be explained by low radioelement abundances in the middle crustal rocks exposed within the core complexes (J.H. Sass, oral commun., 1993).

Areas of potassium metasomatism, related to hydrothermal activity that occurred along and above detachment faults during core complex uplift, are readily distinguished on the K map, especially near the Buckskin-Rawhide and Harcuvar core complexes in west-central Arizona. Potassium aeroradioactivity is thus a potential exploration guide for Au-Cu and Mn deposits that also formed during this hydrothermal activity.

In the southwest quarter of Arizona, first-order features of the aeroradioactivity maps evidently are largely controlled by the distribution of Jurassic granitoids. Two regions in this part of the State have generally high radioelement abundances. One of these regions extends from the Nogales area northwest to Ajo and Organ Pipe Cactus National Monument; the other lies between the lower Gila River and the lower Colorado River. Both are characterized by widespread and voluminous Jurassic granitoids, and many individual aeroradioactivity highs coincide with exposed Jurassic plutons. An intervening region of markedly low radioactivity, in and west of Cabeza Prieta National Wildlife Refuge, coincides with an area where Jurassic granitoids are sparse or absent. This aeroradioactivity low may be related to widespread latest Cretaceous leucogranite, and it forms the southwest end of the Prescott-Jerome-to-Gila Bend-Yuma belt of low radioactivity described previously.

Aeroradioactivity data have considerable potential in Arizona for exploration for several lithophile elements in addition to U and Th. The 1.4–Ga granites in Arizona commonly are highly radioactive; their potential for hosting rare metals may be underappreciated. Tungsten deposits near Bagdad are known to be genetically related to 1.4–Ga granites. About two-thirds of the nearly 30 tungsten districts in Arizona are within or close to 1.4–Ga granites or pegmatites. A few fissure-type U deposits are also spatially related to 1.4–Ga granite. A "red granite" complex of 1.7–Ga hypabyssal and volcanic rocks in the region between Payson and the New River Mountains in the Transition Zone is also highly radioactive and has associated anomalies of Sn, Be, Nb, La, and Y. Modest positive aeroradioactivity anomalies occur in 1.7–Ga granites in northwestern Arizona, where the largest tungsten deposit in the State, the Boriana deposit, is related to a 1.7–Ga two-mica granite. A half dozen tungsten districts in the southwestern part of the State occur within the highly radioactive Jurassic terranes.

Large low-grade uranium deposits are known in the sedimentary rocks of several Tertiary basins in west-central Arizona. The aeroradioactivity maps suggest that the source for the uranium in these basins is in adjacent ranges of highly radioactive bedrock, mainly 1.4–Ga granite. The aeroradioactivity data also indicate high radioelement concentrations in other Tertiary basins.

REFERENCE

Phillips, J.D., Duval, J.S., and Ambroziak, R.A., 1993, National geophysical data grids—Gamma-ray, gravity, magnetic, and topographic data for the conterminous United States: U.S. Geological Survey Digital Data Series DDS–9, 1 CD-ROM.

THE GEOCHEMISTRY AND ENVIRONMENTAL DEGRADATION OF CYANIDE AT THE SUMMITVILLE MINE, COLORADO

Geoffrey S. Plumlee, Walter H. Ficklin,
Maria Montour, Kathleen S. Smith,
Allen L. Meier, and Paul H. Briggs

Among the environmental concerns stemming from recent mining activities at Summitville are past accidental releases of cyanide-bearing heap-leach solutions into the Wightman Fork of the Alamosa River, and the ongoing efforts to remove cyanide from solutions remaining in the heap-leach pad. We have initiated a research project to understand the geochemical processes (1) that are currently active in the Summitville heap-leach pad and (2) that would occur during an accidental release of the heap-leach solutions into the Wightman Fork. Unfiltered heap-leach solutions that are currently being treated in remediation typically have pH values near 9.4 and total cyanide concentrations varying from 120 to 150 ppm (parts per million). Approximately 100–130 ppm of the cyanide is present in WAD (weak-acid dissociable) form as complexes primarily with copper; the remainder is primarily present as free cyanide (CN-, minor HCN), along with lesser amounts as strong complexes with iron, cobalt, and nickel. Copper is the predominant metal in the heap solutions (210 ppm), and reflects the copper-rich nature of the ores and the strength of the copper complexes. Other metals present include Fe, Co, and Ni (1–2 ppm); Al (0.5 ppm); and Ag, Mo, and Zn (0.1–0.2 ppm). High thiocyanate (SCN-) concentrations (250 ppm) show that sulfides are present within the heap and are undergoing oxidation; the thiocyanate forms predominantly by the reactions of free cyanide with intermediate-valency sulfur species formed during sulfide oxidation.

Any surface leaks from the cyanide heap-leach operations that occurred during mining would have flowed into the Wightman Fork. We have designed laboratory experiments to model the mixing of the current heap-leach solutions with the Wightman Fork water. In the experiments, samples of heap-leach solution are mixed with varying proportions of a Wightman Fork water mixture (pH=3.2) consisting of Wightman Fork water from above the Reynolds Tunnel inflow, Reynolds Tunnel water, and Cleveland Cliffs Pond water. The experiments are conducted both outdoors in open containers (to evaluate the effects of photolytic cyanide degradation) and indoors in closed containers (to allow retrieval of volatilized cyanide gas). Compressed air is bubbled through the mixtures to approximate the turbulence that would be encountered during flow along the Wightman Fork. Figure 1 presents results of one experiment that document the progressive loss of cyanide from the mixture, a
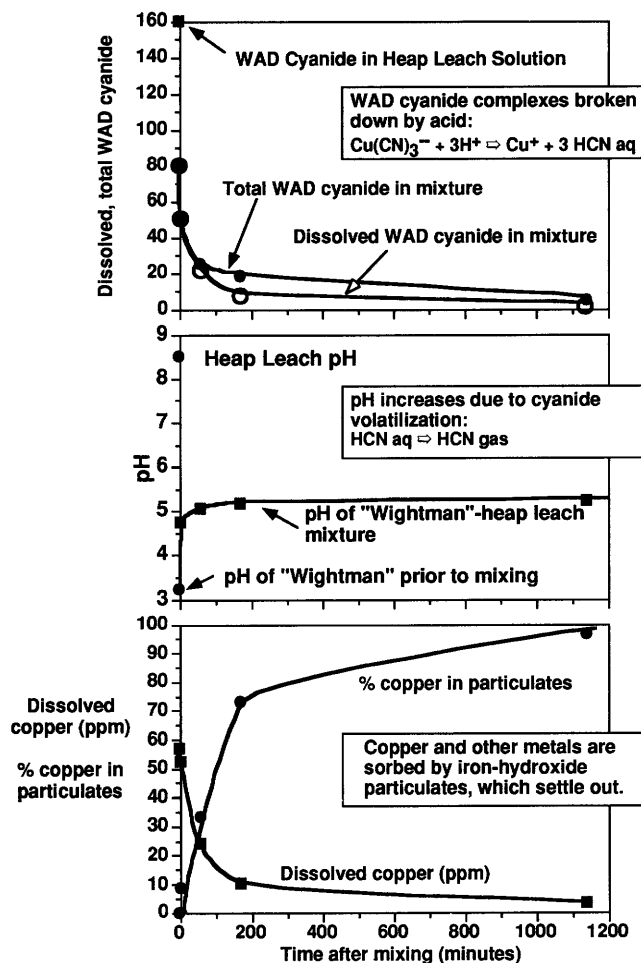
Figure 1 (Plumlee, Ficklin, Montour, and others). Plots showing results of an experiment in which Summitville heap-leach solution is mixed with an equal volume of Wightman Fork water mixture.

transient increase in cyanide associated with solid precipitates, and the formation of abundant iron hydroxide precipitates. We interpret these data to reflect the progressive destruction of the copper-cyanide complexes through acidification by the Wightman Fork waters, and the volatilization of the cyanide as hydrogen cyanide according to the following reaction:

$$Cu(CN)_3^= + 3H^+ = Cu^+ + 3HCN \text{ (g)}.$$
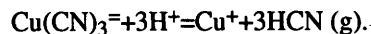
The temporary shift of cyanide into particulates most likely reflects the precipitation of solid copper cyanide; however, this solid cyanide compound is also apparently degraded over time. The copper originally complexed with the cyanide is sorbed onto the abundant iron hydroxides precipitated as a result of the mixing.

Study results to late 1993 indicate that mixing with acidic Wightman Fork waters would likely trigger extensive degradation of cyanide in the heap-leach solutions. In fact, we are exploring further the mixing of heap-leach

solutions with acid-mine drainage as a lower cost remediation tool for treating both heap-leach solutions and mine-drainage.

GEOLOGIC AND GEOCHEMICAL CONTROLS ON THE COMPOSITION OF ACID WATERS DRAINING THE SUMMITVILLE MINE, COLORADO

Geoffrey S. Plumlee, Walter H. Ficklin, Kathleen S. Smith, Maria Montour, John Gray, Philip Hageman, Paul H. Briggs, and Allen L. Meier

The Summitville mine, located at an elevation of 11,500 feet in the San Juan Mountains of southwestern Colorado, generates highly acidic, metalliferous mine-drainage waters from underground mine workings, mine dumps, mill tailings, and seeps both within and outside the mine's open pit. The pH of drainage waters sampled to late 1993 ranges from 1.7 to 3.2. The waters carry extremely high concentrations of metals and other potentially toxic elements, including Cu and Zn (hundreds of parts per million [ppm]); As, Cd, Cr, Co, Li, Ni, rare-earth elements, Se, U, Th, V (hundreds of parts per billion [ppb] to tens of ppm); Be, Ga, Ge, Te (ppb to hundreds of ppb). In general, the acidity and metal content of the waters increase from waters draining underground workings (Reynolds Tunnel, the main drainage tunnel at the site), to waters draining mine dumps and mill tailings (Cropsy waste dump, Cleveland Cliffs Pond), to low-volume seeps and numerous rainwater-derived puddles within the open pit.

The acidic, metalliferous Summitville mine drainage waters are a predictable consequence of the deposit's geologic characteristics. Prior to ore mineralization, the volcanic host rocks were intensely altered by magmatic gas condensates; wallrock alteration grading outward from fractures includes vuggy silica, quartz-alunite, quartz-kaolinite, clay, and propylitic assemblages. Sulfide-rich mineralization then took place in the highly altered rock. Post-mineralization oxidation occurred primarily along the high-permeability vuggy silica zones, occurring to depths as great as 300 feet. In contrast, the low permeability of the clay alteration zones allowed sulfide-rich rock to persist very near the surface; the open-pit mining fractured and exposed large volumes of this sulfide-rich rock to weathering. Many of the ore minerals, including pyrite, marcasite, chalcopyrite, and enargite, generate large amounts of acid during aqueous weathering; the highly altered wallrock coupled with the lack of carbonates in the ores resulted in very little means for buffering the acid generated during sulfide oxidation.

Important geochemical controls on the drainage chemistry, in addition to sulfide oxidation and acid generation, include mineral dissolution/precipitation, evaporation, and, to only a limited extent, sorption. High Cu:Zn ratios in the waters reflect the Cu-rich nature of the ore. The high As concentrations result from the presence of enargite and tennantite. The high concentrations of U, Th, and rare-earth elements in the waters suggest that the acid waters are reacting extensively with wallrocks. The rapid formation of wine-colored, acid puddles in the open pit after rain suggests that readily soluble metal-sulfate salts are being dissolved from the pit rocks; the minerals precipitate again as the puddles evaporate. Sharp increases in metal contents in the Reynolds Tunnel waters during spring runoff may also reflect dissolution of soluble metal-sulfate salts in the old mine workings and fracture systems. Hydrogen isotopic data indicate that evaporation helps enhance the extreme metal contents and acidities of the pit waters; the Reynolds Tunnel waters have isotopic signatures characteristic of snowmelt, whereas the open-pit waters and, to a lesser extent the mine dump waters, show evidence of evaporation. Metal sorption appears to be limited due to the general lack of particulates in the waters.

Geologic and geochemical considerations such as these should be of critical importance to the success of long-term remediation efforts at Summitville.

USGS ENVIRONMENTAL GEOSCIENCE STUDIES OF THE SUMMITVILLE MINE AND ITS EFFECTS ON AGRICULTURE AND WILDLIFE ECOSYSTEMS IN THE SAN LUIS VALLEY, COLORADO—PROJECT OVERVIEW

Geoffrey S. Plumlee and R.C. Severson

The Alamosa River and its tributaries drain several highly mineralized, sulfide-rich areas in the San Juan Mountains of Colorado (fig. 1). These mineralized areas are sources for both natural and mining-related metal loading in the Alamosa River. This metal loading is of concern due to the extensive downstream use of Alamosa River water for agricultural irrigation in the San Luis Valley, for domestic purposes, and for water supply to the Alamosa National Wildlife Refuge and nearby wetlands (seasonal hosts to endangered migratory species such as the whooping crane). The Summitville mining district, located on the Wightman Fork of the Alamosa River, has received considerable public attention in the past year as a result of environmental problems attributed to recent open-pit mining activities. Matters of environmental concern include (1) recent
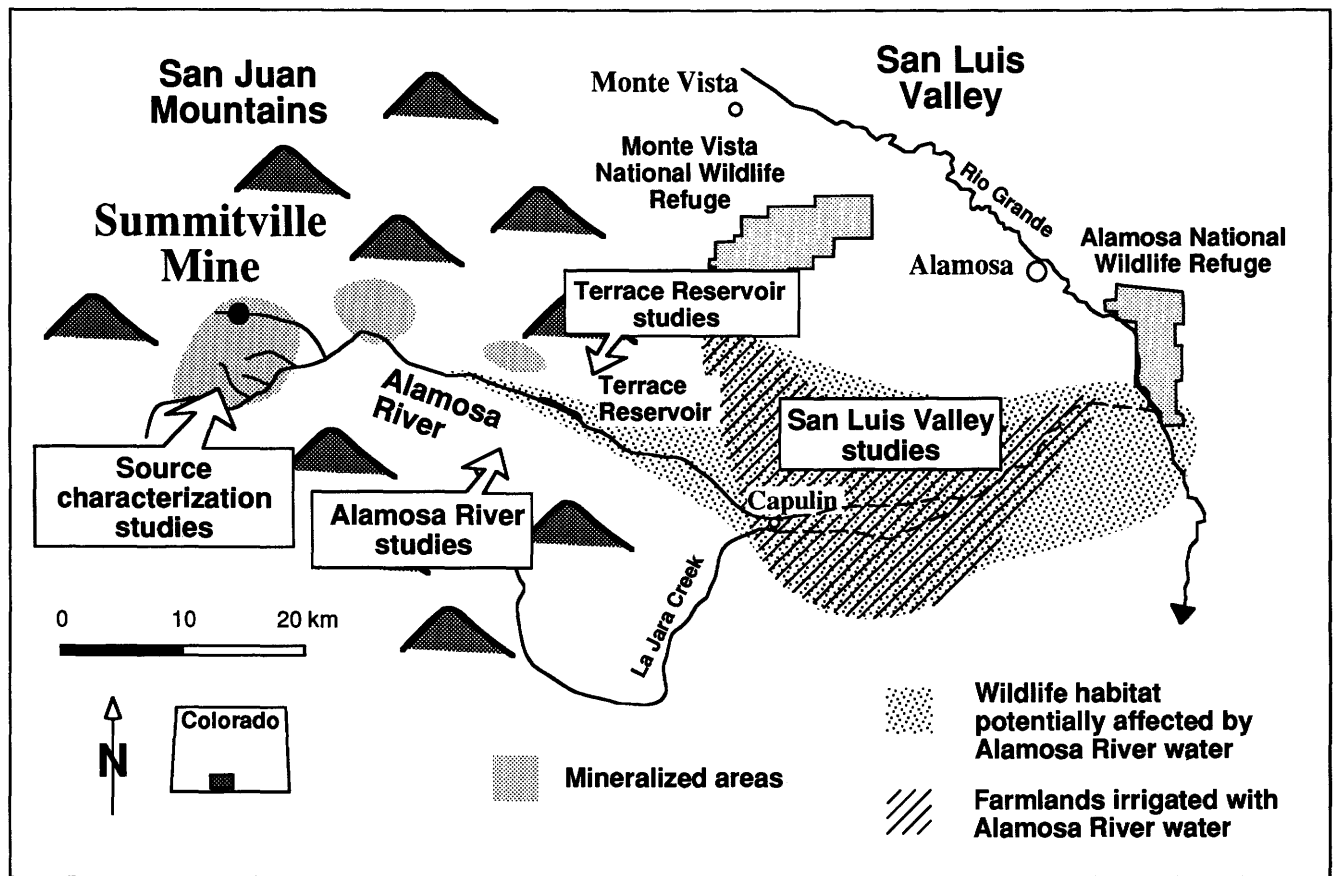
Figure 1 (Plumlee and Severson). U.S. Geological Survey Summitville and San Luis Valley Studies. Cooperators include U.S. Fish and Wildlife Service, U.S.D.A . Forest Service, EPA, State of Colorado, Colorado State University, local extension services, irrigation districts, and farmers.

increases in concentrations of metals and decreases in pH of the Alamosa River waters, San Luis Valley irrigation waters, and irrigated soils; (2) increased corrosion and fouling of irrigation equipment due to the lower pH of the irrigation waters, and (3) reduction of aquatic life in the Alamosa River.

The U.S. Geological Survey Geologic Division (USGS-GD) and Water Resources Divison (USGS-WRD) have initiated multidisciplinary geoscience research projects to provide objective scientific information on Summitville and its downstream environmental effects. Potential users of the results of these studies include valley residents, farmers, regulatory agencies, and industry. The work is being carried out in close cooperation with the State of Colorado, U.S. EPA, U.S. Fish and Wildlife Service, Bureau of Reclamation, U.S.D.A. Forest Service, local agencies (CSU Extension Service), and local farmers. We here present an overview of USGS Summitville activities; many of the projects are discussed in detail in companion abstracts in this volume.

USGS-GD studies at the Summitville mine site include ongoing characterization of the site geology, struc-

ture, mine drainage, and heap-leach geochemistry; these studies will provide information needed to develop effective environmental remediation plans. *Geologic and geochemical characterization of other mineralized areas in the Alamosa River basin (GD)*, as well as *geochemical studies of the Alamosa River and its tributaries (WRD)* will document the origin and nature of metal loadings into the Alamosa River from natural and mining-related sources besides Summitville. The WRD Alamosa River study will also provide insight into processes controlling metal mobility and attenuation downstream from Summitville. *WRD and GD geochemical studies of Terrace Reservoir* evaluate metal cycling between the reservoir sediments and waters. *AVIRIS (Advanced Visible and Infra-Red Imaging Spectrometer) remote sensing data* provide a synoptic view of the surficial geology, mineralogy, environmental geochemistry, and vegetation stress in the southwestern San Luis Valley and Alamosa River basin (including the Summitville area) that is not easily obtained through traditional remote sensing or geologic methods. *Regional geochemical mapping of soils throughout the San Luis Valley* documents the natural distribution

79

of elements in valley soils and any superposition of possible recent metal contamination; the establishment of baseline values serves as a benchmark against which crop studies can be interpreted and any future cleanup of soil contamination can be defined. *The occurrence and distribution of metals in wetlands ecosystems* are being documented to establish pre-mining baseline geochemical signatures in sediments and selected vegetation; additionally, biogeochemical cycling (including fate and transport) of metals through the wetlands and metal uptake by organisms are being assessed. *Metal mobility between soils and major crop types* is being assessed to determine the potential impact of the Alamosa River irrigation water on metal uptake by crops in the southwestern San Luis Valley. The results of the Summitville/San Luis Valley studies will have broad application to the understanding and remediation of existing and future mine sites.

INTEGRATED MINERAL RESOURCE AND ENVIRONMENTAL ASSESSMENTS OF PUBLIC LANDS—APPLICATIONS IN LAND-USE MANAGEMENT

Geoffrey S. Plumlee, Steven M. Smith, Margo Toth, and Sherman P. Marsh

Mineral resource assessments identify the potential for the occurrence of different mineral deposit types based on their characteristic mineralogy, host rock, wallrock alteration, trace-element signature, and structural geology. These same geologic attributes also produce predictable environmental signatures prior to and resulting from mining and mineral processing. Knowledge of mineral deposit geology is therefore critical to effectively predict, mitigate, and remediate the environmental effects of mineral development. In order to facilitate the use of environmental geoscience information in mineral resource development and related land-use planning, the U.S. Geological Survey Office of Mineral Resources (USGS/ OMR) is incorporating environmental risk assessments into its mineral resource assessments of public lands.

A mineral resource assessment of a land unit provides a crucial geologic, geochemical, and geophysical framework upon which an environmental assessment is based. This framework includes compilation of regional geochemical and geophysical data, classifying existing mines and prospects according to deposit type, and identifying terranes favorable for the occurrence of undiscovered mineral deposit types.

The environmental assessment of a land unit has several components. First, regional geochemical and geophysical data are used to establish baselines and to identify natural and anthropogenic sources of metal loadings into the environment. Second, likely environmental effects of mineral resources (mined, known but unmined, and undiscovered) in the land unit can be estimated; this is done using empirical environmental models of mineral deposit types currently under development at USGS/OMR. These models identify, for given mineral deposit types, likely environmental signatures (a) present in soils, waters, and sediments prior to mining, and (b) resulting from mining, including the signatures of mine wastes, mine waters, mineral processing solutions, tailings, and smelter emissions. The environmental signatures take into account data on the abundance, residence, and mobility of metals and other elements of potential environmental concern.

The third component of the environmental assessment is the delineation of "litho-environmental terranes," which are rock units or groups of rock units that have a particular effect on the environment. For example, carbonate terranes generate surface and ground waters with high acid-buffering capacity, and such terranes have large capacity to mitigate the effects of acid mine drainage. The final component is the development of an environmental risk assessment that ranks the deposit types and mining districts identified within the land unit according to the severity of their potential environmental hazards. For example, although a given deposit type may generate extremely acidic, metalliferous acid mine drainage, occurrences of that deposit type in a carbonate-rich terrane or flow of acid waters through a carbonate terrane would lessen the potential environmental effects on the surrounding land unit.

Prototype mineral resource–environmental assessments are currently being completed on a regional scale for the State of Colorado, and on a more detailed scale for the San Juan National Forest in southwestern Colorado. Mineral deposit types in the San Juan National Forest vary from polymetallic carbonate replacement deposits, which tend to generate near-neutral-pH mine drainage waters with high dissolved metal contents, to Summitville-type Au-Cu-Ag deposits, which tend to generate highly acidic waters with extreme concentrations of Cu, Zn, As, Co, Ni, U, Th, and other metals.

Uses for environmental assessments are numerous. By defining baseline environmental signatures for deposit types prior to mining, we can develop geologically realistic remediation standards for post-mining cleanup. The potential environmental effects resulting from the development of different types of mineral deposits can be better predicted and planned for by industry, regulators, and land-use planners. Identifying and prioritizing study of hazardous mine sites on public lands can be accomplished more efficiently. Finally, land managers can better estimate the potential environmental effects resulting from the development of undiscovered mineral resources contained in public lands.

K. Smith, and Plumlee examining geologic controls on mine-drainage chemistry. Geologic and mineral resource information used in the prototype environmental assessments was compiled by S. Ludington, A. Wallace, T. Nash, N. Foley, R. VanLoenen, B. Moring, and G. Green.

GEOLOGIC SETTING OF MINERAL DEPOSITS IN THE OUACHITA–MARATHON–SONORA OROGENIC SYSTEM ALONG THE SOUTHERN MARGIN OF NORTH AMERICA

Forrest G. Poole

The Ouachita-Marathon-Sonora (OMS) orogenic system is a belt of deformed Paleozoic rocks that borders the present southern edge of the North American craton. The collisional-subductional orogenic system extends 3,000 km from central Mississippi in the southeastern United States westward and southward along a sinuous trace into central Sonora in northwestern Mexico. The belt is concealed for 80 percent of its known length; those exposed parts form the Ouachita, Marathon, and Sonora structural salients along the frontal margin. The OMS system is composed of a thick, folded and faulted sedimentary sequence of distinctive, relatively thin, lower Paleozoic eugeoclinal dark-gray radiolarian-graptolitic and siliceous mudstone, chert, sandstone, and limestone, and a relatively thick, upper Paleozoic dominantly olive gray flysch sequence, which includes deep-water turbidites deposited in rapidly subsiding foredeeps. The eugeoclinal sequence of chert, mudstone, siltstone, limestone, and subordinate sandstone, conglomerate, dolostone, barite, tuff, and lava represents offshelf continental slope and rise and oceanic deposits that were deformed and obducted cratonward (northward) onto the once-continuous southern shelf of paleo-North America in late Paleozoic time. During allochthon development and emplacement, foreland basins were formed that received synorogenic flysch and molasse deposits. Rocks of the three orogenic salients have many similarities and differ only in stratigraphic detail, structural scale, and degree of metamorphism. They are separated from each other by the Texas and Chihuahua promontories of paleo-North America.

Rocks within the salients host a variety of Paleozoic and Mesozoic mineral deposits although ore minerals of commercial grades and quantities are present in only a few of the numerous deposits (for example, barite and vanadium in Arkansas and barite in Sonora). Syngenetic stratiform barite and some metal deposits in fine-grained rocks (such as manganese, vanadium, molybdenum) are related to seafloor environments controlled by proximity to hydrothermal vents, salinity of seawater, type and amount of

organic matter, and rates of sedimentation. Other sedimentary mineral deposits formed during diagenesis. Many layers of Devonian chert (originally opaline silica) were converted to novaculite (microcrystalline quartz) during post-depositional episodes of high heat flow. Some deposits formed along epigenetic veins during late Paleozoic and Mesozoic hydrothermal activity. In the Ouachita Mountains, late Paleozoic quartz veins generally are associated with small deposits of copper, lead, zinc, silver, antimony, and mercury. Layers and disseminated grains of pyrite/marcasite are found in barite, chert, and most fine-grained eugeoclinal and foreland-basin rocks. Veins in Arkansas containing mercury, antimony, titanium, and niobium may be related to Mesozoic igneous activity.

Petroleum source and reservoir rocks are present both in the allochthons and in the foreland basins. Although rocks within the three salients exhibit variable temperature histories, oil and solid bitumen/asphalt are more common in lower Paleozoic eugeoclinal rocks and gas is more common in upper Paleozoic foreland-basin rocks. Mississippi Valley-type lead-zinc-barium deposits and petroleum accumulations in the Midcontinent region are probably related to episodic sediment dewatering and expulsion of geopressured metalliferous and petroliferous warm brines from deeply buried basinal black shales of the orogenic system. Similar deposits may exist in margins of shallow basins hosted by outer carbonate-shelf rocks in Texas, Chihuahua, and Sonora. Recognition of hydrothermal activity in many parts of the exposed OMS orogenic system has important implications for regional development of mineral deposits throughout the system in the southern United States and northern Mexico.

SILT HEAVY-MINERAL PLACER DEPOSITS IN A LATERITIC ENVIRONMENT—RIVERS AND INSULAR SHELF OF NORTH-CENTRAL PUERTO RICO

L.J. Poppe, J.A. Commeau, and G. Luepke

Mineralogical studies of sediments from the Rio de la Plata, Rio Grande de Manati, rivers of the Rio Cibuco system, and the insular shelf in north-central Puerto Rico were conducted (1) to examine the effects of lateritic weathering on the silt fraction, (2) to explore the silt fraction for heavy-mineral placer deposits, and (3) to elucidate the active fluvial and shelf processes. The silt fraction, which is enriched in heavy minerals relative to the sand fraction, is mainly detrital but contains a strong authigenic component (fig. 1). The detrital silt heavy-mineral fraction in the rivers is dominated by an amphibole-garnet-pyroxene-epidote assemblage. Amphiboles are more common in the Rio Cibuco; pyroxenes
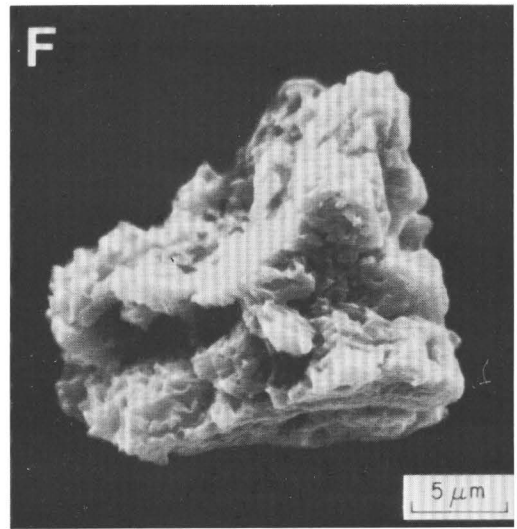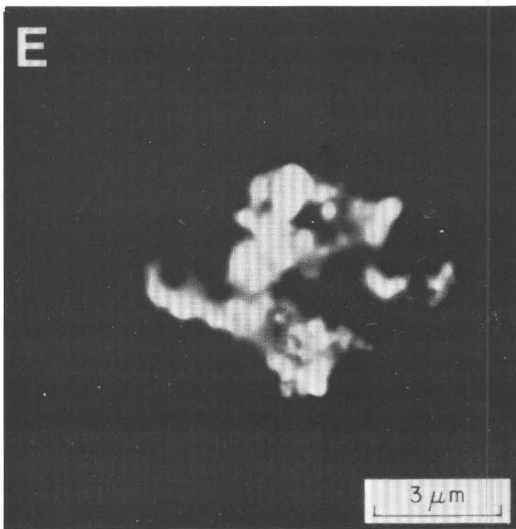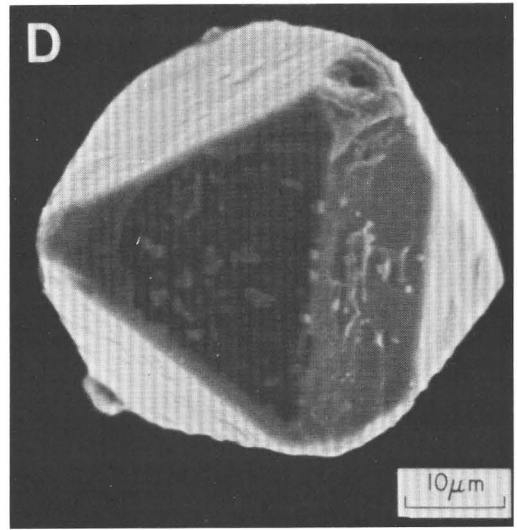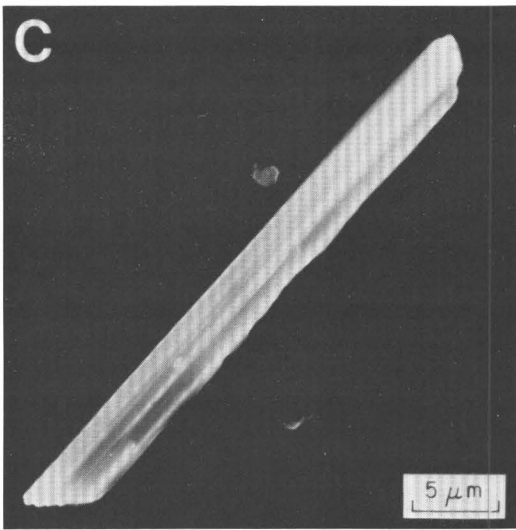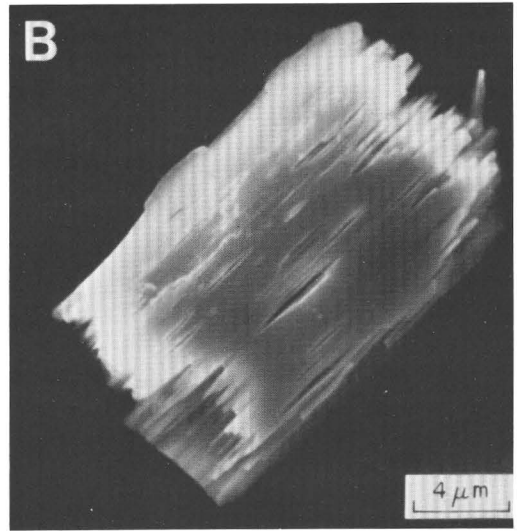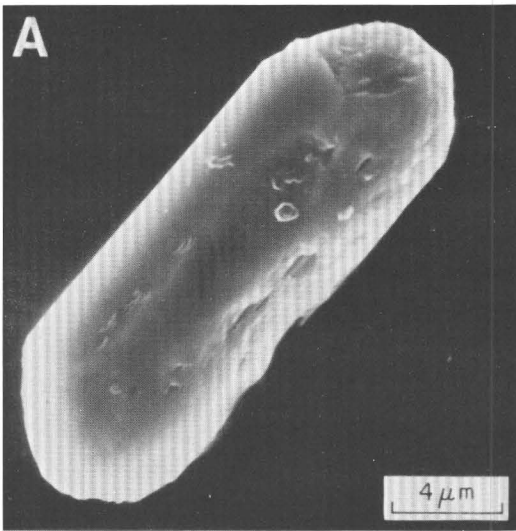
are more common in the Rio de la Plata; epidote and ilmenite are more common in the Rio Grande de Manati. The authigenic silt heavy-mineral fraction, which is largely a product of the lateritic weathering, is dominated by iron oxides (hematite and goethite) and altered grains (cemented mixtures of Fe, Al, Si, and Ti oxides). Grains of bladed rutile and leached ilmenite are common. The lateritization has dramatically altered the relative percentages of the minerals originally present in the source rocks.

Lateral variability in silt-fraction mineralogy is considerable. Within the Rio Cibuco system, the variability is related to the differences in composition of the rapidly eroding source rocks. On the high-energy, wave-dominated shelf, variability in the heavy-mineral distributions is related primarily to differences in the assemblages introduced by the individual source rivers and to differential transport by shelf sorting processes. Silt heavy-mineral abundances on the shelf are greatest near the river mouths (where they can exceed 40 percent by weight) and decrease seaward.

Significant differences are also present between the silt heavy-mineral assemblages in the rivers and those on the adjacent insular shelf, and between the heavy-mineral assemblages in the silt- and sand-sized fractions from these areas. For example, with the possible exceptions of zircon and magnetite, the economically important heavy minerals are much more likely to occur in the silt fraction.

We detected no minerals containing significant amounts of Cu, Ni, Sn, or Zn in any of the river samples, and only traces of Cu, Ni, and Zn on the insular shelf. However, elevated concentrations of chromite, gold, magnetite, and titanium-bearing minerals occur in both the river and shelf samples. Most of the gold occurs as very small crystals (0.6-7.0 μm) encrusted with iron oxides. This close association of gold with iron oxides in lateritic environments has been shown to occur when gold is dissolved from the parent rocks and is reprecipitated in the weathering crusts (Mann, 1984). Cerargyrite, which probably forms during the weathering process from silver-bearing sulfides, is present in the rivers in concentrations of up to 1.9 percent by population, but it is absent in the samples from the insular shelf. Presumably, the abundance of available chloride in the marine environment causes the existing grains of cerargyrite to convert to the much more soluble complexes of $AgCl_2^-$ or $AgCl_3^-$.

Figure 1 (Poppe and others) (facing page). Scanning electron microscope photomicrographs of silt-sized mineral grains representative of those found in the river sediments of north-central Puerto Rico. A, Zircon grain, sample 28, Rio Dos Bocas; B, Corroded epidote grain, sample 28, Rio Dos Bocas; C, Amphibole group mineral, sample 1, Rio de la Plata; D, Chromite grain, sample RP7, insular shelf near Rio de la Plata; E, Backscatter image of an anhedral cerargyrite grain, sample 28, Rio Dos Bocas; F, Extensively corroded and altered potassium feldspar grain, sample 5, Rio de Los Negros.

REFERENCE

Mann, A.W., 1984, Mobility of gold and silver in lateritic weathering profiles—Some observations from western Australia: Economic Geology, v. 79, p. 38–49.

BRIEF DESCRIPTION OF THE GEOLOGY AND MINERAL DEPOSITS OF SOUTHERN SONORA, MEXICO

Jaime Roldan Quintana

Recent compilation of the geology of Sonora at 1:1,000,000 scale has provided new insights into the understanding of the geology of Sonora. The State of Sonora is located south of Arizona, and southern Sonora is herein considered to extend south from lat 28° 30′ N. This region lies south of the Precambrian craton of North America, and no Precambrian rocks are here exposed. Some lower Paleozoic rocks are reported east of Tonichi, representing eugeoclinal offshelf strata of Ordovician age. To the south, scattered outcrops of Paleozoic rocks are located in the region of Navojoa-Alamos, but their lithology and fossil content are poorly preserved, because of younger intrusions. Among these localities, only in El Trigo, northeast of Navojoa, were reported poorly preserved fossils of probable late Paleozoic age.

Triassic rocks present large exposures southeast of Hermosillo, where they are referred to as the Barranca Group. These rocks consist of quartz-feldspathic sandstones, red beds and coal-bearing shales rich in fossil plants. The middle member of the Barranca Group, the Santa Clara Formation, has been dated paleontologically as Late Triassic. The age of the entire group is unknown. At the southern tip of the State of Sonora in Sierra Sonobari, a Late Triassic isotopic age has been obtained from gneisses and amphibolites. However, the age of the metamorphism seems to be younger. No Jurassic rocks have been identified in southern Sonora. Lower Cretaceous marine rocks occur only east of Alamos. Igneous rocks are the most important rock type in southern Sonora. Early Tertiary (62–49 Ma) granitic batholiths are widespread and represent the most continuous rock unit.

Volcanic rocks consist of andesites of Paleocene age unconformably covered by rhyolitic ignimbrites and basaltic andesites of Oligocene-Miocene age. Tertiary extension has produced the basin-and-range structure that characterizes this part of Sonora. Volcanic and clastic fillings of the Baucarit Formation are common in these grabens. Undifferentiated clastic deposits and alluvium cover most of the coastal plain.

The mineral deposits of southern Sonora are concentrated in two areas. One, at lat 28°20′ N., follows a general east-west trend about 40 km wide; it coincides with some of

the outcrops of the Triassic rocks and large exposures of the Late Cretaceous–early Tertiary batholiths. In this mineralized belt are present (1) mantos of coal and graphite, (2) disseminated copper and copper-molybdenum, and (3) veins of silver, lead, zinc, and copper as sulfides.

The second mineralized area is located at lat 27° N. around Alamos in a radius of about 50 km. Most of the deposits are hosted in Tertiary volcanic rocks or in intrusives. The types of mineralization are (1) skarn of tungsten and polymetallic sulfides; (2) disseminated copper-molybdenum deposits, of silver, lead, zinc, copper; (3) veins of silver, lead, zinc, copper with gold values (in the mines near Alamos, silver is present as sulfo-salts); and (4) mantos of graphite. Outside these mineralized areas there are a few scattered mines.

Other nonmetallic minerals that have been exploited include rhyolitic tuffs, limestones, gypsum, halite, and construction aggregates.

PRELIMINARY GEOLOGIC MAP OF THE BIG LUE MOUNTAINS 15-MINUTE QUADRANGLE, GREENLEE COUNTY, ARIZONA, AND CATRON COUNTY, NEW MEXICO

James C. Ratté, William E. Brooks, and Dana J. Bove

The Big Lue Mountains 15-minute quadrangle, in southeastern Arizona and southwestern New Mexico, is at the southwestern margins of the mid-Tertiary Mogollon-Datil volcanic field, just east of the Morenci-Metcalf mining district. It also is at the northwest end of the Laramide Burro uplift near its intersection with the north-northeast-east-northeast-trending Morenci lineament and Morenci Reserve fault zone, at the southeastern margin of the Colorado Plateau.

The Big Lue Mountains quadrangle is covered largely by volcanic and volcaniclastic rocks of Oligocene to Miocene age. Total exposed thickness of the volcanic rocks in the quadrangle is on the order of 1,000 m, but no single section contains all the various extrusive and intrusive units. The mid-Tertiary volcanic rocks unconformably overlie Precambrian and Paleozoic rocks in the Red Hill area in the southwest corner of the quadrangle (fig. 1), presenting the possibility that Laramide intrusive rocks, like those that host the world-class copper porphyry deposits of the nearby Morenci-Metcalf district, could be present beneath the Tertiary volcanic rocks in the Big Lue Mountains quadrangle. Although no signs of significant mineralization are evident in the quadrangle, there are several mineralized occurrences in the pre-Tertiary rocks in the Red Hill area, as well as quartz and carbonate veins as much as 10 m wide along the Dix Creek fault in the north-central part of the quadrangle

(fig. 2), where manganese, silver, copper, and gold (0.04–0.15 ppm) were found (Ratté and others, 1982).

The Tertiary volcanic sequence in the quadrangle in general decreases in age from the southwest corner of the quadrangle to the north, and the most complete sequence is exposed in the southwest-facing slopes of the Big Lue Mountains. The oldest rocks in the sequence in the Big Lue Mountains include the distal outflow facies of several caldera-related ash-flow tuffs (Cooney Tuff, about 34 Ma; Davis Canyon Tuff, 29 Ma; and Bloodgood Canyon Tuff, 28.1 Ma) from the Mogollon Mountains caldera complex to the northeast. The tuffs are overlain by various amygdaloidal and porphyritic andesite lava flows, as much as 500 m thick, and a sequence of dacitic to rhyolitic flows, flow breccias, and pyroclastic beds at least 250 m thick, which are here called the volcanic rocks of the Big Lue Mountains (VRBLM). The VRBLM are overlain by andesitic flows that probably correlate with the Bearwallow Mountain Andesite.

The Big Lue Mountains volcanic sequence (VRBLM) is well exposed in the southeastern part of the quadrangle along State Highway 78, beside Black Jack Canyon, where it is interlayered and intruded(?) by major masses of nearly aphyric rhyolite that have been tentatively dated at about 28–25 Ma. The rhyolites include the rhyolite of Hells Hole, which forms an intrusive(?)-extrusive dome complex of at least 50 km², mainly east of Black Jack Canyon (figs. 1, 2), and the north-northeast aligned rhyolite plug domes known as the White Peaks, in the south-central part of the quadrangle (fig. 2), as well as numerous other intrusive-extrusive bodies. A spectacular carapace breccia at the margin of the rhyolite of Hells Hole Canyon is well exposed at the viewpoint near the Needles Eye, a former narrow highway tunnel that has been eliminated in deference to modern traffic requirements on Highway 78. The carapace breccia is exposed intermittently beneath Bearwallow Mountain Andesite flows for about 8 km along Highway 78 between the Needles Eye and the Arizona–New Mexico State line. Outcrops along the highway south of the Big Lue Ranch road have the typical "honeycomb" vesicular texture of much of the rhyolite on top of the dome complex. The centimeter-size vesicles are lined with crystals of sanidine, niobium-rich pseudobrookite and ilmenite, and garnet.

Except for some older volcanic rocks exposed in the Pat Mountain and Bird Canyon areas in the northwestern part of the quadrangle (fig. 2), the rocks in the north half of the quadrangle are mainly younger than those in the south half, and consist of Bearwallow Mountain Andesite, a bimodal basalt-rhyolite assemblage of Miocene age, and Gila Formation (Neogene) volcaniclastic sediments.

Along the gorge of the San Francisco River in the northeastern part of the quadrangle, the stacked thin flows of Bearwallow Mountain Andesite total as much as 600 m thick. A major eruptive center for at least part of this flow sequence probably is represented by a partially exhumed cinder cone, 0.8–1.2 km in diameter, on the south canyon wall, on the New Mexico side of the State line (fig. 2).
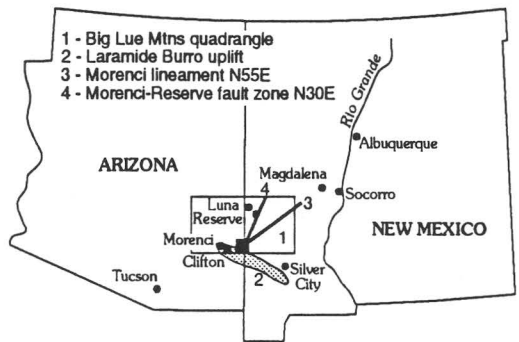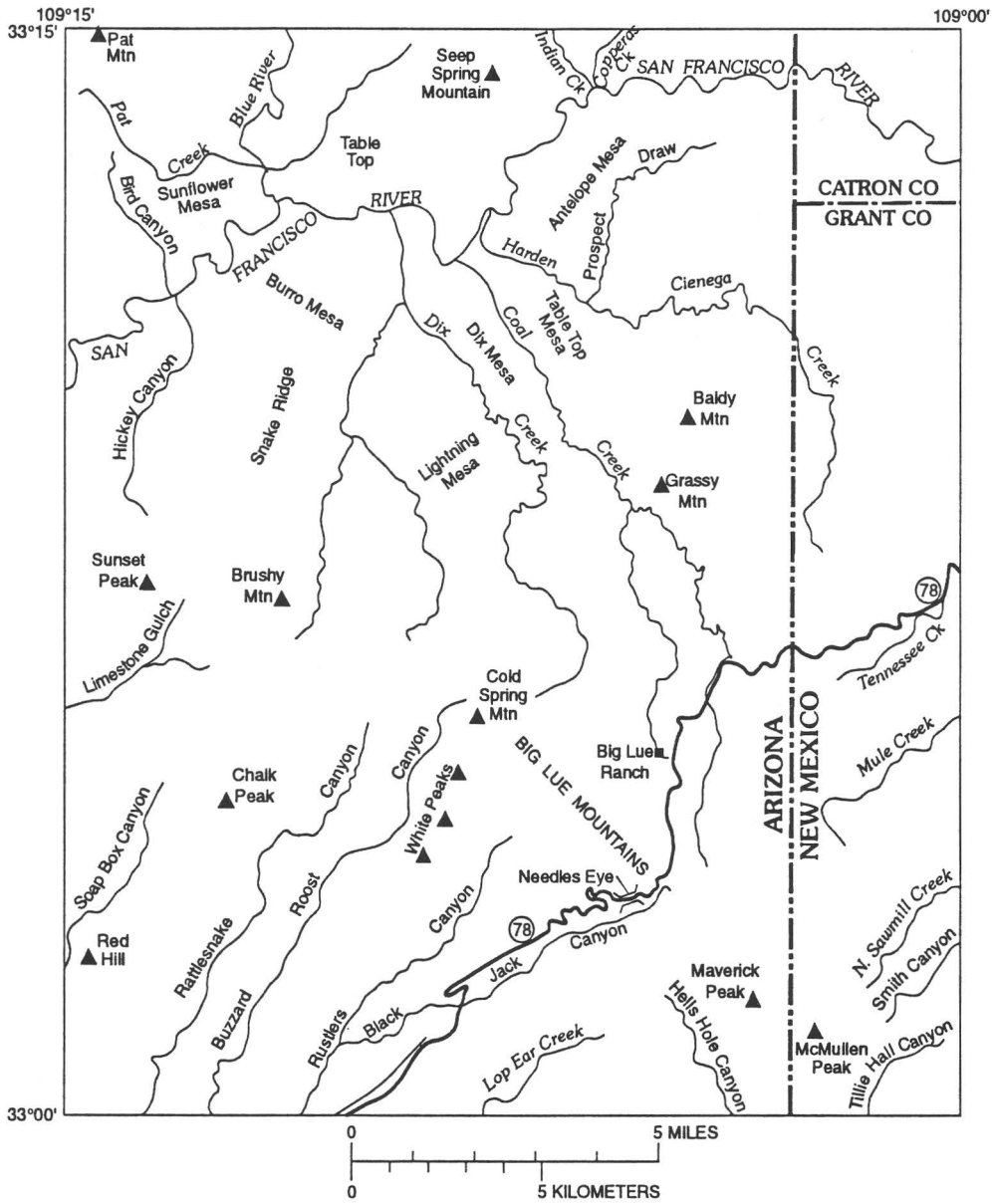
Figure 1 (Ratté and others). Geographic index map and location map for the Big Lue Mountains 15-minute quadrangle, Arizona and New Mexico.
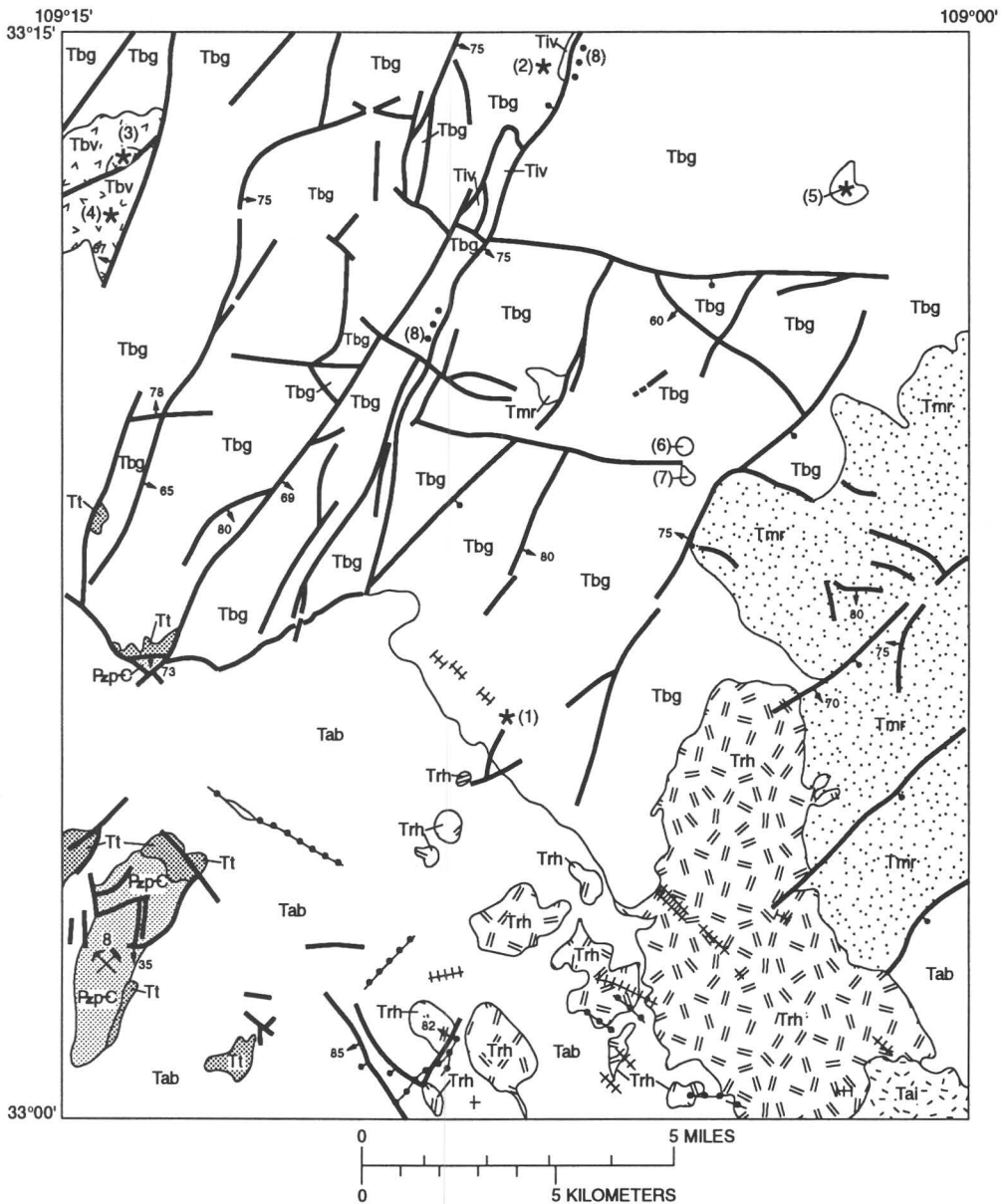
Figure 2 (Ratté and others). Big Lue Mountains 15-minute quadrangle showing generalized fault pattern, mafic dikes (crosshatched lines), silicic dikes (lines with solid dots), prospects and (or) calcite-quartz veins (crossed pick and hammer prospect symbol), selected eruptive centers (stars), and some major geologic bodies and eruptive centers, designated by numbers 1–8, as follows:

1. Cold Spring Mountain eruptive center (uncertain mid-Tertiary age).
2. Indian Creek eruptive center (uncertain mid-Tertiary age).
3. Pat Mountain eruptive center (uncertain mid-Tertiary age).
4. Bird Canyon eruptive center (uncertain mid-Tertiary age).
5. Bearwallow Mountain Andesite eruptive center (≈24 Ma).
6. Bearwallow Mountain Andesite plug at Baldy Mountain (≈24 Ma).
7. Rhyolite plug at Grassy Mountain (≈19 Ma).
8. Prospects and (or) calcite-quartz veins.

86

EXPLANATION
CORRELATION OF MAP UNITS

Tbg

Tmr — Miocene

Tai

TERTIARY

Trh

Tab — Oligocene

Tbv   Tiv

Tt

UNCONFORMITY

Pɛ pɛ — PALEOZOIC / PRECAMBRIAN
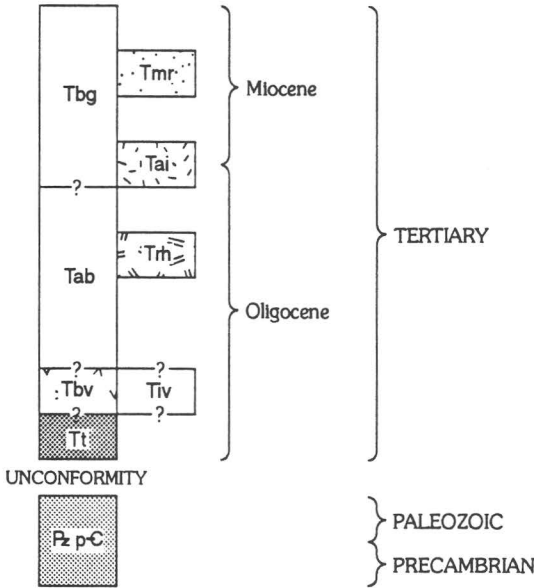
DESCRIPTION OF MAP UNITS

Tbg — Volcanic and volcaniclastic rocks north of the Big Lue Mountains; mainly Bearwallow Mountain Andesite and Gila Formation with interlayered basaltic lava flows (Miocene and Oligocene)

Tmr — Rhyolite of Mule Creek; rhyolite lava flows, domes and tuff rings (Miocene)

Tai — Coarsely porphyritic andesite intrusion (Miocene or Oligocene)

Tab — Amygdaloidal, fine-grained and porphyritic andesite lava flows, overlain by dacitic and rhyolitic flows and pyroclastic rocks of the Big Lue Mountains volcanic sequence (Miocene (?) and Oligocene)

Trh — Rhyolite lava flows and intrusions and minor pyroclastic rocks of Hells Hole (Oligocene (?))

Tbv — Andesitic to dacitic rocks of the Bird Canyon-Pat Mountain volcanic center in northwest corner of quadrangle (Oligocene (?))

Tiv — Dacitic to rhyolitic rocks of the Indian Creek eruptive center in north-central part of quadrangle (Oligocene (?))

Tt — Ash-flow tuffs; distal outflow of regional caldera-forming tuffs. Include Bloodgood Canyon Tuff (28.0 Ma); Davis Canyon Tuff (29.1 Ma); and Cooney (?) Tuff (~34 Ma)

Pɛ pɛ — Pre-Tertiary rocks, undivided; include Cambrian and Ordovician sedimentary rocks and Proterozoic granite (Paleozoic and Precambrian)

★ — Volcanic eruptive center

╫╫╫╫╫╫ — Dike of mafic composition

•-•-•-•-• — Dike of silicic composition

• • • • • — Vein along fault

——— — Contact

——— — Fault—Showing dip; bar and ball on downthrown side

The bimodal basalt-rhyolite assemblage consists mainly of the rhyolite domes and tuff rings of the rhyolite of Mule Creek in the Harden Cienega area near the northeast edge of the quadrangle, and "true" basalt flows and related dikes and small cinder cones that are interlayered with the volcaniclastic sediments of the Gila Formation throughout much of the northern part of the quadrangle. The rhyolite of Mule Creek is dated at about 18 Ma, and the basalts are about 19–18 Ma. A dacite dome in the vicinity of Tennessee Creek in the east center of the quadrangle, near the State line, is about 21 Ma.

Geologic structures in the southwestern part of the quadrangle are mainly faults and dikes that follow the northwest trend of the Burro uplift, which is represented by the small area of pre-Tertiary rocks in the southwest corner of the quadrangle. In the rest of the quadrangle, faults are mainly north-northeast- to east-northeast-trending, high-angle normal faults that form a series of minor horsts and grabens that constitute the southwestern part of the Morenci-Reserve fault zone of basin-and-range age.

REFERENCE

Ratté, J.C., Hassemer, J.R., Martin, R.A., and Lane, M., 1982, Mineral resource potential of the Lower San Francisco Wilderness Study Area and contiguous roadless area, Greenlee County, Arizona, and Catron and Grant Counties, New Mexico: U.S. Geological Survey Miscellaneous Field Studies Map MF–1463–C; scale 1:62,500.

TECTONIC EVOLUTION OF THE SOUTHWESTERN UNITED STATES

Stephen J. Reynolds and Ed DeWitt

The complex tectonic evolution of the southwestern United States resulted in a wide assortment of ore deposits having diverse origins. The oldest Proterozoic rocks in the region mostly represent island arcs and other oceanic terranes that were constructed or accreted against the Wyoming craton between 1.8 and 1.65 Ga. Proterozoic rocks in the Mojave isotopic province include an isotopic component of pre-2.0-Ga crust, whereas those in the Arizona isotopic province were derived directly from the mantle at about 1.78 to 1.65 Ga. Arizona-type crust appears to overlie Mojave-type crust along an irregular boundary that is largely concealed. Another boundary separates older (pre-1.72 Ga) and younger (1.73 to 1.62 Ga) parts of the Arizona isotopic province, and influences the metallogenic signature of subsequent Phanerozoic ore deposits. Regional deformation and metamorphism culminated in major orogenies at 1.7 Ga and about

1.65 Ga. Granites and rare-earth-element-rich alkalic plutons and carbonatite bodies were emplaced at 1.4 Ga.

After regional uplift and erosion, Middle to Late Proterozoic sediments, mafic flows, and silicic pyroclastic rocks were deposited across the beveled landscape and were intruded by subhorizontal diabase sills at 1.1 Ga. Processes capable of producing mineral deposits are intrusion of sills, Keweenawan-age basaltic volcanism, intense chemical weathering of basalt flows and limestones, and widespread potassium metasomatism of the tuffaceous and sedimentary rocks.

A cratonic setting persisted throughout Paleozoic and Early Triassic time, except in the western Mojave Desert where tectonism accompanied and succeeded truncation of the continental margin. Subduction beneath southwestern North America was underway by Late Triassic time and resulted in intermediate to felsic magmatism that was accompanied by uplift at some times and subsidence at others. A major pulse of felsic magmatism at about 160 Ma was accompanied by hydrothermal metasomatism that produced highly aluminous (quartz-kyanite) rocks. During or after this pulse, magmatism jumped westward, probably as an oceanic ridge approached the coast (analogous to mid-Tertiary orogeny?), and sinistral motion may have occurred on the Mojave-Sonoran megashear. In the latest Jurassic and Cretaceous, intracontinental sedimentation (McCoy Mountains Formation and Bisbee Group) was accompanied by emplacement of rift-related(?) alkalic mafic rocks. This was followed by regional Late Cretaceous folding, thrusting, and metamorphism (locally associated with synmetamorphic gold-bearing quartz veins) and by subsequent Laramide magmatism and porphyry copper mineralization related to low-angle subduction. Laramide compression in the Colorado Plateau and Transition Zone formed monoclines over reactivated basement faults. Uplift and erosion occurred both prior to and after Laramide magmatism, and may have been accompanied by Laramide tectonic denudation.

Uplift may have continued until the middle Tertiary, when steepening and foundering of a low-angle subduction zone caused widespread magmatism and crustal extension in an east-northeast–west-southwest direction. Metamorphic core complexes and detachment faults represent gently dipping normal shear zones that penetrated to upper mid-crustal levels. Brines accumulating in detachment-related basins caused regional potassium metasomatism, leached metals from the affected rocks, and flowed up the detachment fault, forming detachment-related base- and precious-metal deposits. At 13 to 15 Ma, the mid-Tertiary style of tectonism was replaced by a basin-and-range style of tectonism characterized by generally east west, small-magnitude extension along high-angle normal faults, and fundamentally basaltic magmatism.

OVERVIEW OF ENVIRONMENTAL MINERAL RESOURCES AND RELATED INVESTIGATIONS IN THE GEOLOGIC DIVISION, U.S. GEOLOGICAL SURVEY

Gilpin R. Robinson, Jr., and Larry P. Gough

The importance of monitoring, characterizing, and remediating past and present-day mining sites in Western North America has led to an increase in environmental geoscience research in the USGS Geologic Division. One specific emphasis of this research is the environmental consequences of mineral resources exploration, development, and remediation. Much of the effort is in response to a growing public awareness of potential point-source contamination and land-use concerns, a need by Federal and State public-land trustees for published information and expert opinions upon which to base management decisions, and a need for sound scientific information to assist regulatory agencies in contaminated-site remediation and litigation. These efforts are being supported by agency funding, international cooperative funding, cooperative agreements between public and private agencies and organizations, and congressional initiatives.

The environmental impacts associated with abandoned mine sites, hazardous waste locations, and natural sources of contamination on Federal lands are important considerations when developing Federal land management plans. These plans attempt to characterize the nature of the sites, minimize environmental impacts, identify appropriate remediation methods, and predict the effects of new mining ventures. For example, acid-rock drainage from natural and mining-related sites, such as Summitville, Colo. (see Plumlee and others, for example, this volume), can create large, toxic metal-bearing water and sediment loads in streams, wetlands, and soils with widespread and long-lasting environmental impact. Such hazardous material sites on Federal lands must be inventoried and characterized in a comprehensive but safe manner before effective cleanup plans can be developed. The environmental geoscience studies in the Geologic Division address these issues by:

1. characterizing the mobility of toxic elements from mineral sources into the soil, water, air, and vegetation;

2. defining the natural dispersion and chemical reservoirs of potentially toxic compounds in unmined mineralized areas to establish baseline geochemical information for different mineral deposit types, regions, and climatic zones;

3. investigating how the processes that control the mobility of toxic elements in the environment can be used in low-cost and low-maintenance remediation methods;

4. developing models based on geologic setting, deposit type, mining method, and climate to predict the diverse environmental effects associated with mining development;

5. developing and applying non-invasive geophysical and remote-sensing techniques to monitor and assess contamination;

6. developing expert-system computer programs to identify the appropriate geochemical and geophysical techniques and technologies to characterize the degree and extent of contamination;

7. developing geochemical and isotopic fingerprinting techniques to identify and segregate contamination sources.

Examples of current USGS research in, and support facilities for, environmental studies include: (1) metal speciation, mobility, and rock/water interface geochemistry (with emphasis on As, B, Cd, Fe, Hg, Pb, S, Se, U, and Zn); (2) characterization of scale-related heterogeneity of geologic materials as they relate to hydrologic properties (using ground-penetrating radar and airborne geophysical techniques); (3) investigations on the relation of mine drainage chemistry to geology and geochemistry of ore deposits; (4) use of the Advanced Visible and Infrared Imaging Spectrometer (AVIRIS), and supporting laboratory techniques, to detect, identify, and map the distribution of hazardous materials; (5) provide geologic and mineral deposit information and expertise to EPA (Environmental Protection Agency) for use in the CERCLA (Superfund) site considerations and Department of Justice for use in CERCLA litigation; (6) studies that help quantify and characterize geologic substances perceived to have significance for human or animal health; (7) surficial geologic mapping studies that emphasize hydrogeologic features, transport corridors, and geologic conditions that affect ground stability and permeability; and (8) studies of metal mobility and environmental consequences downstream from mining operations.

Two units established within the Geologic Division are designed to support, facilitate, and coordinate environmental studies: (1) the Analytical Chemistry Support Group, utilized by industry, government, and USGS personnel for technique development and for inorganic analysis of geologic and biologic materials, and (2) the Center for Environmental Geochemistry and Geophysics, which acts as a focal point and information transfer medium for environmental studies.

PALEOZOIC AND MESOZOIC TECTONIC EVOLUTION OF MEXICO BASED ON GEOCHEMISTRY OF BASEMENT ROCKS

J. Ruiz, E. Centeno-Garcia, P.J. Coney,
R. Torres-Vargas, P.J. Patchett, and P. Yanez

We have used most of the available exposures of basement rocks in Mexico, and lower crustal granulite facies xenoliths, to determine the isotopic and trace-element characteristics of many of the tectonostratigraphic terranes that form Mexico. Basement rocks are exposed in the Sierra Madre, Chihuahua, Mixteca, and Guerrero terranes. Xenoliths are found in the Sierra Madre terrane, in particular. The samples thus represent the basement history of some of the largest terranes of Mexico.

The exposed basement rocks in eastern, southern, and northern Mexico, found at Ciudad Victoria, Molango, Los Filtros, and Oaxaca, have Grenville ages of crystallization and present-day ϵNd values between -7 and -11. The samples represent the basement of the Oaxaca terrane, parts of the Sierra Madre terrane, and the Chihuahua terrane. Most of the samples collected, which include ortho- and paragneisses, show a remarkably consistent 1.6–1.3 Ga model Nd crustal extraction age from a depleted mantle. This model age is similar to other Grenville-age outcrops in Texas (Llano, Van Horn, and Franklin Mountains), in Virginia, and in New York (Adirondack Mountains). Farther north in the Grenville province of Quebec, the model Nd ages are older, demonstrating the involvement of Archean rocks in their evolution. South of Mexico, geochemical analysis of Grenville-age rocks in Colombia is insufficient to make significant comparisons. It is important to note, however, that none of the Grenville-age outcrops in Mexico could have come from much farther north than the Adirondacks because of their model Nd ages.

To the west of the basement exposures in northern Mexico are numerous xenolith localities, where lower crustal granulite facies rocks have been brought to the surface by alkalic basalts of Cenozoic age. The xenoliths are generally similar to the exposed basement rocks in their isotopic chemistry, with the exception that many have Paleozoic model Nd ages. In the south, the polymetamorphic Acatlan Complex, which is the basement of the Mixteca terrane, has Devonian (380 Ma), Carboniferous (290 Ma), and Jurassic (160 Ma) ages. We believe that all the exposures just discussed were formed and deformed by Proto-Atlantic tectonic events.

The westernmost basement rocks studied here are part of the Guerrero terrane. Briefly, the rocks are polymetamorphosed metasediments and basalts with MORB (middle oceanic ridge basalt) geochemistry. The age of sedimentation is thought to be Triassic, based on fossil data. The geochemistry of the sedimentary rocks indicates that they were formed from recycled sediments of Grenville age-type rocks, but they also contain chert. Unconformably overlying these rocks are Jurassic-Cretaceous arc rocks with positive ϵNd values, which indicate that the magmas did not sample old continental crust. The Guerrero terrane and its basement were formed by accretionary processes related to Cordilleran tectonics.

It appears that the Paleozoic evolution of Mexico was dominated by tectonic events related to the opening and closing of the Proto-Atlantic Ocean. The Mesozoic evolution of Mexico was dominated by Cordilleran tectonic events. The

flipover occurred after Devonian but before Permian times, based on the geochemistry of Permian-Triassic granitoids.

ENVIRONMENTAL GEOCHEMISTRY OF ACTIVE AND EXTINCT HOT SPRING MERCURY DEPOSITS IN THE CALIFORNIA COAST RANGES

James J. Rytuba and William R. Miller

Numerous hot springs and fumaroles in the central Coast Ranges of California are actively depositing mercury and associated trace metals. The hot springs and fumaroles are present in and adjacent to mercury deposits in the north end of the 500-km-long Coast Range mercury belt. The mercury deposits in the northern part of the belt are generally younger than 0.5 Ma, and the hot spring and fumarolic activity reflects the waning stage of mercury mineralization. These geothermal systems are related to Pleistocene to Holocene volcanism associated with development of a slab window as the Mendocino triple junction migrated northward along the coast of California. The mines produced mercury primarily from 1870 to 1950; they are now inactive, except for the Manhattan mine, which produces gold and minor mercury (active workings now called McLaughlin mine). The Sulphur Bank mine (fig. 1), the fifth largest mercury producer in the United States (130,000 flasks), is an Environmental Protection Agency Superfund Site; and reclamation efforts are focused on limiting mine tailings and mine waters from entering Clear Lake, a major recreational area. These mitigation measures are complicated by the ongoing deposition of mercury and associated elements from hot springs (fig. 2) and fumaroles in and around the open pit excavated to mine the mercury deposit. Mercury vapor venting from the fumaroles is in part fixed as cinnabar by native sulfur generated from bacterial reduction of sulfate. The remainder of the mercury vapor is discharged into the atmosphere and forms a mercury plume extending from the deposit. Elevated levels of mercury in soils adjacent to the mine area reflect naturally occurring mercury derived from the fumaroles as well as mercury released during past mining.

Hot springs in the Sulphur Creek mercury-gold district, located 20 km northeast of the Sulphur Bank mine, occur in and adjacent to previously mined mercury and gold deposits. Tailings and excavations associated with previous mining activity contribute metals to the drainage basin, but the major component of metals is derived from precipitates from the hot springs. The precipitates are fine black silt and clay composed of (in decreasing abundance) smectite, chalcedony, calcium-magnesian carbonate, pyrite, magnetite, rutile, and cinnabar. Anomalous concentrations of trace metals in the

Figure 1 (Rytuba). Sulphur Bank Mercury mine with Mount Konocti, a 0.6 to 0.4 Ma composite volcano, on the skyline. The open pit mine is partially filled with water and fumaroles depositing cinnabar and native sulfur vent from the walls of the open pit (right side) above the water level. In the near foreground of the lake, fumarolic vents below the water level form disturbed gray areas on the water surface.
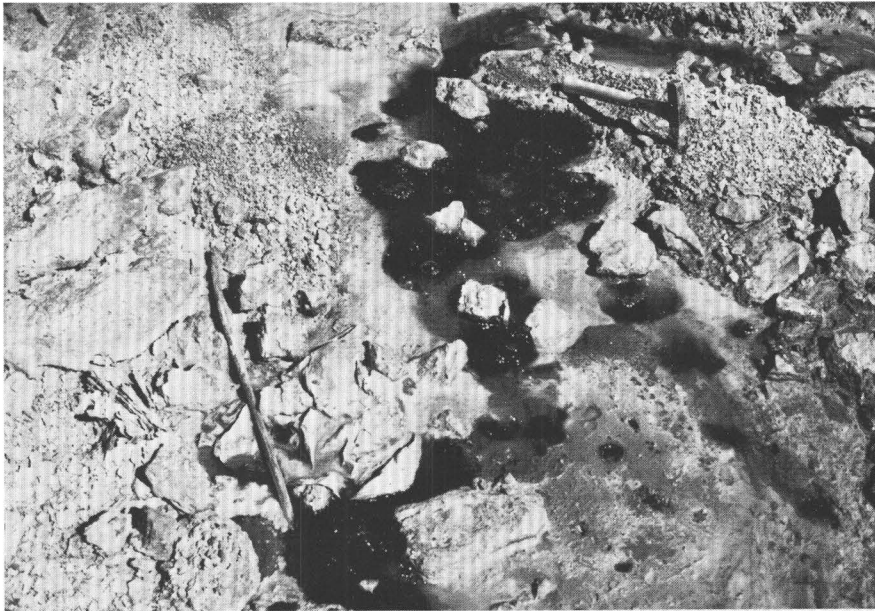
Figure 2 (Rytuba). Hot spring vent at the Sulphur Bank mine exposed on the floor of the open pit. Black precipitate is composed of pyrite and cinnabar. This vent area is now submerged by the lake that fills the open pit (see fig. 1).

precipitate include gold (maximum value, 1.3 ppm), tungsten (50 ppm), cobalt (150), nickel (1,500), chromium (3,000), and titanium (3,000). Mercury content of the hot spring fluid is anomalously high, 10–20 ppb, indicating that only part of the mercury is deposited in the subsurface and that mercury in solution directly enters waters in the drainage basin. Cinnabar grains up to 8 μm in diameter in the precipitate were probably deposited at depth in the hot spring vent and transported to the surface as particulate grains. These enter the drainage basin and are dispersed downstream. Other elements with elevated contents in the high-chloride (2.9 percent), alkaline, hot spring fluid include lithium (maximum content 16 ppm), titanium (600 ppb), bromine (210 ppm), antimony (100 ppb) and tellurium (25 ppb). Extremely high concentrations of tungsten (3,200–7,400 ppb) are present in the hot spring fluids, the highest concentration being in fluid from the Elbow hot spring. These tungsten values are some of the highest known naturally occurring concentrations of tungsten in water. In these alkaline fluids, tungsten is probably present as tungstate anion. Only part of the tungsten is deposited near the hot spring vent; the remainder enters waters in the drainage basin, and elevated levels of tungsten (260–680 ppb) occur in the stream water up to several kilometers from the hot spring discharge site. In the Sulphur Creek district, active hot springs contribute the primary component of particulate mercury and solutes of mercury, tungsten, and other metals to waters in the drainage basin. Previous mining activity contributes only a minor component. Similar dispersion patterns

of metals can be expected adjacent to hot spring type mercury deposits elsewhere in the Coast Range mercury belt, and these patterns provide a base line to measure the effect of mining activity on the environment where natural processes contribute a major component of metals.

GEOLOGIC MAP OF A LATE CRETACEOUS CALDERA AND RELATED PORPHYRY COPPER-MOLYBDENUM ORE DEPOSITS IN THE SILVER BELL MINING DISTRICT, ARIZONA, AND THEIR SUBSEQUENT TERTIARY STRUCTURAL HISTORY

David A. Sawyer

Geologic mapping at 1:24,000-scale in the Silver Bell and West Silver Bell Mountains provides evidence for a close temporal and spatial relationship between caldera volcanism, plutonism, and porphyry copper ore deposition. Intrusion of the precaldera biotite granite has been dated at 72.7±1 Ma (concordant U-Pb age on zircon, E.W. James, written commun., 1984). This was followed by eruption of tuff of Confidence Peak (TCP—equivalent to dacite porphyry of the previous literature), concurrent subsidence along the ring-fracture zone of the Silver Bell caldera, and

formation of caldera-collapse megabreccia composed of Paleozoic sedimentary rocks. The tuff of Confidence Peak accumulated to a intracaldera thickness of >1.2 km in the central Silver Bell Mountains, while a thin outflow sequence of TCP was deposited in the West Silver Bell Mountains. Postcaldera volcanism produced andesite and dacite lava flows and domes, followed by deposition of the Cat Mountain Tuff (equivalent to Mount Lord Volcanics of previous literature), which caps the local volcanic sequence. The TCP, postcaldera andesites and dacites, and Cat Mountain Tuff in the Silver Bell Mountains are indistinguishable in age from the 73-Ma biotite granite. Quartz monzodiorite, granodiorite, and monzodiorite porphyries were intruded at 69 Ma (K-Ar on biotite) as stocks and dikes along the ring-fracture zone of the Silver Bell caldera. Hypogene stockwork Cu-Mo mineralization took place in the apex of complex multiphase intrusions in the Oxide pit area, the El Tiro pit area, and at North Silver Bell, where ring-fracture intrusions intersect major northeast-trending quartz monzodiorite porphyry dike swarms. Significant Cu skarn ore formed in megabreccia blocks of Paleozoic sedimentary rocks in the caldera fill adjoining the ring-fracture intrusions. Later erosion, oxidation, and leaching of hypogene copper deposits formed secondary chalcocite ore that comprises most of the >90 Mt (million tons) of 0.8 percent Cu–0.022 percent Mo (average grade) ore mined in the Silver Bell district.

Beginning in latest Cretaceous time and continuing through the Tertiary, regional faulting and tilting deformed the Cretaceous volcanic and plutonic rocks and their associated ore deposits, and sporadic volcanism took place during Oligocene–early Miocene time. Cretaceous plutons and volcanic rocks were cut by west-northwest-trending strike-slip faults north and south of the Silver Bell Mountains. To the north, the Ragged Top fault offset a Cretaceous granodiorite porphyry pluton and placed it in contact with late Precambrian granite and Apache Group (Middle Proterozoic) sedimentary rocks. Offset on the Ragged Top fault was dextral-oblique having a *minimum* lateral separation of 13–26 km, as geologic histories cannot be matched across the exposed length of the fault. Movement on the fault occurred after 70 Ma but predated the 26-Ma Ragged Top rhyolite lava dome which fills the fault zone. Several west-northwest-trending strike-slip faults also separate the Silver Bell Mountains from the Waterman Mountains to the south. Clockwise vertical-axis rotation of 30 degrees has been documented in the Cretaceous volcanic and plutonic rocks of the Silver Bell Mountains by paleomagnetic studies; these data are consistent with subregional dextral strain. Both Cretaceous volcanic rocks and ore deposits were also tilted 30 degrees to the east-northeast, affecting elevations of alteration and mineralization zoning in the ore deposits. Mid-Tertiary magmatism in the Silver Bell Mountains was limited to emplacement of the Ragged Top rhyolite dome and related north-northwest-trending dikes, and to eruption of basalt to andesite lava flows from 28 to about 20 Ma in the eastern part of the Silver

Bell Mountains, and in the West Silver Bell Mountains. Postvolcanic Neogene faulting cutting through the Silver Bell Mountains was minor in nature, but the faulting was more significant in uplift of the Roskruge Mountains–Silver Bell–Picacho Peak regional horst relative to subsidence of pre-Neogene rocks into the adjoining Avra Valley to the east and the Aguirre Valley to the west.

CONVERSION OF THE MINERAL RESOURCE ASSESSMENT PORTFOLIO OF THE REPUBLIC OF COSTA RICA TO A DIGITAL GEOGRAPHIC INFORMATION SYSTEM

Paul G. Schruben and Robert Swierk

In 1986 and 1987, the U.S. Geological Survey, Dirección General de Geología, Minas e Hidrocarburos, and the Universidad de Costa Rica conducted a mineral resource assessment of the Republic of Costa Rica. The results were published as a large 80×50 cm color portfolio (U.S. Geological Survey and others, 1987). The 75-page document consists of maps as well as descriptive and interpretive text in English and Spanish covering physiographic, geologic, geochemical, geophysical, and mineral site themes as well as a mineral resource assessment. The spatial data layers consist of the following:

1. Physiographic base map at a scale of 1:500,000 with hypsography, place names, and drainage;

2. Geologic map at a scale of 1:500,000;

3. Regional geophysics, including gravity, aeromagnetic, and seismicity maps at various scales;

4. Mineral sites map at a scale of 1:500,000 showing mines, prospects, and occurrences;

5. Volcanological framework of the area important for epithermal gold deposits, at a scale of 1:100,000;

6. Rock sample locations, mining areas, and vein locations for several parts of the country;

7. Permissive areas delineated for selected deposit types.

Conversion to a geographic information system (GIS) was undertaken to facilitate the presentation and analysis of the data. GIS techniques allow combining and overlaying of layers to analyze spatial relationships not readily apparent in the standard paper publication. For instance, themes such as aeromagnetics and rock type can be combined to help define permissive tracts for undiscovered deposits. As part of the original publication effort, many of the layers were compiled in a USGS-authored map-editing program called GSMAP (Selner and Taylor, 1987). Conversion from GSMAP to ARC/INFO was accomplished through the use of GSMARC (Green and Selner, 1988). The ARC/INFO "adjust"
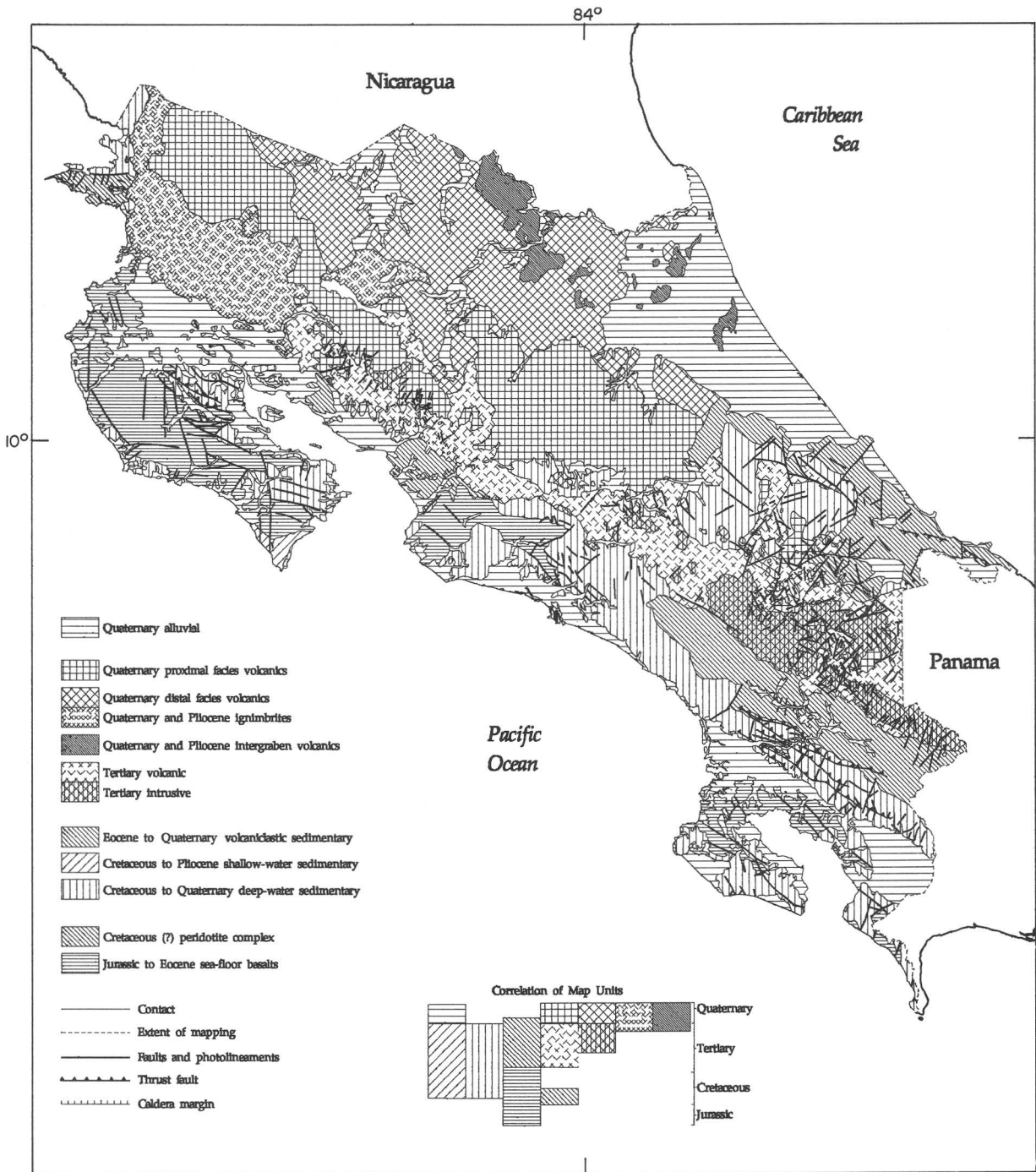
Figure 1 (Schruben and Swierk). Geologic map of Costa Rica.

command was used to apply a rubber-sheet correction to a projection problem of unknown origin. The arcs and polygons were tagged using Alacarte (Wentworth and Fitzgibbon, 1991). The data are presented under ArcView.

The basement of Costa Rica is composed of Jurassic to Eocene oceanic crust, which is overlain by Cretaceous and Tertiary marine deposits that accumulated in a complex series of basins. Uplift during Miocene and later time formed

93

the present isthmus and was accompanied by widespread igneous activity related to subduction along the Middle American trench. The resulting volcanic rocks cover more than half of present-day Costa Rica. The Tertiary volcanic rocks of the gold belt are the coalesced products of several discrete volcanic centers and consist of interlayered andesitic lava flows and fragmental rocks.

The known deposit types of Costa Rica include precious-metal Sado-type quartz-adularia vein, placer gold, podiform chromite, volcanogenic manganese, Cyprus-type massive sulfide copper-zinc, and lateritic bauxite. The most important Sado-type deposit is the Bellavista deposit, with a geologic resource of more than 32 t (1.06 million oz) of gold.

Undeveloped deposit types include hot-spring gold, polymetallic vein, porphyry copper, and porphyry-related skarn. Speculative deposit types include alkaline rock-related Lihir Island type (Ludington and Bagby, in press), zinc-lead skarn, hot-spring mercury, and hematitic copper.

REFERENCES

Green, G.N., and Selner, G.I., 1988, GSMARC—A program and procedure to convert GSMAP data bases into ARC/INFO coverages: U.S. Geological Survey Open-File Report 88-403A and B, 16 p.

Ludington, Steve, and Bagby, W.C., in press, The outlook for volcanic-hosted gold deposits in the Republic of Costa Rica, *in* Symposium on Energy and Mineral Potential of the Central American-Caribbean Region: New York, Springer-Verlag.

Selner, G.I., and Taylor, R.B., 1987, GSDRAW and GSMAP version 4.0: U.S. Geological Survey Open-File Report 87-496A, B, C, and D, 90 p.

U.S. Geological Survey, Dirección General de Geología, Minas *e* Hidrocarburos, and the Universidad de Costa Rica, 1987, Mineral resource assessment of the Republic of Costa Rica: U.S. Geological Survey Miscellaneous Investigations Series Map I-1865, 75 p.

Wentworth, C.M., and Fitzgibbon, T.T., 1991, Alacarte user manual, version 1.0: U.S. Geological Survey Open-File Report 91-587, 267 p.

AUDIO-MAGNETOTELLURIC AND GRAVITY STUDY OF THE MOGOLLON MINING DISTRICT, SOUTHWEST NEW MEXICO

R.M. Senterfit, R.J. Kamilli, G.A. Abrams, D.P. Klein, and J.C. Ratté

Electromagnetic induction (AMT) and gravity data are used to infer subsurface structure and lithology of the Mogollon mining district in southwest New Mexico. The geoelectric AMT data were obtained using distant energy sources, mostly of natural origins in the audio-magnetotelluric frequency range of 4.5–27,000 Hz. The data for each station consist of scalar electromagnetic resistivity measurements at discrete frequencies for two orthogonal magnetic and electric field pairs. A gravity measurement with a Lacoste-Romberg gravimeter was made at each AMT station location, and incorporated with additional gravity data from the University of Texas at Austin and the U.S. Defense Mapping Agency. This work was done by USGS geophysicists, Denver, Colo., in cooperation with the Sierrita-Mogollon transect project, Tucson, Ariz., field office.

The buried structural margin of the Oligocene resurgent Bursum caldera was imaged in three AMT profiles made in the gold-silver-copper-producing Mogollon mining district. The Queen vein zone in the Mogollon district is a high-resistivity feature, probably because it localizes massive quartz and calcite (±gold-silver-copper minerals) in veins as much as 30 m wide, and massive, silicic rhyolite intrusions. To late 1993, all mineral production in the mining district has been to the west of the Queen fault and vein zone. This zone, a reactivated segment of the caldera structural wall, is expressed as a high-resistivity anomaly (400 ohm-m or more) that is about 500 m wide and possibly extends to a depth of 2 km (fig. 1). Low-resistivity zones on either side of the Queen vein correlate with intense propylitic alteration, confirmed by core-drilling, related to the formation of the vein. At depths of 0.5 to 1.5 km, the resistivity decreases to less than 100 ohm-m for a width of about 500 m on both the east and west sides of the vein. This relatively narrow symmetrical resistivity anomaly is centered in a 5-km-wide zone of moderate-resistivity material (250–400 ohm-m) that is bounded by units with resistivities exceeding 400 ohm-m on the east and west. This broad 250–400 ohm-m zone is interpreted to represent the extent of the hydrothermal system that gave rise to the Mogollon mining district. Because a low-resistivity zone is present on both sides of the fault, mineralization may be as likely on the east side of the Queen fault. This characteristic resistivity pattern across the mineralized area becomes weak and incomplete 3 km north of the main area of mineralization, disappearing about 6 km to the north.

Gravity measurements made along the AMT profiles show a dense body, approximately 10 km wide and 2 km below the surface, underlying the Queen fault zone about 5 km to the east and west. This body may have driven the hydrothermal system that caused the mineralization in the Mogollon mining district. The gravity data show no discernable density contrast across the Queen fault zone, whereas the fault zone produces a significant AMT anomaly.

Alongside geologic considerations, AMT and gravity measurements provide evidence that the part of the Mogollon mining district east of the Queen fault, although it has never had any mineral production, may have potential for mineralization.
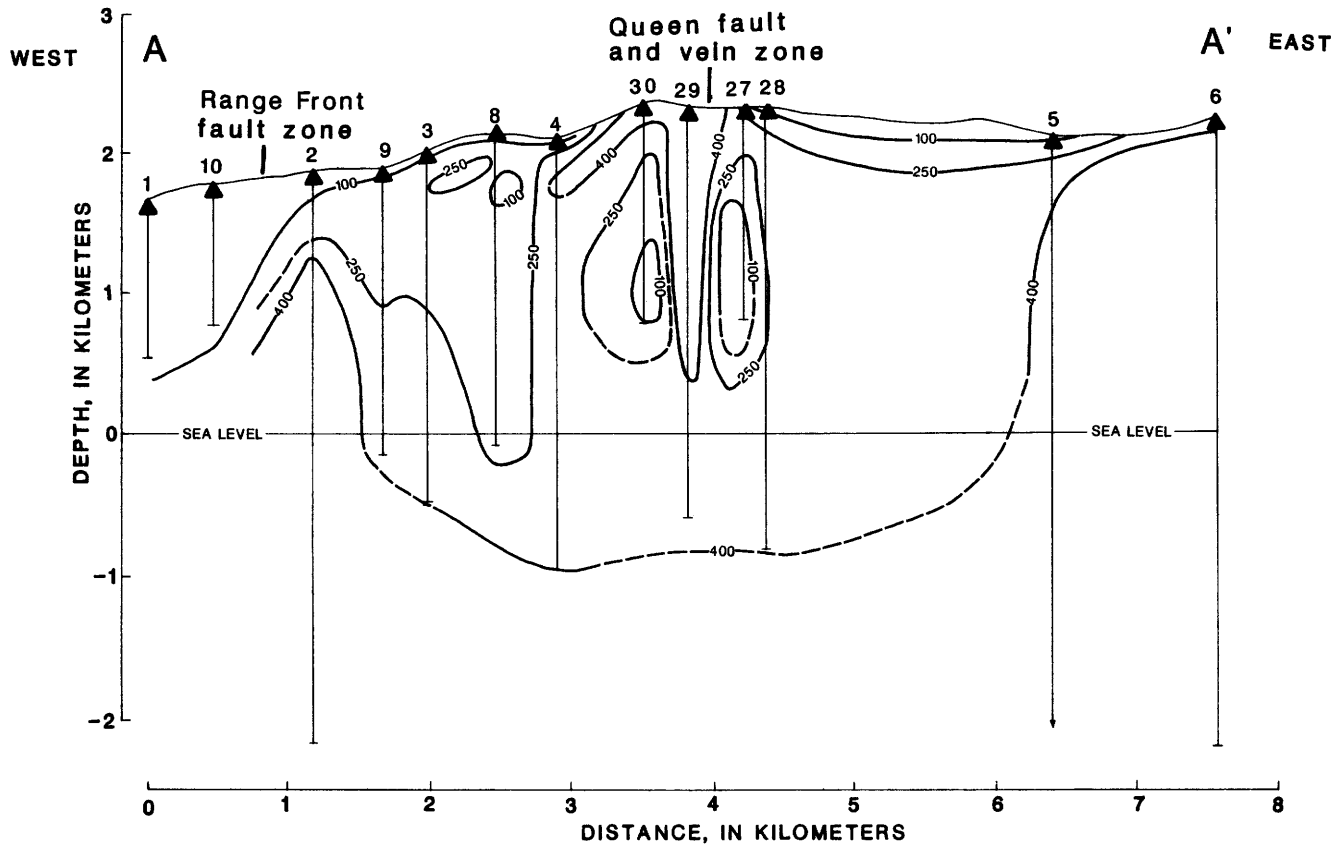
Figure 1 (Senterfit and others). An east-west resistivity section across the Mogollon mining area. Sections are based on the geometric average of the two scalar resistivity soundings taken at each site. Contours are in ohm-meters, with logarithmic contour intervals. Contour lines are dashed where depths are uncertain. Numbered solid triangle, AMT sounding location.

TRENDS IN MINERAL EXPLORATION IN LATIN AMERICA

Douglas B. Silver

The emigration of United States and Canadian companies into Latin America is not a fad, but a trend which both offers the salvation for many mining companies and heralds the demise of industries fundamental to most industrial economies. The exodus is not caused by a single event but by the coalescence of several structural changes to the business fabric. Companies are moving from their original locations or even countries in response to evolving environmental regulations and reforms to the traditional Mining Law of 1872.

Simultaneously, some Latin American countries are being led by politicians trained in many of the West's best business schools. These emerging countries realize that the answers to their economic problems depend on their abilities to build (or rebuild) their country's infrastructure, increase exports and build support for their currencies. An obvious way to achieve these ambitious tasks is to develop their natural resources, because these assets tend to be situated in more remote areas of the country. In the course of developing a new oil field or mineral deposit, the operator will upgrade or create the infrastructure necessary for operating on an internationally competitive basis. Consequently, the country receives foreign investments, jobs, tax revenues, and economic stability, all provided by some of the most technologically advanced and profitable companies in the world.

Approximately 10 percent of the 3,000 North American mining and exploration companies are currently operating in Latin America. However, this seemingly small representation includes most of the major and intermediate metal producers, and, therefore, most of the available funding. Although political boundaries continue to act as the first filter for country selection, these boundaries are slowly giving way to geologic potential. Curiously, the political deterrents to mineral exploration of a few short years ago in Latin America are now considered equal to the perceived and real costs of complying to the growing list of environmental regulations in the United States or Canada.

Mexico and Chile are the dominant countries of choice. Mexico offers a southern extension to the bountiful Great Basin in the western United States. Companies such as

Phelps Dodge are operating gold mines in this high-potential land. Kennecott and Placer Dome continue to expand reserves on their recent (and rumored) one million+ gold discoveries. Eldorado Gold Corporation, a newly formed Vancouver company, is pressing ahead with imminent production from its La Colorada gold project, as is Hecla Mining. Union Miniere acquired the enormous Cananea copper mine. International Curator snatched up the high grade (17 million short tons at 3 percent Cu) Kupferschiefer-style Boleo deposit.

Porphyry copper and gold are also the metallic incentive for going to Chile and, to a lesser extent, to Argentina. MINORCO paid $190 million for a third interest in the Collahuasi copper project. Cominco and Teck are building Quebrada Blanca mine. Lac Minerals continues to find gaudy gold at El Indio. Bema Gold, Amax Gold, and Dayton Mining are trying to develop their large gold deposits. Placer Dome is everywhere as it develops the Zalvidar copper mine. The list of bidders for El Abra represents a who's who in world mining. Cyprus and Lac Minerals were the winners, having paid $404 million for a 51 percent interest, plus committing to their share of a $1 billion capital investment.

The Maricunga gold belt, along the Chilean-Argentinian border, has been presently recognized to extend into Argentina. Previously known but unavailable porphyry copper-gold deposits are candidate targets. American Resource Corporation leads the pack in that it has acquired options on approximately one dozen known porphyry systems. International Musto is developing the massive Bajo El Alumbrera copper deposit with its 8 million ounces of gold and 6+ billion pounds of copper. Meanwhile, Crown Resources Corporation, one of the most successful United States exploration companies, has taken large concessions along the border zone.

Copper is also being explored for in the Caribbean region and Central America. USMX acquired an interest in Cala Abajo, and Adrian Resources and Minnova are advancing the development of the Petaquilla copper porphyry. Miramar Mining, Joutel Resources, and Minnova are independently looking for copper and gold in Cuba, while Mallon Minerals develops the Rio Chiquito gold project in Costa Rica. Canyon Resources and Battle Mountain Gold Company are jointly developing the El Higo gold discovery in the Dominican Republic.

Bolivia, Colombia, and Peru have experienced an influx of new capital for mineral exploration and development. Battle Mountain's success at Kori Kollo in Bolivia is as impressive as Newmont Mining's work in Peru. Less development is taking place in Ecuador, for reasons unknown; however, Armeno Mines and Kookaburra are presently exploring the Chaucha and Peggy porphyry systems.

To the east, aluminum bauxites carry the day. However, Golden Star Resources periodically reminds investors of possible gold potential in Suriname. Cambior's Omai gold mine in Guyana has considerable promise on paper, and their technical people have performed like magicians, exceeding expectations in opening up this mine.

Placer Dome's announcement of a major discovery in the Kilometer 88 area of Venezuela has sparked a land rush akin to those which developed California and the Yukon. But today's rush is not likely to create a world-class mining district because the players appear to have a preference for the performance of their share price rather than the technical quality of their properties.

For the most part, Brazil is being ignored by the northern companies because its foreign repatriation of profits and its export policies are not competitive with those of its neighboring countries. The mineral potential of Paraguay and Belize is too speculative to interest most miners, but Uruguay has its first gold mine, developed by American Resource Corporation.

As Latin American countries successfully vie for United States and Canadian technology and funding, the marketplace will become more competitive leading to resource acquisition prices comparable to those of North America. This will lessen the role of the United States and Canadian companies as primary metal producers while transferring wealth to Latin America.

TOURMALINITES AND STRATA-BOUND MINERAL DEPOSITS—GEOLOGY, GENESIS, AND EXPLORATION APPLICATIONS

John F. Slack

Exploration and research over the past decade have documented a close association of tourmalinites with a variety of strata-bound and generally stratiform mineral deposits. Tourmalinites are strata-bound rocks that contain 20 percent or more tourmaline by volume. They occur in diverse metamorphic terranes but are most common in clastic metasedimentary sequences of Proterozoic and early Paleozoic age. Principal host lithologies are pelitic schist, quartzite, and metagraywacke; metabasaltic amphibolite and metamorphosed felsic volcanic and (or) volcaniclastic rocks are present in some tourmalinite-bearing sequences. Tourmalinites locally are interbedded with coticule (fine-grained spessartine-quartz rock), metachert, and (or) magnetite iron-formation. In weakly metamorphosed terranes (greenschist grade or lower), tourmalinites typically are fine grained (<1 mm) and may be easily misidentified as chert or carbonaceous/graphitic siltstone. In terranes of higher metamorphic grade, the tourmaline generally is coarser grained (>1 mm) as a result of metamorphic recrystallization, producing tourmalinites that may superficially resemble amphibolite.

Most tourmalinites are bedded units <1 m thick that are traceable along strike for tens to hundreds of meters. In complexly deformed terranes, some tourmalinites have been mapped at the same stratigraphic horizon for as much as several kilometers. Structural studies in a few areas have identified metamorphic fabrics that document growth of tourmaline prior to the earliest deformation. Where present, synkinematic to postkinematic granites and pegmatites—some containing tourmaline—commonly postdate tourmalinite formation. Such field relations indicate that, in most cases, the formation of tourmalinites took place prior to deformation, metamorphism, and the emplacement of local granitic intrusions. However, because tourmalinites may also form during regional and contact metamorphism, care must be taken in determining their origin relative to hydrothermal, metamorphic, and granitic processes.

Tourmalinites are metallogenically significant because of their spatial association with ore deposits containing lead-zinc-silver (Broken Hill, Australia; Sullivan, British Columbia), copper-zinc (Prieska, South Africa; Elizabeth, Vermont), gold (Golden Dyke dome, Northern Territory), cobalt-copper-gold (Blackbird, Idaho), tungsten (Felbertal, Austria), and uranium (Rum Jungle, Northern Territory). In these and similar deposits, tourmalinites typically occur either in the immediate wall rocks, or as distal lateral equivalents to the ores. Concentrations of tourmaline are also present in the footwall feeder zones of some massive sulfide deposits (Kidd Creek, Ontario), although these deposits lack associated tourmalinites.

Field relations and geochemical studies indicate that tourmalinites form by the replacement of aluminous sediments or volcanic rocks through chemical reaction with boron-rich hydrothermal fluids. The formation of most tourmalinites apparently takes place below the seafloor by the selective replacement of clays and feldspars; cross-stratal permeability is provided mainly by growth faults. Tourmalinites considered to be of exhalative origin are believed to form by reaction of a boron-rich brine pool with aluminous sediments at or near the sediment-seawater interface, in which the boron and some of the iron and manganese (and perhaps the silicon) in the tourmalinites comes from exhalative hydrothermal fluids. Initial growth of tourmaline occurs either on the seafloor or during early diagenesis. In manganese-garnet-bearing exhalative tourmalinites, some tourmaline may form from precursor manganese-borate minerals such as sussexite $[MnBO_2(OH)]$ and (or) jimboite $[Mn_3B_2O_6]$, based on the observed tourmalinite-coticule connection in many deposits (Broken Hill, Sullivan) and on the occurrence of these minerals in bedded manganese deposits of Switzerland and Japan.

Electron microprobe studies indicate that the compositions of ore-related tourmalines fall mainly along the schorl (iron-rich)–dravite (magnesium-rich) solid-solution join, with a tendency for magnesium-rich tourmalines to predominate. In hydrothermal systems, magnesium-rich tourmalines may form either by premetamorphic replacement from seawater-derived fluids under high fluid/rock conditions, or by sulfide-silicate reactions during metamorphism. Tourmalinization under low fluid/rock conditions (for example, distal tourmalinites) generally produces tourmalinite bulk compositions that are similar to those of tourmaline-free (unreplaced) country rocks, except for major gain of boron and loss of potassium; in contrast, the compositions of tourmalinites that form under high fluid/rock conditions (for example, footwall feeder zones) are generally different from those of the host rocks, being controlled mainly by the chemistry of the hydrothermal fluid. Stable isotope analyses of tourmalines ($\delta^{11}B$, $\delta^{18}O$, δD) in these types of systems suggest boron derivation from clays and feldspars in footwall sediments and (or) felsic volcanic rocks, and in some cases from evaporite borates, with evolved seawater being the major fluid agent.

Tourmalinites may be useful prospecting guides for a variety of strata-bound mineral deposits. In the exploration for largely syngenetic deposits, tourmalinites with a major exhalative component must be distinguished from those that formed significantly below the seawater-sediment (or -volcanic) interface. The former type commonly is closely associated (or in contact) with chemical sediments such as coticule, metachert, and iron-formation, and can be an effective time-stratigraphic marker in district exploration. The presence of sulfide minerals, gold, and anomalous metal concentrations (such as copper and zinc) in tourmalinites are obvious prospecting guides. Also important are abundant manganese-rich garnets, and possibly elevated contents of iron (nonsulfide) and phosphorus, as indicators of a brine-pool origin. Magnesium-rich tourmalines [$\approx Fe/(Fe+Mg)<0.3$], many of which are easily identified by their brown color in hand specimen, are an additional guide; black tourmalines may also be magnesian, however, and electron microprobe analyses are necessary to accurately document tourmaline compositions. Proton microprobe studies, currently underway, suggest that the trace-element composition of the tourmalines can predict the metallogeny of associated mineralization, and may be useful in regional (and district) exploration.

U.S. GEOLOGICAL SURVEY MINERAL RESOURCE STUDIES ON INDIAN LANDS

Bruce D. Smith and E.A. Merewether

The U.S. Geological Survey (USGS) has done both regional and site-specific energy and mineral studies of Indian lands. Regional studies are conducted mainly in USGS internally funded programs that cover a broad base of Federal, State, and Tribal government lands. Through a memorandum of understanding with the Bureau of Indian

Affairs (BIA) Division of Energy and Mineral Resources (DE&MR), the USGS receives funds for three categories of activities in support of resource studies of Indian lands. First, BIA funds are provided for cost-effective sharing of computer assets that pertain to development and utilization of USGS digital energy- and mineral-resource data bases. Second, BIA funds support OUTREACH activities for USGS interaction with Tribal governments in organization and public presentation of resource data. Third, funds are provided for site-specific studies of Indian reservations.

More recently, BIA-funded USGS projects have led to public presentations such as at the Northwest Mining Association (NWMA) annual meeting (Manydeeds and Smith, 1991; Manydeeds, 1992). The DE&MR and USGS coordinate these presentations with Tribal governments, who often send representatives to the meetings. The following summarizes some of the results given at these public meetings.

The Annette Islands Reserve: is located in southeast Alaska near the city of Ketchikan. The USGS mineral assessment project consisted of integrated geophysical (airborne and ground), geologic, and geochemical studies. Ground surveys were made at selected areas identified from the airborne geophysical surveys. A qualitative mineral resource assessment has been made that concludes a moderate potential exists for gold-quartz and polymetallic vein deposits. Detailed results of the project have been presented at the December 1993 NWMA meetings along with a publication of a monograph (Godwin and Smith, 1993).

The Goshute Reservation: is located on the Nevada-Utah border south of the town of Wendover, Nev. Geologic, geochemical, and geophysical studies have been conducted for the entire Reservation. Significant results of these studies reported by Nutt and others (1992) are as follows:

1. Discovery of a jasperoid unit identified with alteration indicative of possible association with igneous rocks;

2. Anomalous geochemical indicator elements for possible gold mineralization have been found to be associated with the jasperoid, and the anomalies extend outside of known prospects;

3. Gravity and electromagnetic studies have been used to interpret the subsurface configuration of igneous rocks, thickness of pediments, and general nature of subsurface lithologies;

4. Various methods to enhance satellite remote sensing data have been used to identify areas of anomalous alteration and to enhance linear features extending beyond known areas of mineralization.

The Red Lake Indian Reservation: covers more than 837,000 acres in north-central Minnesota. Most of the Reservation consists of discontinuous tracts of land in sparsely inhabited swampy areas. A mineral resource assessment of these scattered tracts of land has been completed based on existing USGS data, supplemented by new data and interpretations tailored to the needs of the Red Lake Tribal government for land-use planning purposes. These studies have resulted in a qualitative assessment of mineral resources (base-metal massive sulfide and associated precious-metal deposits, iron-formation, copper-nickel-platinum group element (PGE) deposits, shear-zone gold) ranging from low to high for the Indian lands (Klein and others, 1992).

The Rocky Boy's Reservation: is located in north-central Montana south of the city of Havre. This project entailed a geologic and geochemical study of a known area of mineralization in the southeast part of the Reservation, concentrating on possible gold deposits. Geologic studies have identified four major styles of gold mineralization that have not been considered in previous reports to the Tribe. Geochemical studies have used new analyses of low-level gold and other indicator elements from stream sediments, heavy-mineral pan concentrate, rock, and soil samples. Results from these analyses and from the geologic studies indicate possible gold mineralization in areas outside of the known prospects and mines (Armbrustmacher and others, 1992).

Although proposed BIA-funded USGS mineral resource assessment projects will focus on metallic minerals, the cooperative BIA-USGS program continues to evolve. A new subject in proposals for USGS resource assessments is industrial minerals, particularly the various natural materials considered aggregate. Other industrial minerals, such as phosphates, gypsum, vermiculite, and others, are also being considered in more recent USGS mineral assessment proposals.

Another new component of the proposed USGS work on Indian lands is environmental analyses, for Reservations as well as larger regions which contain several Reservations. USGS data bases can be used to evaluate regions where rock and soil interact with water and air to create possible geologic hazards (for example, radon). Such environmental analyses, using new interpretations of geologic, geochemical, and geophysical data, could aid in prioritizing and designing additional environmental studies.

REFERENCES

Armbrustmacher, T.J., Modreski, P.J., and King, H.D., 1992, Mineral resources of the Black Mountain–Miners Gulch Area, Rocky Boy's Indian Reservation, Bearpaw Mountains, Montana, *in* Manydeeds, S.A., ed., 1992 Mineral frontiers on Indian lands: Bureau of Indian Affairs publication G–92–2, p. 107–116.

Godwin, L.H., and Smith, B.D., 1993, Economic mineral resources of the Annette Islands Reserve Alaska: Spokane, Wash., Northwest Mining Association Monograph.

Klein, T.L., Day, W.C., Clark, J.R., Horton, R.J., and Green, G.N., 1992, Assessment of shear zone-hosted gold deposits for the Red Lake Indian Reservation, Northern Minnesota, *in* Manydeeds, S.A., ed., 1992 Mineral frontiers on Indian lands: Bureau of Indian Affairs publication G–92–2, p. 88–103.

Manydeeds, S.A., ed., 1992, 1992 Mineral frontiers on Indian lands: Bureau of Indian Affairs General Publication, G–92–2, 135 p.

Manydeeds, S.A., and Smith, B.D., 1991, eds., Mineral frontiers on Indian lands: Bureau of Indian Affairs special publication for the Northwest Mining Association 1991 Annual Meeting, 147 p.

Nutt, C.J., Eppinger, R.G., Miller, S.H., Ponce, D.A., and Sampson, J.A., 1992, Geological, geochemical, and geophysical studies for the goshute reservation, Nevada and Utah, Precious-mineral assessment project, in Manydeeds, S.A., ed., 1992 Mineral frontiers on Indian lands: Bureau of Indian Affairs publication G–92–2, p. 50–69.

TECTONIC RECONSTRUCTION OF NORTHWESTERN MEXICO WITH IMPLICATIONS FOR MINERAL RESOURCES—A NEW REGIONAL ORE DEPOSIT SYNTHESIS AND MODEL

John-Mark G. Staude

The metallogeny of northwestern Mexico is intimately related to the magmatic and tectonic histories of the region, and palinspastic reconstructions permit a new evaluation of the time-space development of metallic mineralization in the southwestern Cordillera. This study compiled and compared the host lithologies, age of mineralization, main productive metals, key structural controls, and other features of more than 2,000 metallic mineral occurrences in more than 600 districts. Tectonic reconstructions were completed and mineral deposits restored to their position at the time they formed. These reconstructions and metallogenic model provide a more detailed analysis of mineralization as well as new data for understanding the geologic development of northwestern Mexico.

Metallic mineralization has taken place throughout much of the past 150 m.y., and deposit types changed as magma composition and structural styles developed along the long-lived (>140 m.y.) magmatic arc. Mineralization events can be grouped into five periods corresponding to distinct magmatic and tectonic episodes. Late Jurassic to Early Cretaceous shear zones and mafic to intermediate plutonism generated gold, iron, and possibly copper deposits in a waning transpressional environment. Cretaceous tonalite to granodiorite batholith emplacement generated widespread W skarns and Au-Ag quartz veins in a compressional tectonic environment. Late Cretaceous–early Tertiary (Laramide) porphyry Cu-(Mo), W skarn, and Au-Ag veins are associated with intermediate composition, hypabyssal intrusions. These Laramide ore deposits are coeval with widespread thrust faults in Chihuahua and with local zones of extensional faulting in central Sonora. Late Eocene–Oligocene early intermediate, later felsic to bimodal volcanism is associated
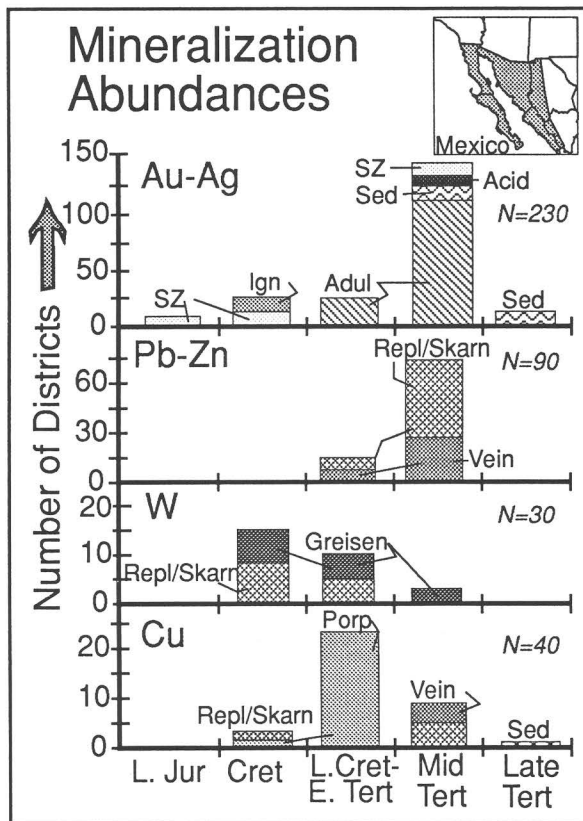
Figure 1 (Staude). Histogram showing number of mining districts in northwest Mexico arranged by age and deposit type. Shading in inset map shows area included for histogram. The number of districts for each commodity is denoted by N=. Abbreviations are L.Jur, Late Jurassic; Cret, Cretaceous; L.Cret-E.Tert, Late Cretaceous–early Tertiary (Laramide); Mid Tert, middle Tertiary; Late Tert, late Tertiary; SZ, shear zone vein districts; Sed, sedimentary-hosted; Acid, acid-sulfate; Ign, intrusion associated veins; Adul, adularia-sericite veins; Repl/Skarn, replacement and skarn districts; and Porp, porphyry deposits.

with many Au-Ag, Ag-Pb-Zn, and Au-Cu districts. Mid-Tertiary extensional features range from basin-bounding, high-angle faults to low-angle detachment faults. From the late Tertiary to Holocene, hot-spring precious- and base-metal deposits were generated in association with rifting of the Gulf of California and mafic magmatism.

Most metallogenic studies of Mexico and other parts of the world use the present geographic distribution of lithologies and ore deposits to interpret their formation conditions; however, in order to relate mineralization to coeval magmatism and tectonism at the time of their formation, palinspastic reconstructions are needed. Reconstructions of northwestern Mexico must account for opening of the Gulf of California, basin-and-range block faulting, and core complex extension to obtain the pre-late Oligocene

relations. Integrating >50 geologic maps and >900 radiometric ages permits restoration of extensional events to the pre-middle Tertiary configuration and provides new insights into the metallogenic history. These reconstructions show that Cretaceous batholithic rocks and associated skarns extend from Baja California into western Sonora, and that Laramide porphyry copper deposits and intrusive centers form a narrower belt than previously thought and are traceable for more than 400 km beneath the younger Sierra Madre Occidental volcanic province. These restorations also indicate that the mid-Tertiary Au-Ag deposits in Baja California represent the western part of the Sierra Madre Occidental metallogenic event and that the sediment-hosted, disseminated Au deposits are related to extension which is synchronous with magmatism in the area.

PROSPECTING FOR GOLD WITH SAGEBRUSH IN THE GREAT BASIN—RESULTS OF GREENHOUSE STUDIES

Kathleen C. Stewart and David M. McKown

Sagebrush has been proposed for use as a biogeochemical prospecting medium for gold in the Great Basin of Nevada because of its widespread growth in areas where Carlin-type disseminated gold deposits are known to exist and because of its extensive root system which may be exposed to ions that migrate in water. Difficulties exist with the use of plants as a prospecting medium, however, where the possibility of aeolian contamination cannot be excluded in the interpretation of data. We designed a greenhouse study to determine if sagebrush accumulates gold in a controlled setting, in order to define its limits for exploration purposes.

Soil collected from Humbolt County, Nevada, was disaggregated to <2 mm, homogenized, and mixed with perlite and disseminated gold ore in a V-blendor. The gold ores were obtained from the Getchell and Pinson mining districts and were ground to <100 mesh and homogenized before mixing. Gold is found in these ores both as metallic gold and associated with pyrite (FeS_2). Other minerals present include realgar (AsS) and orpiment (As_2S_3). Soil mixture M1, prepared to represent a nonmineralized soil from Humbolt County, contained <1 ppb gold, 6 ppm arsenic, 1 ppm antimony, and 2 ppm tungsten. Two additional mixtures (M2 and M3) were prepared to contain anomalous levels of gold, arsenic, antimony, and tungsten: M2 contained 36 ppb gold, 220 ppm arsenic, 13 ppm antimony, and 3 ppm tungsten; M3 contained 190 ppb gold, 230 ppm arsenic, 12 ppm antimony, and 13 ppm tungsten. There was no significant difference in arsenic or antimony concentrations between M2 and M3, but the tungsten concentration was significantly higher in M3 than in the other mixtures. Seedlings of basin big sagebrush
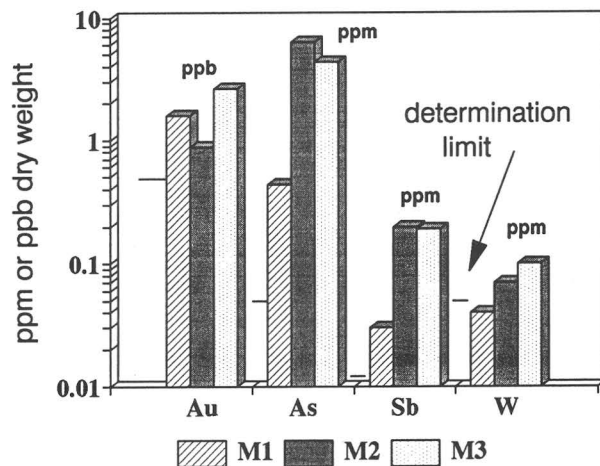
Figure 1 (Stewart and McKown). Mean concentrations of Carlin-indicator elements in above-ground parts of basin big sagebrush after 4 months growth in nonmineralized and mineralized soils under greenhouse conditions, $n=6$. M1 is nonmineralized soil; M2 and M3 contain gold ore from the Getchell and Pinson mining districts in Nevada.

(*Artemisia tridentata* ssp. *tridentata*) were planted in the soil mixtures, placed in a greenhouse in randomized blocks, and maintained at controlled temperature and moisture. After 4 months, all above-ground tissue for each plant was harvested and analyzed as one composited sample by instrumental neutron activation analysis (INAA) for gold, arsenic, antimony, and tungsten.

Sagebrush seedlings showed statistically significant uptake of arsenic, antimony, and tungsten, but not gold. Figure 1 presents the mean concentrations for six plants grown in each mixture. Duncan's F test for multiple ranges (Duncan, 1955) determined that means for sagebrush gold were not significantly different among the plants grown in the three soil mixtures ($P=0.05$), but mean arsenic and antimony concentrations in plants from the mineralized soils were significantly higher than in plants from the nonmineralized soil. Mean plant tungsten levels for the two lowest concentrations of soil tungsten (M1 and M2) could not be distinguished at the 0.05 probability level, but its concentration in plants from the soil with elevated tungsten (M3) was significantly higher than in plants from the other two mixtures. Arsenic showed the greatest absolute uptake from the soils, but the relative uptake of antimony was higher by a factor of 2 compared to its concentration in the soils. Concentrations for all elements measured were above the determination limits, except tungsten in plants grown in the nonmineralized mixture.

The results of the greenhouse study suggest that interpretation of gold data from sagebrush collected in the field cannot rule out the possibility of windblown contamination, because plants in this controlled environment did not

accumulate significant gold, at least over a time period of 4 months. On the other hand, the study indicates that sagebrush has good potential for use in prospecting for concealed Carlin-type deposits in the Great Basin using the pathfinder elements arsenic, antimony, and tungsten. Arsenic and antimony are especially sensitive indicators because sagebrush accumulates these elements in above-ground plant parts to levels that are well above INAA determination limits.

REFERENCE

Duncan, D.B., 1955, Multiple range and multiple F tests: Biometrics, v. 11, p. 1–42.

IMPACT OF ACID MINE DRAINAGE FROM SUMMITVILLE MINE ON BARLEY FIELDS IN THE SAN LUIS VALLEY, SOUTH-CENTRAL COLORADO

P.R. Stout, J.A. Erdman, and J.C. Emerick

Possible contamination from the Summitville gold mine in the San Juan Mountains above Terrace Reservoir on the Alamosa River has raised concerns about using this water to grow barley in the San Luis Valley. Approximately 45,000 acres of farmland with different crops in the San Luis Valley are irrigated with water from Terrace Reservoir. Copper, Mn, Zn, Cd, Fe and Ni have all shown increased concentrations in the reservoir since 1986 when the Summitville mine came into production (Agro Engineering, 1992). The objectives of this study were to examine whether the use of Terrace Reservoir water significantly increased metal uptake in malt barley (*Hordeum vulgare* cv. Moravian III) and to determine relationships between soil chemistry and plant-metal concentrations.

Fields from six farms were selected as sample sites; three of the fields were irrigated with water from Terrace Reservoir and three were irrigated with water, unaffected by Summitville, either from the Rio Grande River or from deep wells (control fields). All the fields had similar physical soil types and were classified as well-drained sandy loams. Samples were collected three times over the summer of 1993 (June 10–15, July 16–19, August 10–13). Three randomly selected, composited soil samples (0–20 cm) were taken from each field on each date and three randomly selected, composited barley samples from each field were taken on the last date. Water samples were taken from the irrigation structures on the first two sampling dates. All samples were analyzed using inductively-coupled plasma atomic-emission spectroscopy (ICP-AES).

The pH of water samples collected from the Terrace-irrigated fields averaged 5.95 and ranged from 5.3 to 6.7.

The pH for control-field water averaged 8.25 with a range of 7.3–9.2. These pH differences between source waters were significant at the 0.01 probability level. Fields irrigated with water from the Terrace Reservoir clearly receive more acidic water than do fields irrigated with water from other sources. No significant difference in pH was observed between the two sampling dates.

Results of total analyses of soils show some differences between fields irrigated with Terrace Reservoir water and control fields. Concentrations of Co, Cu, Fe, Mn, Pb, V, and Zn all were significantly higher in soils from the Terrace-irrigated fields than in soils from the control fields. On the other hand, concentrations of Ca, Li, Mg, Na, and Sr all were significantly higher in the soils from the control fields than in those from the Terrace-irrigated fields. Equally important, metal concentrations in all of the soils sampled were within ranges for Western U.S. soils given by Shacklette and Boerngen (1984). No significant temporal differences were observed among the three sample periods.

DTPA (diethylene triamine pentaacetic acid)-extractable concentrations of La, Ni, Cu, Ce, Mn, Fe, and Zn were significantly greater in soils from the Terrace-irrigated fields than in soils from the control fields. DTPA extractions have been used to estimate the availability of minerals to plants. Significant negative correlations were observed between Fe, Mn, Ce, Cu, Ni, and Zn and soil pH. As with the pH of the irrigation waters, the soil pH of the Terrace fields was significantly lower than that of the control fields. The control-field soils yielded significantly greater DTPA-extractable Pb, K, Ca, Si, and Sr. No significant temporal differences were observed over the season sampled. These data suggest that certain metals become more available to the plants as soil pH decreases and that these metals may be more available to plants in the Terrace-irrigated fields than in the control fields.

Water-extractable Ba was significantly higher in soils of the Terrace-irrigated fields compared to that of the control-field soils. Conversely, water-extractable Ca was significantly higher in the control fields than in the Terrace-irrigated fields. A significant negative correlation between water-extractable Ba and soil pH was observed. No significant temporal changes were observed over the season sampled. These results indicate that few of the metals were extracted by water at concentrations detectable by ICP-AES and that no other detectable differences in water-extractable chemistry existed between the Terrace-irrigated fields and the control fields.

Preliminary results suggest that irrigation with waters from the Terrace reservoir has a measurable impact on both the bulk-soil and DTPA-extractable chemistry. However, the total-metal concentrations of soils irrigated by these waters are well within the ranges for Western U.S. soils reported by Shacklette and Boerngen (1984). The effects on barley of higher metal values in the irrigation water and soils

irrigated by this water are unknown because the analytical data for the barley-grain samples are still pending.

REFERENCES

Agro Engineering, 1992, Water, sediment and soil quality synopsis and literature review Alamosa River, Conejos County, Colorado: Unpublished report prepared for the Alamosa La Jara Water Conservancy District, December 29, 1992.

Shacklette, H.T., and Boerngen, J.G., 1984, Element concentrations in the soils and other surficial materials of the conterminous United States: U.S. Geological Survey Professional Paper 1270, 105 p.

THREE-PART QUANTITATIVE MINERAL-RESOURCE ASSESSMENT FOR SELECTED UNDISCOVERED MINERAL DEPOSIT TYPES, BLM ROSWELL RESOURCE AREA, EAST-CENTRAL NEW MEXICO

David M. Sutphin

The U.S. Bureau of Land Management (BLM) Roswell Resource Area in east-central New Mexico contains approximately 14 million acres within seven counties. Within the area, mining produced several mineral commodities from the turn of the century through World War II; gold was the most important mineral product. As part of the mineral-resource assessment of the Roswell Resource Area, the USGS estimated the undiscovered resources in several mineral deposit types that were permissible in the area and for which grade and tonnage models were available. The resulting mineral resource estimates have been incorporated by BLM into an overall land-use plan.

The technique used in estimating the undiscovered mineral resources for selected deposit types is based upon the three-part type of assessment: (1) using known geologic, geochemical, and geophysical characteristics to delineate tracts that may contain specific deposit types; (2) estimating the probabilities that a certain number of undiscovered deposits exist in these tracts; and (3) estimating the amount of a given commodity contained in the undiscovered deposits by means of comparison with the grades and tonnages of known deposits of the same type. Parts (1) and (2) are conducted by a team of USGS specialists in economic geology, geochemistry, geophysics, and mineral resource assessment who are familiar with the area; part (3) is a computer simulation. This study uses the USGS' MARK-3 program that requires estimates of the number of undiscovered deposits of a given type stated in terms of likelihood of occurrence, resulting in a probability distribution.

Table 1 (Sutphin). Estimates of pre-mining tonnages of commodities in selected undiscovered deposit types, Roswell Resource Area, east-central New Mexico.

	Undiscovered resources (short tons)		
	Probability range		
	.90	.50 (median)	.10
Tract I:			
Barite	520	140,000	1,900,000
Copper	0	8.3	330
Gold	23	290	1,700
Iron	3,400,200	51,000,000	530,000,000
Lead	58	4,400	53,000
Manganese	0	850	160,000
Molybdenum	0	55,000	550,000
Rare-earth oxides	0	0	860
Silver	34	260	1,100
Thoria	0	190	8,800
Zinc	0	1,400	40,000
Tract II:			
Cobalt	0	0	90,000
Silver	0	0	720,000
Zinc	0	0	4,200,000
Tract III:			
Cobalt	0	0	0
Copper	0	0	1,400,000
Silver	0	0	0
Tract IV:			
Gypsum	1.3×10^8	2.0×10^9	2.6×10^{10}

Tracts favorable for the occurrence of undiscovered mineral resources in the Roswell Resource Area were delineated by comparing the geology, geochemistry, and geophysics of the area to the geologic environments and characteristics of deposit types having grade and tonnage models. A consensus by the team on tract borders, the types of deposits permissible in the tract, and the number of those deposits at the 90-, 50-, and 10-percent probability levels was reached after further discussion. By entering deposit estimates into MARK-3, probable quantities of undiscovered resources for selected deposit types in the four tracts within the Roswell Resource Area were calculated (table 1).

Tract I includes areas where geophysical evidence suggests shallow Tertiary intrusive bodies; it includes several historical mining districts and encompasses the most significant identified metal resources in the study area. Using geologic criteria and historical production figures for the Roswell Resource Area, the team estimated that the tract contains undiscovered iron skarns, alkaline-associated gold-silver-tellurium veins, polymetallic veins, epigenetic barite veins, gold-platinum-group-element placers, thorium-rare-earth-element veins, and replacement manganese,

102

porphyry-molybdenum low-fluorine, and fluorite-bastnaes-ite deposits. Tract II delineates an area permissible for sediment-hosted copper and southeast Missouri lead-zinc deposits on the basis of geologic and geochemical data and the presence of nearby mineralization outside the study area. Tract III encloses a 30-mi-diameter area, centered on the Stauber mine in Guadalupe County, that may contain undiscovered sediment-hosted copper deposits. The boundary of Tract IV connects 12 known gypsum occurrences and is likely to contain undiscovered marine-bedded gypsum deposits.

NATIONAL WATER QUALITY ASSESSMENT PROGRAM

Marc A. Sylvester

Many complex water-quality issues face this Nation. Both point (for example, municipal and industrial effluents) and nonpoint (for example, runoff from agricultural and urban land) sources of water pollution have caused water-quality degradation. A clear and comprehensive understanding of water-quality conditions in the Nation does not exist, because most water-quality assessment programs have been local, short-term, independent, single-purpose, and (or) single-agency efforts. Basic questions about water-quality conditions remain unanswered. Is the Nation's water quality getting better or worse? What fraction of the Nation's surface water and ground water is uncontaminated and meets requirements for diverted and instream uses? What is the relative importance of agricultural versus urban runoff in causing water-quality degradation? How variable is water quality across the Nation? How do land alteration and changes in habitat affect water quality? A comprehensive, multiple-scale, interdisciplinary, interagency, and long-term assessment of water-quality conditions using consistent approaches is needed to answer these questions and to provide reliable information for effective management of water resources. The National Water Quality Assessment Program (NAWQA) of the U.S. Geological Survey, which began in 1991, meets these requirements and is designed to answer some of the basic questions regarding water-quality conditions and trends in the Nation. Information from NAWQA will help reduce uncertainty in water-resources planning, management, and regulation, and will be useful for the protection, use, and enhancement of the Nation's water resources.

The goals of NAWQA are to describe the status and trends in the Nation's water quality, and to identify and explain, as possible, the major factors that affect observed conditions and trends. To accomplish these goals, NAWQA is composed of 60 Study Units covering a diversity of conditions across the Nation and 60–70 percent of the Nation's water use. Comparable information from these 60 Study Units will be aggregated to obtain regional and national perspectives on water quality. Interdisciplinary and interagency teams of hydrologists, chemists, and aquatic biologists are doing studies in each Study Unit using consistent approaches. Streamflow and ground-water levels are measured, water-quality samples are collected, processed, and analyzed, and ecological evaluations are made of stream and floodplain habitats and aquatic communities of fish, benthic invertebrates, and algae. Data are stored in a consistent manner in a computerized relational data-base management system so that information is easily accessible and integrated for timely interpretation.

EVALUATION OF METALLIC MINERAL RESOURCES IN THE EAST MOJAVE NATIONAL SCENIC AREA, SAN BERNARDINO COUNTY, CALIFORNIA

Ted G. Theodore, Robert J. Miller, Kenneth R. Bishop, Clay M. Conway, John C. Dohrenwend, Joseph S. Duval, Gordon B. Haxel, John D. Hendricks, Carroll A. Hodges, Robert C. Jachens, Marguerite J. Kingston, David M. Miller, Gary A. Nowlan, James J. Rytuba, and Richard M. Tosdal

Large areas of the East Mojave National Scenic Area (EMNSA) contain indications of various types of metallic mineralization at the surface. These metallic indications can be classified into approximately 20 specific types, or models, of metallic occurrences that are known to show extremely wide ranging concentrations of metals in variably sized accumulations, based on studies elsewhere of similar known deposits. Among metallic occurrences recognized are lead-zinc-silver-gold polymetallic vein; low-sulfide, gold-quartz vein; lead-zinc-silver polymetallic replacement; gold breccia pipe; gold-silver, quartz-pyrite vein; copper-lead-zinc-silver polymetallic fault and skarn; copper, zinc-lead, tungsten, tin-tungsten, and iron skarn; porphyry molybdenum-copper; and quartz-adularia (alunite) gold. Of these 20 types of mineral occurrence, enough geologic information is available only for 10 of them to make highly qualified estimates as to the numbers of additional mineral deposits that remain to be discovered in the EMNSA. Most of approximately 700 individual mineral occurrences known have been extensively prospected for more than a century, and at least 15 percent of them had some production, mostly of minor quantities of metals.

Nonetheless, it is possible that economically significant concentrations of some metals remain to be discovered in the EMNSA, or that some known occurrences may become economic in the future if exploration were allowed. For example, gold ore bodies at three relatively large mineralized systems in the EMNSA (Castle Mountain, Colosseum, and Morning Star) have been brought into production and at another occurrence (Golden Quail) additional resources discovered. The combined gold production from these four deposits in the last 5 years and the gold reserves remaining in them as of 1993 are much greater than that of all the preceding discoveries of gold in the EMNSA. This is partly a reflection of the present availability of low-cost heap-leaching extraction methods.

Some of the mountain ranges that have large numbers of metallic occurrences and that exhibit geochemical anomalies are the Providence Mountains, Clark Mountain Range, Ivanpah Mountains, and the New York Mountains. The general area of Hackberry Mountain lacks abundant metallic occurrences although it is included in a tract of land judged to be favorable for discovery of additional gold deposits similar to those present in the Castle Mountains. These five mountain ranges make up a broad, roughly north-south region in the central part of the EMNSA. Much less endowed with known metallic mineral occurrences are the Granite Mountains, central part of the Piute Range, Fenner Valley area, general area of Cima Dome, Old Dad Mountain area and areas west to Soda Lake, and the Cima volcanic field. These areas lie in the eastern and western parts of the EMNSA.

We have made some judgments about the geology underlying the gravel-covered areas in the EMNSA, including the areal extent of shallow bedrock apparently covered only by thin veneers of gravel. These are areas that would be prime targets for exploration because many of the ores that were exposed at one time in the mountain ranges have been found during past periods of exploration, whereas the pediment areas have remained largely unexplored. But few data are available to us for most of these covered areas. The presence of mineralized rocks, the type of mineral occurrence, and the extent and intensity of the mineralized rocks in the covered areas are essentially unknown. Most covered mineral deposits are undetectable by standard aeromagnetic geophysical methods evaluated in this study, particularly at the broad spacing of our data-collection flightlines.

Restricting estimates concerning presence of undiscovered metal resources, at reasonable levels of probability, only to currently known types of occurrences yields small estimates for volumes of many metals, particularly base and ferrous metals, that might be exploited there at some future date. However, this statement is true only if sizes of most previously discovered deposits in the EMNSA are in fact indicative of sizes of deposits still to be discovered there. Metals from any newly discovered copper, lead, and zinc deposit of the types presently known in the EMNSA probably would be insignificant from the standpoint of national needs. For example, a newly discovered copper skarn deposit in the EMNSA would have roughly a 50 percent chance of containing in excess of approximately 10,000 t (metric tons) contained copper. For comparison, in 1989 domestic production of copper amounted to 1,500,000 t of copper.

Based primarily on the geologic environments of large, recently discovered gold deposits in the EMNSA, some other parts of the EMNSA appear to represent geologic settings capable of hosting significant undiscovered gold and silver resources. In addition, widespread distribution in many parts of the EMNSA of geochemically anomalous samples and numerous mineral occurrences, many of which are associated with intrusion of igneous rock, indicates metal-bearing environments in those parts of the EMNSA that may be sites of additional future discoveries of new types of mineral deposits, if state-of-the-art exploration were allowed to take place in the EMNSA.

INTERACTIVE COMPUTER DISPLAY ON THE GEOLOGY AND MINERAL AND ENERGY RESOURCES OF THE ROSWELL RESOURCE AREA, NEW MEXICO

R.R. Tidball and Susan Bartsch-Winkler

The U.S. Geological Survey (USGS) has assessed the mineral and energy resource potential of the Roswell Resource Area, a seven-county tract in east-central New Mexico administered by the Bureau of Land Management (BLM) (see Bartsch-Winkler, this volume, fig. 1). A comprehensive report (Bartsch-Winkler, 1992; Bartsch-Winkler and Donatich, in press) was provided to the BLM as timely input to a required land-use plan that the BLM must prepare for the Roswell Resource Area. Such land-use plans are required for each area under the jurisdiction of the BLM and other Federal agencies and are periodically reviewed. This report will also be used by the USGS in national mineral resource assessments.

In addition to the published report, the USGS provided the BLM District Office in Roswell, N. Mex., with an interactive computer display that describes the general geology and the commodities present in the resource area. The display may be used to facilitate training of new employees and as an educational tool for use in the BLM Public Inquiries Office in Roswell. The interactive program, which runs on a Macintosh computer, enables a novice to choose alternative pathways through the graphical color displays to access topical information modules including units on the geology, geochemistry, geophysics, mining history, metallic and industrial mineral occurrence, hydrocarbons, and other gas resources. The program was

developed with Aldus SuperCard, version 1.5, software to run on a Macintosh II-series computer. Additional hardware requirements include color-graphics capability, 8 megabytes of memory, and a minimum of 40-megabytes of disk storage. An executable version of the program in compressed form can be loaded from high-density diskettes using standard Macintosh decompression routines.

REFERENCES

Bartsch-Winkler, Susan, ed., 1992, Mineral and energy resources of the BLM Roswell Resource Area, east-central New Mexico: U.S. Geological Survey Open-File Report 92–261, 153 p.

Bartsch-Winkler, Susan, and Donatich, A.J., eds., in press, Mineral and energy resources of the Roswell Resource Area, east-central New Mexico: U.S. Geological Survey Bulletin 2063 [Publication supersedes Open-File Report 92–261].

GEOCHEMICAL MAPPING IN THE SAN LUIS VALLEY, COLORADO—HYDROGEOCHEMICAL AND STREAM SEDIMENT DATA

Ronald R. Tidball, Steven M. Smith, and Kathleen C. Stewart

Figure 1 (Tidball and others). Map of San Luis Valley, south-central Colorado, showing major drainages and Bonanza and Summitville mining districts.

Prime agricultural land in south-central Colorado's San Luis Valley is at risk from metal contamination from several areas of mining activity. The Alamosa River receives acid mine water derived from the Summitville mine, located in the San Juan Mountains west of the valley (fig. 1); it also supplies water for an extensive irrigation system in the valley. The Summitville mine will soon be declared a U.S. Environmental Protection Agency (EPA) Superfund site. The Bonanza district near the north end of the valley is also currently under study by the State of Colorado, the U.S. Forest Service, and EPA as a potential Superfund site. Several creeks drain from this district into the valley. Background geochemical studies of soils and surficial materials in the valley are therefore needed to define the extent of metal dispersion into the valley from several mineralized areas and mining districts.

Previous geochemical sampling in the valley has been sparse. Stream, spring, and pond sediment and water samples, in a project called Hydrogeochemical and Stream Sediment Reconnaissance (HSSR), were collected throughout the State of Colorado during the National Uranium Resource Evaluation (NURE) program in the 1970's. Although overall HSSR coverage of the State is extensive, coverage in the San Luis Valley is generally limited to a few samples in the southeastern and the far northeastern part of the valley. This sampling predates the recent active Summitville mining period of 1986–1992.

The HSSR coverage is currently being supplemented by a soil sampling program by the USGS. The Alamosa River fan and adjacent fans in the southwestern part of the valley are being sampled intensively on a 1-mile (1.6 km) grid interval. A larger interval of 5 km (3.1 miles) is being used in the rest of the valley.

We present here a view of the regional geochemistry based on multielement analyses of HSSR samples to estimate the occurrence of metal-rich source rocks near the valley margin. HSSR data from parts of the Montrose, Pueblo, Trinidad, Raton, Aztec, and Durango 1°×2° quadrangles that surround the San Luis Valley are included.

Intensive HSSR sampling in the eastern part of the Montrose quadrangle showed anomalies of Ag, Cu, Pb, Zn, As, Sb, and Sn bordering the northwest part of the valley. These anomalies are associated with the Bonanza mining district and Kerber and San Luis Creeks, which drain the district. Elsewhere, above-average amounts of Co, Cr, Ni, and V occur in the vicinity of outcrops of basalt in the San Luis Hills in the southern part of the valley and in the vicinity of the Summer Coon stratovolcano north of Del Norte.

The data also show several anomalous sites in the Alamosa River watershed. Wightman Fork, the tributary which drains the Summitville mine area, has Cu values in the range of 100–900 ppm, Pb 150–250 ppm, and Zn about 200 ppm. Below Wightman Fork, Cu and Pb decrease to 50 ppm or less, and Zn decreases to 140–170 ppm. All these samples are from above Terrace Reservoir. The possibility exists that metal-laden sediments are trapped in Terrace Reservoir, but two samples on the upper part of the Alamosa River fan contain 150–170 ppm Cu, 40–50 ppm Pb, and 140–170 ppm Zn, thus suggesting that metals both can migrate and have migrated to the valley. HSSR data on pH show that Alamosa River water is the most acidic (pH 5–5.5) of any stream entering the valley, and corrosion observed in some sprinkler-irrigation systems using river water may be accelerated by its acidic condition. Scattered sites containing anomalous values of Bi, Sb, and Sn, plus above-average values of Cu, Pb, and Zn, are also found in a hydrothermally altered monazite area just north of Terrace Reservoir.

Pb SOURCES IN OLIGOCENE AND MIOCENE PRECIOUS-METAL DEPOSITS OF THE WESTERN ANDEAN CORDILLERA, SOUTHERN PERÚ, WESTERN BOLIVIA, AND NORTHERN CHILE

Richard M. Tosdal

A variety of precious-metal deposits characterize the western part of the Andean cordillera in southern Perú, western Bolivia, and northern Chile. Deposits in this transect include polymetallic vein deposits in southern Perú (Orcopampa, Arcata, Cailloma; lat 15°–16° S.), quartz-adularia and quartz-alunite deposits in western Bolivia and northern Chile (La Española prospect, Choquelimpie; lat 17°–18° 30′ S.), and quartz-alunite and gold-rich porphyry deposits in north-central Chile (Maricunga and El Indio belts; between lat 26° and 28° S.). All deposits are associated with Oligocene and Miocene calc-alkaline volcanic or intrusive rocks erupted from, or emplaced in, stratovolcanos along the main arc.

Lead isotopic compositions from sulfides and whole rocks indicate that three major crustal sources contributed lead to these deposits. The source regions include (1) old nonradiogenic and high-μ ($^{238}U/^{204}Pb$) and high-Th/U lithosphere; (2) high-μ lithosphere with time-averaged Th/U ≈ 4; and (3) lower-μ lithosphere with time-averaged Th/U ≈ 4.

The nonradiogenic lithospheric source is characterized by retarded $^{206}Pb/^{204}Pb$ compositions mostly ≤ 18.2. Thorogenic ($^{208}Pb/^{204}Pb$ versus $^{206}Pb/^{204}Pb$) and uranogenic ($^{207}Pb/^{204}Pb$ versus $^{206}Pb/^{204}Pb$) Pb isotopic compositions lie above the average crustal growth curve of Stacey and Kramers (1975). The elevated $^{208}Pb/^{204}Pb$ ratios demonstrate that Th/U values ≥ 4 dominate this lithosphere, indicating the presence of granulitic rocks, or lower-crustal type Pb reservoirs, where U is depleted with respect to Th. This lower-crustal-like source is present in two adjoining areas. One area is underlain by the Early Proterozoic Arequipa massif in southern Perú, and is characterized by ≈ 2.0 Ga rocks, $^{206}Pb/^{204}Pb$ between 16.0 and 17.1, and $^{208}Pb/^{204}Pb$ between 37.0 and 41.0. The second area underlies western Bolivia and northern Chile where most $^{206}Pb/^{204}Pb$ ratios are between 17.0 and 18.2, $^{208}Pb/^{204}Pb$ ratios are between 37.2 and 41.2, uranogenic Pb isotopic compositions scatter about 1.75-Ga reference isochrons, and U-Pb zircon ages are Middle Proterozoic (1.25 to 1.1 Ga).

The high-μ source is characterized by elevated $^{207}Pb/^{204}Pb$ with respect to a given $^{206}Pb/^{204}Pb$ ($^{206}Pb/^{204}Pb=18.5$–19.9; $^{207}Pb/^{204}Pb=15.63$–15.72) such that most of the uranogenic Pb isotopic compositions lie above and along the extension of the average crustal growth curve, and scatter about late Middle Proterozoic (≈ 1.0 Ga) reference isochrons. Thorogenic Pb isotopic compositions scatter about the average crustal growth curve. These characteristics indicate that the source had high μ values, typical of upper-crustal environments, but average crustal Th/U. Carboniferous, Permian, and Triassic plutonic rocks in north-central Chile, representative of the leading edge of Gondwana, have these Pb isotopic characteristics, and are a product of this source region. Very limited data suggest that this source region also influenced Pb isotopic compositions of some early Paleozoic granitoids in the same region.

The third source is characterized by lower μ values and average crustal Th/U≈ 4. Uranogenic Pb isotopic compositions derived principally from this source generally lie along or below the average crustal growth curve ($^{206}Pb/^{204}Pb<18.7$; $^{207}Pb/^{204}Pb<15.62$). This source is widely recognized in Cenozoic magmas in the Central Andes, and has been interpreted as subcontinental lithosphere that has been fluxed or enriched by material emanating from the subducting slab or as a zone of melting and assimilation at the crust-mantle boundary (Hildreth and Moorbath, 1988). This source represents the least radiogenic isotopic compositions recognized in the deposits.

Present-day Pb isotopic compositions of the deposits and their host volcanic rocks in this region of the Central Andes lie along mixing trends between two of the three sources. Deposits in the Maricunga and El Indio belts are influenced by the lower-μ, subcontinental-type source and the high-μ, upper crustal-type source. A similar mixing trend also appears to explain the lead-isotopic composition in the Orcopampa area, but a steep mixing trend in thorogenic Pb suggests that a third component with high Th/U may also have been involved. In western Bolivia and northern Chile,

the Pb isotopic compositions of the ore deposits reflect mixing between the lower-μ, subcontinental-type source and the Proterozoic lithospheric source.

REFERENCES

Hildreth, W., and Moorbath, S., 1988, Crustal contributions to arc magmatism in the Andes of central Chile: Contributions to Mineralogy and Petrology, v. 88, p. 435–489.

Stacey, J.S., and Kramers, J.D., 1975, Approximation of terrestrial lead isotope evolution by a two-stage model: Earth and Planetary Science Letters, v. 26, p. 207–221.

PRELIMINARY RESULTS OF A SYNOPTIC WATER-QUALITY STUDY OF THE UPPER ALAMOSA RIVER TO THE OUTLET OF TERRACE RESERVOIR

Katherine Walton-Day, Roderick F. Ortiz, and Paul von Guerard

A synoptic study including pH, specific conductance, streamflow, and total copper loads was done from the headwaters of the Alamosa River downstream to the outlet of Terrace Reservoir to assess the source and fate of acid, metal-rich water in the river system. The study was done in cooperation with the Colorado Division of Minerals and Geology and the U.S. Environmental Protection Agency. The study area is located in the San Juan Mountains of southwest Colorado, and the rocks are mostly intrusive bodies and rhyolite ash flows and lava. The Summitville mine (which ceased operation in December 1992) lies within the study area. Acid-rock drainage and some drainage from cyanide heap-leach piles at the Summitville mine site enter the Wightman Fork, a tributary to the Alamosa River.

Water-quality samples were collected every 2 to 4 weeks beginning in late April through mid-August 1993 at eight sites along the Alamosa River and at three sites on tributaries. The Alamosa River sites, listed from upstream to downstream, are upstream and downstream from Iron Creek, downstream from Alum Creek and Bitter Creek, upstream and downstream from the Wightman Fork, and upstream from and at the outlet of Terrace Reservoir. The three tributary sites are Pipeline Creek (tributary to the Wightman Fork) upstream from the Summitville mine, the Wightman Fork directly downstream from the Summitville mine, and the Wightman Fork 5.5 miles (8.8 km) downstream from the mine and directly upstream from the confluence with the Alamosa River.

Preliminary results indicate that (1) seasonal dynamics are complex; (2) multiple sources of water have low pH values (pH<5) in addition to the water from the Summitville mine site; and (3) water quality improves somewhat downstream from the Summitville mine due to dilution and unidentified physical and chemical processes.

Values of pH, specific conductance, and discharge exhibit large seasonal and spatial variation. For example, pH values range from 3.33 on the Wightman Fork downstream from the Summitville mine in late June to 7.59 on the Alamosa River upstream from Iron Creek in mid-May. Specific conductance ranges from 22 to 1,650 microsiemens per centimeter in Pipeline Creek in mid-July and in the Wightman Fork downstream from Summitville in late April, respectively. Streamflow varies from 1.5 ft^3/s (cubic feet per second) in Pipeline Creek in early May to 858 ft^3/s in the Alamosa River upstream from Terrace Reservoir in early June.

Preliminary results indicate sources of acid water to the upper Alamosa River in addition to the Summitville mine. On the Alamosa River upstream from the Wightman Fork, pH values range from less than 4.0 during low flow (April) to about 6.4 during high flow (late June), whereas on the Wightman Fork upstream from the confluence with the Alamosa River, pH values range from about 7.5 during low flow to about 4.5 during high flow. These results indicate that sources for acid water to the Alamosa River exist upstream from the Wightman Fork. Specific sources, although not identified, are most likely located between the Wightman Fork and Iron Creek, as only pH values upstream from Iron Creek were circum-neutral throughout the study period. In addition, during a rainfall-runoff event, lower pH values were measured upstream from Terrace Reservoir than immediately downstream from the Wightman Fork, indicating sources of acid water to the Alamosa River between the Wightman Fork and Terrace Reservoir.

Some increase in pH and decrease in specific-conductance values occur as water moves down the Wightman Fork from the Summitville mine to the confluence with the Alamosa River during and following runoff (late May to late June). For example, on the Wightman Fork directly below Summitville, pH values ranged from about 3.3 to about 3.7 during and following runoff and specific conductance ranged from 932 to 1,242 microsiemens per centimeter. During that same period, on the Wightman Fork above the confluence with the Alamosa River, pH values ranged from 4.4 to 5.0 and specific conductance ranged from 372 to 592 microsiemens per centimeter. Streamflow increased as much as seven-fold between the two sites, indicating that dilution from other water sources contributed to these improvements. However, over the same reach of stream, instantaneous total copper loads (in kilograms per second) decreased as much as six-fold during early runoff. This decrease indicates that processes other than dilution, such as sorption and precipitation of solid phases, contribute to water-quality improvements. Evaluation of the complete data set will help identify these processes.

Au-Ag POLYMETALLIC MINERALIZATION IN THE MUSIC MOUNTAIN AREA, ARIZONA, ALONG THE SOUTHWESTERN EDGE OF THE COLORADO PLATEAU

Karen J. Wenrich and Miles L. Silberman

The Music Mountain mining district lies at the base of the Grand Wash Cliffs, a major fault-line scarp along the Grand Wash fault, which marks the southwestern margin of the Colorado Plateau (fig. 1). Nearly vertical Au-Ag polymetallic quartz veins are parallel to, and in contact with, altered diabase and granite porphyry dikes that cut Proterozoic granite, schist, and gneiss. The gold-bearing veins range in thickness from several centimeters to 1 m, and they contain significant amounts of sulfide minerals, principally galena, sphalerite, and pyrite, with minor chalcopyrite, pyrrhotite, arsenopyrite, and tennantite. Microprobe analyses of the sulfides showed the sphalerite to contain high Fe (Zn:Fe=4:1 atomic proportion), and tennantite to be high in Zn and Fe (As:Zn:Fe=3:1:1 atomic proportion). Bulk rock geochemical analyses yielded as much as 7.2 ppm Au, 1,000 ppm Ag, 2.4 percent Pb, 1.7 percent Zn, 1.7 percent Cu, 500 ppm Cr, 460 ppm Ni, 350 ppm Cd, 300 ppm Co, and 2.8 ppm Hg. Two types of quartz veins occur in the district and surrounding area: (1) veins, associated with pegmatites and some diabase dikes, that consist of coarse- to medium-grained bull quartz with occasional pyrite cubes—the pyrite has generally been altered to limonite or weathered out entirely leaving empty molds; (2) veins and stringers within diabase dikes, along the contact between diabase dikes and granite, and within shear zones in granite that are parallel to the dikes. Type-2 quartz is medium to fine grained with coxcomb crystals lining vug walls; the gold-bearing quartz veins are of this type.

Stream-sediment and panned-concentrate samples were collected at 269 sites from all drainages in Precambrian rock within a 15 mi² (40 km²) area directly north of the Music Mountain mines and eastward between the Grand Wash Cliffs and the Aubrey Cliffs, in an effort to locate gold-rich veins beyond the Music Mountain mines. Several samples had anomalous Au and Ag concentrations, including one panned concentrate with 528 ppm Au. In each case there were diabase dikes with adjacent quartz veins above the anomaly site.

Diabase dikes and quartz veins in the district and to the north consistently strike N42°W to N57°W, which is one of the most prevalent Precambrian fracture orientations throughout northwestern Arizona (the other being approximately N45°E). Drifts and trenches of the mines in the district form striking N45°W arrays (fig. 2) that roughly parallel the Grand Wash fault in this area. In contrast, quartz veins associated with pegmatites generally strike N40°E to due east. In the Gold Basin–Lost Basin districts to the north, the gold occurs in such pegmatite-quartz veins that strike northeast. Thirty miles (48 km) east along Diamond Creek, quartz veins and diabase dikes strike N45°E and have associated gold and silver anomalies in stream sediments and panned concentrates. To the west, major Au-Ag polymetallic quartz veins of the Wallapai mining district rarely show strikes outside of the range N30–60°W. Such northwest and northeast trends can also be seen in alignments of mineralized solution-collapse breccia pipes on this southwestern part of the Colorado Plateau.

All diabase dikes were hydrothermally altered to some extent. K-Ar ages from four of the dikes with quartz veins along their margins range from 935±35 to 755±21 Ma. One vein was mineralized. Within the Music Mountain mines area, mineralized type-2 quartz veins occur at one location along the margins of a dacite dike where it contacts diabase intruded along a northwest-trending structure. Sericite from this dacite dike gave a K-Ar age of 72±2 Ma. These data suggest that the northwest-trending diabase dikes, and one stage of mineralized quartz veins, are late Precambrian, and that a later stage of mineralized quartz veins is Late Cretaceous.

Fluid-inclusion studies of 36 quartz veins in the Music Mountain area indicate that the vast majority of the quartz veins, most of which were of type 1, appear to have a "deep" mesothermal origin. Two localities containing type-1 quartz veins are exceptions to this: (1) several quartz veins within the Music Mountain mines, and (2) quartz veins located 2 miles (3.2 km) northeast of the mines. Quartz veins from these two areas contain clear cores surrounded by ratty, dendritic, outer growth zones. Fluid-inclusion filling temperatures >350 °C were observed in quartz cores from both areas. Sulfides and sericite in the Music Mountain mines are associated with fluid inclusions in the outer growth zones with temperatures <200 °C and salinities commonly <7 wt. % NaCl eq. Exceptions to this include sphalerite inclusions adjacent to, and located in the same outer quartz growth zone with, primary inclusions; these inclusions yielded temperature <200 °C and variable compositions: (1) 22 wt. % NaCl eq., (2) 7 wt. % NaCl eq., and (3) vapor-CO_2-bearing. Such highly variable salinities adjacent to each other suggest a very saline brine mixed with a low-salinity fluid. In the area northeast of the Music Mountain mines are three types of inclusions similar to what might be expected from a porphyry system: (1) NaCl-saturated brines (fig. 3—indicated by halite daughter minerals adjacent to vapor bubble within the liquid inclusion), (2) low-salinity inclusions, and (3) vapor-rich inclusions. Salinities as high as 38 wt. % NaCl and temperatures as high as 380 °C were observed in quartz cores from this area. The variable salinities in the outer quartz zones, and the high temperature–high salinities found within the cores of the quartz, suggest that initial fluids were high-temperature saline brines that were diluted by later low-salinity, low-temperature, sulfide-bearing fluids to produce the outer quartz growth zones.
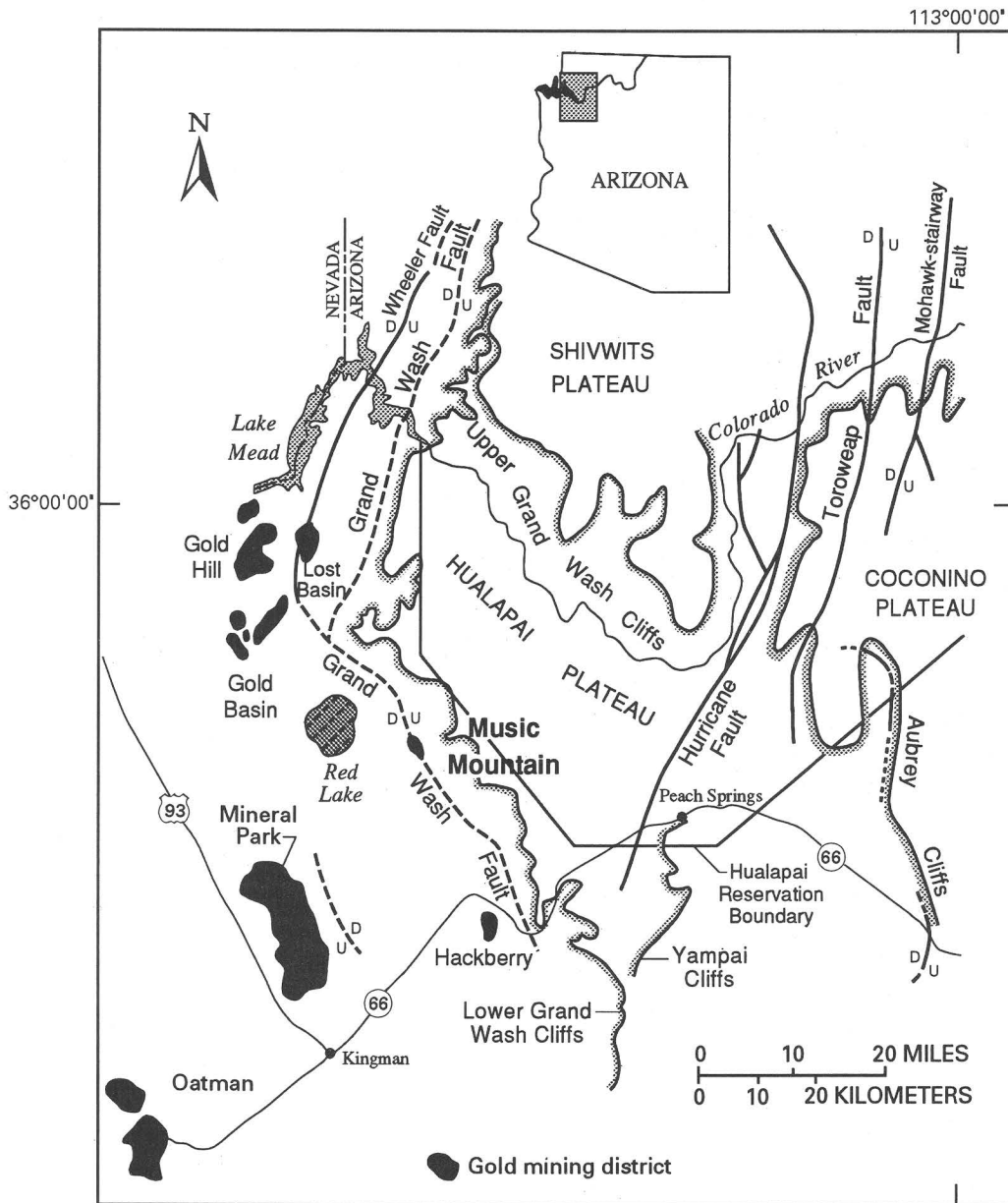
Figure 1 (Wenrich and Silberman). The Music Mountain, Gold Basin–Lost Basin, and Hackberry mining districts lie at the edge of the Colorado Plateau at the base of the Grand Wash Cliffs. The Au-Ag polymetallic mineralization occurred within quartz veins associated with diabase dikes or pegmatites that commonly strike either northwest or northeast.

All the geochemical sites (within a 1,000 mi² (2,500 km²) area) determined to be anomalous in gold during this study lie within 2 miles (3.2 km) of either the Grand Wash or the Hurricane faults. Although the overall trend of the Hurricane fault is north-south, it is composed of northwest- and northeast-trending segments. The Gold Basin and Lost Basin mining districts also lie close to the Grand Wash fault. Recurrent tectonism along northwest and northeast trends in

the region is reflected not only in the faulting but also in multiple episodes of mineralization. The Hurricane and Grand Wash faults, both major Precambrian fault zones that have probably been reactivated in the Phanerozoic (adjacent, approximately parallel faults, such as the Cremation, Bright Angel, Palisade, Butte, and Muav faults, have documentable Phanerozoic displacement), appear to be good exploration targets for gold-rich quartz veins associated with pegmatite

Figure 2 (Wenrich and Silberman). Music Mountain mines. Note the four lines of trenches striking N45°W. Hualapai Valley is in the background and the Grand Wash Cliffs, the southwestern edge of the Colorado Plateau in Arizona, lie along the upper right side of the figure. The Lost Basin district lies in the far distance on left side of photograph. View is to the north-northwest.

or Precambrian diabase dikes, many of which may be buried beneath the thick alluvium of Hualapai Valley. The occurrence of NaCl-saturated brines, vapor-rich inclusions, and low-salinity inclusions in the quartz veins, along with occasional filling temperatures in the range of 350–380 °C, suggests that Music Mountain gold mineralization may be peripherally related to a porphyry Cu-Mo system, perhaps similar to Mineral Park.

Figure 3 (Wenrich and Silberman). Fluid inclusion from a quartz vein that lies adjacent to a northwest-trending diabase dike located 2 mi (3.2 km) northeast of the Music Mountain mines. Such an inclusion suggests that this quartz was deposited from a NaCl-saturated brine—note the cubic salt crystal and the vapor bubble. Salt crystal is 50 μm long.

View eastward from Hualapai Valley (Basin and Range) to the Grand Wash Cliffs, the southwestern boundary of the Colorado Plateau (northern Arizona). Note the flat-lying strata of the Cambrian Tapeats Sandstone and the Muav Limestone capping the top of the cliffs. Original slide by Karen J. Wenrich.

Northwest-trending, Precambrian diabase dike cutting a ridge 1 mile (1.6 km) north of the Music Mountain mine. This dike is similar to the diabase dikes in the Music Mountain mine area in that it too has a quartz vein following its margin (note darker, higher relief area on left edge of the dike). Original slide by Karen J. Wenrich.

AUTHOR INDEX

H

Hageman, Philip, USGS, Denver   78
Hammarstrom, J.M., USGS, Reston   44
Hardyman, Richard, USGS, Denver   48
Haxel, G.B., USGS, Flagstaff   75, 103
Hemley, J.J., USGS, Reston   26
Hendricks, J.D., USGS, Flagstaff   103
Herring, J.R., USGS, Denver   45
Hodges, C.A., USGS, Menlo Park   46, 103
Hoffman, J.D., USGS, Denver   47
Hofstra, Albert, USGS, Denver   35, 48
Hon, Ken, USGS, Denver   48
Houser, B.B., USGS, Tucson   49

J

Jachens, R.C., USGS, Menlo Park   103
John, D.A., USGS, Menlo Park   4
Johnson, K.M., USGS, Spokane   4
Jones, A.E., P.O. Box 7633, Reno, NV 89510   64

K

Kamilli, R.J., USGS, Tucson Field Office, University of Arizona,
    Gould-Simpson Rm 430, Tucson, AZ 85721   52, 94
King, T.V.V., USGS, Denver   53
Kingston, M.J., USGS, Reston   103
Klein, D.P., USGS, Denver   54, 94
Knepper, D.H., Jr., USGS, Denver   37
Kover, A.N., USGS, Reston   56
Krohn, M.D., USGS, Reston   58
Kulik, D.M., USGS, Denver   44, 58

L

Lamothe, P.J., USGS, Menlo Park   70
Landis, G.P., USGS, Denver   27
Lee, G.K., USGS, Denver   44
Lichte, F.E., USGS, Denver   59
Light, T.D., USGS, Anchorage   19
Lindsay, James, USGS, Spokane   12
Lindsey, D.A., USGS, Denver   4
Lipman, Peter, USGS, Menlo Park   48
Long, K.R., USGS, CIMRI, Tucson   60, 73
Ludington, S.D., USGS, Menlo Park   4
Luedke, R.G., USGS, Reston   61
Luepke, G., USGS, Menlo Park   81

M

Manydeeds, S.A., Bureau of Indian Affairs, Division of Energy and
    Mineral Resources, 730 Simms St., Lakewood, CO   62
Marsh, S.P., USGS, Denver   47, 80
Martins Pereira, Sérgio Luiz, Unamgen Mineracao e Metalurgia
    S.A. Santa Barbara, Minas Gerais, Brazil   27
McCafferty, A.E., USGS, Denver   69
McGuire, D.J., USGS, Denver   62, 64
McHugh, J.B., USGS, Denver   68
McKee, E.H., USGS, Menlo Park   23, 48, 65
McKown, D.M., USGS, Denver   100
McLean, Hugh, USGS, Menlo Park   66
Meier, A.L., USGS, Denver   67, 78
Merewether, E.A., USGS, Denver   97

Miller, D.M., USGS, Menlo Park   103
Miller, R.J., USGS, Menlo Park   103
Miller, W.R., USGS, Denver   68, 90
Miranda, F.P., Petroleo Brasileiro S/A (Petrobras), Cidade
    Universitaria, Ilha do Fundao, Rio de Janeiro, RJ, 21949–900,
    Brazil   69
Montour, Maria, USGS, Denver   77, 78
Moring, B.C., USGS, Menlo Park   19

N, O

Naeser, C.W., USGS, Reston   23
Nash, J.T., USGS, Denver   70
Nelson, C.H., USGS, Menlo Park   70
Noble, D.C., Mackay School of Mines, University of Nevada-Reno,
    Reno, NV   65
Nowlan, G.A., USGS, Denver   35, 72, 103
Orris, G.J., USGS, Tucson   42, 73
Ortiz, R.F., USGS, Norwest Bank Building, 8th and Main,
    Suite 200, Pueblo, CO 81003   107

P

Page, N.J, USGS, Tucson   40, 42, 73
Palanques, A., Ciencias del Mar, Barcelona, Spain   70
Pallister, J.S., USGS, Denver   30
Patchett, P.J., Department of Geosciences, University of Arizona, Tucson,
    AZ 85721   89
Peacock, T.R., USGS, Denver   33
Peterman, Z.E., USGS, Denver   1
Peterson, D.W., USGS, Menlo Park dpetersn@mojave.wr.usgs.gov   15
Pierce, H.A., USGS, 210 E. 7th St., Tucson, AZ 85705   40, 74
Pitkin, J.A., USGS, Denver   75
Plumlee, G.S., USGS, Denver   34, 77, 78, 80
Poole, F.G., USGS, Denver   81
Poppe, L.J., USGS, Woods Hole   81

Q, R

Quintana, J. R., Estacion Regional del Noroeste, Instituto de
    Geologia U.N.A.M., Apartado Postal 1039, Hermosillo,
    Son., 83000 Mexico   83
Raines, G.L., USGS, Mackay School of Mines, University of
    Nevada-Reno, Reno, NV 89557   17
Ratté, J.C., USGS, Denver   84, 94
Reynolds, S.J., Dept. of Geology, Arizona State University,
    Tempe, AZ 85287–1404   87
Robinson, G.R., Jr., USGS, Reston   88
Ruiz, Joaquin, Department of Geosciences, University of Arizona,
    Tucson, AZ 85721   13, 89
Rye, R.O., USGS, Denver   23
Rytuba, J.J., USGS, Menlo Park   22, 90, 103

S

Sanjines, Orlando, Servicio Geologico de Bolivia   48
Sawyer, D.A., USGS, Denver   91
Schoonmaker, J.W., Jr., USGS, Reston   56
Schruben, P.G., USGS, Reston   92
Senterfit, R.M., USGS, Denver   94
Severson, R.C., USGS, Denver   78
Sidder, G.B., USGS, Denver   42
Silberman, M.L., USGS, Denver   108

ORGANIZATION OF THE U.S. GEOLOGICAL SURVEY

Office	Name	Telephone	City
Office of the Director			
Acting Director	Robert M. Hirsch	703/648-7411	Reston
Acting Associate Director	Bonnie McGregor	703/648-7412	Reston
Assistant Director for Research	Steven E. Ragone	703/648-4450	Reston
Assistant Director for Engineering Geology	James F. Devine	703/648-4423	Reston
Assistant Director for Administration	Jack J. Stassi	703/648-7200	Reston
Assistant Director for Programs	Peter F. Bermel	703/648-4430	Reston
Assistant Director for Intergovernmental Affairs	John J. Dragonetti	703/648-4427	Reston
Assistant Director for Information Systems	James E. Biesecker	703/648-7108	Reston
Public Affairs Officer	Donovan B. Kelly	703/648-4459	Reston
Chief EEO Officer	Bruce D. Palmer	703/648-4417	Reston
Assistant to the Director for Human Resources	J. Lynn Smith	703/648-7111	Reston
National Mapping Division			
Chief	Allen H. Watkins	703/648-5748	Reston
Geologic Division			
Chief Geologist	Benjamin A. Morgan	703/648-6600	Reston
Water Resources Division			
Chief Hydrologist	Philip Cohen	703/648-5215	Reston
Information Systems Division			
Assistant Director	James E. Biesecker	703/648-7108	Reston
Administrative Division			
Assistant Director	Jack J. Stassi	703/648-7200	Reston

ORGANIZATION OF THE GEOLOGIC DIVISION

Office of the Chief Geologist			
Chief Geologist	Benjamin A. Morgan	703/648-6600	Reston
Associate Chief Geologist	David P. Russ	703/648-6601	Reston
Assistant Chief Geologist for Program	Bonnie McGregor	703/648-6640	Reston
Assistant Chief Geologist, Eastern Region	Nancy Milton	703/648-6660	Reston
Assistant Chief Geologist, Central Region	Harry A. Tourtelot	303/236-5438	Denver
Assistant Chief Geologist, Western Region	William R. Normark	415/329-5101	Menlo Park
Office of Mineral Resources			
Chief	Willis H. White	703/648-6100	Reston
Chief, Branch of Alaskan Geology	L. David Carter	907/786-7403	Anchorage
Chief, Branch of Eastern Mineral Resources	Klaus J. Schulz	703/648-6327	Reston
Chief, Branch of Central Mineral Resources	Gary R. Winkler	303/236-5568	Denver
Chief, Branch of Western Mineral Resources	Ronald G. Worl	509/353-2639	Spokane
Chief, Branch of Geochemistry	David B. Smith	303/236-1800	Denver
Chief, Branch of Resource Analysis	Richard B. McCammon	703/648-6150	Reston
Chief, Branch of Geophysics	David L. Campbell	303/236-1212	Denver
Office of Energy and Marine Geology			
Chief	Gary W. Hill	703/648-6472	Reston

Chief, Branch of Petroleum Geology	Thomas S. Ahlbrandt	303/236-5711	Denver
Chief, Branch of Coal Geology	Robert C. Milici	303/236-7726	Denver
Chief, Branch of Sedimentary Processes	Christine Turner	303/236-1644	Denver
Chief, Branch of Pacific Marine Geology	Michael E. Field	415/354-3184	Menlo Park
Chief, Branch of Atlantic Marine Geology	Bradford Butman	508/457-2211	Woods Hole
Chief, Center for Coastal Geology and Regional Marine Studies	Abby Sallenger	813/893-3684 ext. 3002	St. Petersburg

Office of Regional Geology

Chief	Mitchell W. Reynolds	703/648-6960	Reston
Chief, Branch of Eastern Regional Geology	Wayne L. Newell	703/648-6900	Reston
Acting Chief, Branch of Central Regional Geology	William D. Johnson, Jr.	303/236-1258	Denver
Chief, Branch of Western Regional Geology	John (Jack) W. Hillhouse	415/329-4909	Menlo Park
Chief, Branch of Isotope Geology	Carl E. Hedge	303/236-7880	Denver
Chief, Branch of Astrogeology	Philip Davis	602/527-7201	Flagstaff
Chief, Branch of Paleontology and Stratigraphy	John Pojeta, Jr.	703/648-5288	Reston

Office of Earthquakes, Volcanoes, and Engineering

Chief	Robert L. Wesson	703/648-6714	Reston
Chief, Branch of Earthquake and Geomagnetic Information	John R. Filson	703/648-6785	Reston
Chief, Branch of Seismology	Allan G. Lindh	415/329-4778	Menlo Park
Chief, Branch of Earthquake and Landslide Hazards	Kaye M. Shedlock	303/273-8579	Denver
Chief, Branch of Earthquake Geology and Geophysics	William H. Prescott	415/329-4860	Menlo Park
Chief, Branch of Volcanic and Geothermal Processes	Peter Lipman	415/329-5228	Menlo Park
Chief, Branch of Lithospheric Processes	Bruce Hemingway	703/648-6740	Reston

Office of Scientific Publications

Chief	John M. Aaron	703/648-6077	Reston
Chief, Branch of Eastern Technical Reports	Herbert A. Wolford	703/648-4326	Reston
Chief, Branch of Central Technical Reports	Lawrence F. Rooney	303/236-5457	Denver
Chief, Branch of Western Technical Reports	James B. Pinkerton	415/329-5043	Menlo Park
Acting Chief, Library and Information Services	Edward H. Liszewski	703/648-4305	Reston
Chief, Branch of Visual Services	John R. Keith	703/648-4357	Reston

Office of International Geology

Chief	A. Thomas Ovenshine	703/648-6047	Reston
Associate Chief	Richard D. Krushensky	703/648-6060	Reston
Deputy Chief for European Geology	Richard D. Krushensky	703/648-6060	Reston
Deputy Chief for Asian and Pacific Geology	Jack H. Medlin	703/648-6062	Reston
Deputy Chief for Latin American Geology	Jean N. Weaver	703/648-6012	Reston
Deputy Chief for Middle Eastern and African Geology	Frederick O. Simon	703/648-6055	Reston
Deputy Chief for Geologic Hazards and Risk Assessment	Ted Algermissen	703/648-6051	Reston
Deputy Chief for International Polar and Environmental Studies	Bruce F. Molnia	703/648-4120	Reston
Deputy Chief for Russian and NIS Programs	Paul Hearn	703/648-6287	Reston

Addresses

U.S. Geological Survey
Reston, VA 22092

U.S. Geological Survey
Box 25046
Denver Federal Center
Denver, CO 80225

U.S. Geological Survey
345 Middlefield Road
Menlo Park, CA 94025

U.S. Geological Survey
Branch of Alaskan Geology
4200 University Drive
Anchorage, AK 99508-4667

U.S. Geological Survey
2255 North Gemini Drive
Flagstaff, AZ 86001

U.S. Geological Survey
384 Woods Hole Road
Woods Hole, MA 02543-1598

U.S. Geological Survey
Hawaiian Volcano Observatory
Hawaii National Park
HI 96718

U.S. Geological Survey
David A. Johnson Cascades Volcano
  Observatory
5400 MacArthur Boulevard
Vancouver, WA 98661

U.S. Geological Survey
600 4th Street, South
St. Petersburg, FL 33701

Cosponsoring Organizations

Frances Pierce
President, Arizona Geological Society
U.S. Geological Survey
210 East 7th Street
Tucson, AZ 85705

Dr. Larry Fellows
State Geologist
Arizona Geological Survey
845 North Park Avenue, #100
Tucson, AZ 85719
602/882–4795

Dr. Clem Chase
Chairman
Department of Geosciences
Gould-Simpson Building #77
University of Arizona
Tucson, AZ 85721
602/621–2417; –6024; –4051